

AD-A046 704

MCDONNELL AIRCRAFT CO ST LOUIS MO
REMOTE VIEWING SYSTEM.(U)
JUN 77 R W FISHER

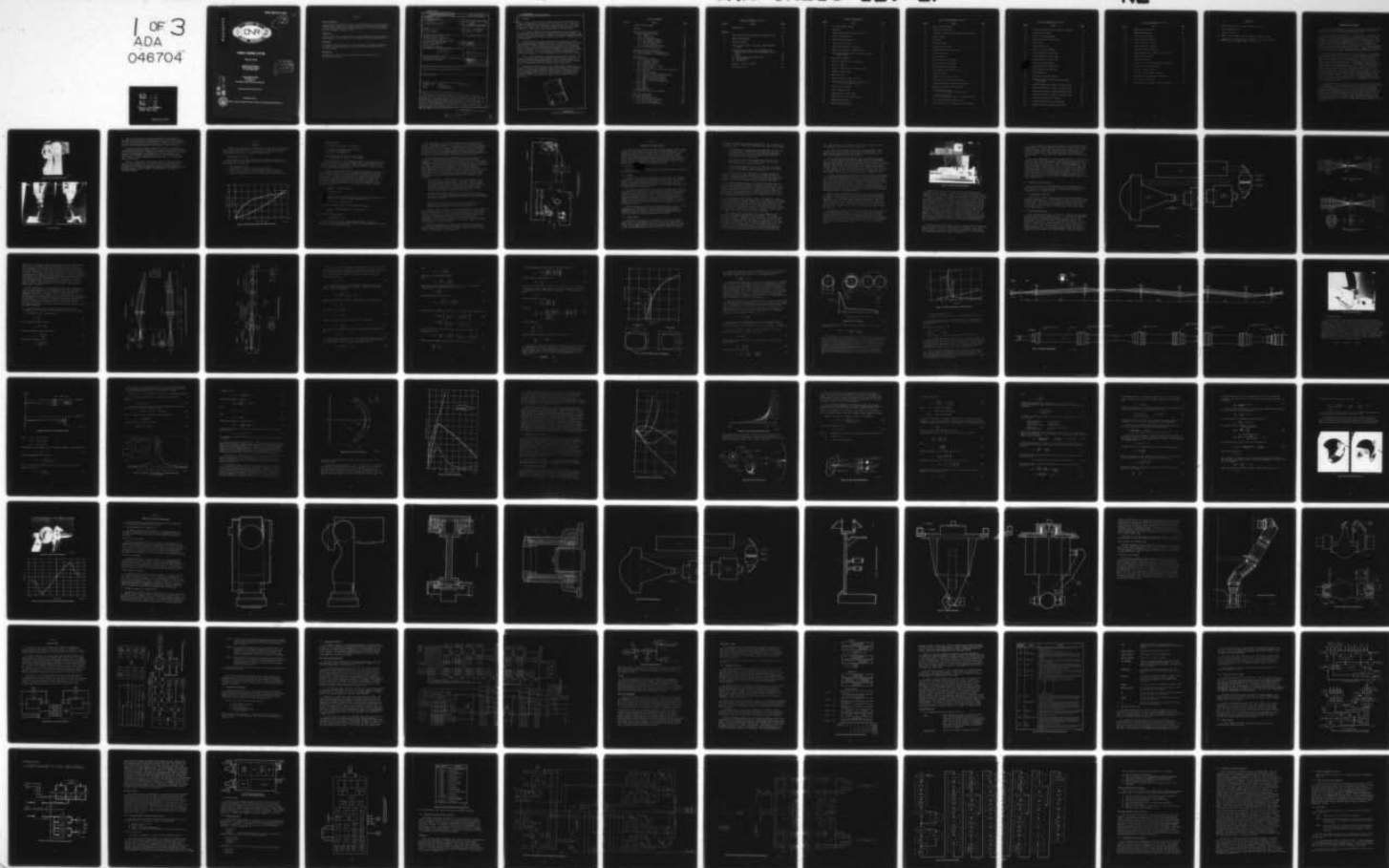
F/G 17/2

UNCLASSIFIED

ONR-CR213-129-2F

N00014-75-C-0660
NL

1 OF 3
ADA
046704



AD A 0 4 6 7 0 4

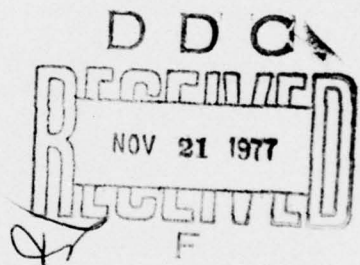


12

REMOTE VIEWING SYSTEM

RALPH W. FISHER

McDonnell Aircraft Company
McDonnell Douglas Corporation
St. Louis, Missouri 63166



Contract N00014-75-C-0660
ONR Task 213-129
June 1977
Final Report for Period 1 July 1975 - 30 May 1977

Approved for public release; distribution unlimited.

AD No. —
DDC FILE COPY



PREPARED FOR THE

OFFICE OF NAVAL RESEARCH • 800 N. QUINCY ST. • ARLINGTON • VA • 22217

NOTICES

Change of Address

Organizations receiving reports on the initial distribution list should confirm correct address. This list is located at the end of the report. Any change of address or distribution should be conveyed to the Office of Naval Research, Code 221, Arlington, Virginia 22217.

Disposition

When this report is no longer needed, it may be transmitted to other authorized organizations. Do not return it to the originator or the monitoring office.

Disclaimer

The findings in this report are not to be construed as an official Department of Defense or Military Department position unless so designated by other official documents.

Reproduction

Reproduction in whole or in part is permitted for any purpose of the United States Government.

UNCLASSIFIED

SECURITY CLASSIFICATION OF THIS PAGE (When Data Entered)

19 REPORT DOCUMENTATION PAGE		READ INSTRUCTIONS BEFORE COMPLETING FORM	
1. REPORT NUMBER (18) ONR-CR-213-129-2F	2. GOVT ACCESSION NO.	3. RECIPIENT'S CATALOG NUMBER	
4. TITLE (and Subtitle) REMOTE VIEWING SYSTEM.		5. TYPE OF REPORT & PERIOD COVERED Final Report. 1 Jul 75 - 30 May 77.	
7. AUTHOR(s) (10) Ralph W. Fisher		8. CONTRACT OR GRANT NUMBER(s) (15) N00014-75-C-0660	
9. PERFORMING ORGANIZATION NAME AND ADDRESS McDonnell Aircraft Company McDonnell Douglas Corporation P.O. Box 516, St. Louis, Mo. 63166		10. PROGRAM ELEMENT, PROJECT, TASK AREA & WORK UNIT NUMBERS	
11. CONTROLLING OFFICE NAME AND ADDRESS Office of Naval Research 800 N. Quincy St. Arlington, VA 22217		12. REPORT DATE (11) June 1977	
14. MONITORING AGENCY NAME & ADDRESS (if different from Controlling Office) (12) 207p.		13. NUMBER OF PAGES 196	
		15. SECURITY CLASS. (of this report) UNCLASSIFIED	
16. DISTRIBUTION STATEMENT (of this Report) Reproduction in whole or part is permitted for any purpose of the United States Government.		15a. DECLASSIFICATION/DOWNGRADING SCHEDULE	
17. DISTRIBUTION STATEMENT (of the abstract entered in Block 20, if different from Report) "Approved for public release distribution unlimited"			
18. SUPPLEMENTARY NOTES			
19. KEY WORDS (Continue on reverse side if necessary and identify by block number) Variable Acuity Displays Optical Detection Optics Remote Sensing Vision Television Systems			
20. ABSTRACT (Continue on reverse side if necessary and identify by block number) A fully operable laboratory model of the Remote Viewing System was designed and built. The system consists of a TV camera and TV projector both equipped with a non-linear lens, i.e. a lens that matches the human eye acuity function with excellent resolution capability near the optical axis, but greatly reduced resolution capability in the peripheral areas. The camera and projector are slaved together by a digital servo system. An operator can steer the camera and thus the projector by use of a helmet mounted tracker. → next page			

DD FORM 1 JAN 73 1473 EDITION OF 1 NOV 65 IS OBSOLETE

UNCLASSIFIED

SECURITY CLASSIFICATION OF THIS PAGE (When Data Entered)

403 111 ✓

LB

UNCLASSIFIED

SECURITY CLASSIFICATION OF THIS PAGE(When Data Entered)

20. ABSTRACT.

cont. → As the operator rotates his head to observe off axis display detail, the camera is commanded to rotate and the projector follows. Thus, high acuity detail is retained on the foveal axis of the observer's eyes. This system allows wide field-of-view (160°) remote viewing of scenes, with resolution comparable to human vision, using conventional TV system bandwidths.

The gimballed camera and projector mechanical and optical designs are presented along with the method of relaying the optics thru the gimbals. The digital servo system is described along with the associated computer programs. The head tracking system includes sections on the tracker, illuminator, optics and electronics.

Considering that the system is the first of this type, the results were very encouraging. Equipment developed to perform conventional functions worked perfectly including the servo control, TV camera, TV projector, and Head Tracker. The most challenging problem encountered in the development were associated with the state-of-the-art advancement required in non-linear optics. Problems were also encountered in maintaining optical quality in the camera and display. The maximum resolution attained is approximately 1.5 milliradians compared to the 0.5 milliradians that is theoretically possible.

Even with this limitation, system performance was very impressive. The value of the wide field in maintaining observer orientation within the full 160° field-of-regard was readily apparent. Target tracking capability by head control was very good and peripheral cueing by motion and glints proved to be of significant value in the acquisition and tracking task.

Detailed performance analyses of the current design indicate better acuity is possible by fabricating new rear spline elements for the non-linear lenses and redesigning the projector optical relay. Through these efforts, 1 milliradian performance should be readily obtained. Performance better than this appears to be limited by a diffraction problem inherent in the projector Schlierin optics and would require use of a different type of projector.

ACCESSION for

NTIS ☒ Section ☒
DDC ☐ B. Section ☐
UNCLASSIFIED
J. S. K. 1977

EXCLUDED FROM AVAILABILITY CODES
or SPECIAL

A

UNCLASSIFIED

SECURITY CLASSIFICATION OF THIS PAGE(When Data Entered)

TABLE OF CONTENTS

<u>Section</u>	<u>Title</u>	<u>Page</u>
1	INTRODUCTION AND SUMMARY	1
2	APPROACH	4
3	ELECTRO-OPTICAL SYSTEM DESIGN	8
3.1	Camera Subsystem Design	8
3.1.1	Camera	8
3.1.2	Optical Relay	8
3.2	Projector Sub-System Design	12
3.2.1	The Projector Selection	12
3.2.2	Optical Relay Design	12
3.2.3	Focus Correction	26
3.2.4	Projection Surface Design	32
3.3	Head Tracking System Design	32
4	MECHANICAL DESIGN AND FABRICATION	42
4.1	Camera Assembly (P/N 71A050002-1001)	42
4.2	Projector Assembly (P/N 71A050003-1001)	42
5	CONTROL SYSTEM	52
5.1	Microprocessor Hardware	54
5.1.1	Diagnostic Hardware	55
5.1.2	Diagnostic Software	58
5.2	Camera Electronics Box	62
5.2.1	System Clocks and Timing	63
5.2.2	Control Logic	63
5.2.3	Camera Box Electro Mechanical Description	66
5.3	System Software	67
5.3.1	PROM Programming	67
5.3.2	PROM #1, Interrupt Handler Software	69
5.3.3	Transmitter Service Routine	73
5.3.4	PROM #2 Yaw Control Equations	74
5.3.5	PROM #3 Diagnostic Software	75
5.3.6	PROM #4 Pitch Control Equations	75
5.4	Math Models	75
5.4.1	Mode 1	76
5.4.2	Mode 2	79
5.4.3	Mode 3	84
5.5	System Operation	84
5.6	Head Tracker Interface Electronics	91
6	RESULTS AND CONCLUSIONS	94
6.1	Camera Performance	98
6.2	Total System Performance	98
6.2.1	Low Contrast Performance	103
6.2.2	Demonstration Results	107
6.3	Conclusions and Recommendations	107

TABLE OF CONTENTS (Continued)

<u>Section</u>	<u>Title</u>	<u>Page</u>
7	REFERENCE LIST	109
<u>Appendix</u>		110
A	BRIEF DESCRIPTION OF THE REMOTE VIEWING SYSTEM (RVS)	110
B	CAMERA CONSIDERATIONS	113
C	PROJECTOR STUDIES	116
D	PROM 1, PROM 2, PROM 3, AND PROM 4 COMPUTER PROGRAM LISTINGS	129
E	APPLICATION OF THE NIGHT VISION LABORATORY (NVL) THERMAL VIEWING SYSTEM STATIC PERFORMANCE MODEL TO THE RVS	176
	E.1 MTF's	176
	E.2 Noise Equivalent Modulation (NEM)	181
	E.3 MRM Calculations	183
	E.4 Conclusions	184
	APPENDIX - LIST OF REFERENCES	186
	DISTRIBUTION LIST	187

LIST OF ILLUSTRATIONS

<u>Figure</u>	<u>Title</u>	<u>Page</u>
1	Two Axis Gimbaled Cameras	2
2	Projector	2
3	Remote Viewing System Optical Requirements	4
4	Control System Elements	7
5	Camera and Relay Brassboard	11
6	Camera Optical Elements	13
7	Light Valve Operation - No Output	14
8	Light Valve Operation - Maximum Output	14
9	Light Valve Nonlinear Lens Interface for Single Element Relay	16
10	Basic Relay Parameters	17
11	Effect of Magnification on Brightness	21
12	MTF of an Annulus	23
13	Effect of Magnification on System Acuity	24
14	Projector Optical Relay	25
15	Relay Test Setup	26
16	Projection Lens Conjugate Geometry	27
17	Image Plane Position Relative to Infinity Focus for 54 In. Conjugate Distance	28
18	Focus Corrector Geometry	30
19	Corrector Angular Blur	31
20	Display Error vs Actual Angle	33
21	Nodal Point Shift of Nonlinear Lens	34
22	Head Position Sensing	34
23	Head Tracking Radiometrics	35

LIST OF ILLUSTRATIONS (Continued)

<u>Figure</u>	<u>Title</u>	<u>Page</u>
24	Helmet Mounted Detector	40
25	Projector Mounted Source	41
26	Response of Infrared Head Tracking Detector System	41
27	Camera Assembly	43
28	Pitch Axis	44
29	Yaw Axis Assembly	45
30	Camera Optical Elements	46
31	Camera Optical Mounting Surfaces	47
32	Projector Assembly	48
33	Relay Assembly	50
34	Projector Pitch Axis Assembly	51
35	Servo Control Block Diagram	52
36	Block Diagram Control System	53
37	Wiring Diagram SBC-80 Front Panel	56
38	Interrupt Channel	57
39	Computer Input and Output Ports	59
40	Display Processor Keyboard Explanation	61
41	Universal Asynchronous Receiver/Transmitter	64
42	Camera Electronics Box Block Diagram	65
43	Camera Electronics Box (a) Top View Camera Electronics Box)	67
43	Camera Electronics Box (b) SBC-80/Remote Camera Data Transfer Board	68
44	Camera Electronics Box Component List	69
45	Camera Electronic Box Transmitter Circuit Diagram	70

LIST OF ILLUSTRATIONS (Continued)

<u>Figure</u>	<u>Title</u>	<u>Page</u>
46	Camera Electronics Box Receiver Circuit Diagram	71
47	Software Flow Diagram	72
48	Mode 1 Servo Block Diagram	76
49	System Response for Stick Input	77
50	Servo Gains	78
51	Camera Azimuth Axis	79
52	Mode 2 Servo Block Diagram	80
53	System Response for Stick Input	81
54	System Response for Stick Input	82
55	System Response for Stick Input	83
56	Pitch Servo Block Diagram	85
57	System Response for Ramp Input	86
58	System Response for Step Input	87
59	System Math Model	88
60	Head Control Detector Amplifier	93
61	Geometry to Convert Shaft Encoders Readings to True Angles	95
62	Threshold Resolution vs Angle from Optical Axis	99
63	Threshold Resolution vs Angle from Optical Axis	100
64	Threshold Resolution vs Angle from Optical Axis	101
65	Threshold Resolution vs Angle from Optical Axis	102
66	Horizontal Display Error vs Angle	104
67	Vertical Display Error vs Actual Angle	105
68	Minimum Resolvable Modulation Predictions	106

LIST OF ILLUSTRATIONS (Continued)

<u>Figure</u>	<u>Title</u>	<u>Page</u>
A-1	Human Eye Characteristics	111
A-2	Bandwidth Requirements	111
A-3	Electro-Optical Schematic	112
A-4	Camera/Projector Interface	112
C-1	General Projection Geometry	117
C-2	Display Brightness Geometry	118
C-3	Normalized Display Brightness	121
C-4	Optimum Geometry for Specular Screen Coatings	122
C-5	Optimum Screen Coating	124
C-6	Light Valve Geometry	128
D-1	Prom No. 1 Service Interrupt Handler Software	130
D-2	Prom No. 2 Yaw Control Software	138
D-3	Prom No. 3 Monitor Program	151
D-4	Prom No. 4 Pitch Control Software	160
E-1	Scan Distortion Introduced by Foveal Lens	177
E-2	Optical Relay Parameters	179
E-3	NVL Model Adapted to VARVS for Visual Spectrum	185

APPENDICES

- A Brief Description of the Remote Viewing System (RVS)
- B Camera Considerations
- C Projector Studies
- D PROM 1, PROM 2, PROM 3 and PROM 4 Computer Program Listings
- E Application of the Night Vision Laboratory (NVL) Thermal Viewing System Static Performance Model to the RVS

Section 1

INTRODUCTION AND SUMMARY

This final report documents the results of Contract No. N00014-75-C-0660. The objective of this contract was to design and build a fully operable laboratory brassboard of the MCAIR Remote Viewing System.

Under a previous ONR Contract (Ref. 1), MCAIR proved the feasibility of a unique non-linear lens which made this effort possible. This lens takes advantage of the "variable acuity" characteristics of human vision to reduce the amount of information (or bandwidth) that must be transmitted in a wide field-of-view high resolution imaging system. A brief description of the remote viewing system concept which utilizes this lens is presented in Appendix A. The brassboard system constructed under this contract represents a significant advancement in the state-of-the-art of remote viewing because for the first time a variable acuity picture that is designed to be compatible with human vision was recorded, transmitted, and displayed in real time.

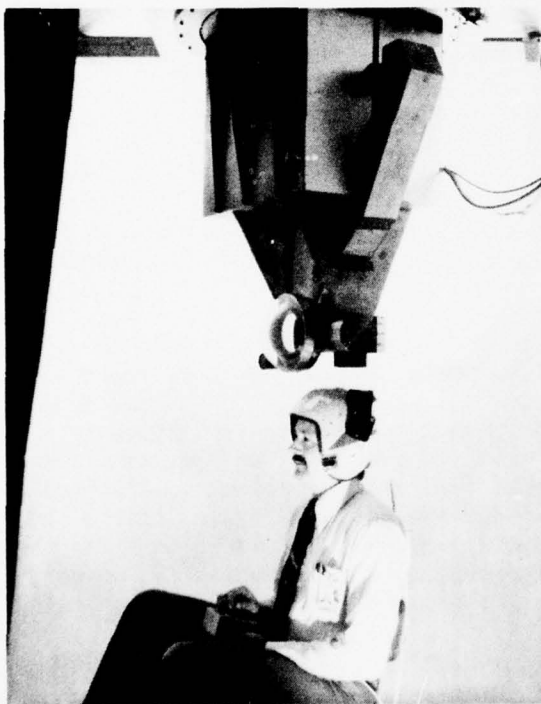
The ONR Brassboard Remote viewing system consists of a two axis gimbaled TV camera as shown in Figure 1 and a two axis gimbaled TV projector as shown in Figure 2(a) and (b). A serial transmission link and low loss TV cable allow the camera to be located up to 400 ft. from the projector. The operator of the system can steer the camera under servo control using a helmet mounted tracker shown in Figure 2, approximately 90 degrees right and left and can look up and down $\pm 45^\circ$. A microprocessor implements two axis servo control of the camera and projector servos. The system can track angular rates up to 1 rad/sec. It is capable of looking at the sun with no catastrophic failure. The projector subsystem consists of a 9 ft. dia sphere, a TV projector, and mounting support frame. It requires a floor area of 15 ft. by 15 ft. The lower portion of the sphere is cut away, thus an 8 foot ceiling is adequate. Interconnecting cables between the microprocessor and the operator allow the operator to position himself at the center of the sphere. He is required to be at the spherical center directly below the projector to realize the best optical performance of the system and for optimum head control.

Considering that the system is the first of this type, the results were very encouraging. As should be expected the only serious problems encountered in the development were associated with the state-of-the-art advancement required in non-linear optics. All conventional functions or equipment worked perfectly including the servo control, TV camera, TV projector, Head Tracker, etc. Problems were encountered in maintaining optical quality in the non-linear image when transmitted through the optical relays, both in the camera and display. While most of these problems were overcome, the resulting resolution was still about 3 times lower than anticipated, about 1.5 milliradians compared to the 0.5 milliradians that should be theoretically possible.

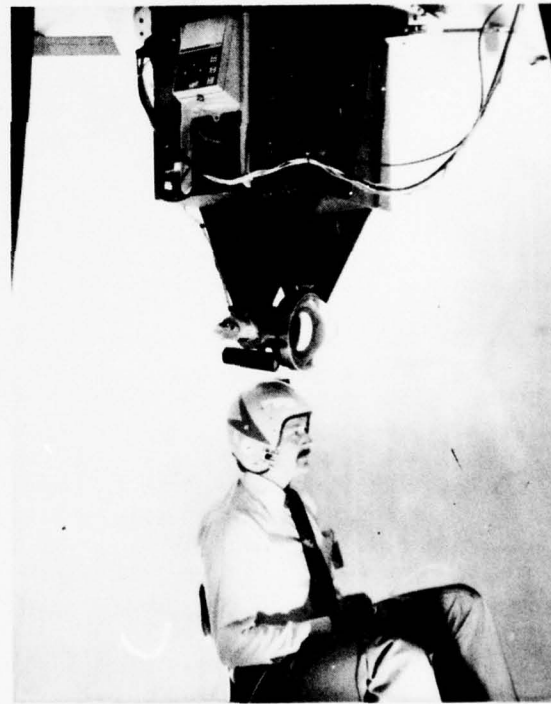


GP77-0549-71

Figure 1 Two Axis Gimbaled Camera



(a) Left Side Showing Detector Mounted on Helmet



(b) Right Side Showing Source on Projector Assembly

Figure 2 Projector

GP77-0549-70

Even with this limitation, system performance was very impressive. The value of the wide field in maintaining observer orientation within the full 180° field-of-regard was readily apparent. Target tracking capability with head control was very good and peripheral cueing by motion and glints proved to be of significant value in the acquisition and tracking task.

Detailed performance analyses indicate better acuity is possible by fabricating new rear spline elements for the non-linear lenses and redesigning the projector optical relay. Through these efforts, 1 milliradian performance should be easily obtained. Performance better than this appears to be limited by a diffraction problem inherent in the light valve's Schlieren optical output. Further improvement would require use of a different type light valve projector.

Finally it appears that the laboratory demonstration which involved viewing a scene in which most of the spatial detail is stationary does not show the true potential of the system for the highly dynamic airborne application. It is therefore highly recommended that the brassboard hardware be flight tested in order to obtain a true performance assessment in a dynamic environment.

Section 2

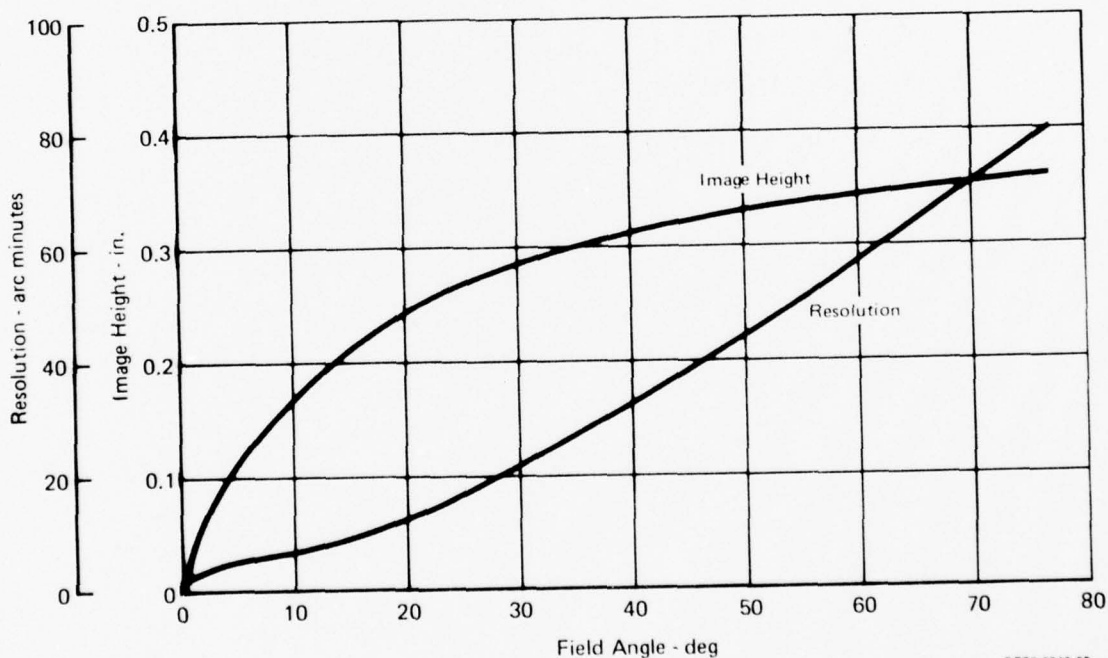
APPROACH

The basic design philosophy is discussed and the rationale for the approach used is presented in this section. In subsequent sections detailed design of the equipment is developed. As a starting point for these discussions the original design goals from our proposal are listed below.

Electro-Optical Subsystem

The design goal of the video subsystems is to generate a projected display that fully supports human vision in both field-of-view and resolution. More specifically the goals are:

- o 160° hemispherical FOV
- o Image transfer characteristics as shown in Figure 3
- o Resolution as a function of viewing angle as shown in Figure 3
- o Display brightness greater than 1 ft-lambert over the entire FOV
- o Standard TV bandwidth video transmission between camera and projector



GP77-0549-55

Figure 3 Remote Viewing System Optical Requirements

Control Subsystem

Camera platform with motion capabilities of:

- o Coverage - 360° azimuth, + 60° elevation
- o Acceleration - 3000°/second²
- o Slew rate - 300°/second

Projector platform with the same specifications

Servo static position accuracy - 30 arc minutes

The starting point for the design was presented in the proposal for this study (References 2 and 3). As this design evolved, considerable change was dictated by practical considerations. Salient differences occurred in the gimbaling philosophy and electronic servo control system. The basic design and these changes are summarized below.

The camera electro-optical design followed the proposal very closely. A silicon vidicon camera was used for solar damage protection (See Appendix B). This necessitated use of an optical relay with a mechanical iris for light level control. A significant change from the proposal was the decision to utilize a 1023 line raster TV system which was selected to obtain greater resolution. The basic non-linear lens has an on-axis focal length of 2 inches and an image plane height of 0.72 inches (for maximum FOV of 160°). In a 525 line raster system (488 effective lines), the angular separation between scan lines is:

$$\frac{.72}{488 \times 2} = 0.738 \text{ milliradians}$$

2.5 minutes of arc

Angular resolution results when this separation is multiplied by the Kell factor which is 1.4. Thus the angular resolution is:

$$2.5 \times 1.4 = 3.5 \text{ minutes of arc}$$

By utilizing a 1023 line system, the scan line separation is:

$$\frac{.72}{937 \times 2} = .384 \text{ milliradians} = 1.32 \text{ minutes of arc.}$$

The angular resolution then is:

$$1.85 \text{ minutes of arc}$$

This value is much closer to the desired performance. It will be shown later, however, that only a small fraction of this improvement was actually achieved for various technical reasons.

The camera gimbal approach changed somewhat from that outlined in the proposal. The azimuth gimbal axis was not at the lens nodal point but was offset as illustrated in Figure 4. The primary reason for this was simplicity of fabrication and the wide azimuth coverage available with this arrangement. The use of gimbal position encoders shown on Figure 4 reflects our decision to employ digital electronics wherever possible. This approach eliminated the need for rate and acceleration sensors on the camera platform because these functions can be derived digitally from the position encoder outputs.

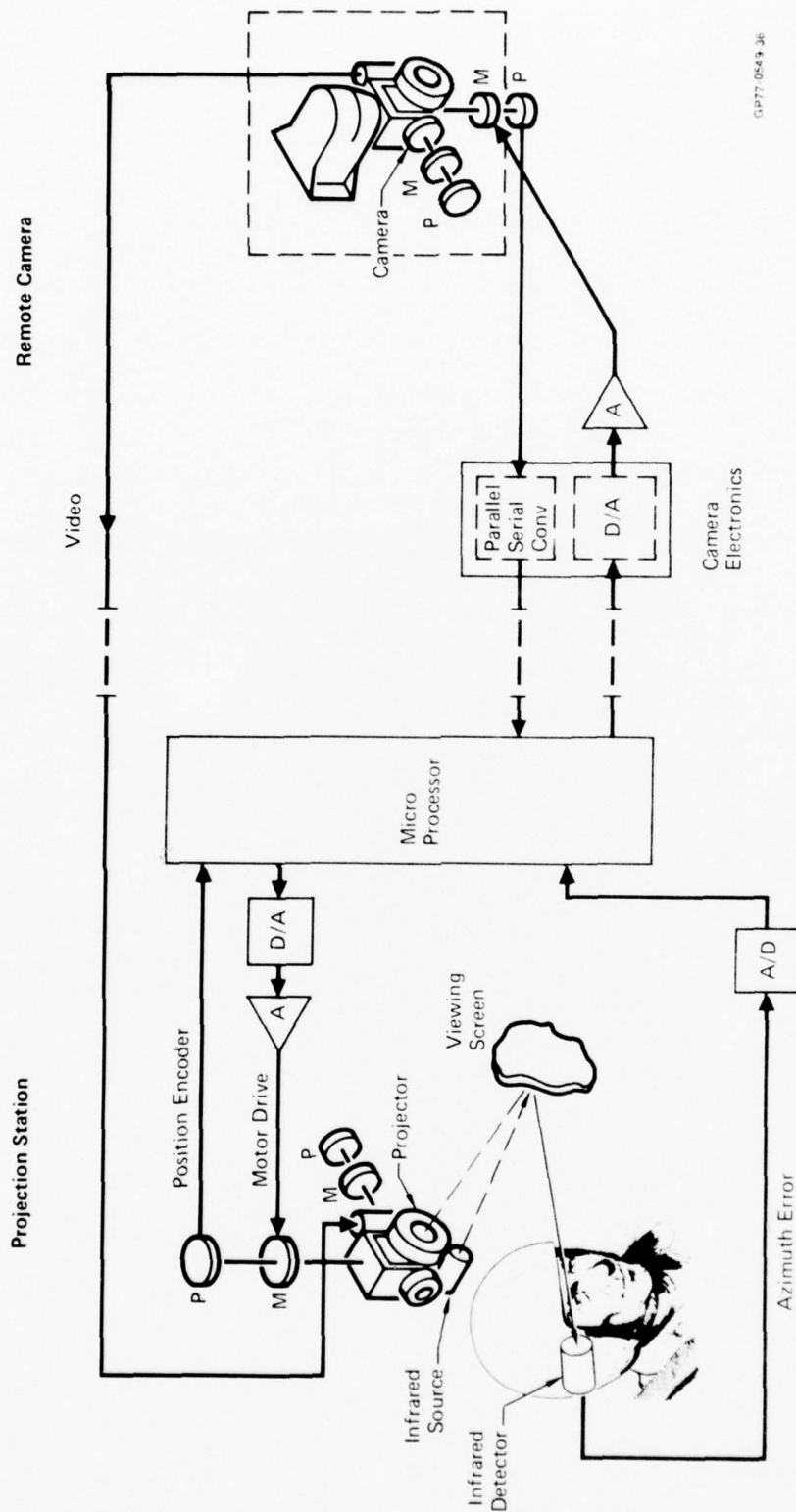
The projector design deviated substantially from that outlined in the proposal, the difference being primarily in the mechanical gimbaling arrangement. After consultation with General Electric Co. (G.E.) on mechanical constraints of the light valve projector, we decided to gimbal the projector in azimuth. This simplified the optical relay because it required articulation in one dimension only, the pitch direction. This could be handled by a simple half-angle mirror and eliminated the need for image derotation. Besides making the relay much simpler and easy to align, this approach assured a much higher level of light output, a critical concern with this system (See Appendix C). The resulting projector gimbaling arrangement is shown in Figure 4. Other minor problems that impacted on the projector system design were:

- o Focus correction is required because of the close proximity of the projection screen to the projector. This arises because the lens has a flat focal plane when focused at infinity. When the plane is shifted to obtain correct on-axis focus, the variable focal length makes this location incorrect for all other field angle points. An additional lens element was required to correct this problem. Design of this element is discussed in Section 3.2.3.
- o Incompatibility between the projector Schlieren optics and the non-linear lens. This rather complex problem is described in Section 3.2 and caused inefficient optical relay performance for projection angles near the optical axis.

This problem required refabrication of the rear element of the projection lens and relay design revision to obtain greater magnification between projector and non-linear lens.

A digital control system was selected primarily because of its flexibility. Since a control system for a variable acuity optical link of this type had never been constructed, we felt a great number of changes in control system dynamics and modes would be required before successful operation would be achieved. A digital system with microprocessor control met these requirements. In addition, this approach will make future additions of more sophisticated control modes possible e.g., eye control. Figure 4 shows the basic elements of this control system.

Head position sensing was as outlined in the proposal except that the source and detector locations were interchanged. The IR source had to be mounted on the projector instead of the helmet so that it would be additive with the infrared output from the projector.



GP77-0544-36

Figure 4 Control System Elements
Azimuth Axis Shown Only

Section 3

ELECTRO-OPTICAL SYSTEM DESIGN

The electro-optical design is divided into three separate efforts, those relating to the camera, the projector, and the head tracking system. For the camera, this effort includes TV camera selection and optical relay design to mate the camera with the non-linear lens. For the projector, this effort covers TV projector selection, relay design, and focus corrector design. The head tracking system design uses an infrared source boresighted with the projector and a detector assembly mounted on the helmet and is a part of the control system which is described in Section 5. Each of these items is discussed in detail in the following sections.

3.1 CAMERA SUBSYSTEM

The camera subsystem design consisted of the camera subsystem integration and optical relay design.

3.1.1 Camera

The camera electro-optical configuration followed that of the proposal very closely. The original TV camera purchased as the sensor was a GE model 4TE33A1. This camera was selected because it utilized a silicon vidicon which is necessary for solar burn protection. It was compact and self contained and was believed to be compatible with the GE light valve projector which was selected for the display.

During early evaluation of the camera/projector combination, a vertical jitter was noted on the display. This problem was traced to the random scan interlace of the GE camera. The projector however, requires a precise 2/1 interlace to maintain a stable picture. This problem was corrected by using an external sync generator. Later in the systems integration effort, numerous intermittent electrical connections were encountered in the TV camera. This, plus poor optical performance of the automatic iris assembly caused us to conclude that the GE camera would not be suitable for the demonstration system.

Therefore, another camera was selected and we elected to choose one with a higher line rate capability to obtain greater resolution. After a thorough search of available TV cameras, a General Electrodynamics Co. Model 6073B camera was selected. This system had the desired 1023 line rate and a stable 2/1 interlace required by the projector.

3.1.2 Optical Relay

The function of the optical relay system is to relay a good quality image from the non-linear lens to the TV camera vidicon with no loss of field-of-view or any noticeable vignetting. It must also magnify the image to the size compatible with the vidicon requirements and provide exposure control for the camera system. Exposure control is obtained by using an

electronic controlled iris on one of the relay lens. For convenience and to reduce cost, this element was purchased with the camera. Relay design requirements are:

- o Its input must be the non-linear lens image which is 0.72 inches in diameter and is located about 0.070 inches from the last (aft) lens element. An F/5.6 ray bundle must be accommodated and imaging is nearly telecentric where all chief rays are nearly parallel to the optical axis.
- o Its output must be to vidicon faceplate which has an active scanning area of 0.5 X 0.375 inches. Later this was found to be a circular area 0.7 inches in diameter.
- o One relay element must be a 50 mm F/1.4 lens with an installed automatic iris assembly. This iris must be properly integrated to form an aperture stop without vignetting.

Using these optical relay requirements, the design progressed as follows. The relay optics were designed to use lenses that could be purchased off-the-shelf rather than custom designed and fabricated special lenses. The lenses were chosen with sufficient aperture and format to transmit the F/5.6 cone of light forming the non-linear lens image.

Use of the available automatic iris/lens assembly dictated that the relay use lenses operating at infinity conjugates. A pair of lenses are therefore required to relay an image. The first lens collimates the image and the second forms an image from the collimated bundle of light. The lens speed required is the same as the speed of the cone of light to be relayed. The image-to-image distance is approximately the sum of the two focal lengths. Magnification of the relayed image is equal to the ratio of the focal lengths of the two lenses.

If the purchased camera with the automatic iris assembly is used as the second relay lens, the focal length of the first relay can be calculated if the final image size is known. Selection of a final image size, requires a tradeoff of resolution and field-of-view. The problem is that a 4 X 3 aspect raster is used to scan the circular image from the non-linear lens. The aspect ratio of the TV raster must be 4 X 3 because the projector system uses a light valve television projector with a fixed 4 X 3 raster format. The image should cover as much of the raster as possible.

If the raster height is made equal to the image diameter, no FOV is lost but it does waste a large part of the TV format. If the image is larger, the angular resolution would be improved but the top and bottom of the FOV is cutoff. A compromise solution is to let the raster height cover 90% of the image diameter. The part of the image that is lost lies in an area of low interest. The non-linear lens image which is 0.72 inches in diameter should be demagnified to be 0.417 inches in diameter for a standard 1/2 by 3/8 inch television raster. An 86 mm focal length lens when paired with the 55 mm Vicon lens will give the desired image size. An 85 mm F/2.0 Olympus lens was selected for the first relay lens which

has an aperture that is large enough to collect all the light from the non-linear lens without the need for a field lens.

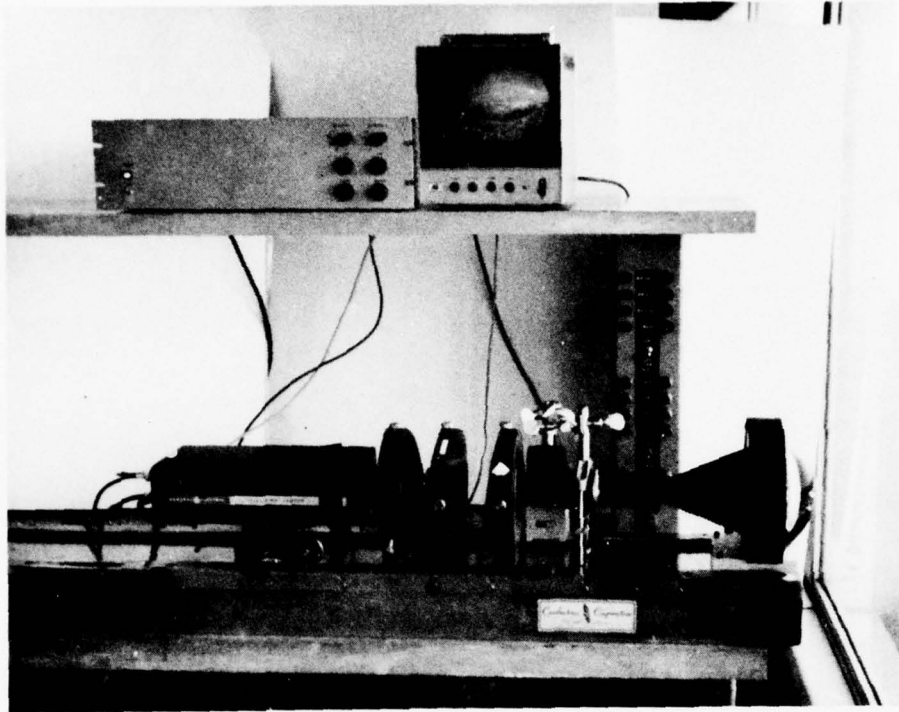
The second relay lens has an auto-iris to provide exposure control. However, this is the case only if the iris is the aperture stop. The aperture stop is defined to be the stop that effectively restricts the cone of rays passing through the lens system.

The following analysis shows how the auto-iris becomes the aperture stop. The first element restricting the light bundle is the non-linear lens which has a speed of $F/5.6$. The non-linear lens is telecentric in the image plane which means the non-linear lens' exit pupil is located at infinity. Therefore, the next lens, the 85 mm Olympus, will reimage the non-linear lens exit pupil in it's back focal plane. The 85 mm lens is fast enough so that it doesn't restrict the $F/5.6$ light bundle. Therefore, if the 50 mm lens is positioned so that it's entrance pupil is coincident with the back focal plane of the 85 mm lens, the auto-iris will be the aperture stop.

The relay system described above fulfills all of the optical requirements but is mechanically awkward when coupled to the camera and non-linear lens. It is about three feet long and the two heavy elements are located on the ends. It can't be folded into a more compact package without severe vignetting unless a second relay is added. Therefore, an additional pair of relay lenses are used to fold the optical system 180° so that the vidicon is located directly above the first relay. The back focal distances of the second pair of relay lenses are large enough to accommodate folding mirrors. Each mirror folds the system 90° . Two 80 mm $F/2.8$ Xenotars are used for the second relay giving it unity magnification.

Adding a second relay makes it necessary to use a field lens to keep the auto-iris as the aperture stop and to keep vignetting from becoming noticeable. The field lens is a double convex lens located in the second image plane. With the image actually being formed inside the lens, the field lens doesn't affect the image and dust particles on the field lens surface are not in focus. The focal length of the lens is chosen to form an image of the exit pupil of the 50 mm relay lens onto the iris of the last relay lens. Using the lens maker's formula the focal length is found to be 52 mm.

The vidicon has typical silicon detector response and is very sensitive to near-infrared energy. However, the non-linear lens and relay optics are not optimized for this spectral band and the image suffers if the infrared is not filtered out. Various narrow band and low pass filters were tried and the one that worked best was a Schott KG-3 infrared absorbing glass. It is placed in the collimated region of the relay. A brassboard of this system was constructed and evaluated. This setup is shown in Figure 5.



GP77-0549-67

Figure 5 Camera and Relay Brassboard

After initial testing of the camera and projector systems, some modifications were necessary. First the camera vidicon was rotated 90° to compensate for the 90° image rotation which occurs in the projector system. This gave more vertical FOV coverage than horizontal FOV coverage due to the 4 X 3 raster. Previously, the image size was chosen so that the part of the image falling outside of the raster was the top and bottom of the FOV. Now the 10% image loss occurs in the horizontal direction where the full FOV is desired. To get full coverage of the horizontal FOV, the circular image from the non-linear lens must fit within the rectangular raster but the system resolution must not suffer. The solution was to magnify the image and increase the raster size so that the image would cover as many of the discrete diodes that makeup the sensitive surface area of the vidicon as possible. The vidicon has a sensitive area about 0.7 inch in diameter. The image which is also circular is made slightly smaller. The raster size is increased to 0.93 X 0.70 inches so that the raster height is about the same as the image diameter. Consequently the image covers more discrete sensitive elements than before and the resolution is improved with no loss of FOV.

The relative size of the image to the 4 X 3 aspect raster is smaller now than it was because the full image lies within the raster. This causes the projected image to be smaller. Consequently, the projector relay optics must be altered to provide increased magnification of the television image. This modification is described later in Section 3.2.

As in the projector, the camera relay optics had to provide increased magnification. The second relay pair which before operated at unity magnification was made to magnify the 0.417 inch diameter image to 0.703 inches. The larger image was obtained by replacing the last 80 mm Xenotar with a 135 mm, F/4.7 Xenar lens. This required only mirror modifications in mounting hardware. The other optics were unchanged with the same field lens used.

The optical components are located as shown in Figure 6. The television image is formed in the following way. Light from the object enters the non-linear lens from the left and is imaged immediately behind the non-linear lens. This image is collimated by a 85 mm F/2.0 Zuiko Olympus lens. The collimated bundle is imaged a second time by a Vicon 50 mm F/1.4 lens that contains the aperture stop for the system. A field lens is located in the second image plane. The first mirror folds the optical axis up 90° where a 80 mm F/2.8 Xenotar lens collimates the second image. A 135 mm F/4.7 Xenar lens picks up the collimated bundle and the final image. The second mirror folds the optical axis 90° to make the image hit the vidicon. An infrared absorbing filter is placed in the collimated bundle between the last pair of relay lenses.

3.2 PROJECTOR SUB-SYSTEM DESIGN

The second effort in the system design was the electro-optical subsystem design of the projector which consisted of projector selection, relay design, focus corrector design, and projection dome design and is detailed in the following sections.

3.2.1 The Projector Selection

Logic for the original selection of the GE light valve projector is presented in Appendix C. It was the lowest cost approach that could produce adequate display brightness. A PJ7000 light valve was originally purchased for the system. This unit had a 525 line raster and an optical output of 700 lumens. Later this unit was updated to a 1023 line raster for reasons stated earlier in Section 2 and 1000 lumen output thereby making it a PJ7150 projector.

3.2.2 Optical Relay Design

After receiving the projector from GE it was coupled to the non-linear lens with a simple single element optical relay. Problems were immediately encountered with the optical energy transfer. The problem was traced to the Schlieren optical technique used in the projector. This is shown schematically in Figure 7, for the no output case and Figure 8 for full output. The light output is proportional to the rate of change of oil film thickness. This rate of change is generated by an electron beam which writes on the oil film. As can be seen in these figures, the result is a centrally obscured bundle of illuminated segments. When this bundle is coupled into the non-linear lens a problem results. This is illustrated

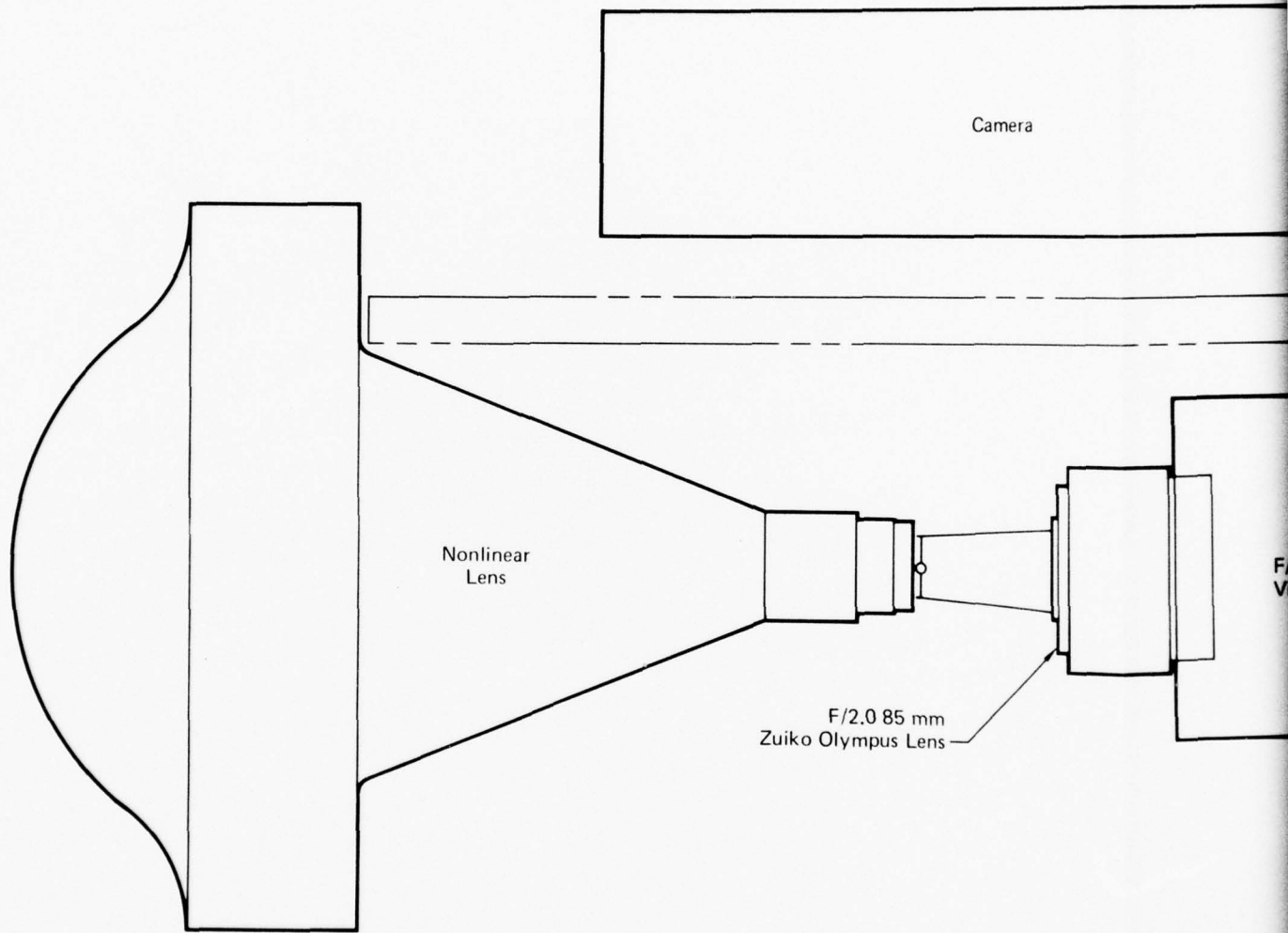
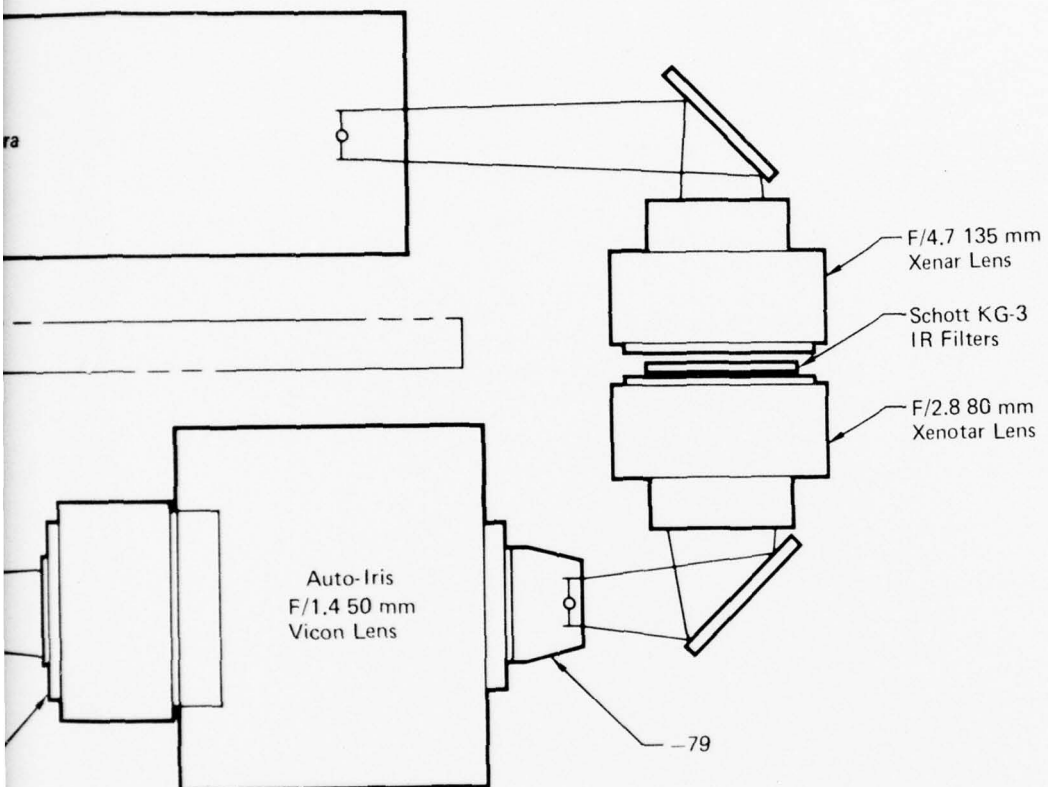


Figure 6 Camera Optical Elements

GP77-0549-51



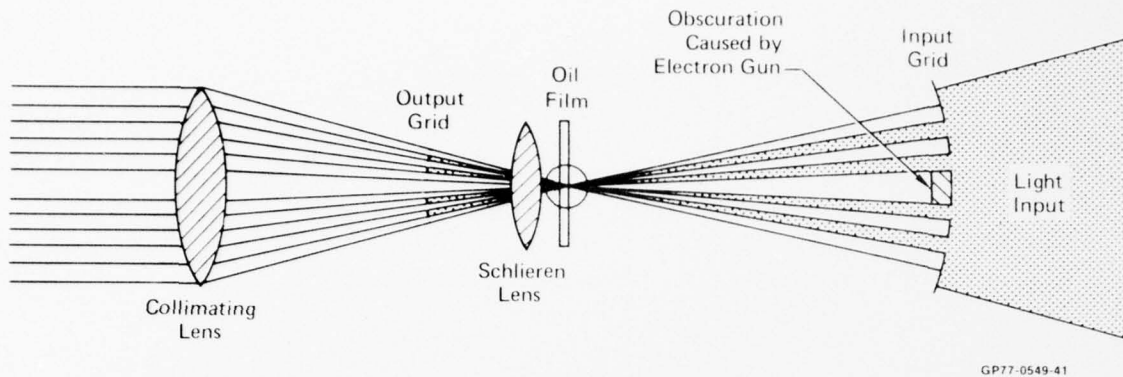


Figure 7 Light Valve Operation
No Output

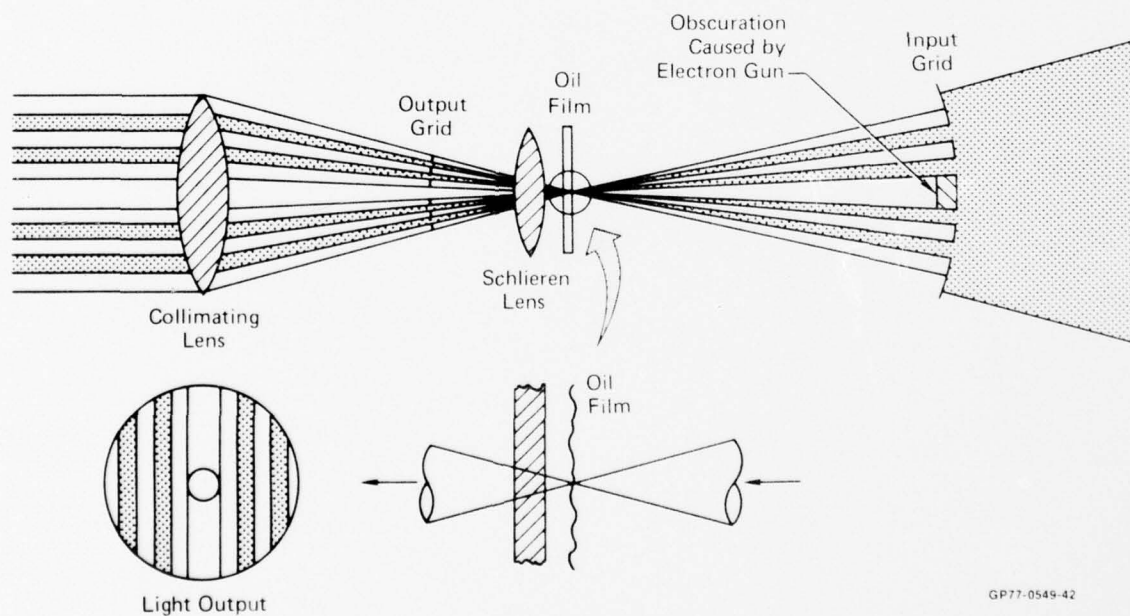


Figure 8 Light Valve Operation
Maximum Output

in Figure 9 for a simplistic one element relay used in our original experiment. In this experiment a dark spot was noted at the center of the projected image. In the on-axis case, the reason for this is that almost all of the energy from the light valve falls outside of the acceptance cone of the non-linear lens as can be seen in Figure 9. This causes two areas of concern. The low light in the central high acuity area of the image can seriously reduce the observer's visual capabilities. In addition, the annular shaped input to the lens provides energy in the worst possible portion of the acceptance ray cone if good image quality is desired. The latter is known from original ray trace data on the lens. In addition, the annular input by itself can cause serious diffraction problems. All of these problems can lead to low display acuity in the central region where the highest acuity is desired.

GE was consulted to see if the projector output could be modified to correct for this situation. After considerable study, they concluded that a major redesign would be required to make the light valve output more compatible with our lens. This left only the relay parameters as a possibility to effect an improvement. From an optical viewpoint, the only relay parameter that can be varied which affects the output ray cone geometry is magnification. This parameter can expand or compress the F/number cone from the projector. In our case, we need to reduce the cone size which requires more magnification within the relay. A derivation will be presented which relates the F/number and magnification to the ratio of source and display brightness.

The entire optical system is shown schematically on Figure 10. The symbols to be used in this derivation are also defined on this figure.

The illumination (E_s) of the source is:

$$E_s = \frac{F}{A_s} \quad (1)$$

Thus the source brightness (B_s) is:

$$B_s \approx \frac{E_s}{\omega_s} = \frac{F}{A_s \omega_s} \quad (2)$$

Now from cone geometry the solid angle is:

$$\omega_s = \frac{\pi}{4 \text{ FNO}_s^2} \quad (3)$$

where $\text{FNO}_s = \text{F/number of source}$

$$B_s = \frac{4 \text{ FNO}_s^2 F}{\pi A_s} \quad (4)$$

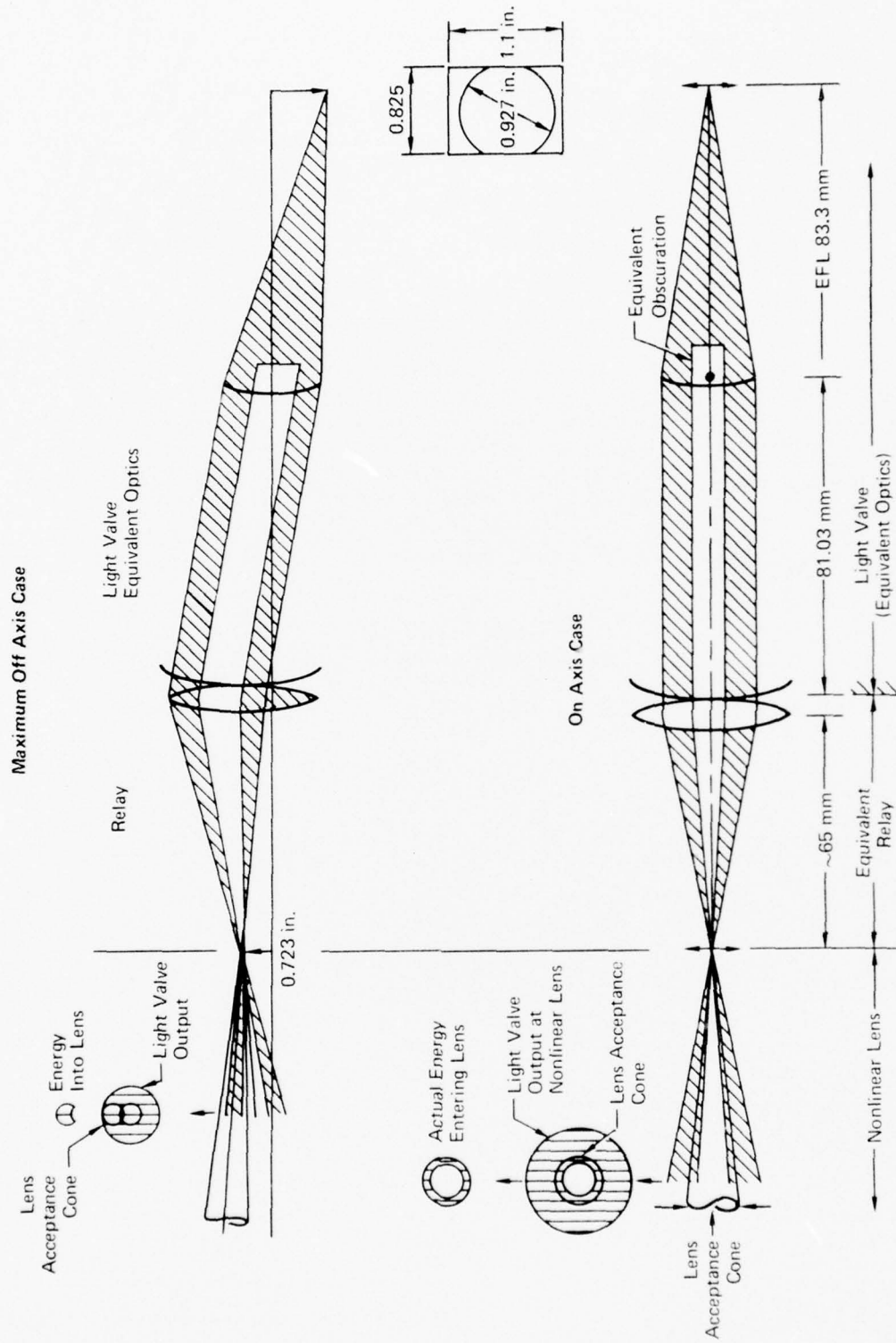
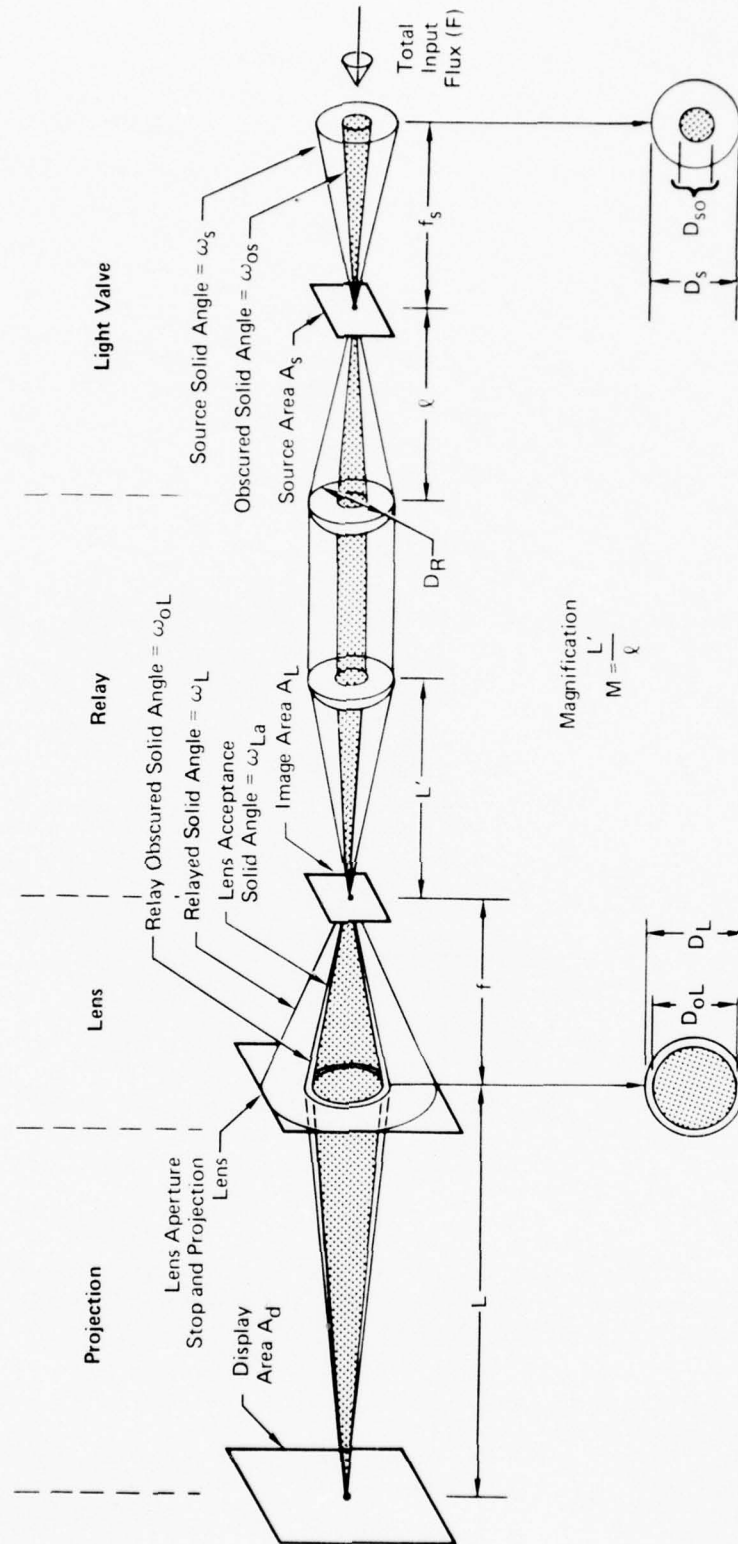


Figure 9 Light Valve Nonlinear Lens Interface for Single Element Relay



GP77-0549-39

Figure 10 Basic Relay Parameters

This (B_s) is also the brightness of the image at the lens. For those who are not familiar with this fact it can be proven as follows: The total flux passing through the source area (A_s) will arrive at the lens area (A_L) assuming good relay design. The area A_L is related to A_s by the magnification (M), viz:

$$A_L = M^2 A_s \quad (5)$$

Since the output of relay is collimated as any good relay is, the output ray diameter equals the input diameter. Therefore, the ratio of output to input solid angle is

$$\frac{\omega_L}{\omega_s} = \frac{\pi D_R^2}{L^2} \frac{L^2}{\pi D_R^2} = \frac{1}{M^2} \quad (6)$$

In addition, the areas A_L and A_s are also related by the magnification viz:

$$M^2 = \frac{A_L}{A_s} \quad (7)$$

The brightness of the image is:

$$B_L = \frac{F}{A_L \omega_L} \quad (8)$$

Substituting Equations (5), (6), and (7) into (8) results in:

$$B_L = \frac{F}{A_s \omega_s} \quad (9)$$

The right side of Equation (9) is equal to the right side of Equation (2), thus:

$$B_L = B_s \quad (10)$$

Now we will determine the effect of the lens obscuration, magnification, and F/number on the screen brightness. The light flux actually entering the projection lens from an incremental image area (dA_L) is:

$$F = B_L dA_L (\omega_{La} - \omega_{LO}) \quad (11)$$

where

$$\omega_{La} = \frac{\pi}{4 \text{FNO}_L^2}$$

where FNO_L = Lens acceptance F/Number

Also:

$$\omega_{Lo} = \frac{\omega_{so}}{M^2} = \frac{\pi D_{so}^2}{M^2 f_s^2} \quad (12)$$

Now if we define an obscuration factor (K) as the ratio of the obscured diameter (D_{so}) to the aperture diameter (D_s), viz:

$$K = \frac{D_{so}}{D_s} \quad (13)$$

Substituting Equation (13) into (12)

$$\omega_{Lo} = \frac{\pi K^2 D_s^2}{M^2 f_s^2} = \frac{\pi K^2}{M^2 \text{FNO}_s^2} \quad (14)$$

where FNO_s is the F/number of the source. Now substituting into Equation (11).

$$F = B_L dA_L \left[\frac{\pi}{4 \text{FNO}_L^2} - \frac{\pi K^2}{4 \text{FNO}_s^2 M^2} \right] \quad (15)$$

$$= \frac{\pi B_L dA_L}{4} \left[\frac{1}{\text{FNO}_L^2} - \frac{K^2}{\text{FNO}_s^2 M^2} \right] \quad (16)$$

All of this flux falls within area dA_d on the projection screen. The illumination is then:

$$E_d = \frac{F}{dA_d} = \frac{\pi B_L dA_L}{4 dA_d} \left[\frac{1}{\text{FNO}_L^2} - \frac{K^2}{\text{FNO}_s^2 M^2} \right] \quad (17)$$

However the focal lengths and differential areas are related by:

$$\frac{dA_L}{dA_d} = \frac{f^2}{L^2} \quad (18)$$

Substituting Equation (18), (3) and (2) into (17) results in:

$$E_d = \frac{F f^2}{L^2 A_s} \left[\left(\frac{FNO_s^2}{FNO_L} \right) - \left(\frac{K^2}{M} \right) \right] \quad (19)$$

Now the display screen brightness is:

$$B_d = \frac{E_d}{\omega_d} \quad (20)$$

where ω_d is the solid angle over which E_d is reflected. For our purpose of studying the effects of magnification, the relative brightness referenced to an unobscured source will simplify the analysis. For an unobscured source:

$$K = 0$$

And then Equation (19) becomes:

$$E_r = \frac{F f^2}{L^2 A_s} \left(\frac{FNO_s^2}{FNO_L} \right) \quad (21)$$

Therefore:

$$\frac{B_d}{B_r} = \frac{E_d}{E_r} = \frac{\left(\frac{FNO_s^2}{FNO_L} \right) - \left(\frac{K^2}{M} \right)}{\left(\frac{FNO_s^2}{FNO_L} \right)} = 1 - \left(\frac{K FNO_L^2}{M FNO_s^2} \right) \quad (22)$$

For our light valve

$$K = 0.36$$

$$FNO_s = 2.8$$

$$FNO_L = 5.6$$

Substituting these values into Equation (22) results in:

$$\frac{B_d}{B_r} = 1 - \frac{.518}{M^2} \quad (23)$$

This curve is plotted in Figure 11(a). This curve clearly illustrates the problem noted in our first experiments. During this exercise we had the full width of the light valve format filling the lens image plane as shown in Figure 11(b). Here the magnification was the ratio of the non-linear lens diameter of 0.72 inch to the camera scanning width of 1.1 inches, viz:

$$M = \frac{0.72 \text{ inch}}{1.1} = 0.65$$

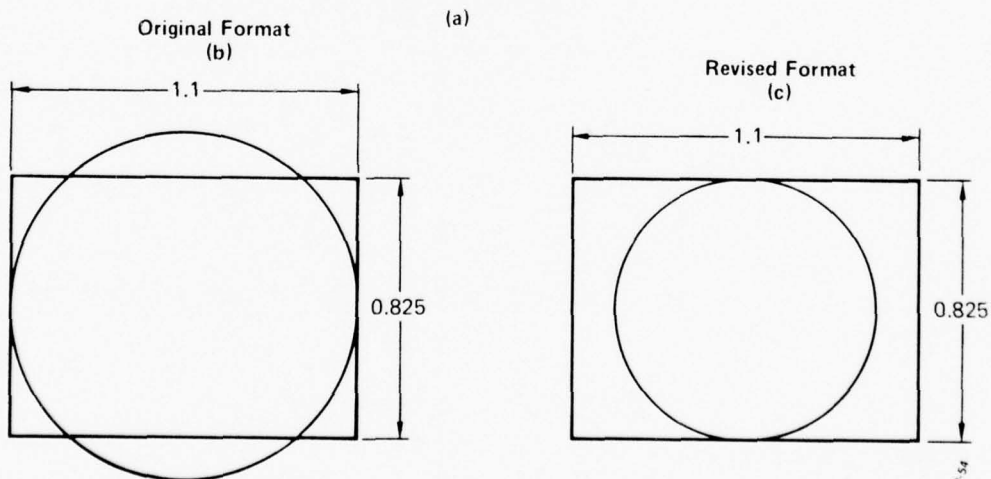
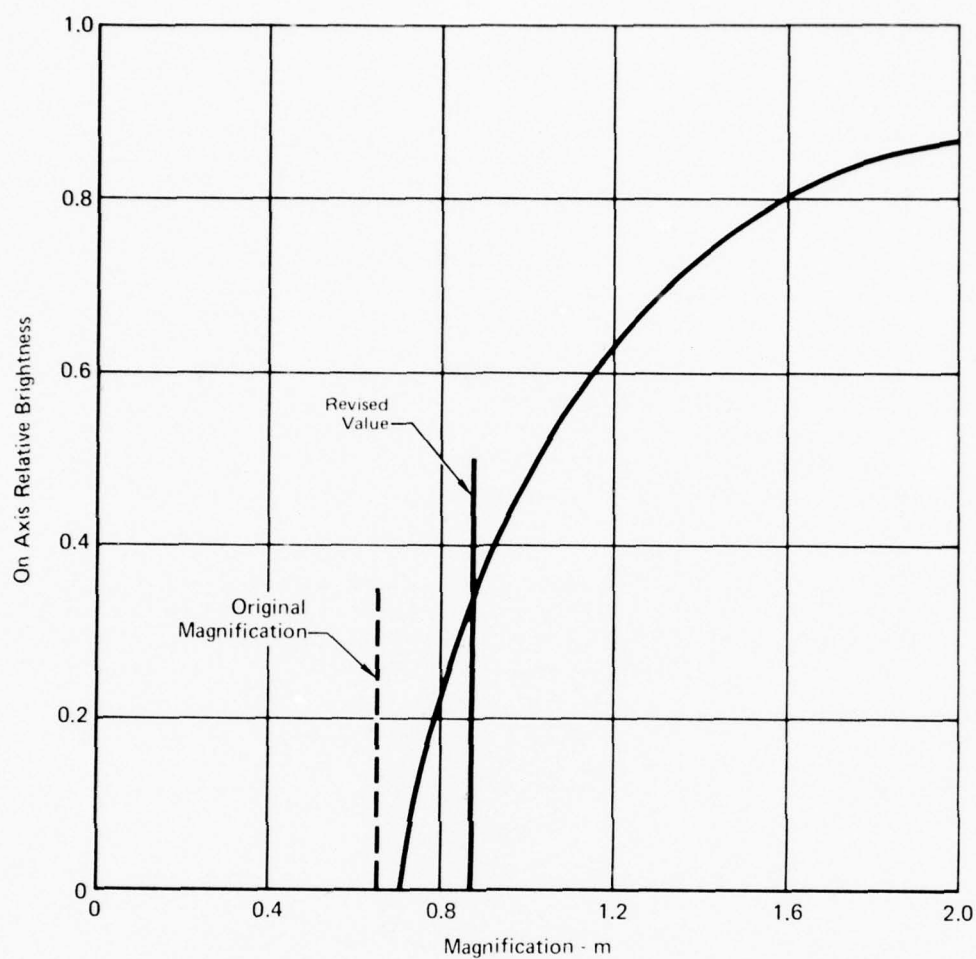


Figure 11 Effect of Magnification on Brightness

GP71-0549-54

Under these conditions no light was entering the lens. The system was made useable by reducing the portion of the source area occupied by the lens image as shown on Figure 11(c). Thus, the magnification is:

$$M = \frac{0.72}{0.825} = 0.87$$

Now the display brightness is 0.3 that of an unobscured or conventional optical system. Since considerably more light is available in the central area of the display (See Appendix C), this is an acceptable situation. In fact it helps to make the display brightness more uniform if the relay is correctly designed. Such a design was shown on Figure 9. Note that for the edge ray bundle that the lens acceptance cone shifts to a more desirable portion of the light valve cone. The result is essentially an increase in output when compared to that of an unobscured system at the field edge. Since the above solution appears to be satisfactory from a brightness standpoint the question of acuity was then considered.

While the exact effect of an annular aperture function is very difficult to predict precisely, an approximation of its affect on resolution is rather easy. Figure 12 shows such an aperture and its associated diffraction MTF. For a thin annulus where the inner (D_{OL}) and outer (D_L) diameters are approximately the same, the MTF shows a pronounced drop in response at a spatial frequency (S_1) proportional to the difference in the diameters divided by twice the light wavelength (2λ), viz:

$$S_1 = \frac{D_L - D_{OL}}{2\lambda} \quad (24)$$

Therefore, a good approximation to the MTF is to assume that the spatial frequency (S_1) is the limiting factor in performance. For this reason this frequency was calculated in terms of the parameters of Figure 12.

At the projection lens output, the lens diameter (D_L) and focal length (f) are related to F/number (FNO_L) by:

$$D_L = \frac{f}{FNO_L} \quad (25)$$

Substituting Equation (13) into (25) and relating FNO_L to FNO_s by the magnification

$$D_{LO} = \frac{K f}{M FNO_s} \quad (26)$$

Substituting into Equation (24)

$$S_1 = \frac{f}{2\lambda} \left[\frac{1}{FNO_L} - \frac{K}{M FNO_s} \right] \quad (27)$$

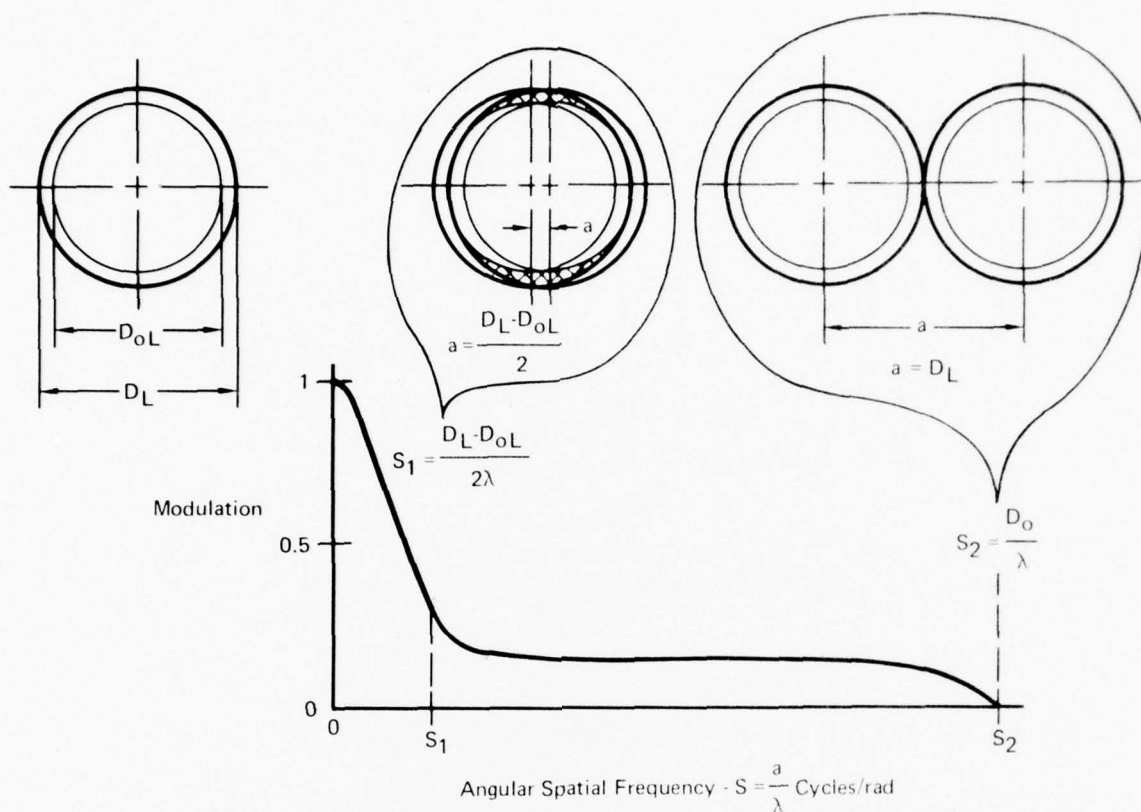


Figure 12 MTF of an Annulus

GP77-0549-43

In more conventional terms the resolution is approximately the width of a half cycle.

$$\alpha = \frac{1}{2S_1} = \frac{\lambda}{f \left(\frac{1}{FNO_L} - \frac{K}{M FNO_S} \right)} \quad (28)$$

This function is plotted in Figure 13 for the light valve output for an obscuration ratio ($K \approx 0.36$) and F/number of 2.8 and variable magnification and the non-linear lens focal length of 2 inches and F/number of 5.6. Note that for the revised raster format, the serious MTF degradation occurs at a resolution of 0.34 milliradians or 1.2 minutes of arc. While it would be desirable to have better performance than this, it is comparable to scan line subtense and no further improvement could be made. Any further increase in relay magnification would result in an increase in scan line subtense, also shown in Figure 13 for a 1023 line raster. Based on the above effort the design requirements for the relay were established, and are:

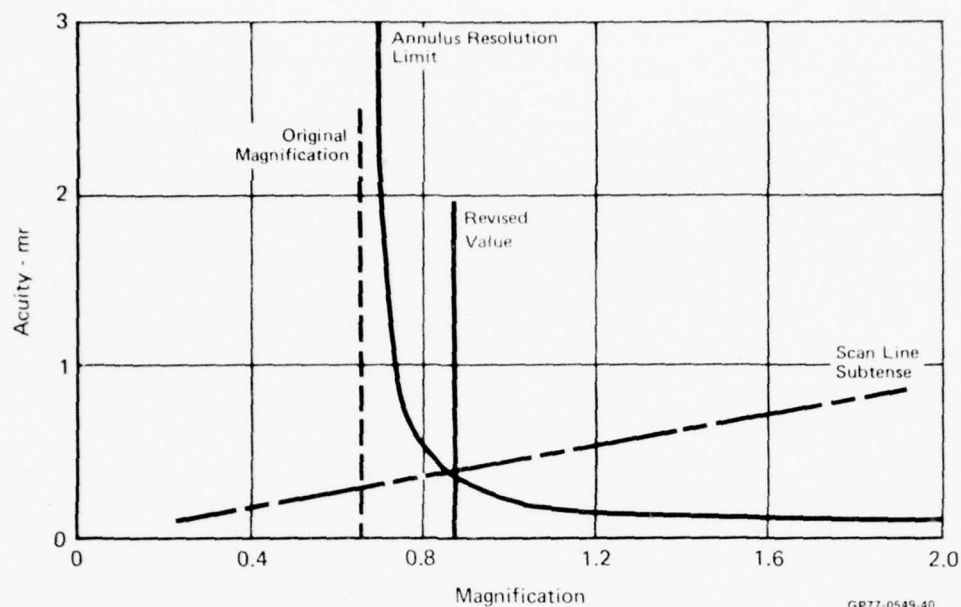


Figure 13 Effect of Magnification on System Acuity

1. A magnification of 0.87
2. Aperture shift geometry with field angle as shown in Figure 9.

The final requirement was to iterate the overall relay mechanical design including overall length, fold point locations, and diameter with the designer.

Basically, these parameters are:

Overall Length = 4 feet

Diameter = 3 inches

Critical Folds = 12 inches required between last two lenses

After considerable design effort the relay of Figure 14 evolved. On this figure an edge ray bundle is drawn to show how the desired aperture shift is achieved. Note no field lenses are utilized. This was necessary to maintain the desired aperture shift. The large size penalty normally associated with a relay design of this type is eliminated by allowing vignetting of the unused part of the light valve optical output.

The lens elements were purchased and the relay set up on an optical bench. After a small decollimation at the projector output to achieve the required magnification, performance was exactly as expected. The relay configuration using available lenses is shown in Figure 14. Figure 15 is a photograph of the relay test set-up.

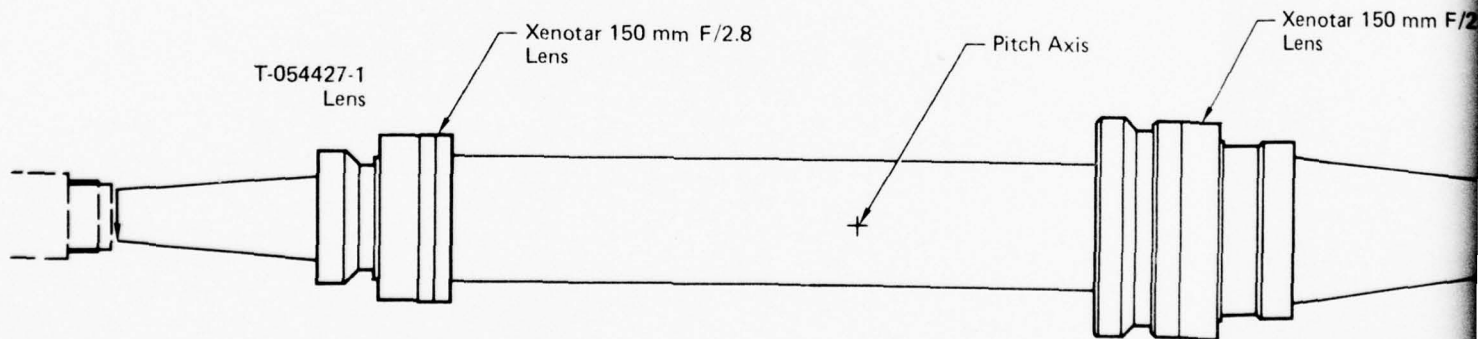
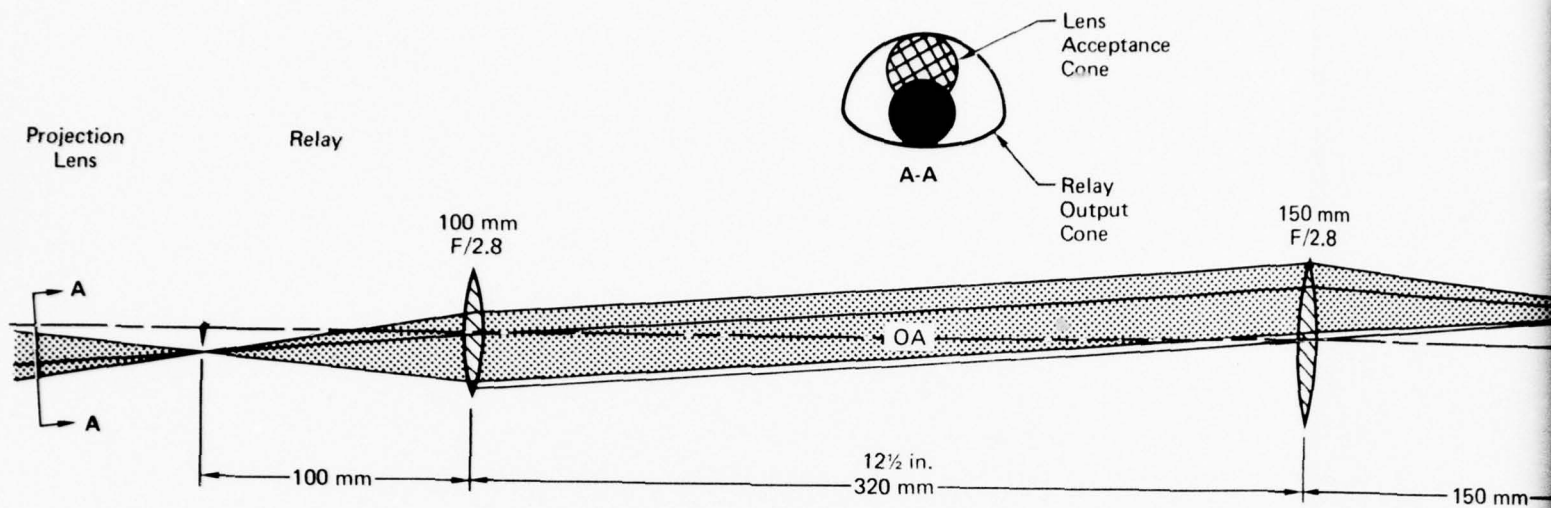
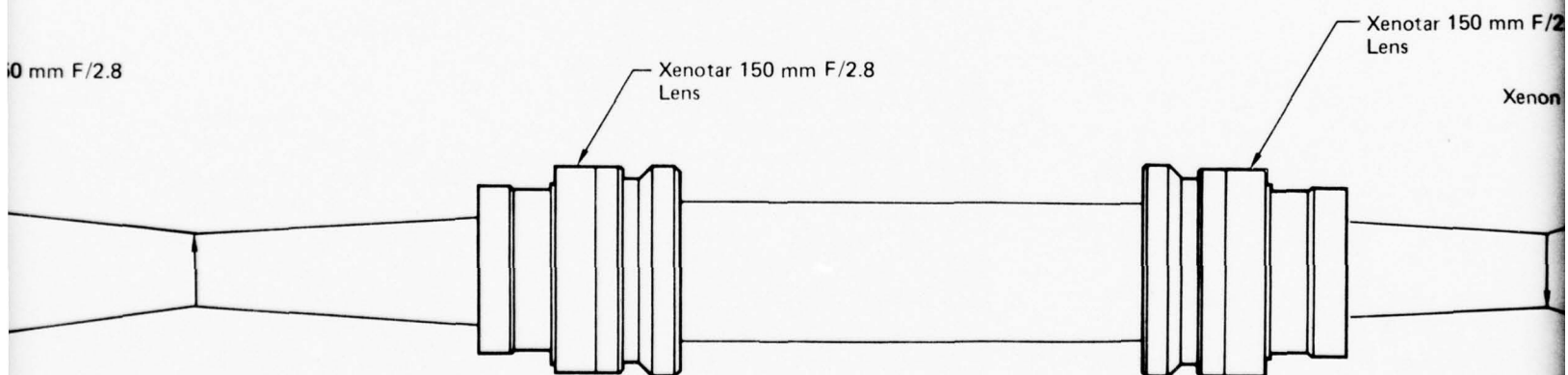
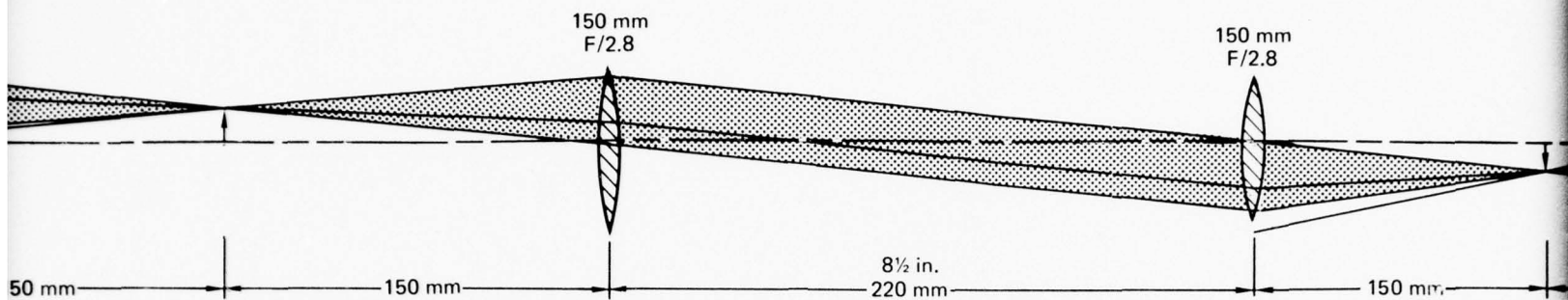
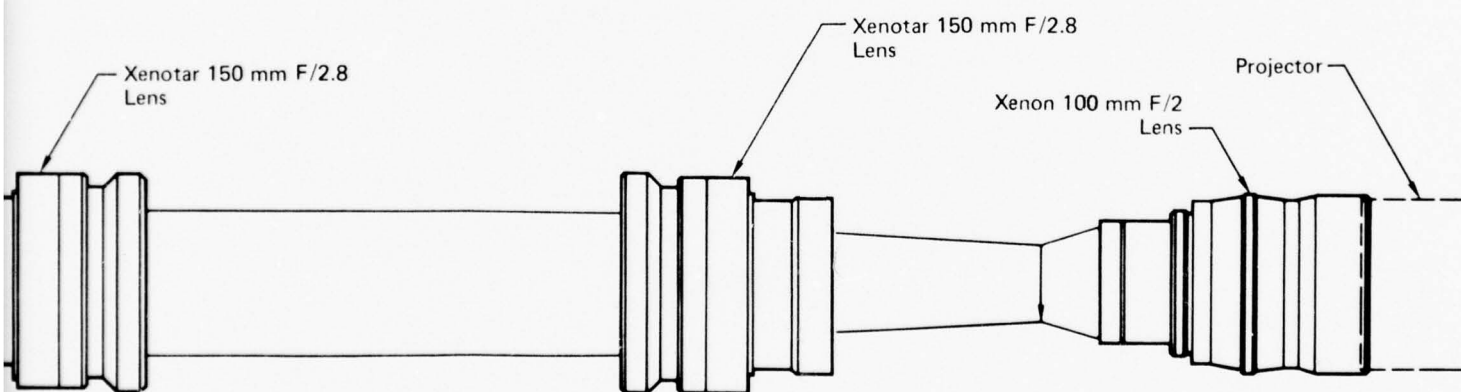
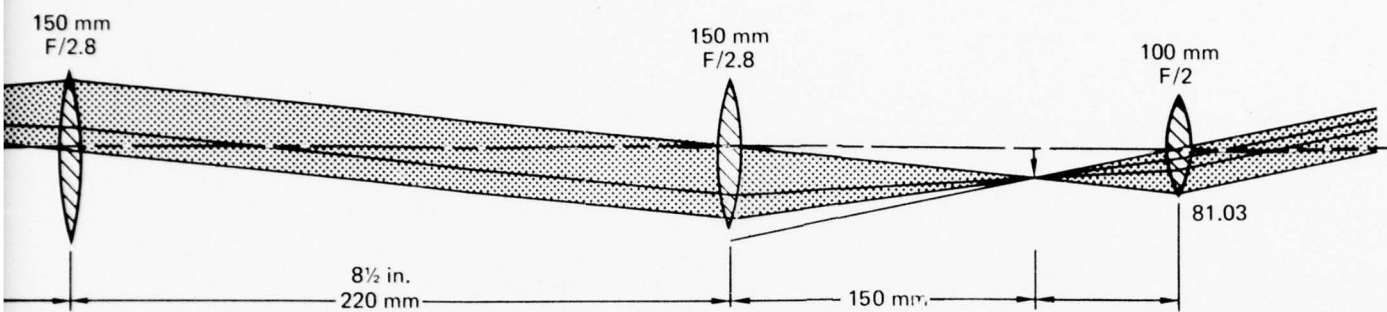


Figure 14 Projector Optical Relay

GP77-0549-53





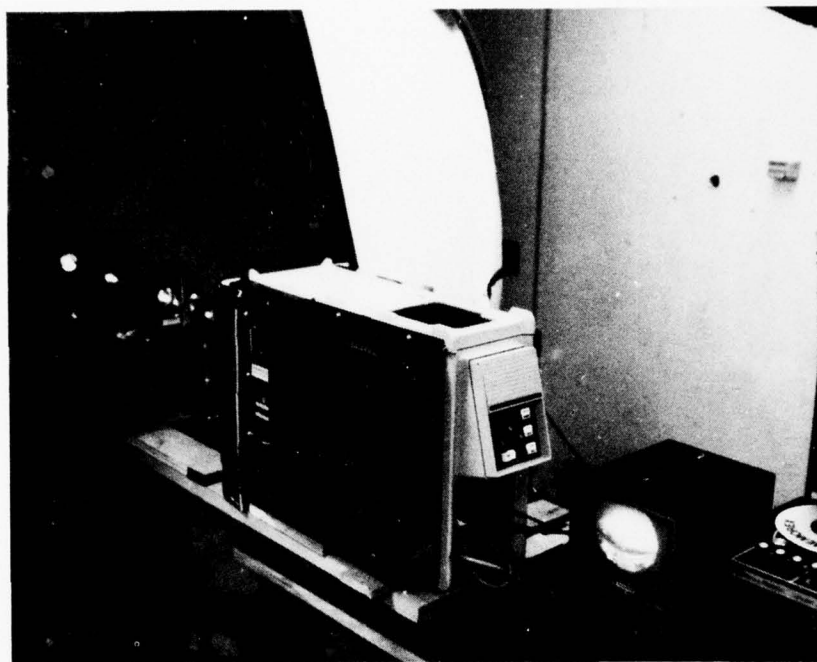


Figure 15 Relay Test Setup

GP77-0549-78

3.2.3 Focus Correction

The variable focal length nature of the projection lens creates a serious focus problem. This problem arises because the projector lens is identical to the camera lens and designed for an object located at infinity. For projection, the lens focal plane must be shifted aft by about 0.08 inch to obtain optimum on-axis focus where the lens focal length is 2 inches. At an 80° object field angle, the focal length is down to 0.04 inches. An 0.08 inch shifted image plane is obviously grossly out-of-focus for this short off-axis focal plane. To determine the magnitude of this problem, the focal plane profile for optimum focus was computed. The general case geometry of Figure 16 was used for this purpose. Here the lens equivalent optical geometry for on-axis and off-axis object angle θ is shown. For either case the general lens equation applies.

$$\frac{1}{s_1(\theta)} + \frac{1}{s_2(\theta)} = \frac{1}{f(\theta)} \quad (29)$$

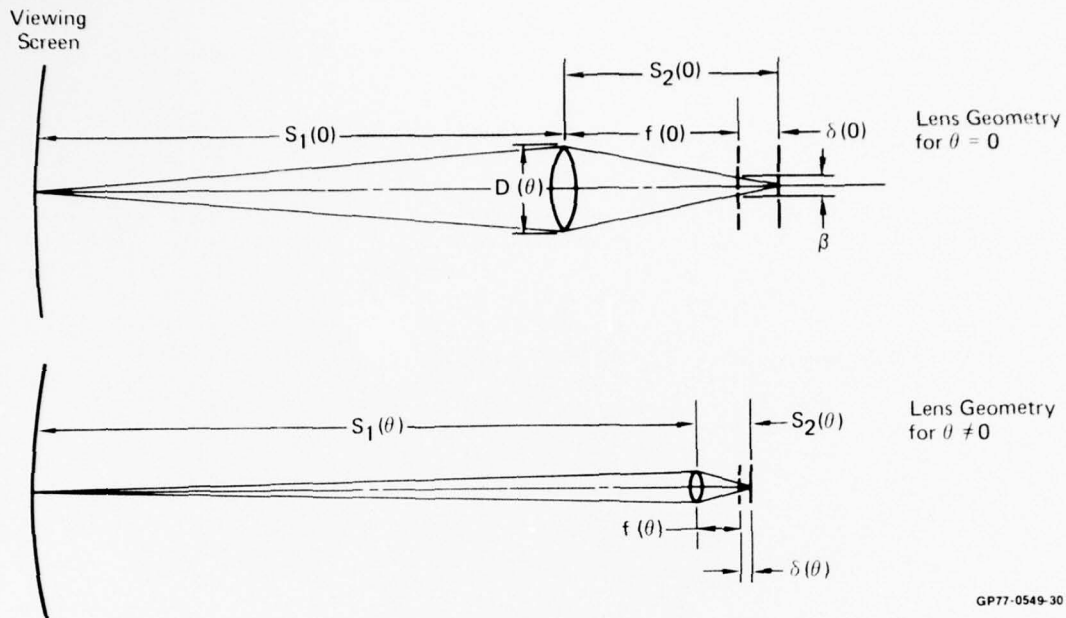


Figure 16 Projection Lens Conjugate Geometry

where $S_1(\theta)$ = Object distance
 $S_2(\theta)$ = Image distance
 $f(\theta)$ = Focal length

From Figure (16) and because $S_1(\theta)$ is relatively constant, the focus error is

$$\delta(\theta) = S_2(\theta) - f(\theta) \quad (30)$$

Substituting Equation (29) into (30)

$$\delta(\theta) = - \frac{f^2(\theta)}{S_1(\theta) - f(\theta)} \quad (31)$$

For a 54 inch object distance, ($S_1(\theta)$), the error in focus for a system focused at infinity is:

$$\delta(\theta) = \frac{f^2(\theta)}{54 - f(\theta)} \quad (32)$$

This equation is plotted in Figure 17. In order to maintain optimum focus, the image plane would have to be the shape of the Figure 17 curve, i.e., 0.08 inch further back in the center relative to its edge.

Now the effect of this defocus will be related to focal plane resolution.

If $\phi(\theta)$ is the required resolution, the allowable focal plane blur ($\beta(\theta)$) is

$$\beta(\theta) = f(\theta) \phi(\theta) \quad (23)$$

Since the focal plane spatial resolution is uniform; that is the off-axis resolution is equal to the on-axis value,

$$\beta = \text{constant} = f(\theta) \phi(\theta) = f(0) \phi(0) \quad (34)$$

If ϕ is in minutes of arc the allowable focal plane blur is

$$\beta = \frac{f(0) \phi(0)}{3440} \quad (35)$$

Relating similar triangles on Figure 16

$$\frac{D(\theta)}{S_2(\theta)} = \frac{\beta}{\delta(\theta)} \quad (36)$$

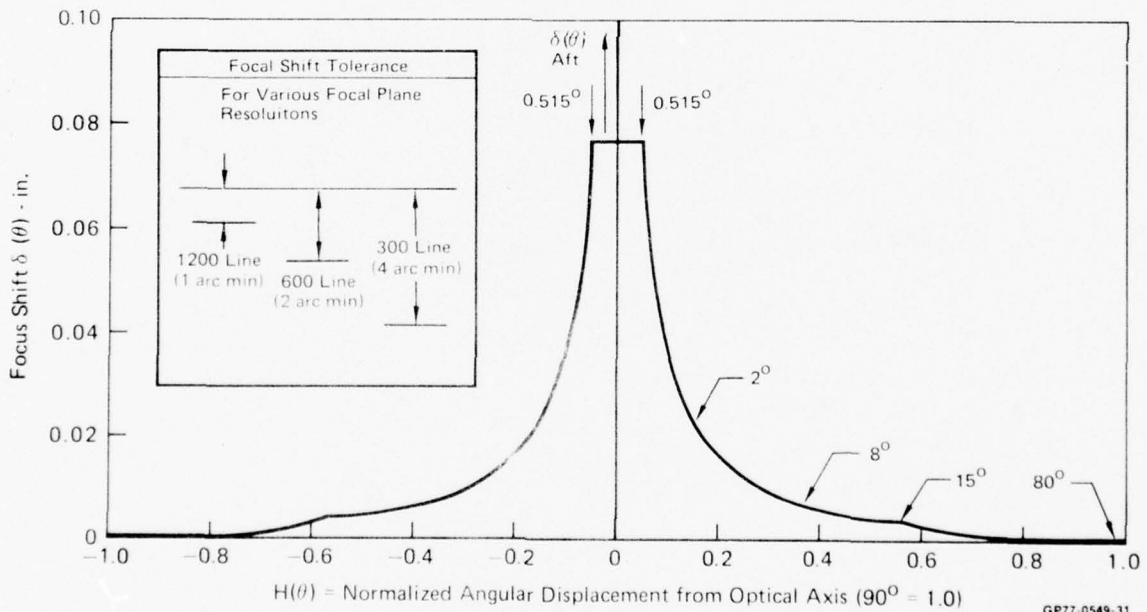


Figure 17 Image Plane Position Relative to Infinity Focus for 54 In. Conjugate Distance

Solving for $\delta(\theta)$

$$\delta(\theta) = \frac{\beta S_2(\theta)}{D(\theta)} \quad (37)$$

Since the F/number is defined as

$$FNO \triangleq \frac{f(\theta)}{D(\theta)} = \text{constant} \quad (38)$$

and

$$S_2(\theta) \approx f(\theta) \quad (39)$$

Then

$$\delta(\theta) = \beta F/No. \quad (40)$$

Substituting Equation (35) and (39) into (40)

$$\delta(\theta) = \frac{\phi(0)}{3400} F/No. f(0) \quad (41)$$

For our lens the $F/No. = 5.6$ and $f(0) = 2$ inch, the allowable focal plane mislocation is

$$\delta(\theta) = 3.294 \times 10^{-3} \phi(0) \quad (42)$$

This equation is plotted on Figure 17 for resolutions ($\phi(0)$) of 1, 2, and 4 arc minutes.

There are two ways of correcting this focus shift problem. The image plane can be tailored to Figure 17 with a corrector element in the lens image plane or the lens can be operated at the infinity focal plane position and a positive optical element placed at the lens output to converge the lens output to a 54 inch conjugate distance. After some experimentation with a focal plane corrector, the latter approach was selected as the only feasible method of focus correction. This is not without its problems however.

The only way of achieving a positive (converging) lens effect outside of the non-linear lens is as shown in Figure 18. It must be a deep double convex element in order to accommodate the entire field-of-view while its thickness must be held down to reduce weight and inertia of the projector pitch axis.

The following technique was used to design this element. Curvature of the surface closest to the lens was selected by fit geometry. Then the second surface radius was computed to converge the on-axis ray bundle at the 54 inch distance. Then the angular blur size as seen from the center of the dome was computed for all other field angles. These results were then compared to the inherent system acuity. The resulting lens curvature are shown on Figure 18 while blur data are shown on Figure 19.

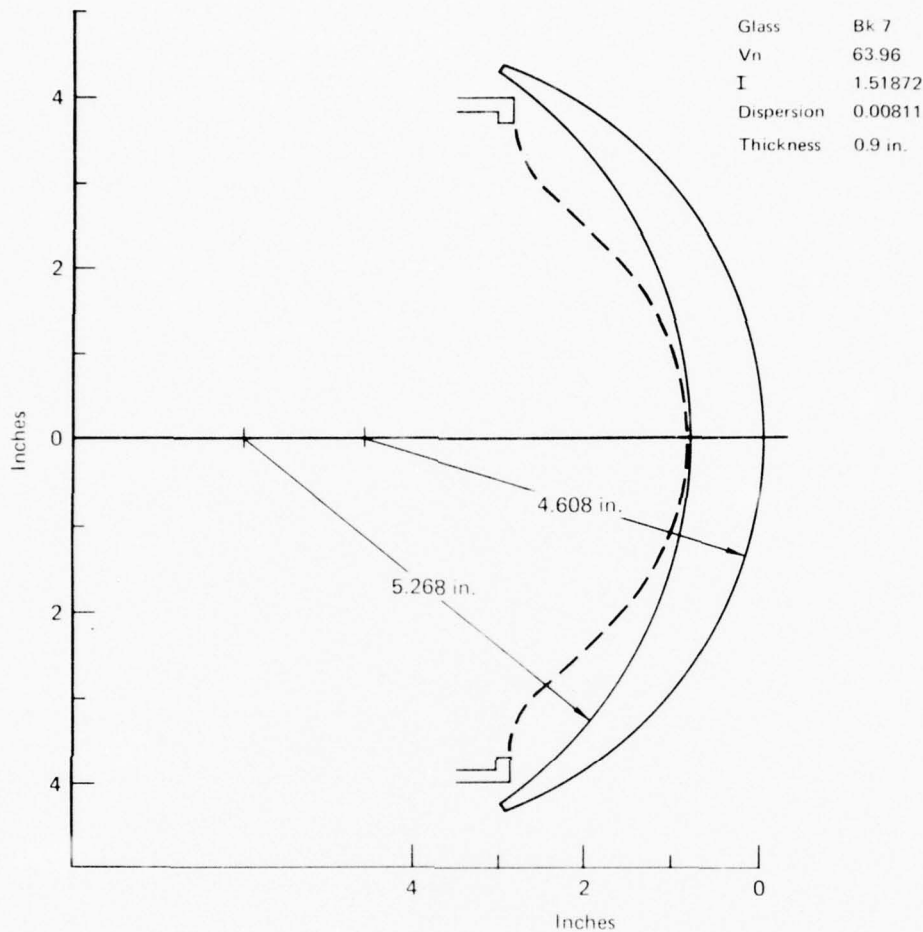


Figure 18 Focus Corrector Geometry

GP77-0549-32

The blur after correction was well within the acuity tolerance for the entire 160° field.

The problem with this method of focus correction is that it generates a distortion to the non-linear lens output. Rays exiting the non-linear lens are bent towards the optical axis by an increment that increases with field angle. This is to say that while blur is acceptable, the centroid of the blur falls on the screen at the wrong location. This can and will cause false motion of points on the display as gimbal angles vary.

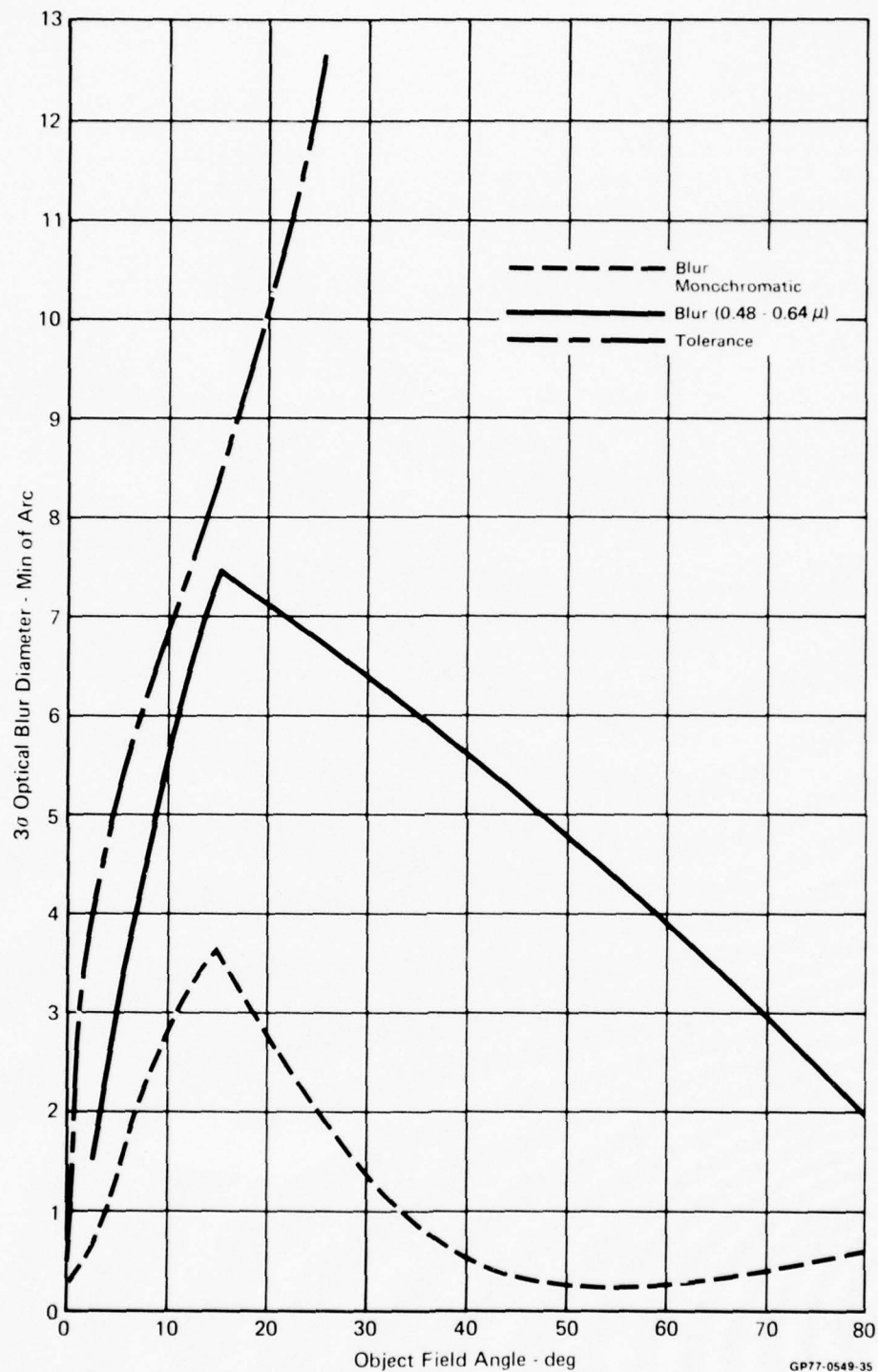


Figure 19 Corrector Angular Blur

To study importance of this effect, rays were traced from the lens to the screen at various field angles without and with the corrector lens. The angular error resulting from both cases as observed from the dome center are shown on Figure 20. With no corrector lens, an error is generated because of the nodal point shift in the non-linear lens. This shift can be seen on the chief ray trace data shown on Figure 21. The gimbal axis of the projection lens intersect very near the 45° nodal point. This make the projection correct only at 0° and 45° .

As the nodal point shifts aft or forward for the angles other than 45° , they fall on the screen at larger or smaller angles (measured from the sphere center) than they should to maintain no distortion. The worst case occurs at 80° where points are advanced by 2° , Figure 20 curve c. If the focus corrector is installed on the lens, points are directed in an opposite direction as shown by the curve e of Figure 20. Here the error increases continuously, reaching about 9° at 80° command angle. This suggests that if the size of the non-linear lens image is increased, this problem must be reduced. This was analyzed and a 2% value was found to produce minimum error over the entire field, curve d. The maximum error is about the same magnitude as it would be with no corrector. The only problem is a slight loss in field-of-view, from 160° to 140° . Since resolution is very low in this region, this is believed to be an acceptable tradeoff for a better acuity close to the optical axis. A corrector of the design shown in Figure 18 was fabricated and installation hardware designed for the projector lens.

3.2.4 Projection Surface Design

It was apparent from early experimental projections on the interior surface of the sphere that a diffuse unity gain white screen surface did not yield enough edge brightness. This was predicted and the calculations are contained in Appendix C. As also described in the appendix, the projection/viewer geometry was optimized for a specular screen coating. The work of Reference (4) indicated that a silver screen material would increase brightness by a factor of four. Based on this, we evaluated several types of aluminum paint on the surface and we found that a screen gain of four was easily achieved. By visual observations, we concluded that sufficient brightness was being obtained out to field angles of 120° . Beyond this, performance was questionable. However, high contrast objects were easily detected out to 140° .

The aluminum paint, however, caused the imperfections in the dome joints to become very noticeable. This required expenditure of considerable effort to refill and sand the joints smooth.

3.3 HEAD TRACKING SYSTEM DESIGN

The function of the head tracker servo control system is to maintain angular alignment of projector's optical axis and the observer's nominal sightline. A head angular position sensor or a relative head/projector angular position sensor will not accomplish this because of the close proximity of the viewing surface. To correctly accomplish this sensing

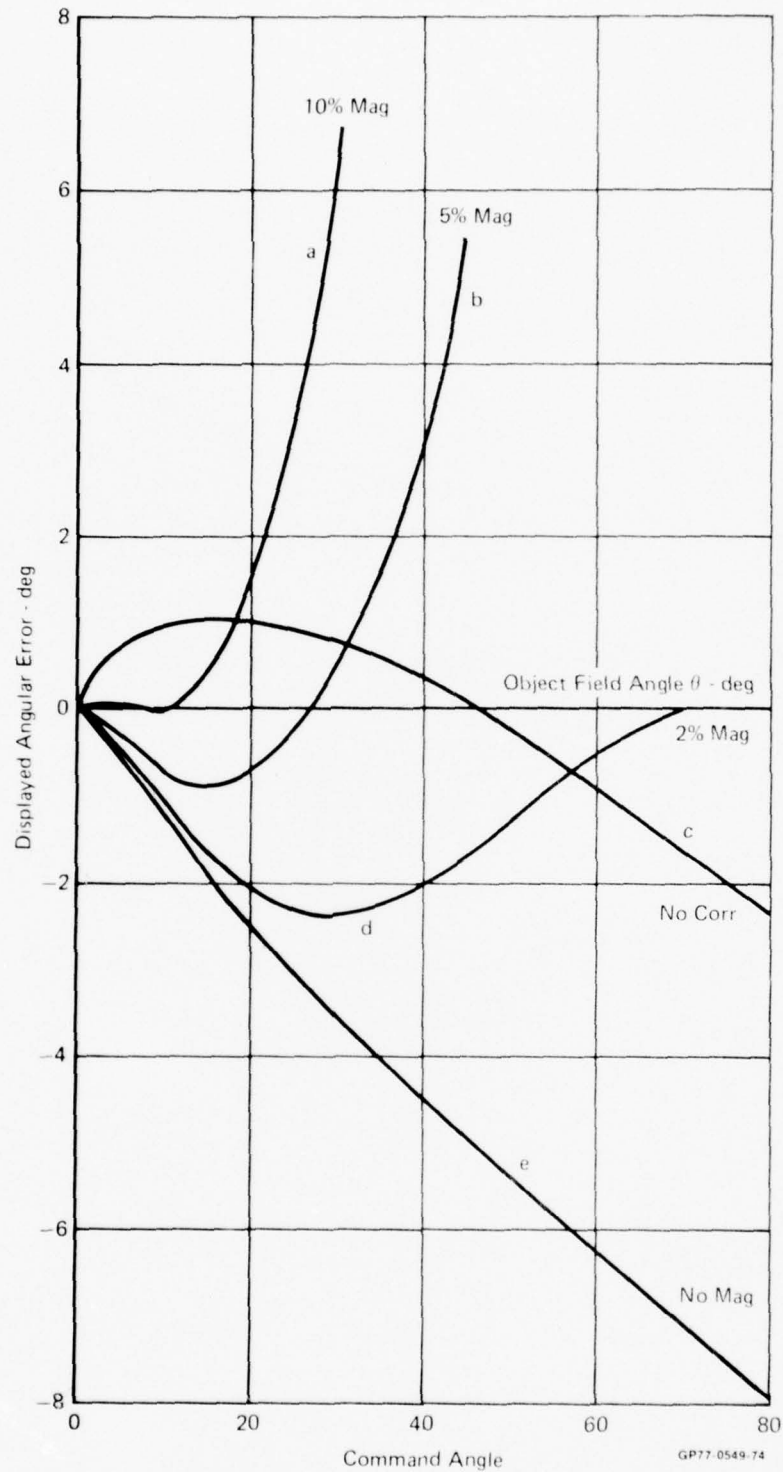
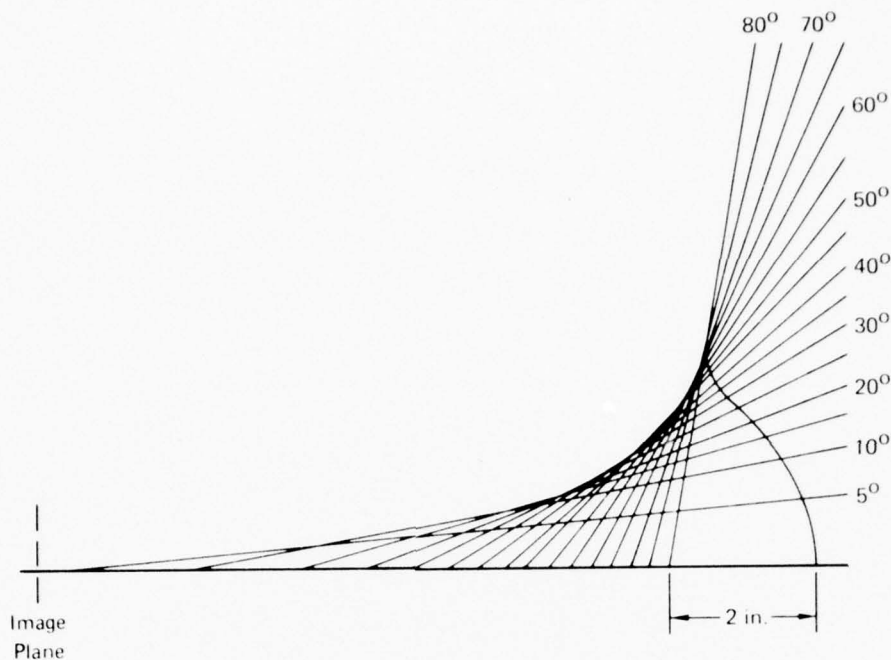


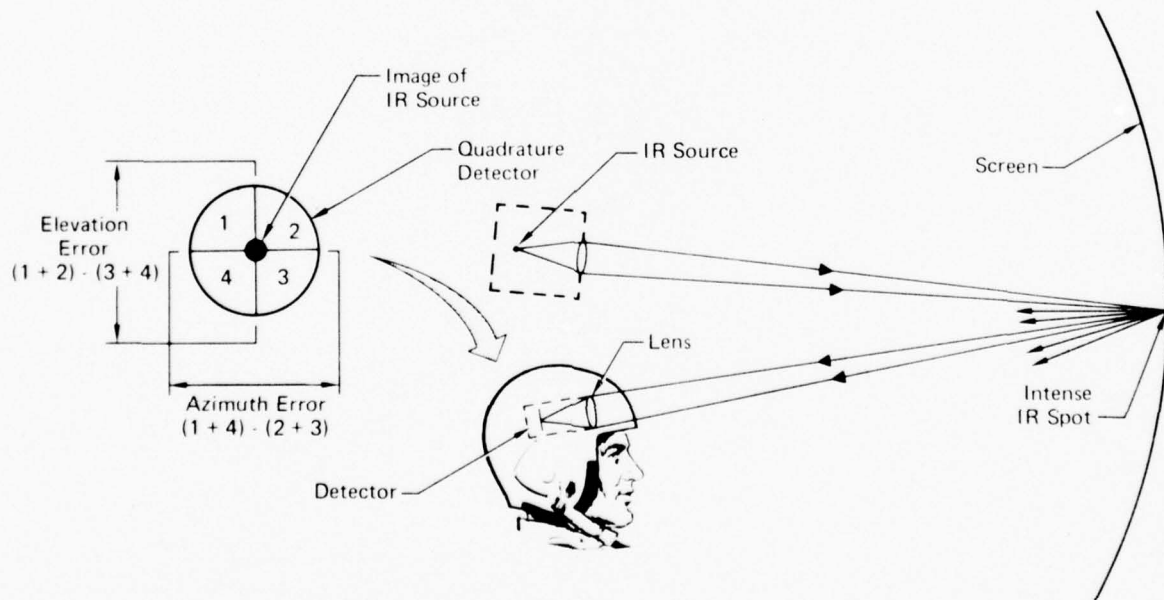
Figure 20 Display Error vs Actual Angle



GP77-0549-33

Figure 21 Nodal Point Shift of Nonlinear Lens

task, the head position must be sensed relative to the projection lens coordinates in all six dimensions. To avoid a complex sensing and computational task, an electro-optical approach was devised that inherently senses the required parameters and is shown in Figure 22.



GP77-0549-37

Figure 22 Head Position Sensing

For the head tracker to function properly it must have adequate sensitivity and no significant deadband. From an optical standpoint the image of the source that falls on the detector must be of sufficient size and strength to provide a useable signal/noise ratio around the null point. For this system, where uniform acuity exists over about $\pm 1^\circ$, a threshold sensitivity of about 0.20° would seem adequate.

In the following paragraph, the sensitivity of the source will be related to other system parameters. An optical schematic and definition of terms is shown in Figure 23. The source has a radiant emittance of W_λ watts/cm²-μ. Assuming the source has a focal length (f_1), and F/number (FNO_1), the power output of the source assembly can be computed as follows:

Assuming the source is a Lambertian emitter, its radiance is

$$N_\lambda = \frac{W_\lambda}{\pi} \text{ in } \frac{\text{watts}}{\text{steradian cm}^2-\mu} \quad (43)$$

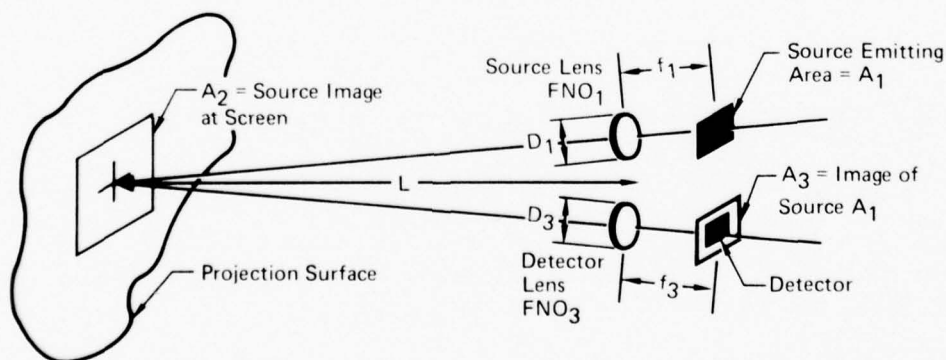
The power exiting the source is:

$$P_1 = N_\lambda \omega_1 A_1 \Delta\lambda \quad (44)$$

where ω_1 = Solid angle subtended by the projection lens (See Figure 23)

A_1 = Source area

$\Delta\lambda$ = Source emitting bandwidth



GP77-0549-38

Figure 23 Head Tracking Radiometrics

The solid angle (ω_1) is

$$\omega_1 = \frac{\pi D_1^2}{4 f_1^2} = \frac{\pi}{4 \text{FNO}_1^2} \quad (45)$$

where D_1 = Source lens diameter
 f_1 = Source lens focal length
 FNO_1 = Source lens F/number

It is also assumed that $\Delta\lambda$ is small enough so that N_λ remains essentially constant. If the source assembly is focused to form an image on the viewing screen a distance L from the source, the irradiance at the screen surface is

$$H = \frac{P_1}{A_2} \quad (46)$$

where A_2 = Screen area illuminated by source

From geometrical optics the source and screen areas are related by:

$$\frac{A_1}{A_2} = \left(\frac{f_1}{L} \right)^2 \quad (47)$$

and

$$A_2 = A_1 \left(\frac{L}{f_1} \right)^2 \quad (48)$$

Substituting Equation (44) through (48) into (46)

$$H = \frac{W_\lambda \Delta\lambda}{4 \text{FNO}_1^2} \left(\frac{f_1}{L} \right)^2 \quad (49)$$

Assuming a screen gain of G , the radiance of the screen is:

$$N_2 = \frac{G H}{\pi} = \frac{G W_\lambda \Delta\lambda}{4\pi \text{FNO}_1^2} \left(\frac{f_1}{L} \right)^2 \quad (50)$$

The power from the screen entering the detector aperture also located a distance (L) from the screen is:

$$P_3 = N_2 \omega_3 A_2 \quad (51)$$

Where

$$\omega_3 = \frac{\pi D_3^2}{4L^2} \quad (52)$$

Substituting Equations (48), (50), and (52) into (51) results in an equation defining the power incident on the detector as a function of system parameters.

$$P_3 = \frac{G W_\lambda \Delta \lambda D_3^2 A_1}{16 FNO_1^2 L^2} \quad (53)$$

The detector selected was a UDT, Inc. PIN SC/25. Salient characteristics for this cell are:

Spectral Response	+ 5% 350-1100 nm
Dark Current	7.5 μ amps Max
Position Sensitivity	0.32 amps/watt-cm
Active Area	3.5 cm ² (.74x .74 inches)
Minimum Spot Size	0.05 inch

For this application an output exceeding the dark current of 7.5 μ amps for an angular spot displacement of 0.2° is desired. Thus the desired sensitivity to angular inputs should be:

$$S_o = \frac{\text{Dark current}}{\text{Threshold}} = \frac{7.5 \mu\text{amp}}{0.2 \text{ deg}} = 37 \mu\text{amp/deg} \quad (54)$$

To define the sensitivity in terms of linear displacements, Equation (54) must be adjusted by the detector focal length, thus the desired position sensitivity is:

$$S_L = \frac{2120}{f_3} \frac{\mu\text{amps}}{\text{cm}} \quad (55)$$

We can equate the desired position sensitivity to the cell actual position sensitivity, thus

$$S_L = \text{Actual position sensitivity} \times \text{Incident Power} \quad (56)$$

Substituting Equation (55) into (56) and solving for the incident power results in:

$$P_3 = \frac{2120}{f_3} \frac{\mu\text{amp}}{\text{cm}} \times \frac{1}{.32 \frac{\text{amp}}{\text{w-cm}}} \quad (57)$$

$$= \frac{6.62 (10^{-3})}{f_3} \text{ watts} \quad (58)$$

The incident power (P_3) was defined in Equation (53). The focal length (f_3) in Equation (58) is defined in terms of F/number and lens diameter, viz:

$$f_3 = D_3 \text{ FNO}_3 \quad (59)$$

Substituting Equation (53) and (59) into (58) results in an equation which interrelates the detector and source parameters, viz:

$$\frac{G W_\lambda \Delta\lambda f_3^3 A_1}{16 \text{ FNO}_1^2 \text{ FNO}_3^2 L^2} = 6.62 (10^{-3}) \quad (60)$$

Of the above parameters, G and L are available from display geometry. The parameters ω_λ , $\Delta\lambda$, A_1 can be obtained from the source parameters.

A 1763 prefocused incandescent standard light bulb was chosen for mechanical reasons and has the following characteristics:

- o Temperature 4000°K
- o Source Dimensions 0.06 x 0.12 inches = 0.4645 cm²

A Wratten No. 88A filter was selected to attenuate the visual and transmit the infrared wavelengths. This filter cuts off below 300 nm. The cell response limits the upper responsivity to 1000 nm. This establishes the wavelength band to:

$$\Delta\lambda = 200 \text{ nm} = 0.2\mu$$

The 4000°K source has an average radiance over this wavelength band of

$$W_\lambda = 1000 \frac{\text{watts}}{\text{cm}^2 - \mu}$$

Using a screen gain of 4 and distance to the screen of 54 inches (137 cm) and substituting these values into Equation (60) results in

$$f_3 = 1.75 \text{ FNO}_1^{\frac{2}{3}} \text{ FNO}_3^{\frac{2}{3}} \quad (61)$$

The aperture diameter of the source and receiver are related by their respective focal lengths, viz:

$$\frac{D_1}{D_3} = \frac{f_1}{f_3} \quad (62)$$

The detector aperture (D_3) has a diameter of 0.05 cm and if the smaller dimension of the source is equal to its aperture (D_1), the focal lengths are related by:

$$\frac{f_1}{f_3} = \frac{0.1524}{0.05} = 3.05 \quad (63)$$

A 2 inch focal length lens with a 1.5 inch aperture diameter was selected for the source optics. Thus the F/number is:

$$FNO_1 = \frac{2.0}{1.5} = 1.33$$

The focal length of the detector from Equation (63) is:

$$f_3 = \frac{2}{3.05} = 0.66 \text{ inch}$$

The required detector F/number is therefore

$$FNO_3 = \sqrt{5.35 \frac{FNO_1^2}{f_3}} \quad (64)$$

$$FNO_3 = \sqrt{5.35 \frac{(1.33)^2}{(0.66 \times 2.54)^3}} = 1.42$$

The chosen detector field-of-view can be determined by:

$$\tan \frac{\theta}{2} = \frac{\text{detector size}}{2 \times f_3} = \frac{0.74}{2 \times 0.66} \quad (65)$$

Thus the field-of-view is:

$$\theta = 58^\circ$$

After a search of available lenses, a double convex aspheric was selected. This lens had a focal length of 0.94 inches and a diameter of 1.5 inch. Therefore its F/number is:

$$FNO_3 = \frac{.94}{1.5} = 0.63$$

While the field-of-view would be somewhat reduced with this lens i.e.,

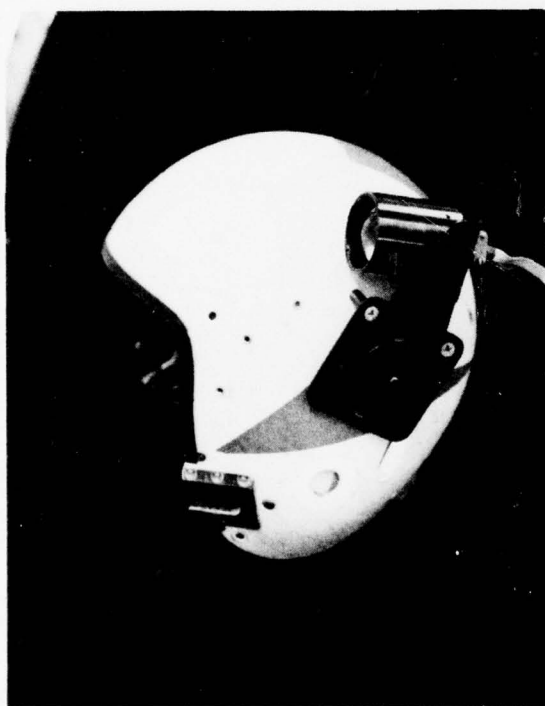
$$\theta = 43^\circ$$

the threshold will be improved by the ratio

$$\frac{f_3^3}{FNO_3^2} \frac{(FNO_3)^2}{f_3^3} = \frac{.94^3}{.63^2} \frac{1.42^2}{.66^3} = 14.5$$

This allows sufficient margin for more filtering if required and/or allows operation of the source at a lower power input.

The assembled sensor can be seen on Figure 24 while the source is seen on Figure 25. An additional Wratten 88A filter was found to be necessary on the detector to reduce its sensitivity to visual wavelength band. The response of the final detector system is shown on Figure 26.



(a)



(b)

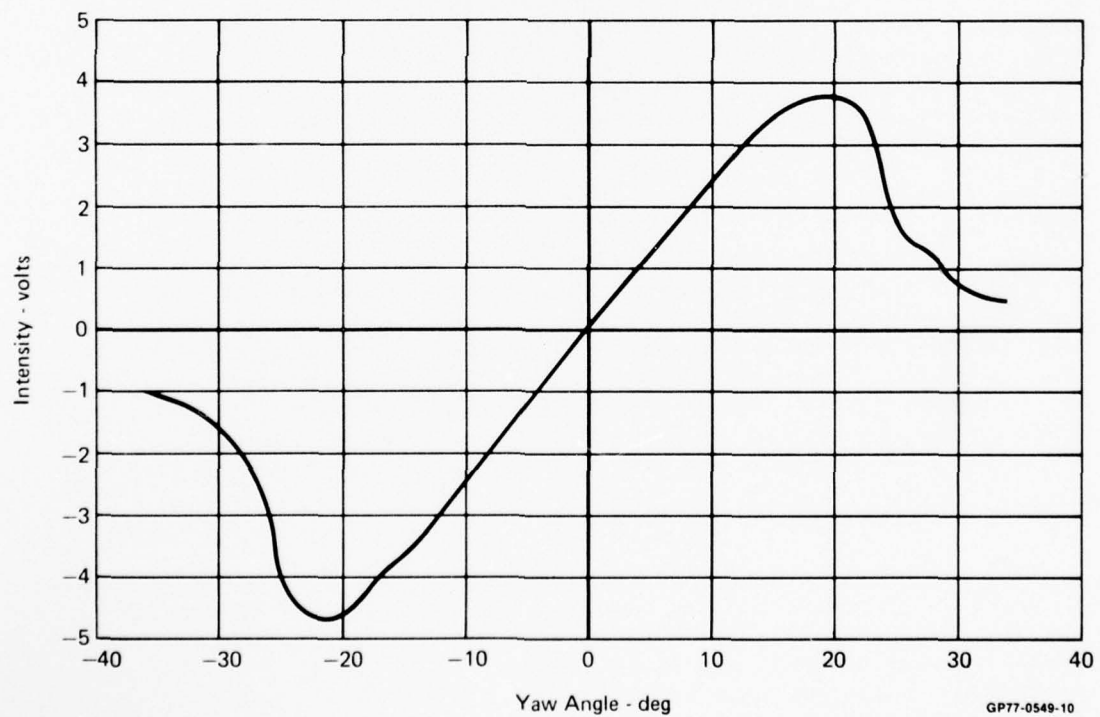
GP77-0549-69

Figure 24 Helmet Mounted Detector



GP77-0549-68

Figure 25 Projector Mounted Source



GP77-0549-10

Figure 26 Response of Infrared Head Tracking Detector System

Section 4

MECHANICAL DESIGN AND FABRICATION

Detail drawings of the camera assembly and projector assembly and their components are included in this section.

4.1 CAMERA ASSEMBLY (P/N 71A050002-1001)

The camera assembly is shown in Figure 27. Camera and pitch axis assembly is supported by forks from the yaw axis assembly. Wiring for TV camera and pitch position encoder are flat cables secured to one of the forks.

PITCH AXIS (P/N 71A050002)

The pitch axis assembly is shown in Figure 28. Pitch shaft (-27) is supported on bearings in both forks. Bearings are fully retained in both forks. The pitch axis torque motor (Inland T-5135, 4 lb.-ft.) is mounted in the -49 fork, pitch position encoder (Baldwin 5X232BL) and pitch stops in the -51 fork. The pitch stops, -39 and -41 permit $\pm 60^\circ$ rotation (from horizontal) with the yaw axis vertical as in Figure 27 or horizontal. A removeable pin is provided to lock the pitch axis in the horizontal position.

YAW AXIS (P/N 71A050003)

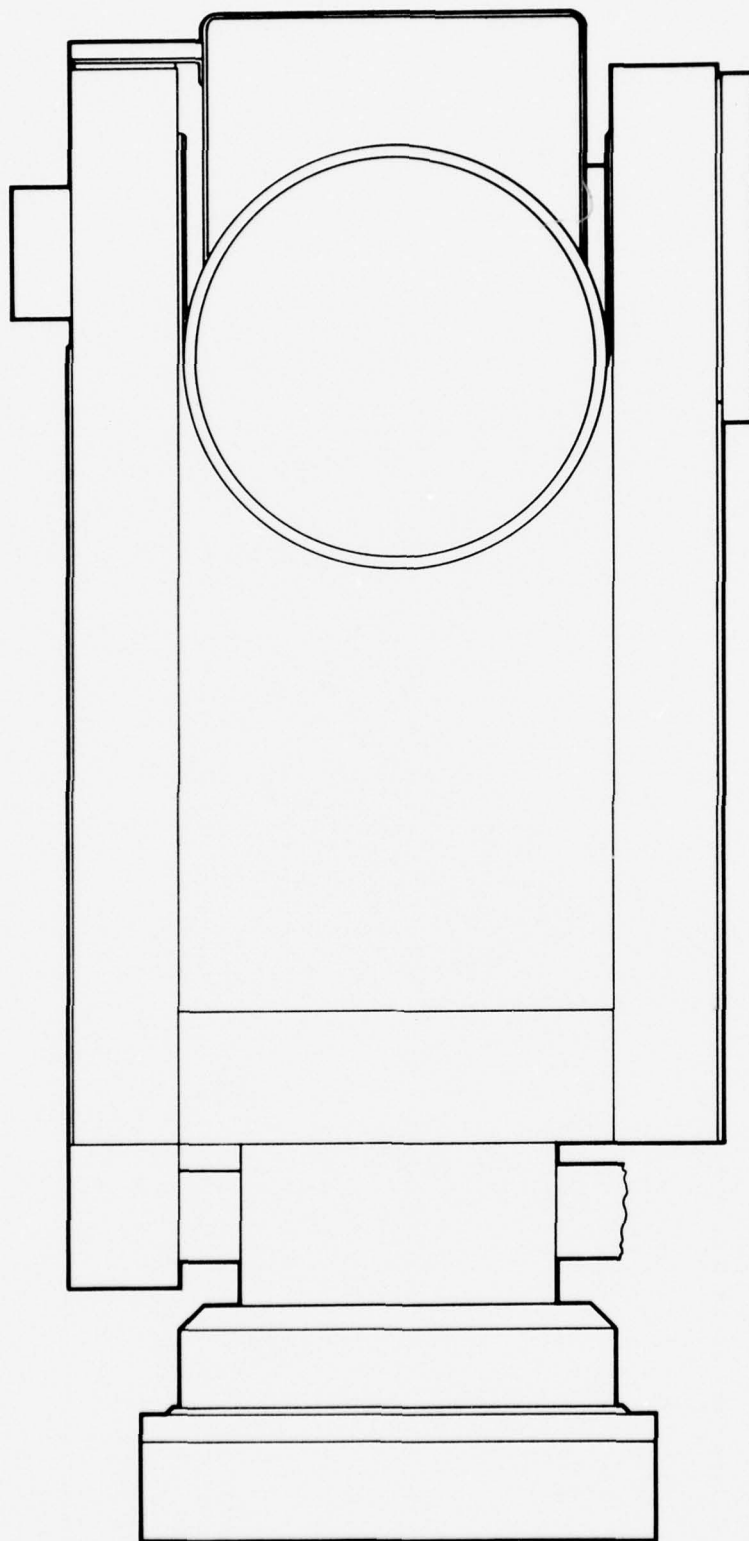
The yaw axis assembly is shown in Figure 29. Fork supported block is mounted on -57. Yaw shaft (-59) is supported by 2 bearings the lower of which is fully retained, the upper is free to move axially in the support housing (-65). The yaw torque motor (Inland T-5730, 7 lb.-ft.) and yaw position encoder are mounted within the support housing. Stops (not shown) limit yaw travel to $\pm 90^\circ$, and a removable pin locks the yaw axis at 0° .

OPTICAL ELEMENTS AND MOUNTS

The optical elements layout is shown in Figure 30. The attach points are located as shown in Figure 31. The -1 base plate is mounted on -27 pitch shaft and provides the mount for the non-linear lens (T-054427-1) the relay optics, and television camera. The optical centerline of the non-linear lens is 2 inches below the pitch axis. The axial position of all relay optics except a field lens mounted in -79 shown in Figure 30 is adjustable along the optical axis. Folding mirrors are adjustable about 2 axes. A cover (not shown) is provided and is attached to the -1 base plate.

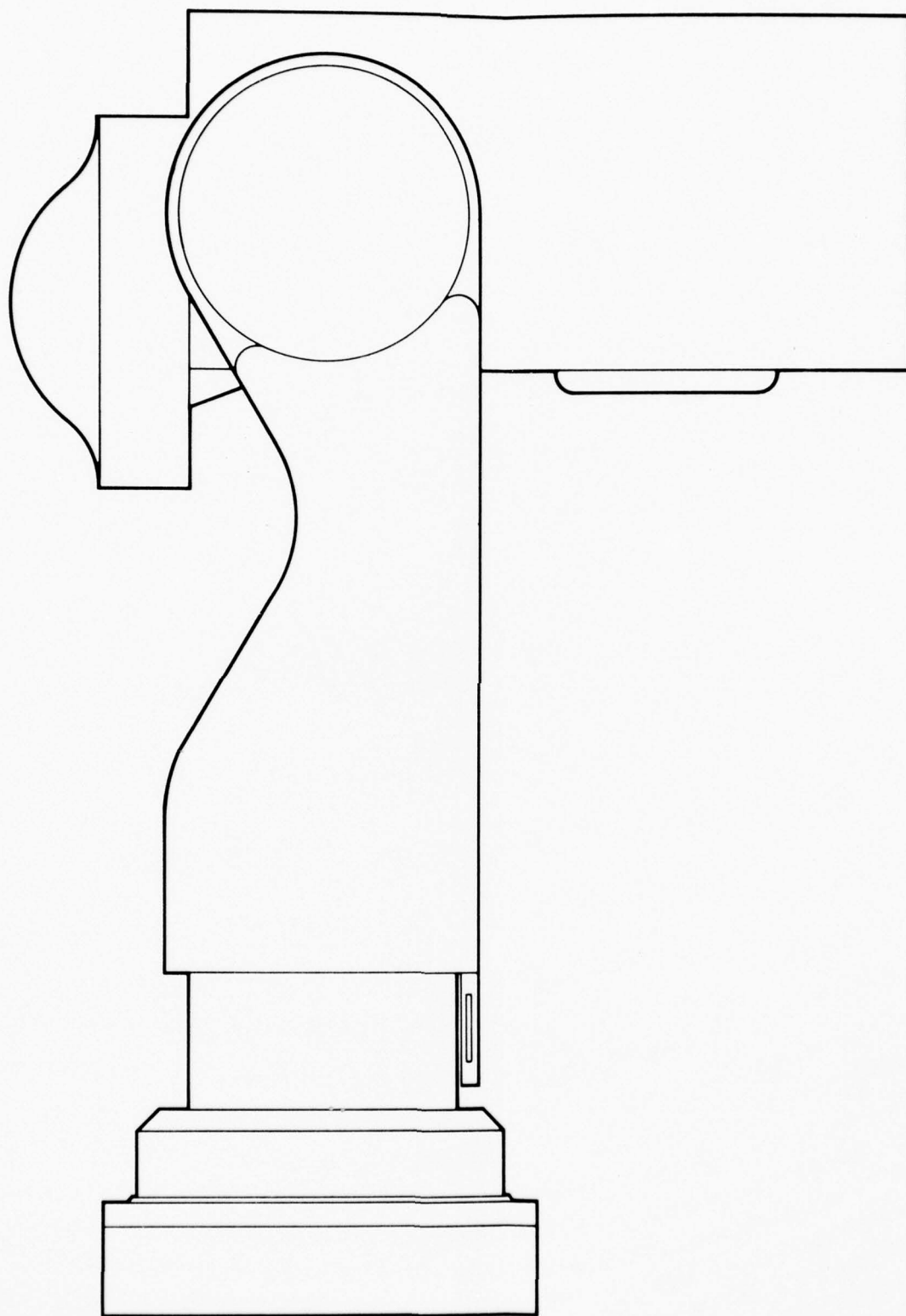
4.2 PROJECTOR ASSEMBLY (P/N 71A050003-1001)

The projector assembly is shown in Figure 32(a) and (b) and is supported by 71A050004 support structure shown on the upper part of Figure 32(b). The yaw axis bearing is a single 25 inch I.D. "x" section bearing designed to carry moments as well as axial and radial loads. This support method was selected to preclude a long yaw axis shaft (and a pair of conrad type bearings) and permit mounting the entire assembly within the dome. The yaw torque motor



GP77-0549-45

Figure 27 Camera Assembly



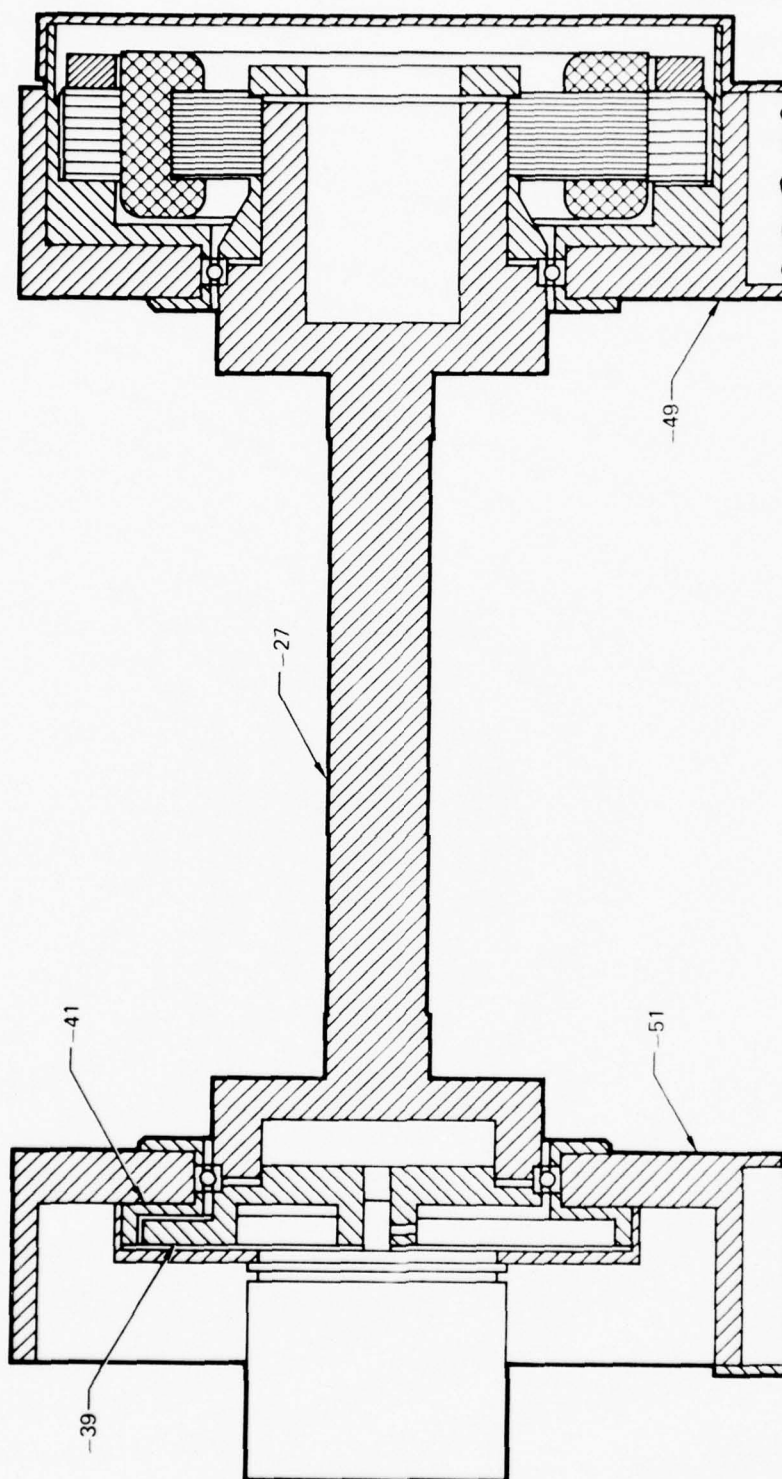


Figure 28 Pitch Axis

GP77-0549-49

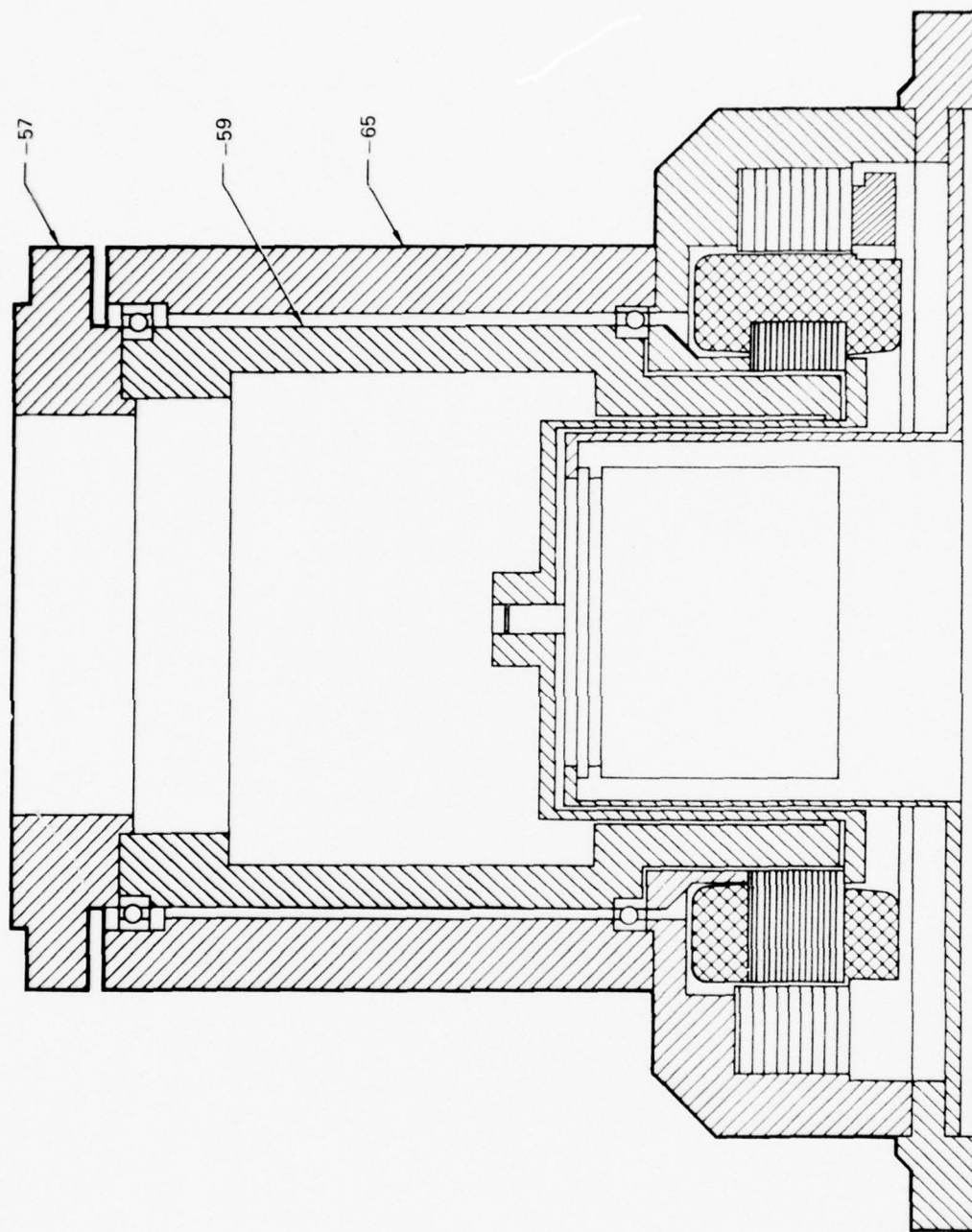


Figure 29 Yaw Axis Assembly

GP77-0549-50

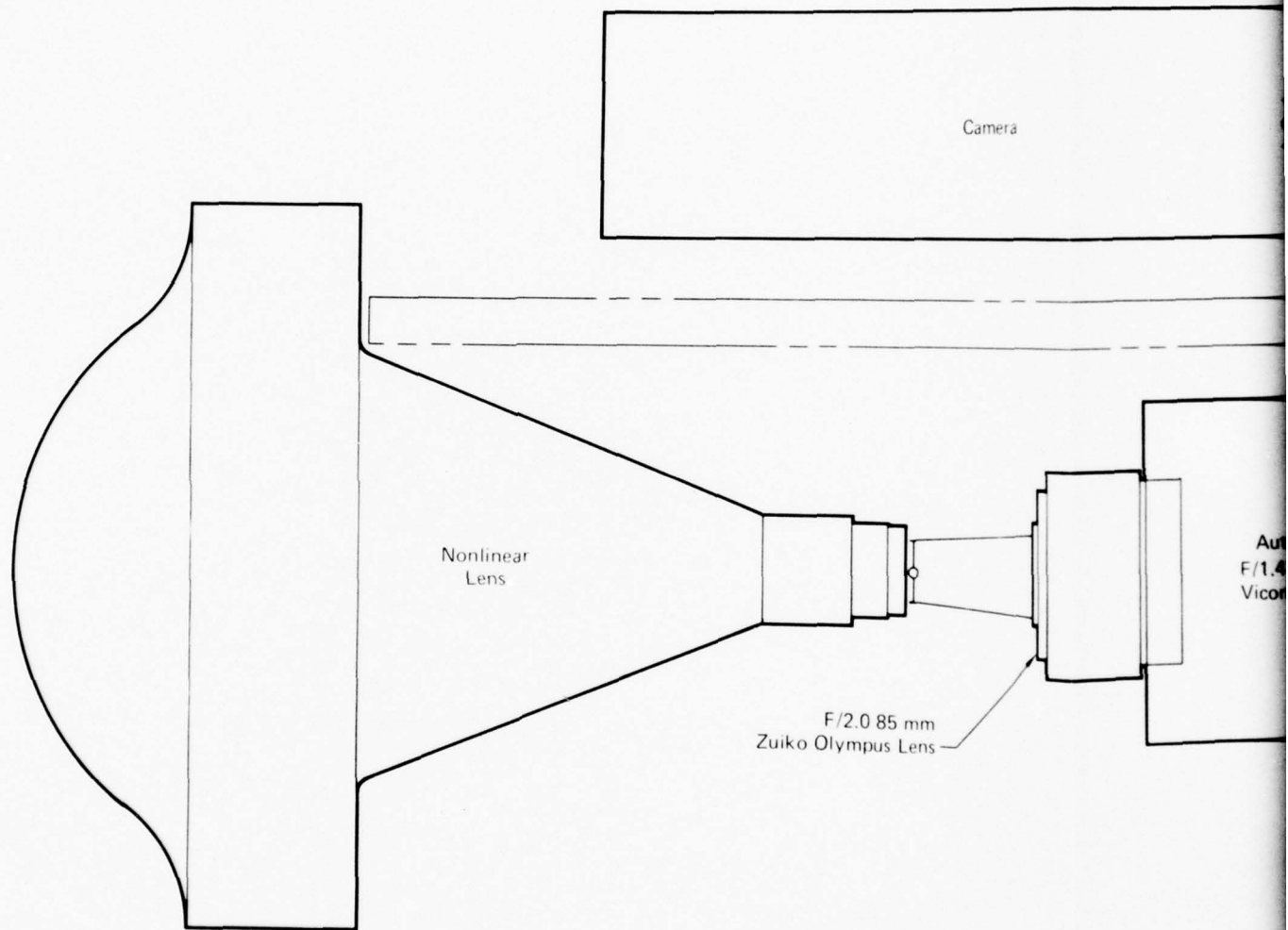
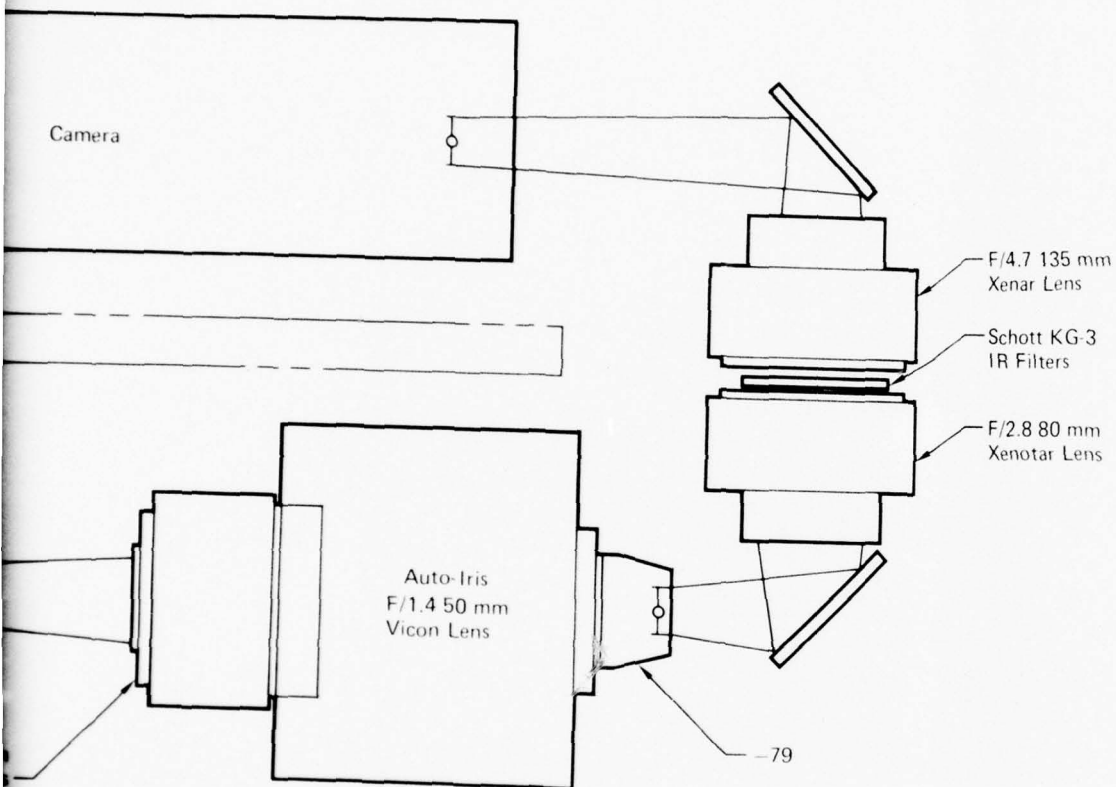
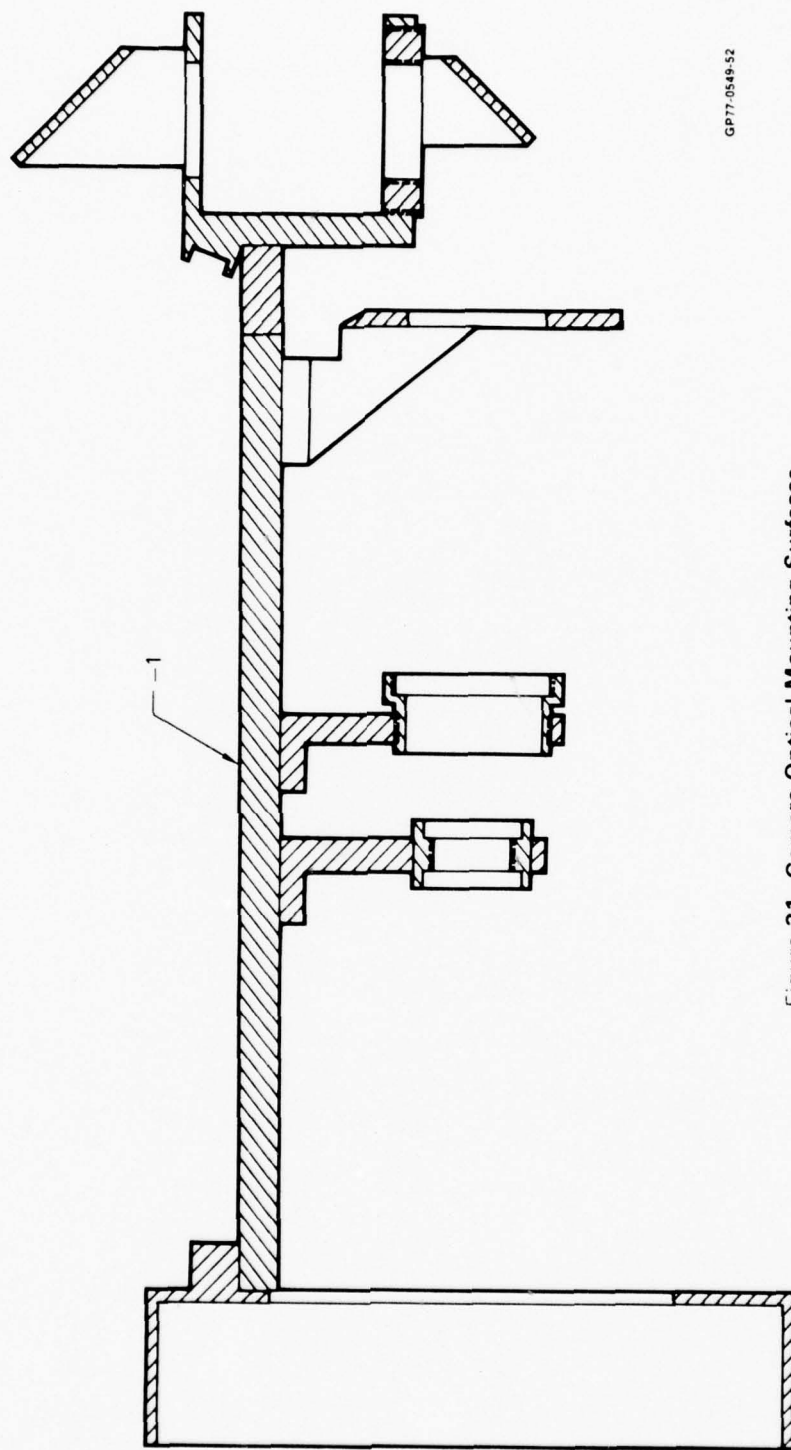


Figure 30 Camera Optical Elements

GP77-0549-51





GP77-0549-52

Figure 31 Camera Optical Mounting Surfaces

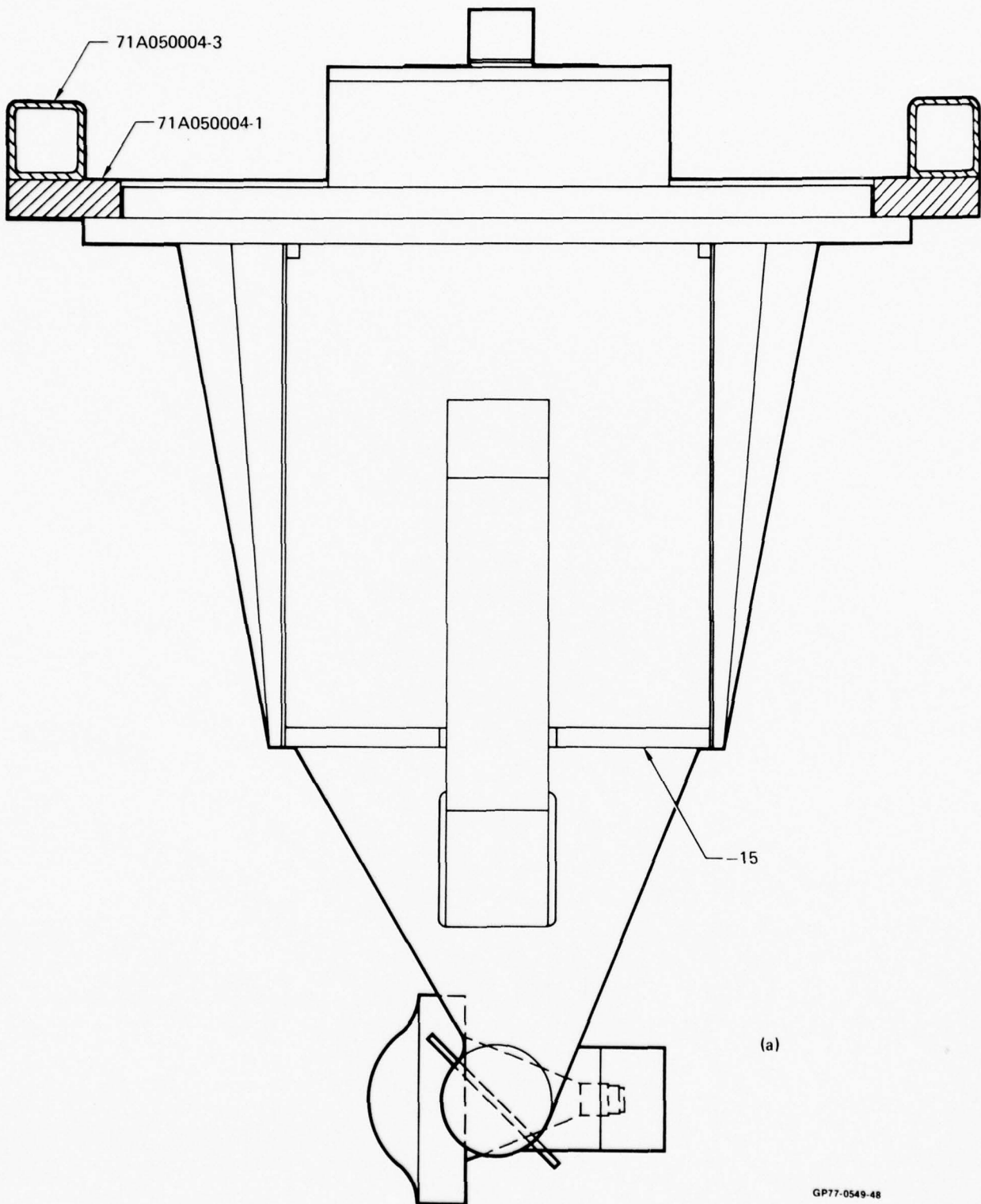
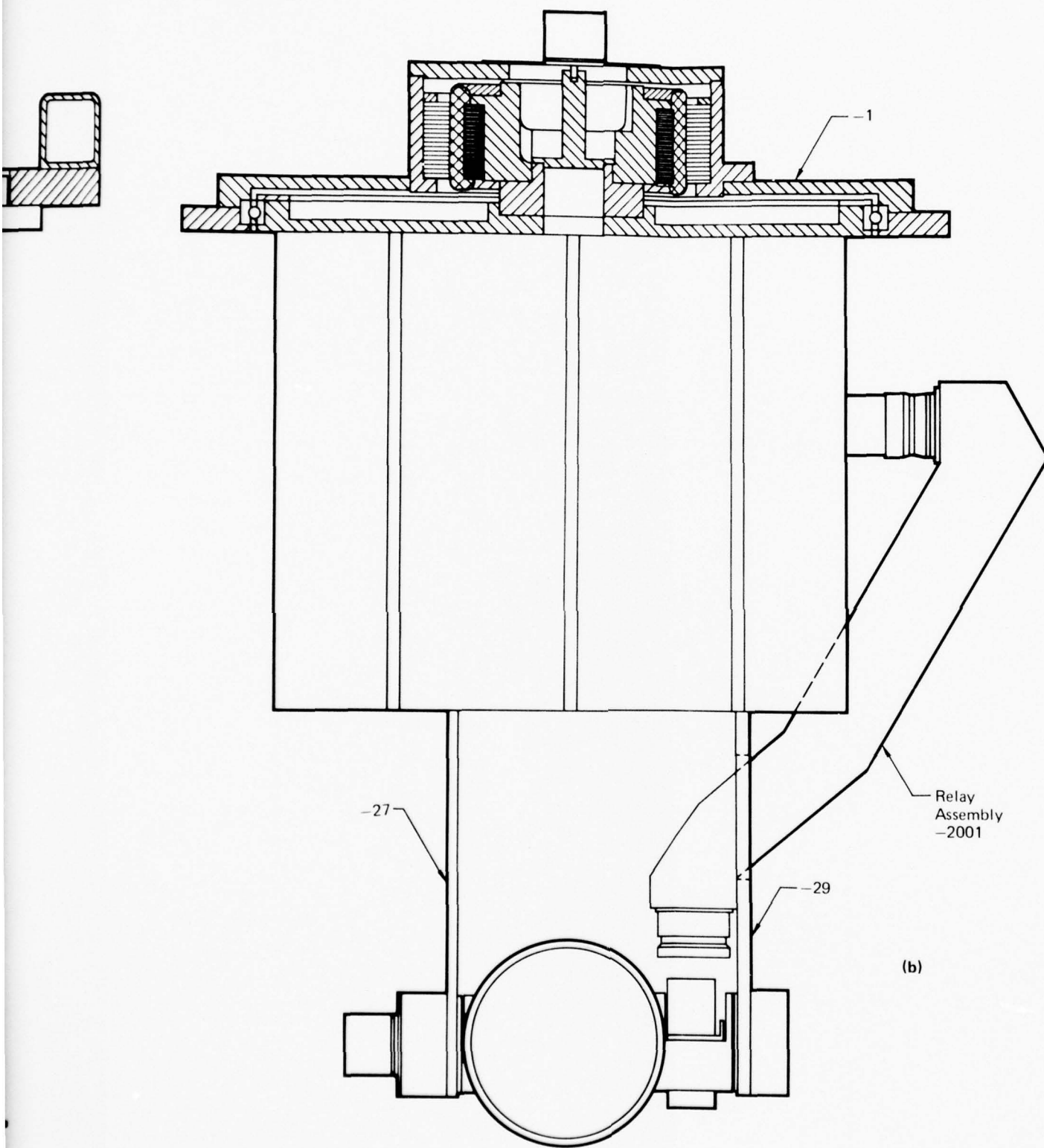


Figure 32 Projector Assembly



(Inland T-10035, 100 lb.-ft.) and yaw position encoder are mounted on the -1 plate above the bearing. The projector is mounted within a box structure supported by the yaw bearing. Holes in the box at appropriate locations provide access to projector controls. Bottom plate of the box supports the pitch axis forks. Yaw travel is limited by stops (not shown) on the 71A050004-1 plate to approximately $\pm 120^\circ$. The stops are spring loaded to provide essentially uniform deceleration for 15° of rotation (of the yaw axis) before becoming "hard" stops. Limit switches short the yaw motor just before engaging either stop.

Fork arms (-27 and -29) support the pitch axis assembly. The -29 fork and bottom plate (-15) of box structure support the -2001 relay assembly.

RELAY ASSEMBLY (P/N 71A050003-2001)

The relay assembly is shown on Figure 33 and supports and locates 4 of the 5 required relay lenses and 3 of the 6 required mirrors, the remaining lens and mirrors are mounted within the pitch axis assembly. All lenses in the relay assembly are adjustable along the optical axis, and all mirrors are adjustable about 2 axes.

PITCH AXIS (P/N 71A050003)

The pitch axis assembly is shown in Figure 34. The -27 fork mounts the pitch axis torque motor (Inland T-2950, 1.2 lb.-ft.) and pitch position encoder (Baldwin 5V232BL). Stops are provided to limit pitch travel to $\pm 60^\circ$ (from horizontal). A removeable pin (in the -29 fork) locks the pitch shaft in the horizontal position. A "half angle" drive is provided for the relay mirror mounted on the -55 mirror support. The "half angle" is obtained by a differential on the -29 fork. A ring gear (PIC N3-4-5) is fixed to the differential case (-99, -47, -45), a second gear is fixed to the pitch shaft (-43, -39). The planet gears, to which is mounted the "half angle" mirror (-51, -53, -55), rotate in the same direction as the pitch shaft but at one-half the angular rate. The mirror may be "zeroed" by rotating the -47 cover with respect to the -45 housing. The -109 ring is the mount for the corrector lens (not shown).

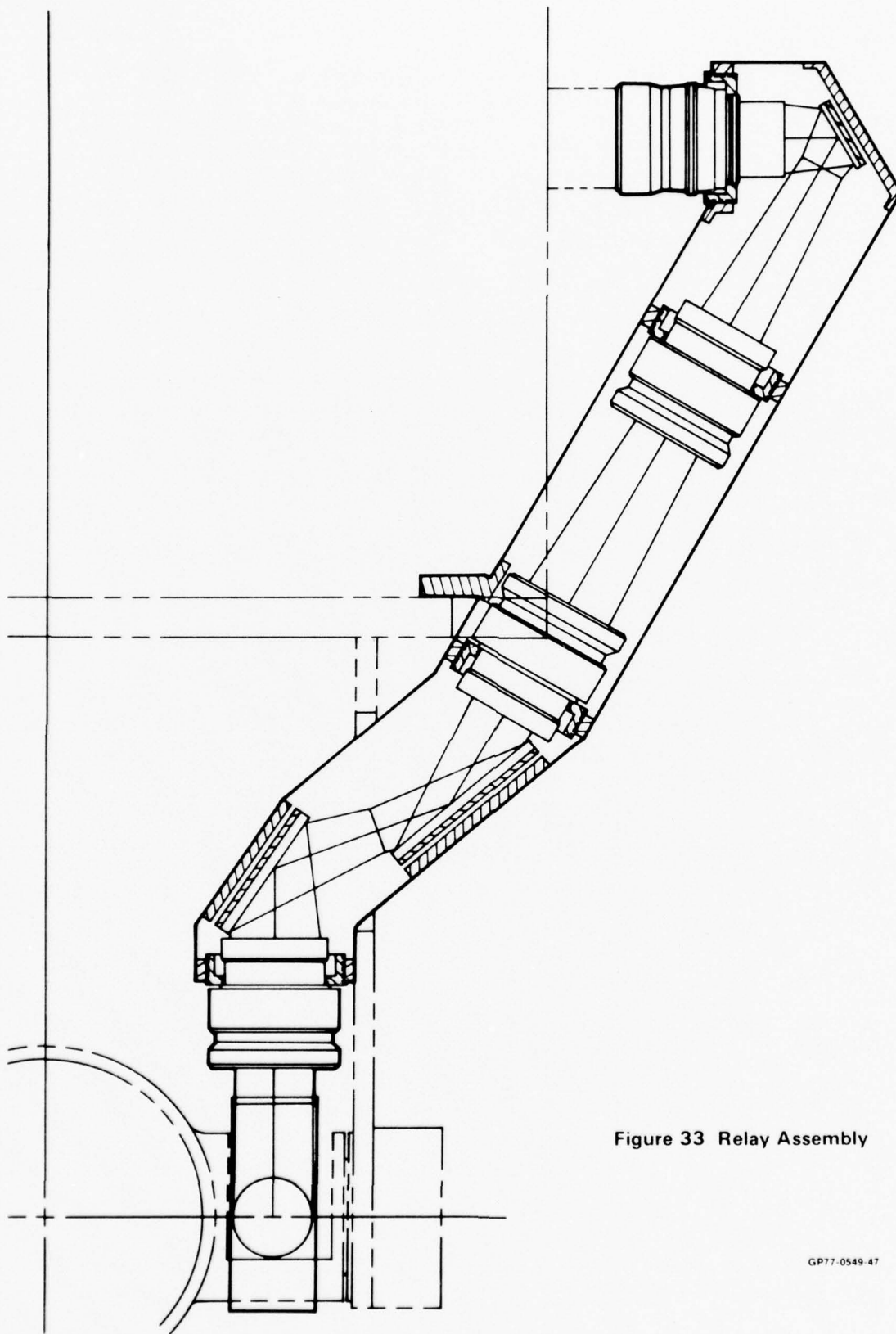


Figure 33 Relay Assembly

GP77-0549-47

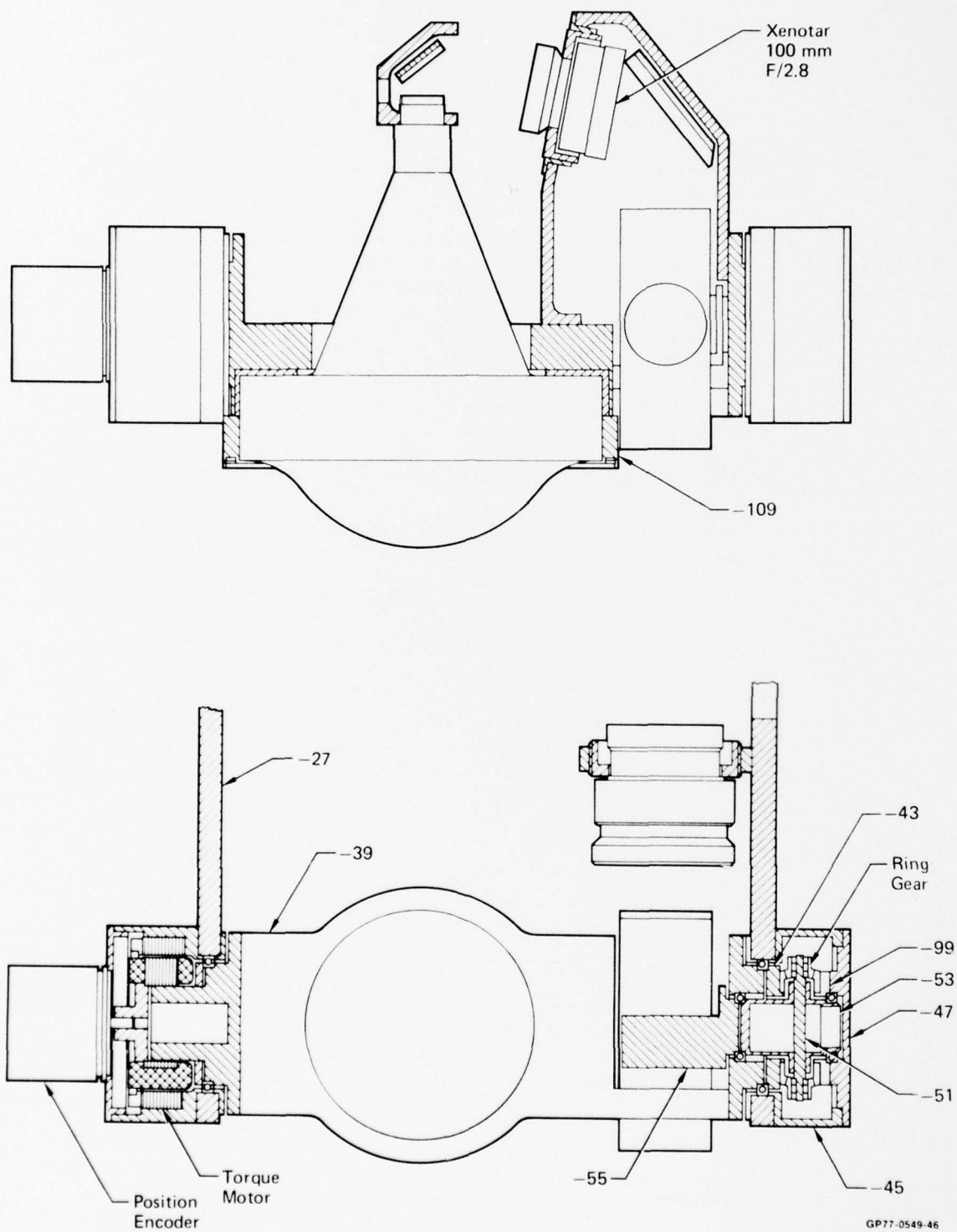


Figure 34 Projector Pitch Axis Assembly

Section 5

CONTROL SYSTEM

The function of the Control System is to command the projector to follow changes in camera angle. Camera angle changes are commanded by changes in operator head position or joy stick input. It consists of these major parts; the microprocessor, the camera electronics box, and the software.

The general design of the control system has been done digitally. The digital design of this system is in general immune from the kind of problems such as drift and error due to the manufacture of position and rate signals that beseech common analog servos. The mathematic production of rate signals from position data and digital (PCM) transmission of control signals eliminate many noise and signal related problems, although some signal errors still show up. In the case of a digital system these errors show up in varying degrees. For example, a lower order bit could be dropped and probably not be noticed by the system, but the system would surely jump if the sign bit or one of the higher bits suddenly is in error. Filters and other protective software have been programmed to help smooth out the results of such signal errors.

Figure 35 is a block diagram showing the camera and projector servos, the microprocessor which is located at the home station and the camera electronics box at the remote site. The system uses serial data to communicate between the microprocessor and the camera electronics box. Figure 36 shows a more complete block diagram of the hard wired control system. The microprocessor allows the system to be operated in three basic modes:

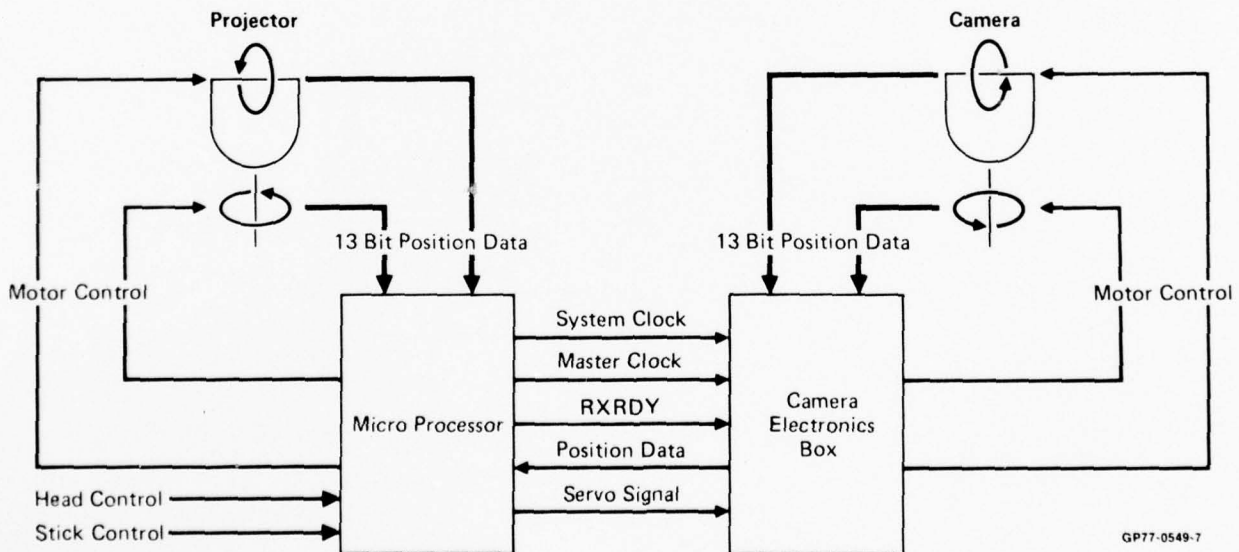


Figure 35 Servo Control Block Diagram

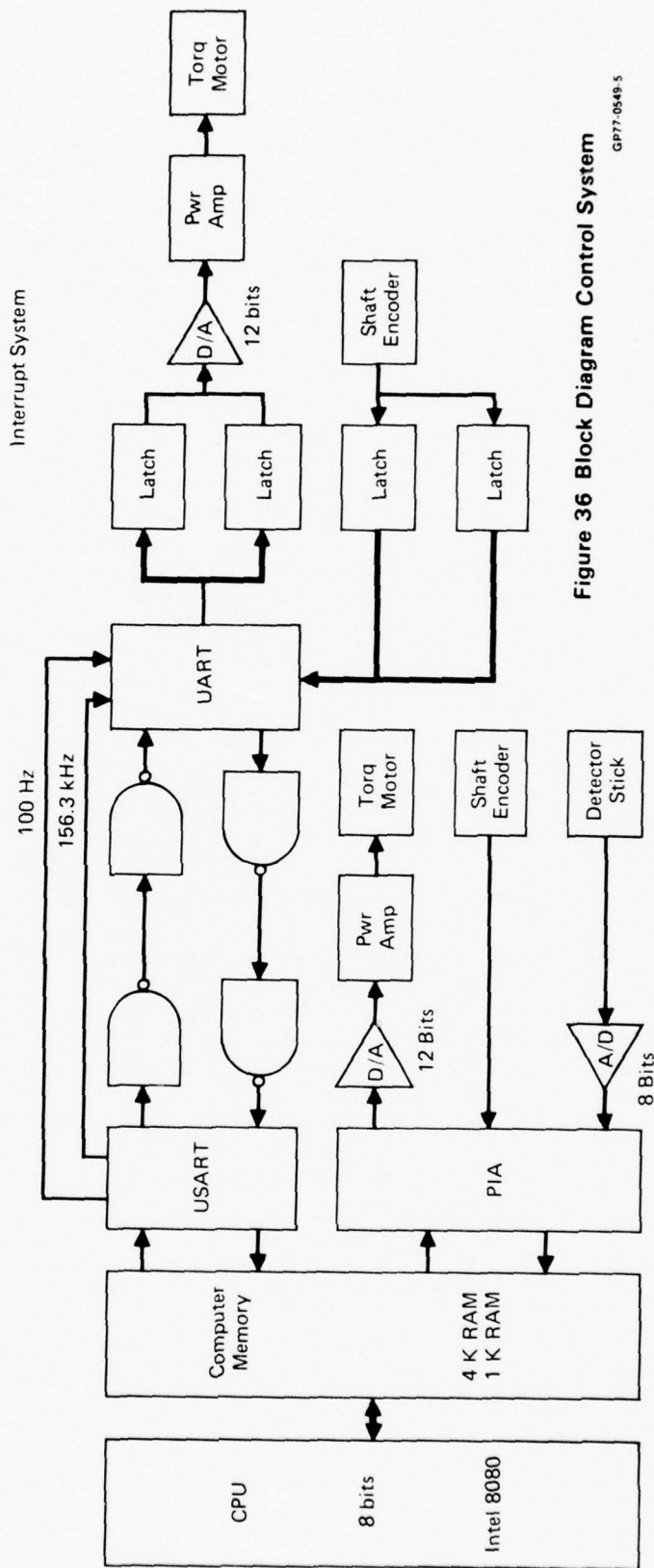
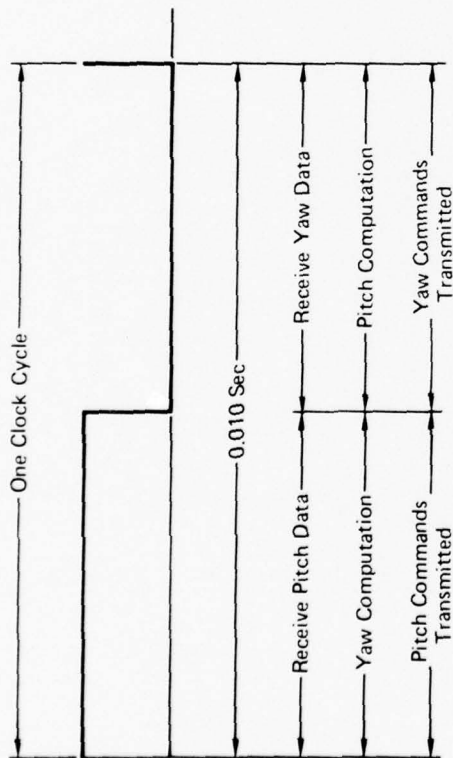
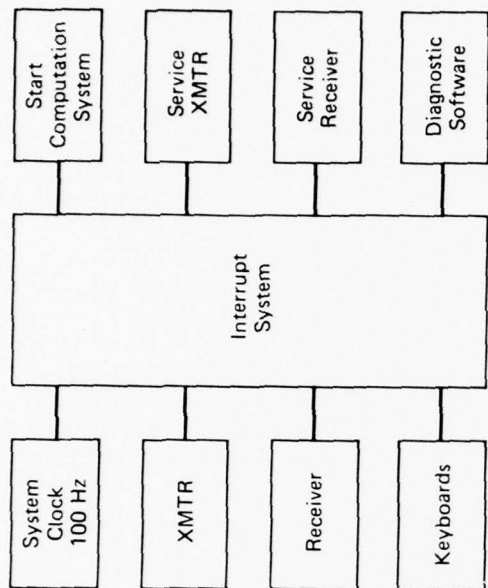


Figure 36 Block Diagram Control System

GP77-0549-5

- MODE 1) Camera servo fully operational, the projector axes are pinned and the system is joy stick controlled. In this mode the high acuity spot is stationary while the "whole picture" moves about the dome.
- MODE 2) The camera and projector servos are fully operational. The display picture is stabilized and the system is joy stick controlled. In this mode, the high acuity portion of the image is slewed about, using the joy stick control to the point of interest while the picture as a whole is stationary.
- MODE 3) Camera and projector servos are fully operational and head controlled. This is generally the preferred mode of operation and the display is the same as in Mode 2 except that the camera and projector follow-up are controlled via a helmet mounted position detector.

These three modes allow the user to tailor the remote viewing system to his own particular needs.

This section contains a description of the control system and is divided into task oriented subsections which are: a description of the microprocessor, the camera electronics box, and software. In addition, included is a section on the head tracker and a section on the math models on which the software is based. Finally in the last section are system operation procedures.

5.1 MICROPROCESSOR HARDWARE

The basic microprocessor is the Intel 80/10 packaged in the SBC80 Modular Backplane/Card Cage with an I/O expansion board and prototype board. Diagnostic hardware, real time interrupt logic, power supplies, and some analog hardware were integrated with the Intel SBC 80 into one package resulting in a mini-computer for the Remote Viewing System.

The 80/10 Intel microprocessor board contains:

- 1 - 8080A Central Processor
- 1 - 8251 Serial I/O
- 1 - 8255 Parallel I/O
- 4 - 8708 1K-PROM-UV eraseable
1 K BYTES OF RAM

and line drivers and terminators. In addition to the hardware listed, a computer emulator and PROM programmer were available at the suppliers for scheduled use.

5.1.1 Diagnostic Hardware

The hardware consists of two hexadecimal keyboards, 5 hexadecimal LED displays, address comparators, and miscellaneous gates and logic and is shown in Figure 37. One keyboard is implemented as a function keyboard via the software and the other keyboard is implemented as a data/address keyboard via the software. The keyboards and LED Displays are front panel mounted on the computer. The rest of the hardware is mounted on the back of the front panel and on the prototype board.

Real Time Interrupt Hardware

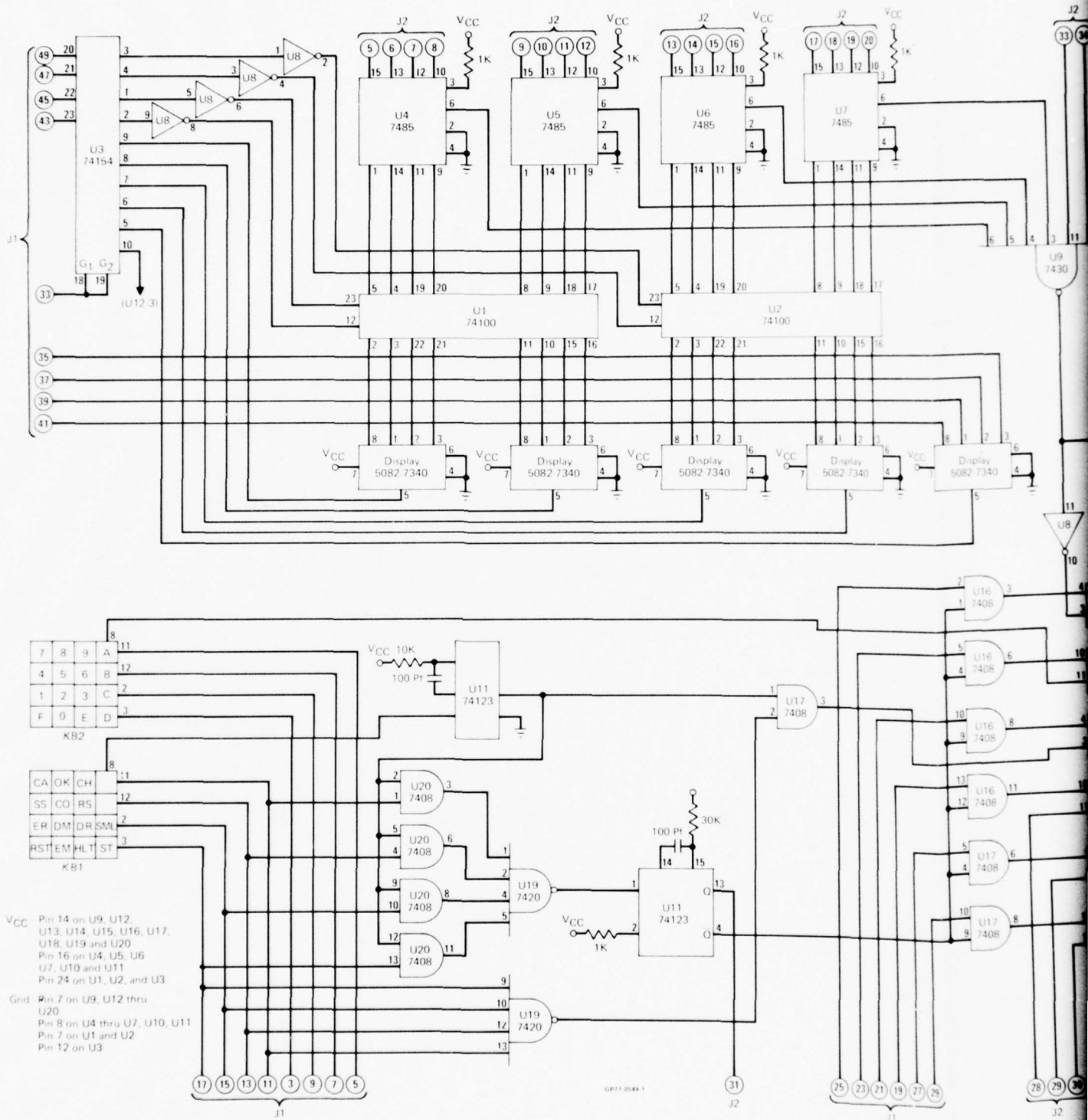
The processor has provisions for six real time interrupts. They are designated MCLR, RXRDY, TXRDY, KB1, KB2, AND COMPARATOR on Figure 37. The basic interrupt channel is shown in Figure 38.

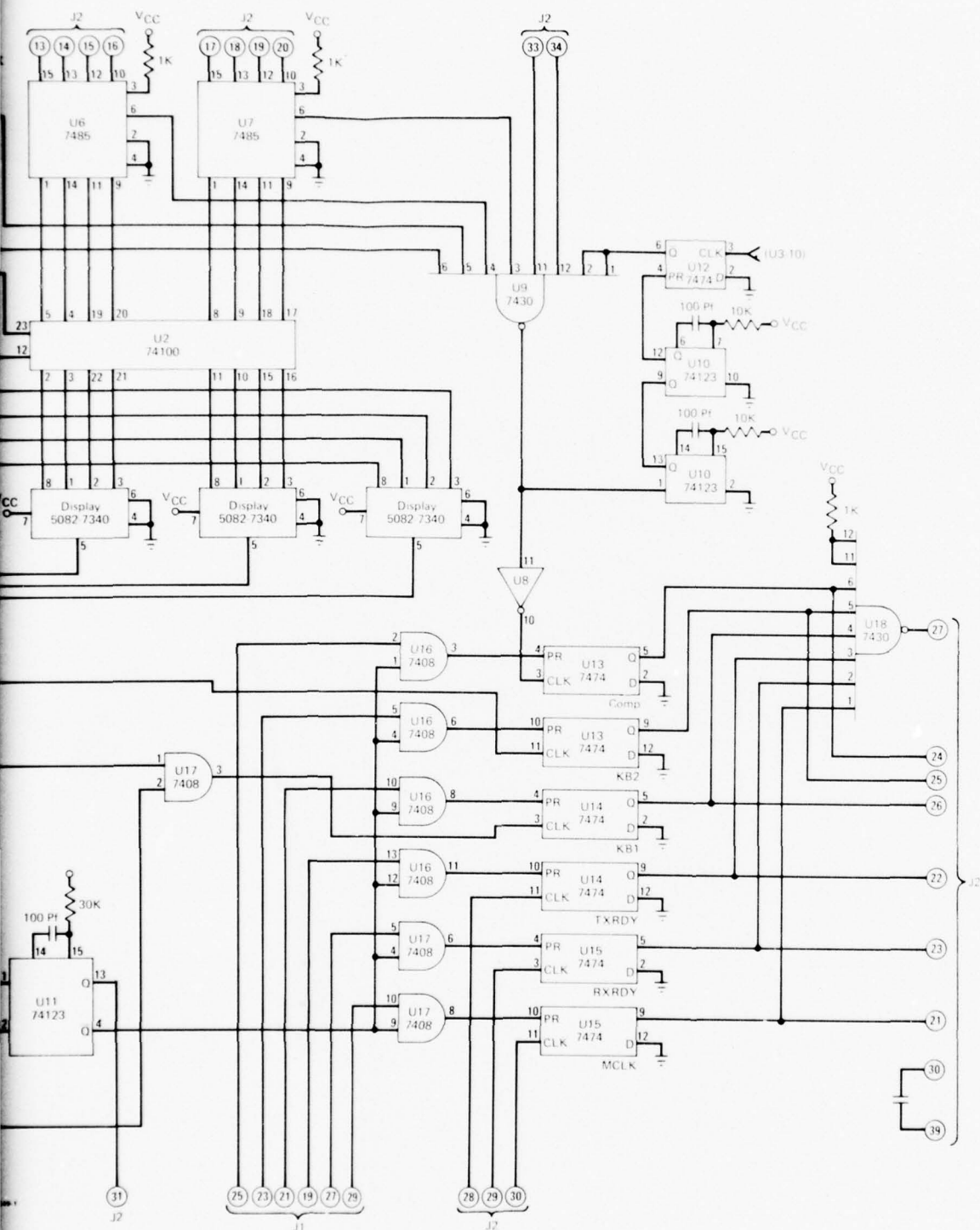
The computer controls the active status of the interrupt channel by inputs to the channel enable and reset gate. When the channel is active, an interrupt from an external device sets the Q output of the flip-flop. The Q output generates an interrupt pulse to the computer and sets a bit in the computer interrupt input port. The computer software interrupt handler service routines polls the interrupt input port to determine the source of the interrupt and thereby takes the desired path. During this time all other low priority interrupts are disabled. For example, if an RXRDY interrupt came in while a TXRDY interrupt was being serviced, it would not recognize the RXRDY request until the TXRDY service was completed. High priority interrupts from the keyboards are always active.

All six interrupt channels operate in the same way and are mixed together at the eight input NAND Gate. The output of this gate drives the computer interrupt line. The hardware involved in an interrupt channel is a computer output port, computer input port, and gate, and a Flip-Flop.

Operation of one interrupt channel can be described as follows. The computer has instructions which enable and disable the external interrupt line. With the interrupt line enabled, the software sets the bit that is assigned to the channel being discussed. This bit appears as input to the 7408 gate as shown in Figure 37. The line from Reset is normally high and so the input to the preset channel of the Flip-Flop is high and active. The inputs to the NAND gate are all high and the channel is ready to accept an interrupt. An interrupt from an external source causes the Flip-Flop to go low. The Flip-Flop output causes the NAND gate output to go high generating a computer interrupt and it also sets a bit assigned to this channel at a computer input port.

Software samples the input port, determines which interrupt channel has requested service, sets the active status of all interrupt channels according to the priority level of the interrupt that has just occurred and proceeds to service the interrupt. When service is complete, software resets the output port which sets the Flip-Flop and then sets the output port so that the channel is again active. It also resets the other channels and





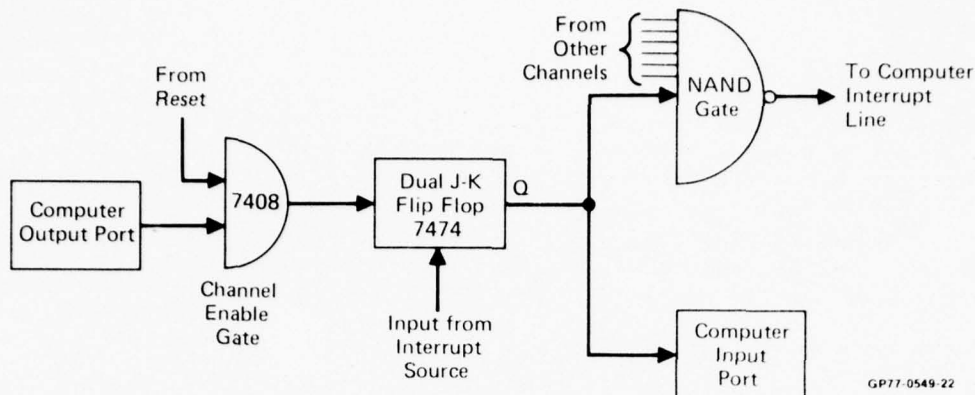


Figure 38 Interrupt Channel

makes them active. In summary, the output of the Flip-Flop is normally high, goes low when an interrupt occurs, stays low during software service, goes high when software is finished, and becomes active when the 7408 and gate output is high.

Restart

The restart function key causes U-19 on Figure 37, to change its output which in turn causes U-11 to trigger. The output of the one shot U-11 goes to the computer reset line which causes the computer to go to memory location zero. No interrupt is generated. When other keys are depressed, an interrupt is generated via U-17 as described above. In addition the keyboard output is routed via J-1, pins 17, 15, 13, 11, 3, 9, 7 and 5 to a computer parallel input port. As a consequence the software can determine which key was depressed and perform the necessary functions.

LEDS and Comparators

Circuits driving the LED displays and compare address functions involve the components U-1, U-2, U-3, U-4, U-5, U-6, U-7. J-1 pins 35, 37, 39, 41 are a computer output port on which the computer outputs the data desired to write to a specific LED. The software then outputs the code on pins 43, 45, 47, 49 of J-1 which causes U-3 to select the appropriate LED. The pins of J-2 are the address bus of the computer. When the comparators U-4, U-5, U-6, U-7 "see" the address set on the latches U-1 and U-2, a computer interrupt is generated via U-9. The one shots U-10 and U-11, reset U-12 so that the gate U-9 is disabled after the compare address has been executed. U-12 enables the gate U-9 when the software selects it via U-3. In summary, software loads the comparators with the desired address similar to the previous discussion about LED's and then software enables U-9. When the address appears at the comparators, U-9 generates an interrupt and the one shots U-10 disable the U-9 gate. Pins 34, 33 of J-2 are signals from the computer which enable U-9 only when an address is on the address bus of the computer. This is necessary since other computer data appears on the address bus and creates a timing problem solved by these inputs.

Input/Output PORTS

The system uses a total of eight input ports and five output ports. They are assigned as shown in Figure 39. The computer low order bits is shown at the right in the figure. High priority interrupts are at Input Port 1, low priority interrupts come in at Input Port 3. The A/D converters start the A/D conversion process when SYS CLK goes positive. The software checks Port E4 to verify that conversion is complete before reading the data at Ports E5 and E6.

The low order LED is selected by a 4 at port E8 and toggling bit 6 at port E-A.

5.1.2 Diagnostic Software

Intel has a computer emulator designated as ICE-80 which is used with the Intel MDS system. The in-circuit emulator interfaces to any user configured 8080 system. With the ICE-80, the designer can emulate the system 8080 in real time, single step the system program, and substitute Intellec memory and I/O for user system equivalents. It will provide address data and 8080 status information on the last 44 machine cycles emulated. It allows the user to share Intellec memory and I/O facilities and is indispensable for initial debugging. The ICE-80 was used with the RVS during Monitor Program debugging.

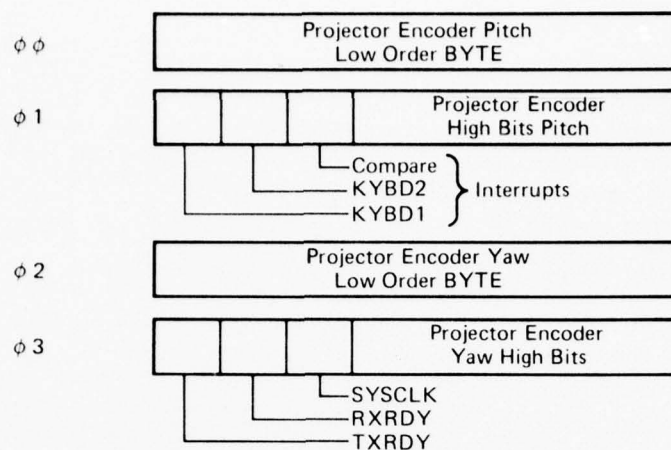
The RVS microprocessor has diagnostic software referred to as the Monitor Program designed primarily to facilitate operational program checkout and for enhancement of computer operation. One PROM in the processor is devoted to the Monitor Program. It is the only program input/output the computer has. Initial checkout of the processor monitor program utilized the computer emulator available on the Intel MDS System. After the Diagnostic Software checkout on the emulator was completed, it was used to troubleshoot other PROM software.

PROM #3 is devoted to the Diagnostic Software. It is stand alone software. While the computer is operational with the system software, Diagnostic Software is not used. The Monitor program is accessed when the operator depresses the Halt Key. Exit from the diagnostic software is accomplished when the Return Key is depressed.

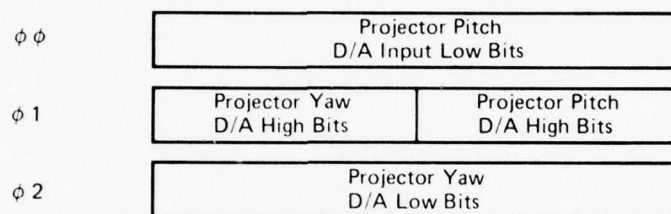
The primary purpose of the monitor program is to implement keyboard functions which allow the operator full utilization of processor capability. Under monitor, the operator can display the contents of all memory positions, program RAM, single step the processor, and access all processor registers.

The Monitor Program contains all of the diagnostic software required to couple the two keyboards with the processor. All keyboard functions are implemented by software as opposed to hardware. Keyboard generated interrupts are routed via the interrupt handler to the monitor. Keyboard 1 is a function keyboard and Keyboard 2 is for data in hexadecimal. When a Keyboard 1 key is depressed the monitor jumps to the appropriate routine corresponding to the function represented by the key. Concurrently, the interrupt handler has

Input Ports



Output Ports



I/O Port Assignments

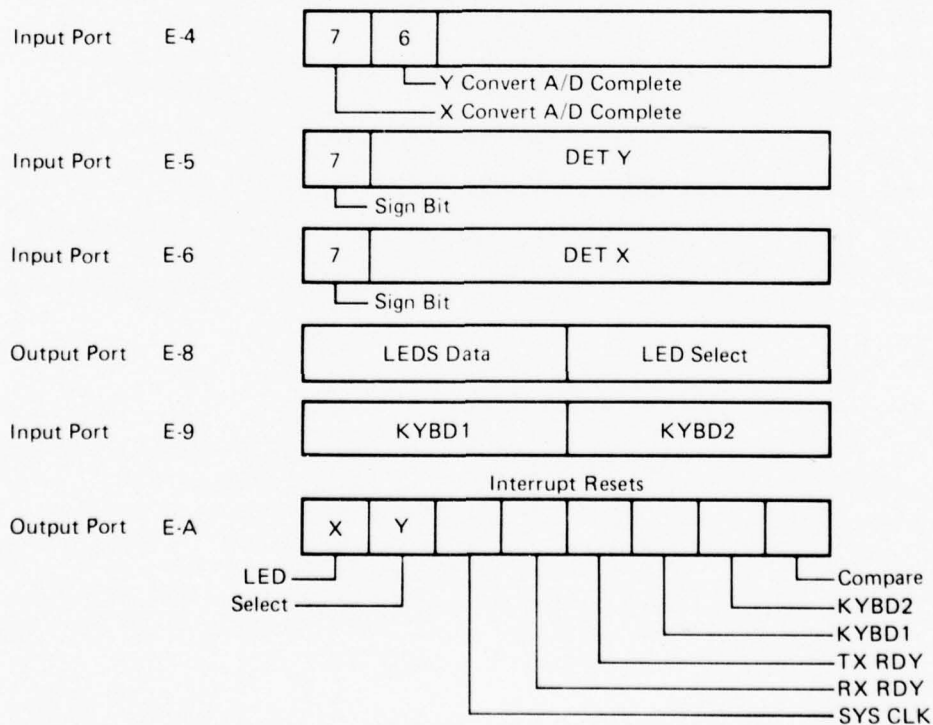


Figure 39 Computer Input and Output Ports

GP77-0549-23

disabled all other interrupts so that once a keyboard interrupt has occurred they have priority. This assumes that the operator desires complete processor control. When the operator has finished his input, depressing the RST key, returns the machine to the program with all interrupts enabled.

Figure 40 is a brief explanation of keyboard functions implemented. These functions allow the operator to display contents of all memory locations, to load data into RAM, to display the contents of registers and load registers, to halt the program, to single step the program, and to stop the program at a specific program address. The SML Key used with the OK and Change Key allow the user to load or change any of the fixed multiply constants. The monitor generates fast multiply routines for each multiply constant and loads RAM with these routines. Twenty multiply constants are programmed and loaded in RAM from 3D90 to the top of RAM.

The stack pointer starts at 3CFF. The lower portion of RAM is assigned to the stack. Scratch pad RAM starts at 3D00 to 3D90. Since there are 608 locations above 3D90 and only 400 are required by the multiply routines, residual memory is available at the top of RAM.

An example of monitor will illustrate how it works. The example will illustrate how to examine a memory position (i.e., display contents of memory on the LEDS). First the operator presses the Halt button. Monitor recognizes the interrupt, halts the computer and displays on the LED's the address of the next program instruction that will be executed. Next the operator presses the display memory key. Monitor determines that the display memory function is required. It displays a 2 on the highest order LED indicating that the EM key was depressed. Then it prepares to fetch a memory location, and then halts and waits for the operator to proceed. Next the operator depresses in succession 4 keys which are the memory address entering, highest order hexadecimal number first. Monitor then moves the memory contents of that position to the LED display and waits for the next keyboard instruction. In summary, the operator presses Halt, EM, XXXX, on the numeric Keyboard and Monitor displays on the LED's the contents of memory location XXXX. If the operator wishes to see the next position he presses the continue button. This button sequences thru memory one step at a time executing the function initially loaded (i.e., deposit, or examine memory).

Keyboard Functions

The following describes the keyboard functions:

Reset

Reset causes the processor to start at location zero. The PROM program at location zero initializes the problem (see related section under software) and then the processor is programmed to Halt. This allows the operator to do necessary tasks prior to system operation. Subsequently, the operator causes the processor to proceed by depressing the Start key.

Examine Memory

Displays the contents of memory on the LED's.

Keyboard Mnemonic	Meaning	Description																		
HLT	Halt	Pressing this key causes an interrupt, sending program control to the diagnostic software.																		
RST	Reset	Hardware reset. Restores program counter to zero.																		
EM	Examine memory	After pressing this function key, the diagnostic software will expect four hexadecimal numbers to be input from the data keyboard, indicating the address to be examined. It will then display the contents of that memory location.																		
DM	Deposit memory	The DM routine expects six entries from the data keyboard. The first four of these are formed into the 16-bit address and the last two form the 8-bit data byte to be stored.																		
CO	Continue	Following an EXAMINE MEMORY or DEPOSIT MEMORY, the operator may automatically increment the address pointer by pressing CONTINUE. The software will then display the contents of this new location or will be ready to accept two hexadecimal digits for data entry.																		
ER	Examine register	After pressing ER the software expects one hexadecimal digit from the data keyboard indicating which of 8 registers is to be displayed. The routine will then display the contents of this register.																		
DR	Deposit register	After pressing DR the software expects three entries from the data keyboard, the first digit indicating which register is to be modified, and the last two digits formed into the 8-bit byte to be moved into the register. The registers are given the following numerical assignment: <table><tr><td>Register</td><td>Number</td></tr><tr><td>B</td><td>0</td></tr><tr><td>C</td><td>1</td></tr><tr><td>D</td><td>2</td></tr><tr><td>E</td><td>3</td></tr><tr><td>H</td><td>4</td></tr><tr><td>L</td><td>5</td></tr><tr><td>A</td><td>6</td></tr><tr><td>PSW</td><td>7</td></tr></table> (Processor status word)	Register	Number	B	0	C	1	D	2	E	3	H	4	L	5	A	6	PSW	7
Register	Number																			
B	0																			
C	1																			
D	2																			
E	3																			
H	4																			
L	5																			
A	6																			
PSW	7																			
RS	Return	By pressing this key, the software will restore all register contents and condition bits to their values prior to entering the diagnostic software and will then return program control to the location being executed prior to entry into the diagnostics.																		
CA	Address compare	This function uses comparators to compare the address bus to a software stored 16-bit number. After pressing this key, the software will expect four entries from the data keyboard which are formed into the 16-bit number loaded into the comparator. A RETURN is executed automatically by the software and upon occurrence of the inserted address, program control is returned to the diagnostic software.																		
SS	Single step	After pressing this key, the software will automatically execute the RETURN routine and will execute the instruction prior to entering the diagnostic software. Program control is then returned to the diagnostics.																		
ST	Start	Causes the processor to return.																		
SML	Set Multiply Constant	This function expects the OK or change key to be depressed. If change is signaled it expects two hexadecimal entries. It will then generate a fast multiply routine load it in RAM and display the next multiply constant for the operator to OK or CHANGE. Twenty constant must be approved.																		
OK	Okay	Indicates to SML approval of constant.																		
CH	Change	SML expects two hexadecimal numbers to be input from the data keyboard. SML then generates multiply routine from numbers loaded and loads in RAM.																		

Figure 40 Display Processor Keyboard Explanation

GP77-0549-72

<u>Halt</u>	Causes the computer to stop and wait for a keyboard input. Halt displays the next instruction address.
<u>Examine Register</u>	Displays register contents on LED's.
<u>Deposit Memory</u>	Allows user to load any RAM position.
<u>Deposit Register</u>	Allows user to deposit register.
<u>Set Multiply</u>	User may change any multiply constant. The next constant is displayed on the LED's. Once this mode is entered all twenty multiply constants must be OK or changed.
<u>Single Step</u>	The computer executes one program step. The address of the next instruction is shown on the LED's.
<u>Continue</u>	Is used with the Examine memory, a Deposit memory function. It sequences to the next memory position implementing the same function used previously.
<u>Restart</u>	Is used to reenter the program from the Halt mode.
<u>Compare Address</u>	The computer stops at the desired address. The next instruction is displayed.
<u>OK</u>	Is used with SML. It leaves the constant unchanged and the next constant is displayed.
<u>Change</u>	Is used with SML. The user enters the desired constant on Keyboard 2.
<u>ST</u>	After pressing this key, the software will execute the RVS control software.

5.2 CAMERA ELECTRONICS BOX

The Camera Electronics Box (CEB) interfaces the remote camera shaft encoders and servo amplifier via the serial data transmission line to the home station microprocessor. The CEB's primary function is to send and receive data. It sends gimbal position data to the microprocessor and receives servo-motor commands from the microprocessor.

The transmitter system is split into two identical sections, one handling pitch axis data, and the other yaw axis data. The transmitter section sends the 13 bit shaft encoder word (one for each axis) up the serial line in two eight bit words to the processor. The first byte contains the eight low order bits, the second byte contains the remaining five higher order bits. The 3 excess bits (the highest bits unused) are set to zero.

The receiver system, like the transmitter is split into two identical subsystems; one for each axis, pitch and yaw. The receiver subsystem output consists of two 8 bit parallel-parallel data latches which are input to two 12 bit digital-to-analog converters.

The heart of the camera electronics box is the Universal Asynchronous Receiver/Transmitter (UART). This device is an LSI subsystem which accepts parallel binary words consisting of 5 to 8 data bits, and outputs them as serial words with one or two stop bits and a parity option. The UART is a single monolithic chip, is TTL compatible and its strobed outputs are tristate logic.

Block diagrams of the UART's Transmitting and Receiving sections are shown in Figure 41(a) and (b).

5.2.1 System Clocks and Timing

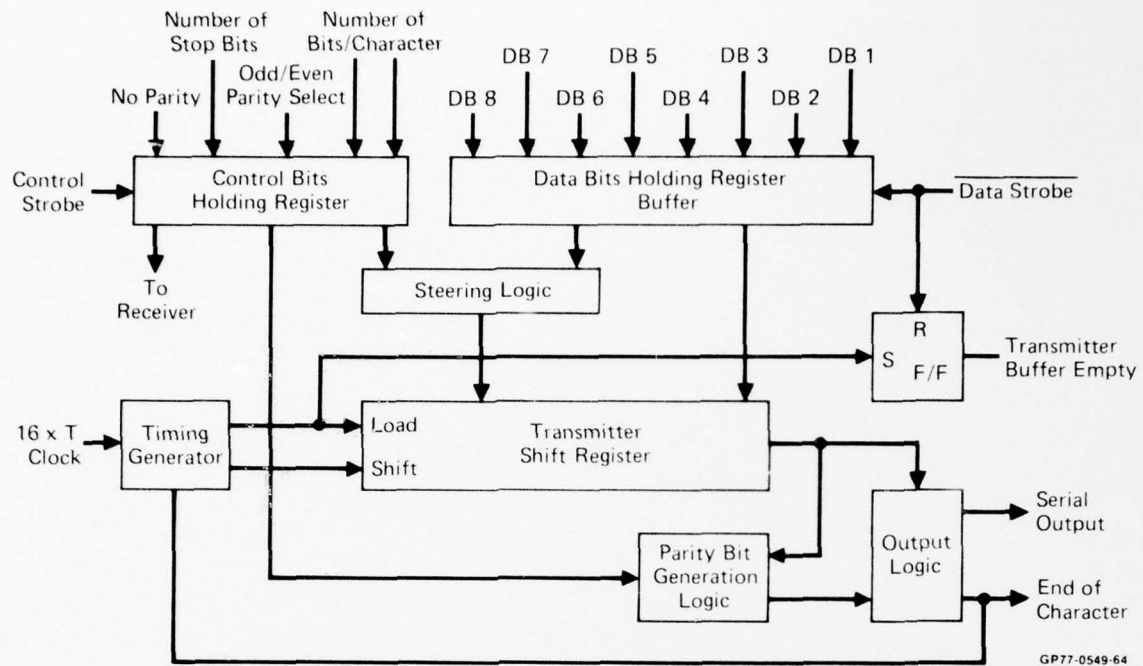
The basic computation cycle (M-clock) runs at 100 Hz. The system clocks runs at 153.6 KHz, the frequency required by the UART to establish a baud rate of 16. This is the maximum asynchronous baud rate of the Universal Synchronous Asynchronous Receiver/Transmitter (USART) and UART. The transmission of one byte takes approximately 1.2 μ sec. Two bytes per half cycle of M-clock are required, thus the timing margin of the system is approximately 50%. No measurements were made of the computation cycle length but some results indicated the computer timing margin is greater than 50%. Thus, the serial transmission line determines the maximum M-clock frequency.

Increasing M-clock would allow the design of a wider bandpass system, however since many factors must be considered (i.e., motor saturation, noise levels, accuracy, load disturbances) there is not a clear cut ratio between bandpass and M-clock frequency.

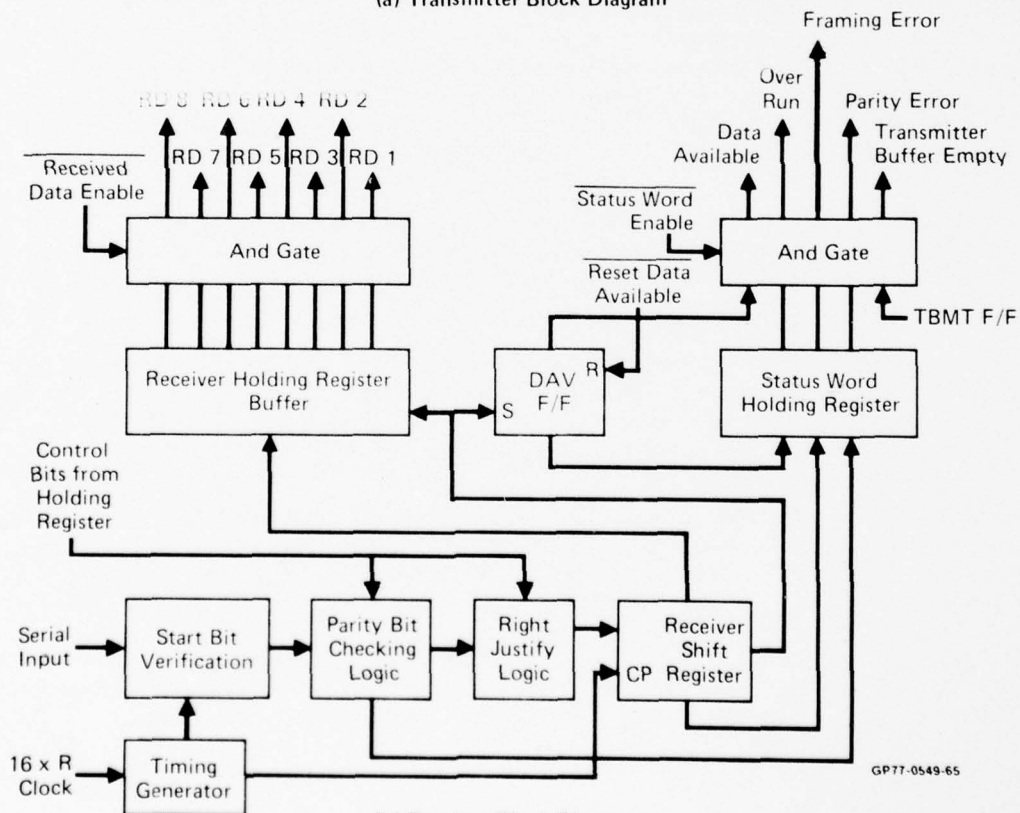
The initial design proceeded with an M-clock of 100 Hz, thus the basic sample rate of the system is 10 msec, 5 msec for each axis. Synchronous transmission was considered but preliminary work indicated that it might prove difficult to operate a 400 ft. transmission line in the synchronous mode. The asynchronous mode allowed design flexibilities because the 156.3 KHz clock could be a local oscillator or it could, if feasible, be sent over the transmission line. The final design sends the system clock over the transmission line. This required careful attention to the line driver selection and impedance matching of the receiver.

5.2.2 Control Logic

The control logic routes the incoming and outgoing bytes to the transmitter and receiver sections.



(a) Transmitter Block Diagram



(b) Receiver Block Diagram

Figure 41 Universal Asynchronous Receiver/Transmitter

Transmitter Section

The control logic is symmetric for both axes. Figure 42 contains a block diagram of the CEB Design. The pitch axis is enabled by the positive

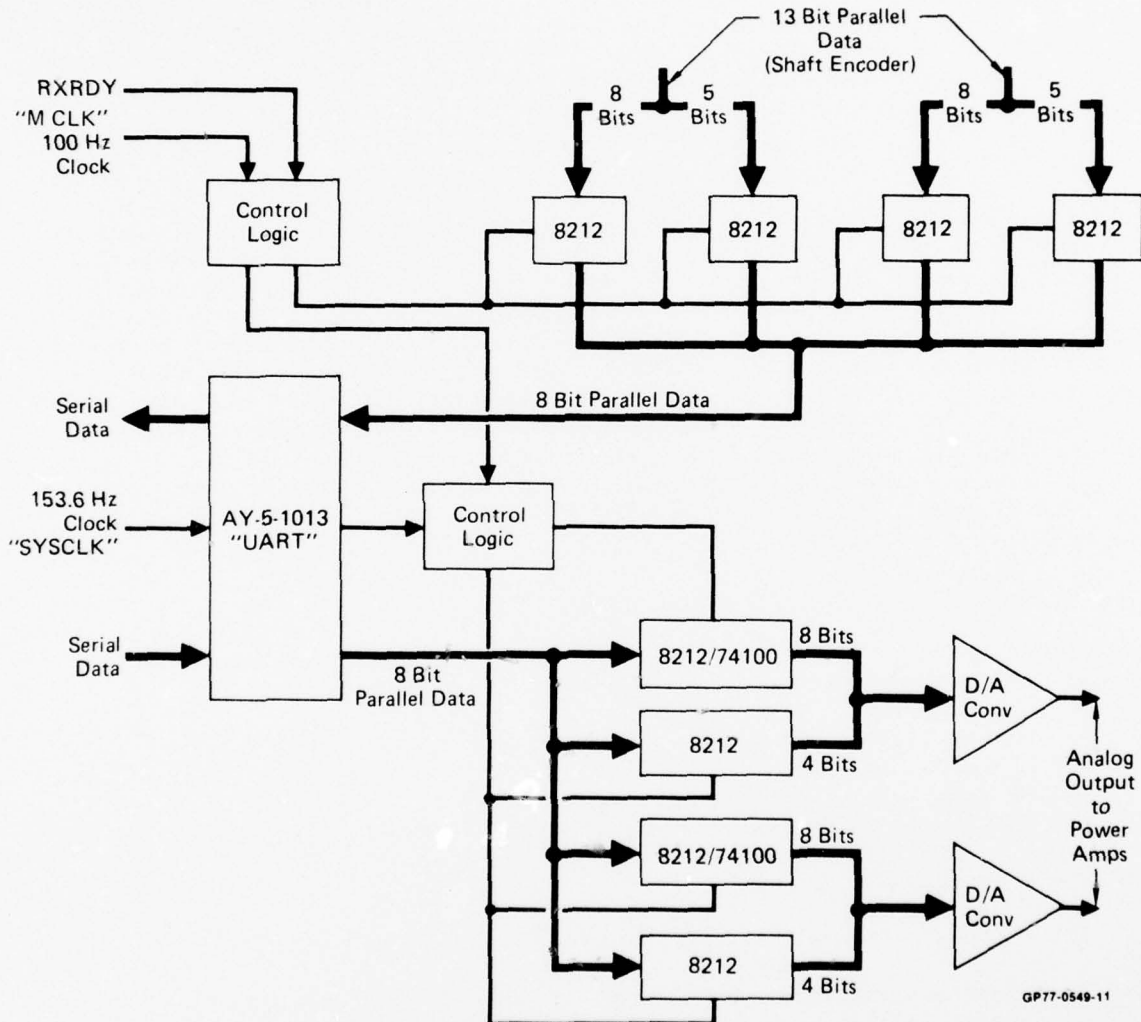


Figure 42 Camera Electronics Box Block Diagram

M-clock and the yaw axis is enabled by the negative M-clock. When M-clock goes positive the pitch axis encoder output is stored in data buffers, (the shaft encoder output continually tracks shaft position). The first buffer, (the low order bits) is strobed onto the data bus, while the other three latches are in the high impedance state. The falling edge of the data strobe (DS) pulse on the UART causes the shift register to transmit the data out on the serial output line. When the first byte of the transmission is complete, a real time interrupt is generated at the microprocessor. The microprocessor services the interrupt and generates a RXRDY pulse to the CEB. Upon receipt of the pulse, the second byte is strobed onto the data bus to the UART and the sequence is repeated. The second RXRDY pulse sent down by the microprocessor is ignored by the CEB and the box now waits for M-clock to go negative and then sends up the yaw information in the same manner. In summary, for each half cycle of the M-clock the encoders are read, stored in latches and sent to the microprocessor in two eight bit words. These bytes are received by the microprocessor and stored in memory and the microprocessor acknowledges receipt of these words to the CEB via the RXRDY pulse.

Receiver Section

The receiver section is independent of the transmitter section including UART functions, thus allowing for complete asynchronous operation. When M-clock goes positive, the microprocessor initiates transmission of the first (high order bits) pitch axis command byte. When this transmission is complete, the receiver's control logic strobes the first byte into a buffer. The microprocessor then initiates transmission of the second byte. Upon completion of the second byte transmission, the control logic loads the second byte into a buffer and then it inputs both bytes to the digital-to-analog converter for the pitch axis. The D/A (12 bits) receives a full word at one instant in time just after the receiver has loaded both bytes of information into data storage. This word remains on the D/A input until the end of the next cycle of the M-clock.

5.2.3 Camera Box Electro Mechanical Description

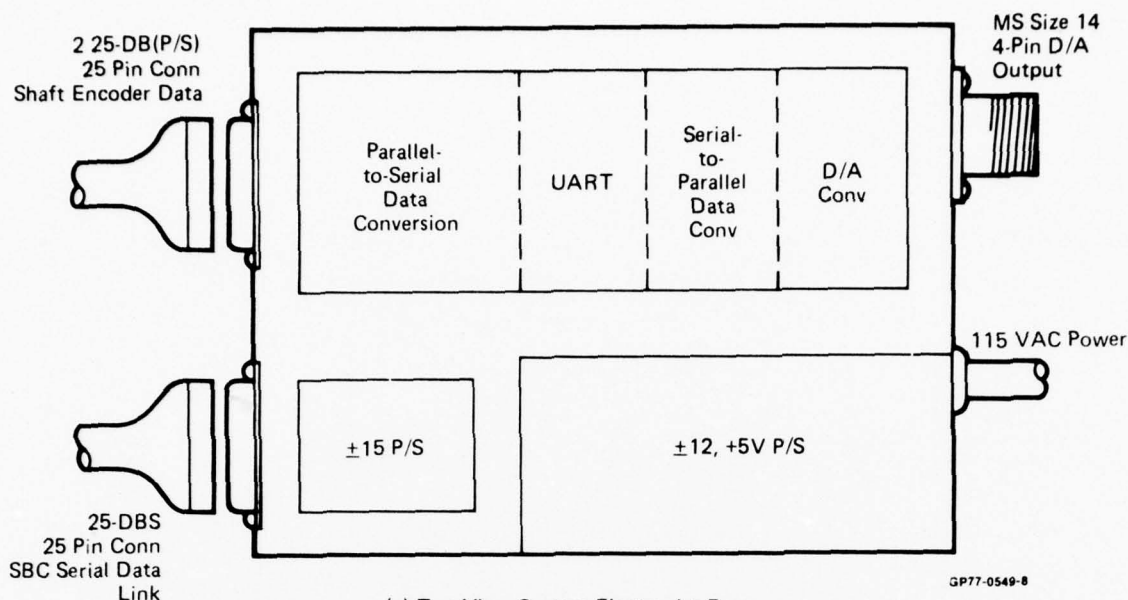
The camera electronics box is connected to the microprocessor via five twisted pair cables. The processor supplies the system with:

- 1) System clock - 153.6 KHz
- 2) M-clock - 100 Hz
- 3) RX Data - Servo-amp command signal
- 4) RXRDY - Microprocessor acknowledgement of receipt of Position Data

The camera box sends

- 1) TX Data - A Position Data down to the SBC 80 microprocessor.

The shaft encoder words are brought to the CEB from the gimbals using 2-18 wire ribbon cables and DB25 connectors, and the D/A output is sent to the power amp over two twisted pairs, through an MS3106-14S-4P connector. The power amp outputs are run in separate cables to the torque motors. Thirteen (13) bit Baldwin shaft encoders are used to determine shaft position. Figure 43(a) shows the CEB LAYOUT and Figure 43(b) shows the board layout. Component descriptions shown in the board are listed in Figure 44. Figure 45 and 46 are schematics of the transmitter and receiver sections, respectively of the CEB.



(a) Top View Camera Electronics Box
Figure 43 Camera Electronics Box

5.3 SYSTEM SOFTWARE

Each of the four PROMS are assigned a system software function for ease of PROM management. PROM #1 (memory locations 0-3FF) is devoted to the system initialization and the interrupt handler. PROM #2 (memory locations 400-7FF) contains the Yaw Axis control equation software. PROM #3 (memory locations 800-BFF) contains the diagnostic software. PROM #4 (memory location C00-FFF) has the software for the system pitch axis. The detailed line by line listing of the software for all of the PROMS is included in Appendix D. Software flow diagrams are shown in Figure 47.

5.3.1 PROM Programming

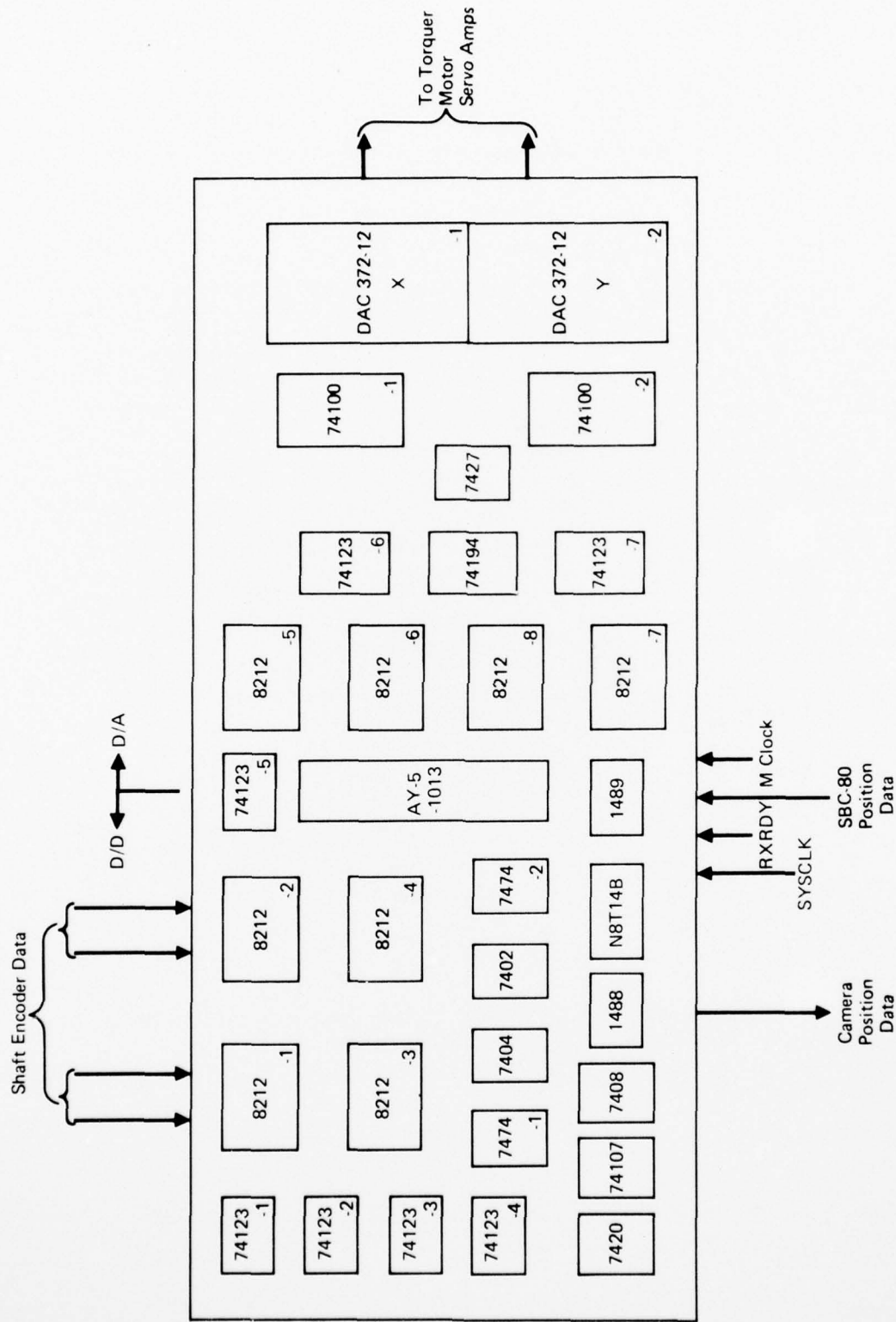
An Intel 8080 Cross assembler is available on the PDP 11 Digital Equipment Computer. To program a PROM, a source program is created on the PDP 11 computer. It is assembled on the PDP-11 by the following commands into an 8080 binary language which is used as an input to the PROM programmer. Commands for using the assembler are:

```
$ AS KB:, CMI
RU INXAS
File, LP: < File since the assembler cannot handle a full PROM, a
program MERGE can be used to link two programs together:
```

```
$ AS File 1.OBJ, 1
AS File 2.OBJ, 2
AS File 3, 3
RU MERGE
```

Subsequently, the .OBJ files can be punched on paper tape with commands

```
$ AS File 3, 1
$ AS PP:, 4
RU CHANGE
```



(b) SBC-80/Remote Camera Data Transfer Board
Figure 43 Camera Electronics Box

Qty	Part No.	Description
8	8212	Eight Bit Input/Output Port
7	DM74123	Dual One-Shot
2	7474	Dual D-Type Flip Flop
1	7404	Hex Inverter
1	7402	Quad 2 Input NOR
1	7420	Dual NAND
1	74107	Dual J-K Flip Flop
1	7408	Quad 2 Input AND
1	1488	Line Driver
1	1489	Line Receiver
1	74194	4 Bit Shift Register
1	7427	Triple 3 Input Positive NOR
2	74100	8 Bit Latch
2	DAC372-12	D/A Converter
1	AY5-1013	Universal Asynchronous Receiver/Transmitter
1	N8T14B	Line Receiver

GP77-0549-63

Figure 44 Camera Electronics Box Component List

The resulting paper tape can then be read into the PROM programmer.

5.3.2 PROM #1, Interrupt Handler Software

As real time interrupts are generated to the microprocessor, it is routed to memory location 38, whereas the reset button causes the computer to start at memory location zero. As a consequence, memory locations zero thru 37 are devoted to the necessary housekeeping functions required to initialize the system. The processor then encounters a program Halt. The start button causes it to advance past the Halt where it enters the active system program. The program enables all interrupts and waits in a backward forward loop located at memory positions 30 and 33 for interrupts. A listing of the program is shown in Figure D-1, Appendix D.

Interrupts

There are three system interrupts; system clock, receiver, and transmitter. The system clock generates an interrupt every 0.010 sec. Each system interrupt causes the computer to proceed thru the yaw and pitch control equations and update the system commands. Concurrently, the receiver and transmitter send data over the serial transmission line link to the remote camera. The receiver interrupt causes the computer to store the received word in memory. The transmitter interrupt causes the computer to load the transmitter with a new command word.

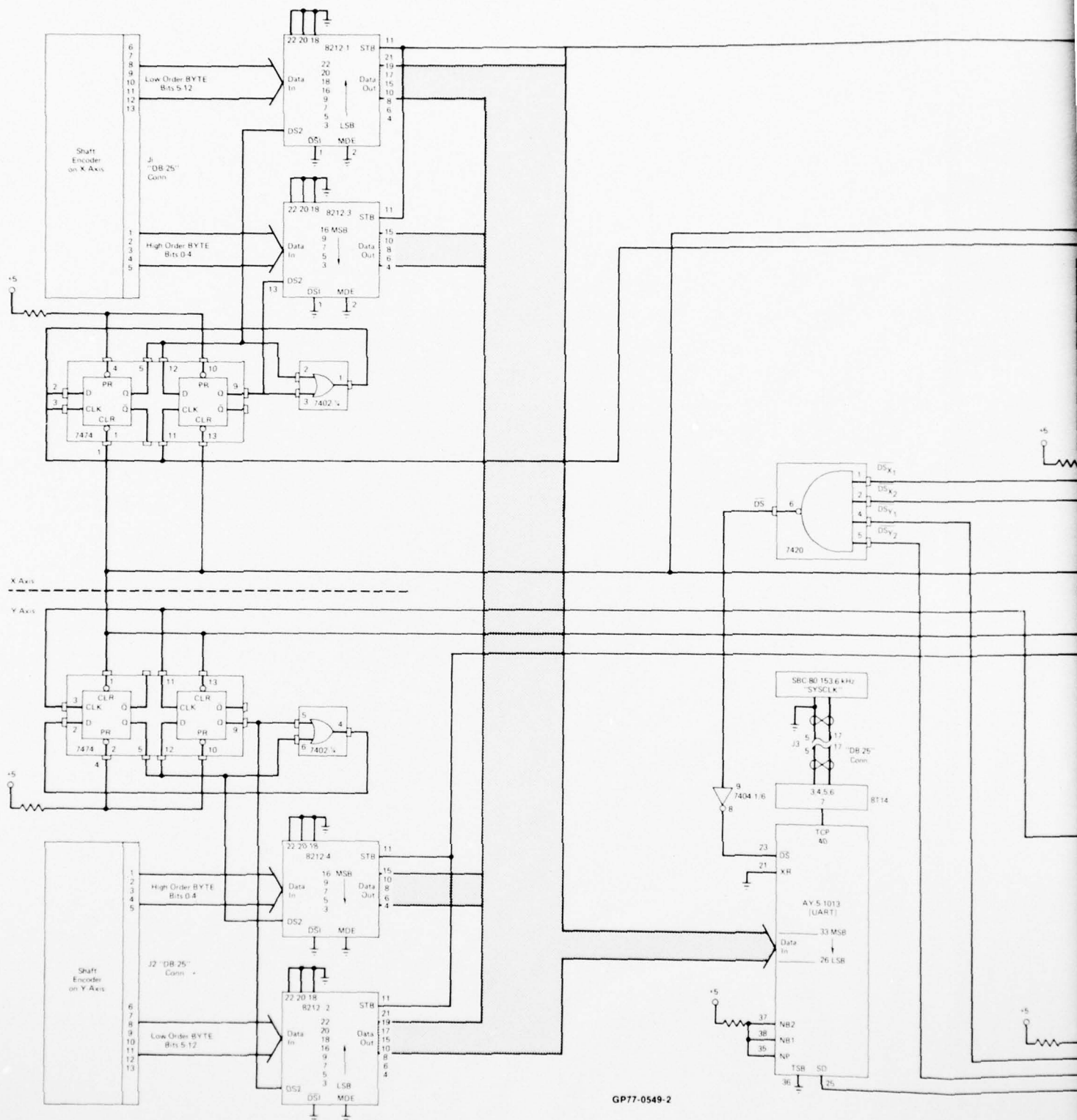
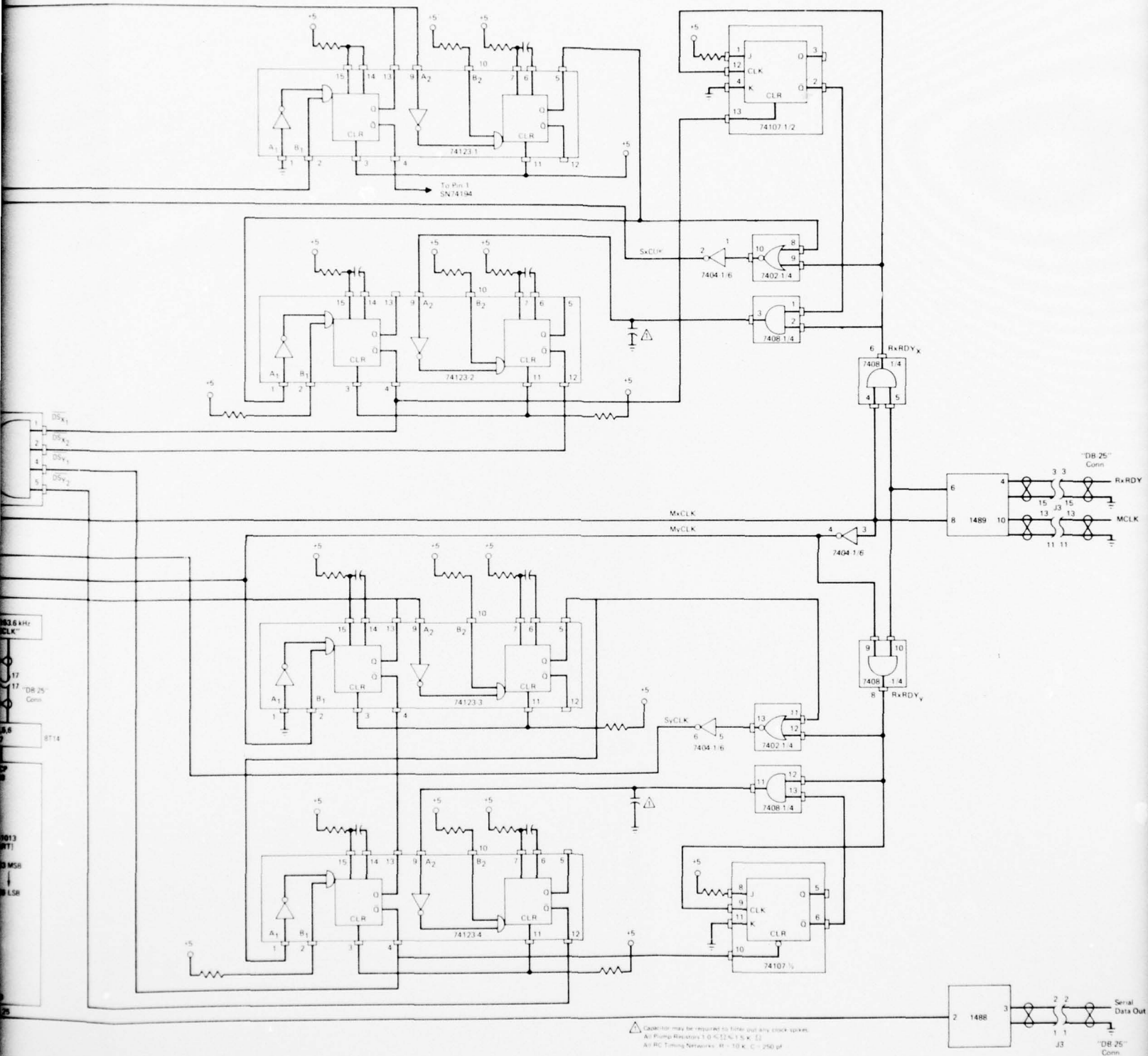
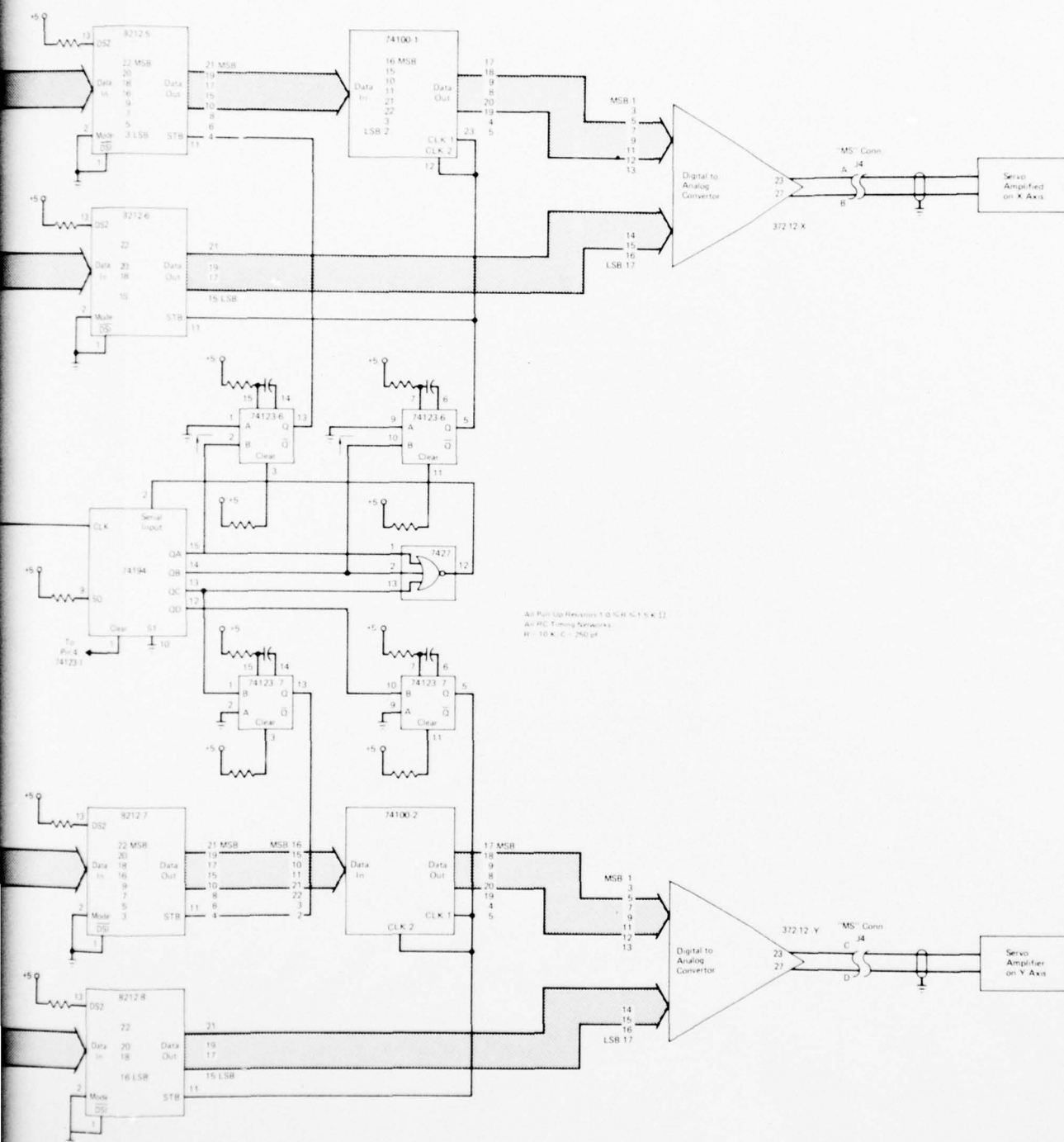


Figure 45 Camera Electronic Box Transmitter Circuit Diagram



GP77-0549-3



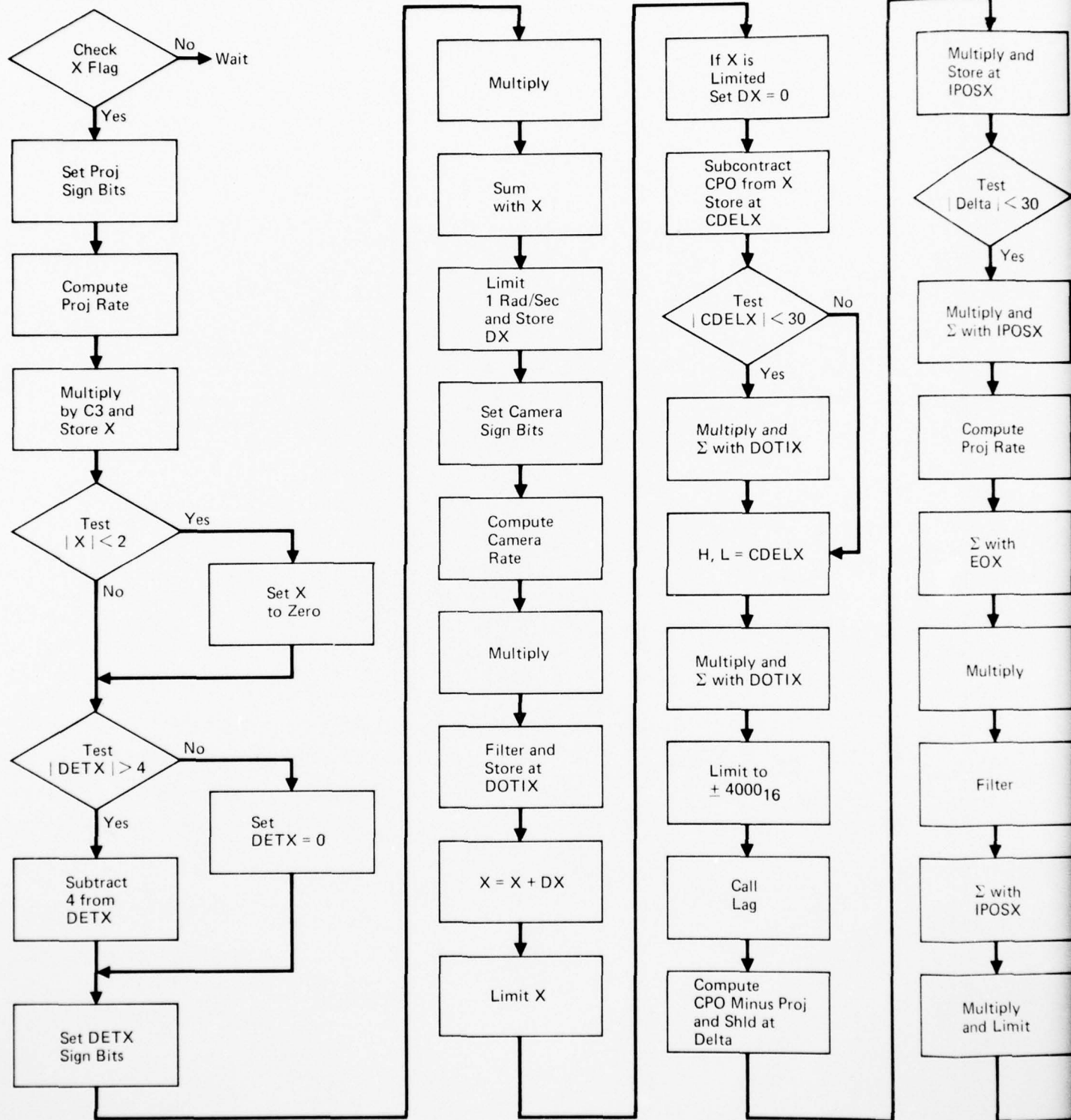
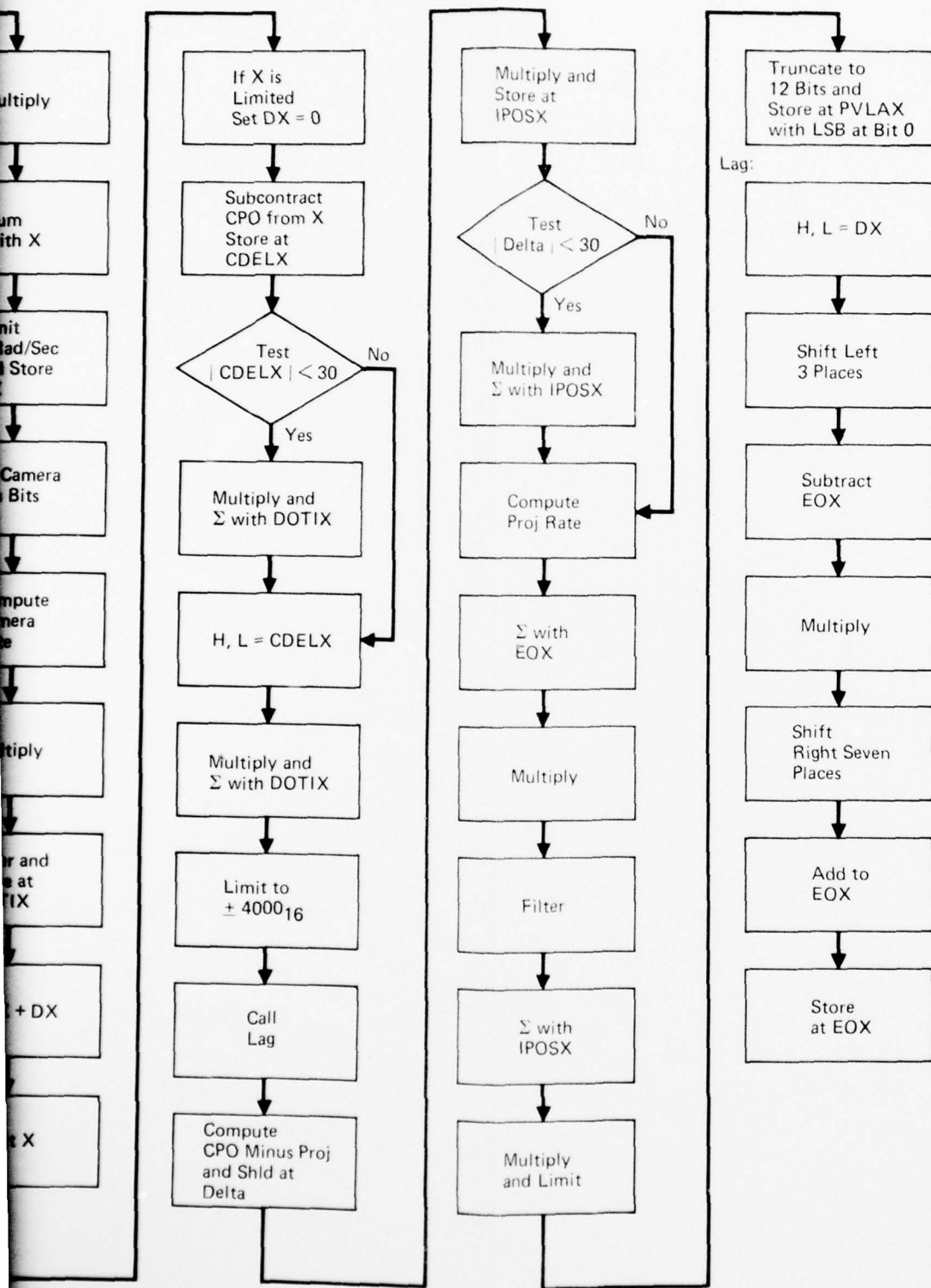


Figure 47 Software Flow Diagram

GP77-0549-29



GP77-0549-29

When an interrupt occurs, the following sequence is executed:

- 1) Save the status of the machine,
- 2) Poll the interrupt ports and determine the specific interrupt,
- 3) Reset all interrupts, make appropriate interrupts active determined by priority of interrupt requesting service,
- 4) Jump to interrupt service routine,
- 5) Restore status of machine and return to sequence prior to the interrupt.

System Interrupt Service Routine

This routine is the primary or key interrupt which determines the system data sample rate. The following events happen after a system interrupt:

- 1) Load the transmitter with a new word and load the transmitter counter used by the transmitter service routine
- 2) Initialize the receiver counter, Y Flag, and X Flag
- 3) Read the Projector Encoders
- 4) Output command updates to the Projector Power Amplifiers
- 5) Read the X and Y A/D's
- 6) Compute the Yaw and Pitch control equations. The output of these equations update system commands.

Receiver Interrupt Service Routines

This routine stores the word just received in memory and resets the receiver. The receiver is then ready for the next word. Initially, the service routine loads the receiver counter. Since the receiver normally reads four words per sample interval, the service routine checks the counter. If more than four words have been received an error has occurred. In this case, the data from the last cycle is loaded into the yaw axis data memory positions. If the counter is correct, the routine reads in the receiver contents and stores the data in the memory position indicated by the counter. Next the routine increments the counter and stores it in memory. When two words have been received, X Flag is loaded. This indicates that new data is ready for processing in the pitch axis control equations. If the third word has been received the routine loads the transmitter and returns to the previous program before the interrupt occurred.

5.3.3 Transmitter Service Routine

This routine loads the transmitter with words from memory each time the transmitter is ready to send a new word. The pitch data is sent out first since it is always ready at the beginning of a clock cycle. The routine loads the transmitter counter, decrements the counter and sends a word to the transmitter from memory. When the counter indicates Yaw commands (i.e. third word) the routine checks Y Flag. Y Flag indicates that the Yaw axis computation is done and that new Yaw commands are ready. If data is available the routine sends the data and returns the computer to the previous program.

5.3.4 PROM #2 Yaw Control Equations

These equations are on PROM #2 and start at location 400. Due to the complexity of the system every effort was made to keep the pitch and yaw equations alike. As a consequence PROM #4 except for changes peculiar to the pitch axis is similar in program flow to PROM #2. First the new data word is called from memory and the bits 14 thru 16 are set so that the computer treats the encoder as a double precision word with the LSB of the encoder located at the LSB of the computer. The compensation equations are calculated and placed in intermediate storage at CAMAY. CAMAY is limited to 1 rad/sec and is input to the integrator driving the camera. Next the camera servo equations are processed. These equations represent a rate command position hold servo. The camera encoder is converted to a double precision word with the LSB of the encoder corresponding to the LSB of the computer. The unfiltered first difference is computed and stored at location 3FF0. The filtered gimbal rate is limited and multiplied by the constant MYLVB. MYLVB is stored at location 3D82 as a double precision word with the decimal at the left with one sign bit. At location 4F9 the digital integrator sums in the update CAMAY and limits the integrator output at gimbal stops of $\pm 90^\circ$. These stops are inside the mechanical stops of the gimbal. The camera encoder is subtracted from the integrator output and stored at CDEL location 3D72. Next the position feedback is limited and multiplied by the constant MYLVK. Subsequently, the rate feedback signal is summed with the position signal. This sum is multiplied by TORQY and limited. It is stored at CCMAY as a double precision word. The transmitter service routine sends CCMAY to remote station where via the hardware it is truncated to a 12 bit word as input to the D/A driving the power amp. Next LAG is called. This subroutine is a filter which provides a signal to the projector. The signal provides accurate projector to camera tracking. The camera error is tested. If it is too large, the camera input is taken as the input to the projector. The program now computes the projector servo equations which are a basic position servo with a modified rate command from LAG. The program proceeds as follows: Beginning at memory position 696 the position feedback is calculated, limited and multiplied by MULBY. This result is stored at IPOSY. At location 6C5 an integral channel is implemented for small input errors. If the error is large the integral channel is bypassed. The output is summed with the contents of IPOSY and stored at IPOSY. Next the first difference of position is calculated and stored at 3FF2 with the LSB of the result at the LSB of the computer. This unfiltered difference is summed with EOY, the LAG signal mentioned previously and the result is limited and filtered to provide a suitable rate feedback signal. It is stored at 3D64.

This result is summed with the position feedback signal. The computer word has one sign bit and the decimal to the left in the double precision word. Since the hardware requires the decimal to the right, the software truncates the word to 12 bits and shifts the result to the right so that the LSB of the word is at the LSB of the computer. This result is stored at PVLAY. Y Flag is set to indicate that new data is at PVLAY. Next the routine checks if the transmitter has already tried to send the data. This is indicated by the high order bit of Y flag. If it has the routine it initiates the transmission. If not, the routine continues to the Pitch control. The computer listing is contained in Figure D-2.

5.3.5 PROM #3 Diagnostic Software

Discussed earlier in Section 5.1.2. Computer listing is contained in Figure D-3.

5.3.6 PROM #4 Pitch Control Equations

X Flag is tested to determine if new data has been received. If not the routine waits for new data. After new data has been received, the pitch equations are processed similar to the yaw equations described above. Different multiply constants are used. A complete listing of the equations are shown in the Figure D-4. In the software equations X is used to designate the Pitch Axis and Y is used to designate the Yaw Axis of the system. The new Pitch Axis commands are stored at PVLAX as a double precision word. At the beginning of the next clock cycle the transmitter service routine sends the new words to the remote station. At the end of the Pitch Axis equations, the computer has completed all required up data processing per clock cycle and returns to loop waiting for the next interrupt. Timing margins indicate that the next interrupt will be from the receiver and transmitter routines.

5.4 MATH MODELS

The Remote Viewing System servos can be operated in three different modes. They are:

- MODE 1) Stand alone servos closed around each gimbal.
- MODE 2) Camera as a rate command position hold servo with rate inputs from the stick. The projector in a position servo follower to the camera.
- MODE 3) Camera and Projector in closed loop with the head controller. This option includes capability to insert the stick control in lieu of the head controller without changing the control equations.

The first mode allows the camera to be used with the projector servos disabled. It simplifies system power up because the system is stable for all gain modes.

The second mode uses the stick control as input. It can be implemented by minor program changes in the microprocessor. It can be used to achieve accurate pointing and projector to camera tracking. It is ideally suited for fine pointing but is less advantageous for tracking moving targets.

The third mode is the final system configuration which provides helmet mounted control by the operator.

AD-A046 704

MCDONNELL AIRCRAFT CO ST LOUIS MO
REMOTE VIEWING SYSTEM.(U)
JUN 77 R W FISHER

F/G 17/2

UNCLASSIFIED

ONR-CR213-129-2F

N00014-75-C-0660
NL

2 OF 3
ADA
046704



5.4.1 MODE 1

Linear Transfer Function

A simplified linear model of the servo used for each gimbal is shown in Figure 48. The integral channel was implemented and used as required for fine pointing. The equivalent transfer function is:

$$H_1(s) = \frac{AKS + AM}{S^3 + ACS^2 + AKS + AM} \quad (66)$$

where $A = 1/I$
 $K = \text{ft \# / rad}$
 $M = \text{ft \# / sec / rad}$
 $C = \text{ft \# / rad / sec}$
 $I = \text{Gimbal Inertia}$

Computer studies of ramp type inputs to the servo showed that the 100 ft. lb. torque motor on the projector azimuth axis was the system limiting factor and significant saturation occurred around 1 rad/sec. The servos were designed to minimize this saturation and provide the best possible frequency response. Figure 49 shows the response of the camera to a ramp input of

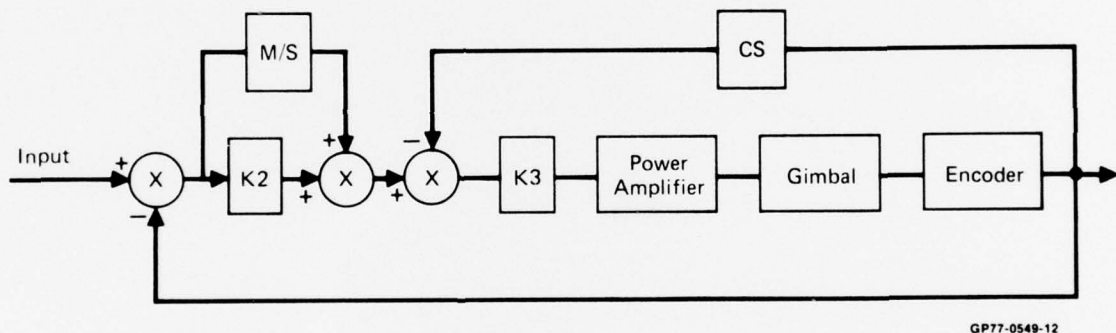


Figure 48 Mode 1 Servo Block Diagram

1 rad/sec for 0.25 sec. The camera lag is less than 0.1 sec as shown in the figure. This is consistent with an operators reaction time using stick control. Note that this lag does not cause image motion on the projector screen. The image will move because the projector remains stationary in Mode 1 operation.

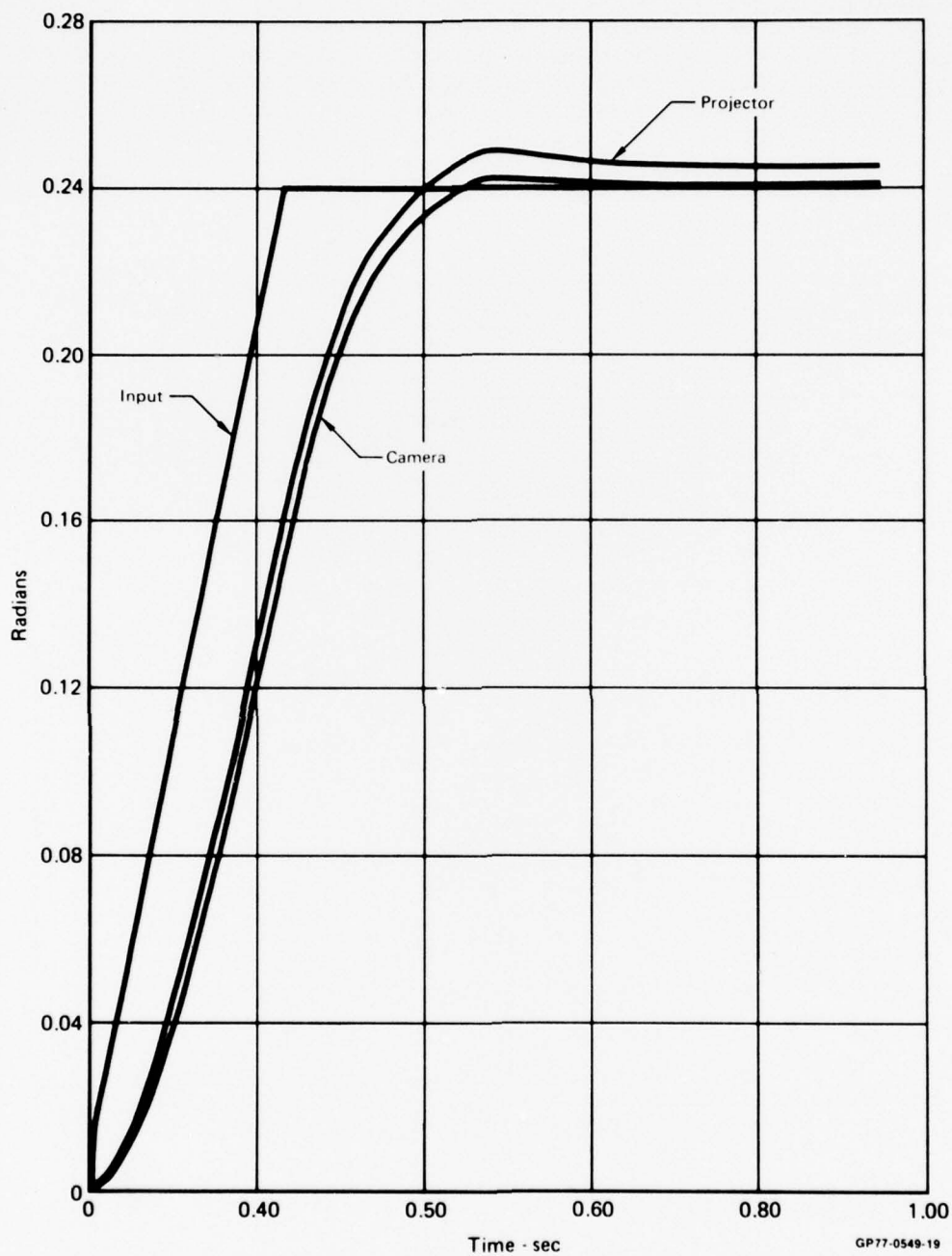


Figure 49 System Response for Stick Input
Lag = 0.12 Sec

Gains

Important gains for each axis are summarized in Figure 50. Inertias shown in the table were results of measurements made when the system was first assembled. Subsequent changes in optics and mechanical design caused these inertia figures to change. Accurate information on inertias associated with the final design are unavailable. The channel gains shown in the table were used to derive the first estimate of computer gains cognizant of the effects of non-linearities. The important non-linearities in the system are saturation, threshold, and friction. These result in overall gain reduction and apparent increase in damping.

The gains of Figure 50 were required during software development. They served as a basis for software scaling and for sizing multiply routines. Subsequently, they were used during initial system checkout.

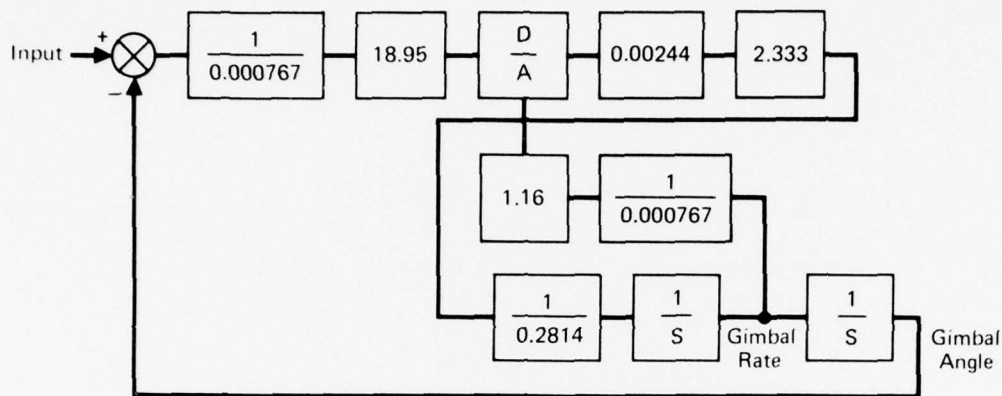
Name	Symbol	Units	Projector Azimuth	Projector Pitch	Camera Azimuth	Camera Pitch
Inertia	I	ft-lb/sec ²	1.58	0.052	0.28	0.113
Proportional Channel Gain	K	ft-lb/rad	632	20.8	112.5	45.2
Rate Channel Gain	C	ft-lb/rad/sec	63.2	2.08	11.25	4.52
Integral Channel Gain	M	ft-lb/rad/sec	7015	230	1249	501
Pwr amp Gain	KA	ft-lb/Computer Volt	19.2	0.493	2.28	1.4
Computer Rate Gain	G _C	—	413	530	619	406
Computer Prop Gain	G _K	—	165	212	15	10
Computer Integral Gain	G _M	—	18	23	1.7	1.1
	C	ft-lb/rad/sec	0.1528 G _C	0.0039 G _C	0.018 G _C	0.011 G _C
	K	ft-lb/rad	3.82 G _K	0.098 G _K	7.27 G _K	4.45 G _K
	M	ft-lb/sec/rad	380 G _M	9.76 G _M	726 G _M	445 G _M

Figure 50 Servo Gains

GP77-0549-14

Gains for Camera Azimuth Axis

An example of the gains involved for the camera azimuth axis are shown in Figure 51. Non-linearities not shown in the figure cause gain reduction and some phase shift. Consequently, gains were adjusted on the actual hardware to optimize gimbal performance and camera-to-projector tracking as evidenced by picture motion. The non-linearities of the system make



GP77-0549-20

Figure 51 Camera Azimuth Axis

the frequency response of the system a function of amplitude and frequency. They tend to reduce the system bandwidth. The system was designed and optimized for ramp type inputs.

5.4.2 MODE 2

Using the projector in a servo follower mode to the camera requires careful system servo design. Any error in projector-to-camera tracking **causes** picture motion on the spherical screen as viewed by the observer. The servo follower inherently has dynamic lag even though integral feedback could be used to reduce steady state errors. From qualitative considerations some dynamic error is allowable because the observer cannot follow dynamic motion faster than a few hundredths of a second. Consequently, camera and projector instantaneous rates can be unequal for short time intervals providing the steady state position error remains within acceptable limits of approximately 0.01 radians.

While there are several approaches to the problem, the **one used** in the RVS was to feed the camera rate command signal forward to the projector. This required insertion of a lag network in series, which compensates the projector for camera velocity lag. Since the camera lag is insensitive to component changes by virtue of the feedback in the servos the circuit should remain in calibration. Adjustment of the lag can cause the projector to lead

the camera or to lag the camera. Computer studies indicate the system is easier to stabilize in Mode 3 if the projector leads the camera by a slight amount. While some dynamic error still exists its magnitude and time of decay are such that no deleterious system operation is evident to the observer. A simplified linear block diagram is shown in Figure 52.

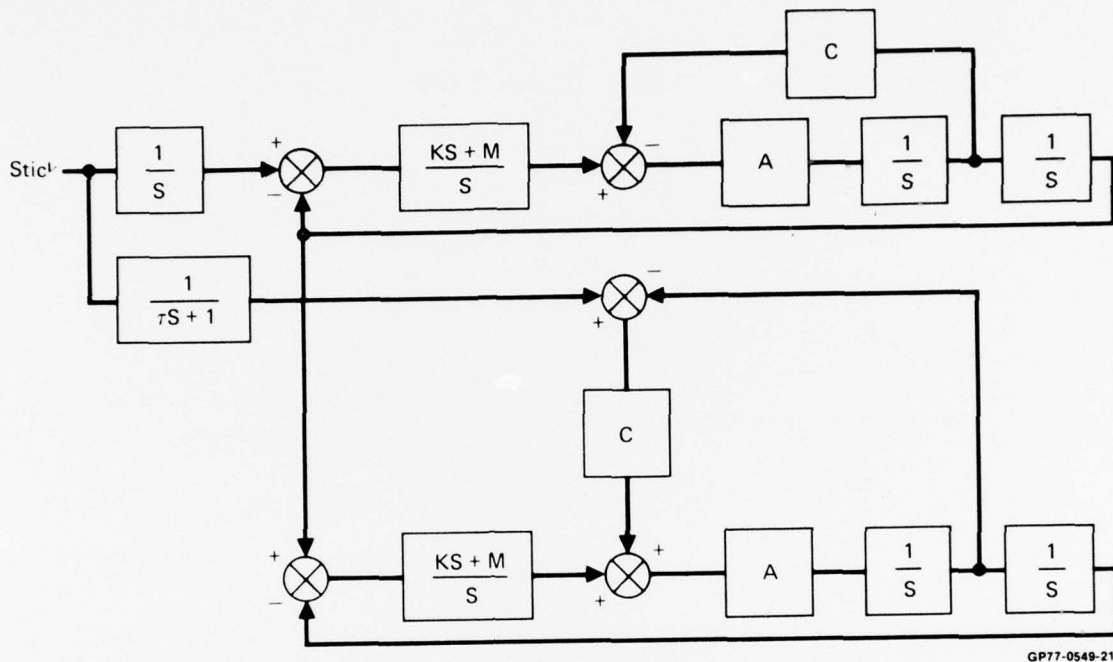


Figure 52 Mode 2 Servo Block Diagram

The output of the lag network approximates the camera velocity. If the camera velocity were being fed forward the linear projector response can be shown to be

$$H_2(s) = \frac{ACS^2 + AKS + AM}{S^3 + ASC^2 + AKS + AM} \quad (67)$$

System Response Versus Lag

Figures 49, 53, and 54 show the response of the system to maximum stick inputs of 1 rad/sec for .25 sec with values of lag in the forward loop of 0.1 and .12 sec and .14 sec. The figures show that this range of lag causes the projector to cross over the camera and change from lag to lead. The parameter was adjusted on the actual hardware to enhance projector tracking and achieve minimum picture motion.

The Figure 55 shows the system response for a stick input of max plus for 0.25 sec and then max negative for 0.25 sec. with the lag set at an optimum of 0.14 sec.

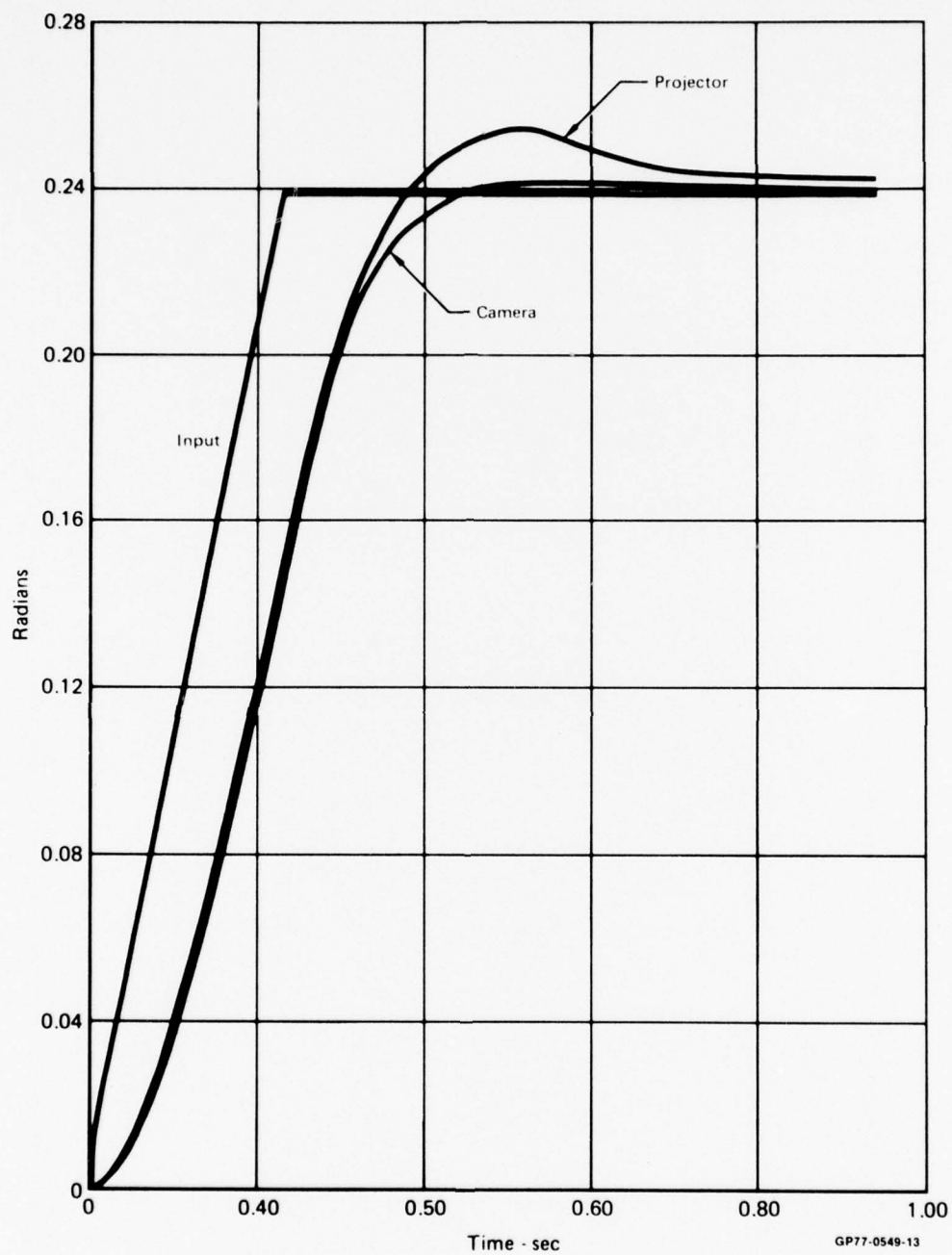


Figure 53 System Response for Stick Input
Lag = 0.10 Sec

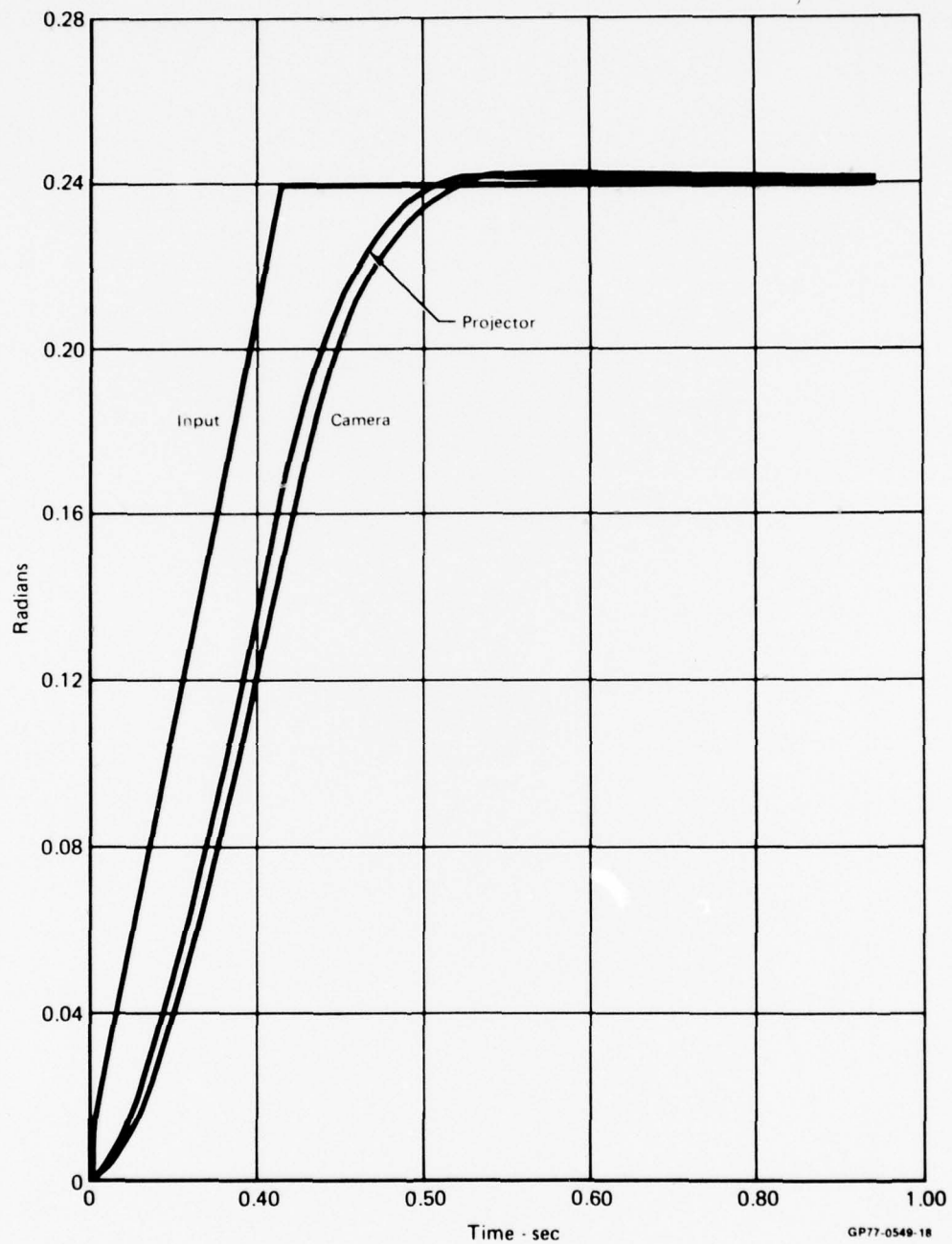


Figure 54 System Response for Stick Input
Lag = 0.14 Sec

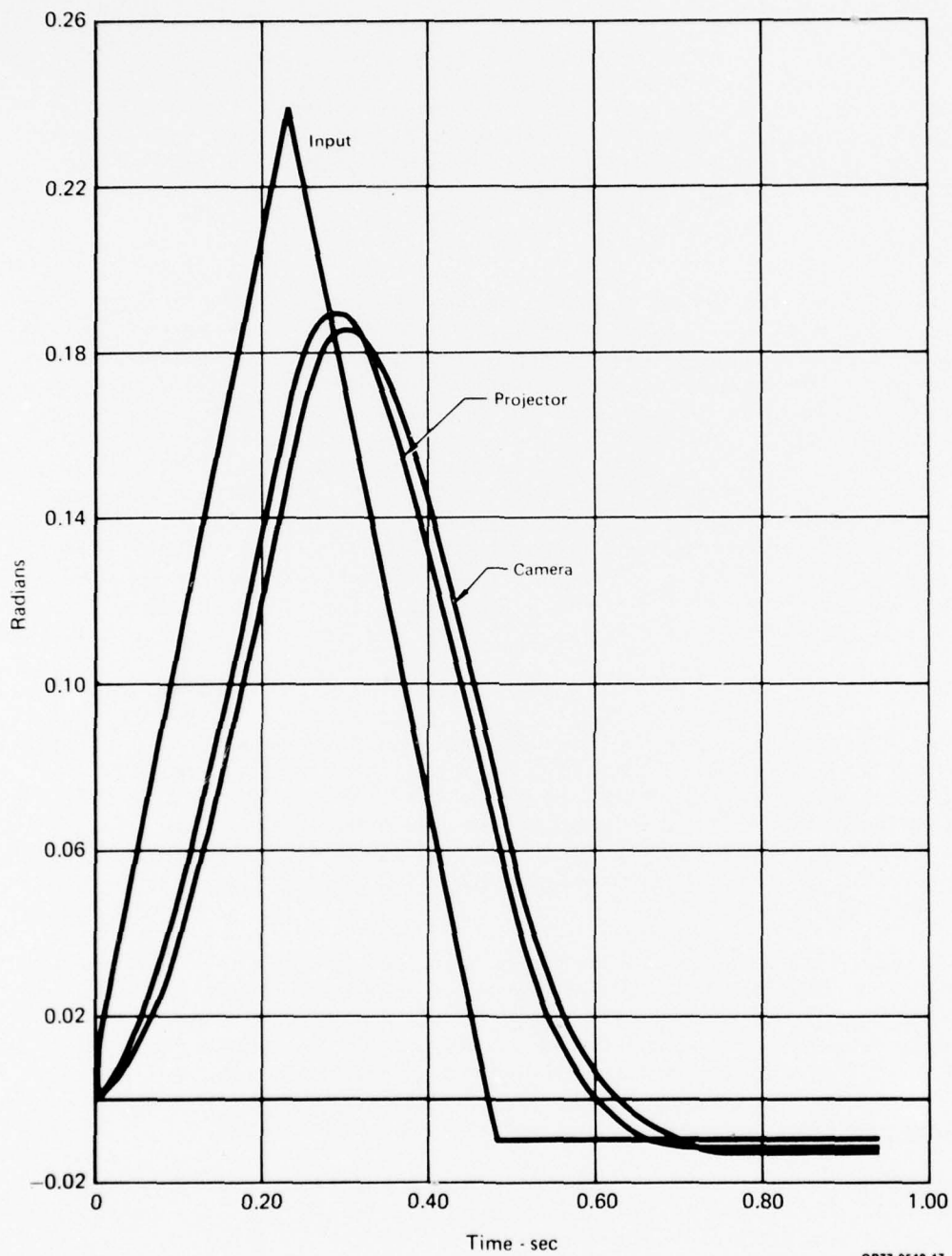


Figure55 System Response for Stick Input
Lag = 0.14 Sec

5.4.3 MODE 3

Non-Linear Block Diagram

Figure 56 is a block diagram of the final mechanization showing the feed-back loops implemented in the microprocessor. For simplicity the gimbal model is not included. The gimbals are shown as a double integration of the accelerating torque. Figures 57 and 58 show the response of the system to step inputs of the detector and for smooth Lead motion of 7 rad/sec for 0.25 sec.

Digital Model

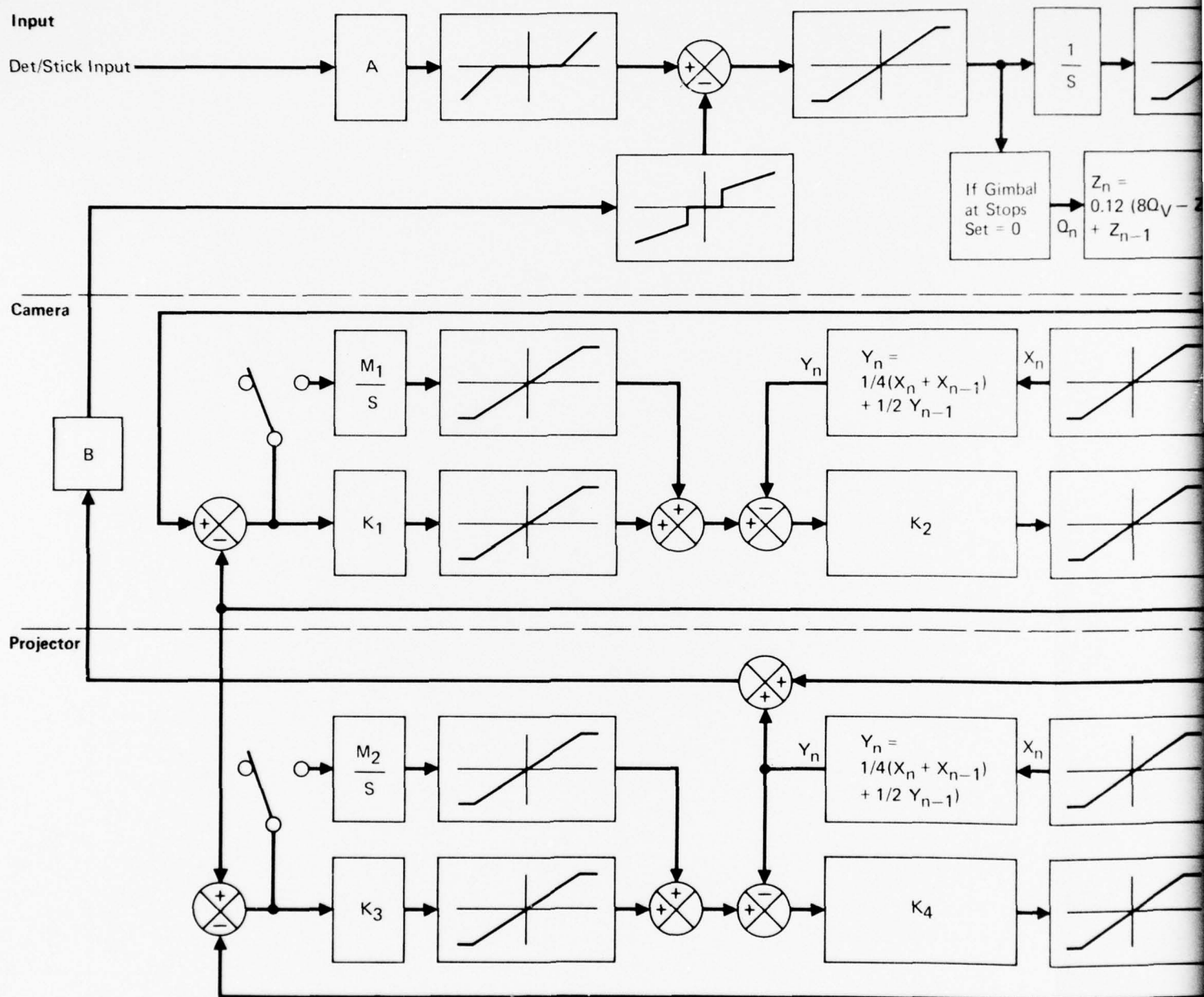
A digital simulation of one axis of the system is shown in Figure 59. This model was used to conduct parametric studies and to determine the effects of various system non-linearities. The arithmetic and sample times of the microprocessor inherent in a sampled data system were included in the model to the extent possible. This was required to accurately predict hardware performance. Dynamic friction for the camera and the projector gimbals are included. The power amplifiers were modeled as voltage amplifiers. The torque motors for each gimbal were modeled from motor specifications and gimbal inertias were taken from experimental results. The actual or final gains used in the microprocessor are in good agreement with those predicted by the model and in general correlation between hardware performance and that predicted by the model was very good. Quantitative information on the as built system non-linearities would further improve the simulation results.

5.5 SYSTEM OPERATION

At system power-up, check to see that all cable connections are made. At the base, the microprocessor has two ribbon cables with DB25 connectors coming from the pitch and yaw shaft encoders, an analog output with connector (MS3106-MS-2P) which goes to two potentiometers on the input of the servo amplifiers, and the serial I/O cable (DB25) box. Also, located on the rear panel of the microprocessor are connections for the joystick control and helmet control.

The camera electronics box requires the serial cable from the microprocessor, two ribbon cables (DB25 connectors) from the shaft encoders and the analog output (MS3106-14S-4P) cable to the servo amplifiers. When all cables have been connected and the servo amplifier input gain pots turned to the off position, the microprocessor, camera electronics box, and servo amplifiers can be powered in any order. The microprocessor may now be started by pushing the "RST" button (reset) and then the "Go" button.

Next the operator turns each camera servo gain pot to maximum. He verifies that the camera is pointed straight ahead and that it is stable. Subsequently, the projector servo pots should be set to a maximum, one at a time. When the pot is maximum the camera and projector should be stationary and both pointing at the same position.



GP77-0549-6

Figure 56 Pitch Servo Block Diagram



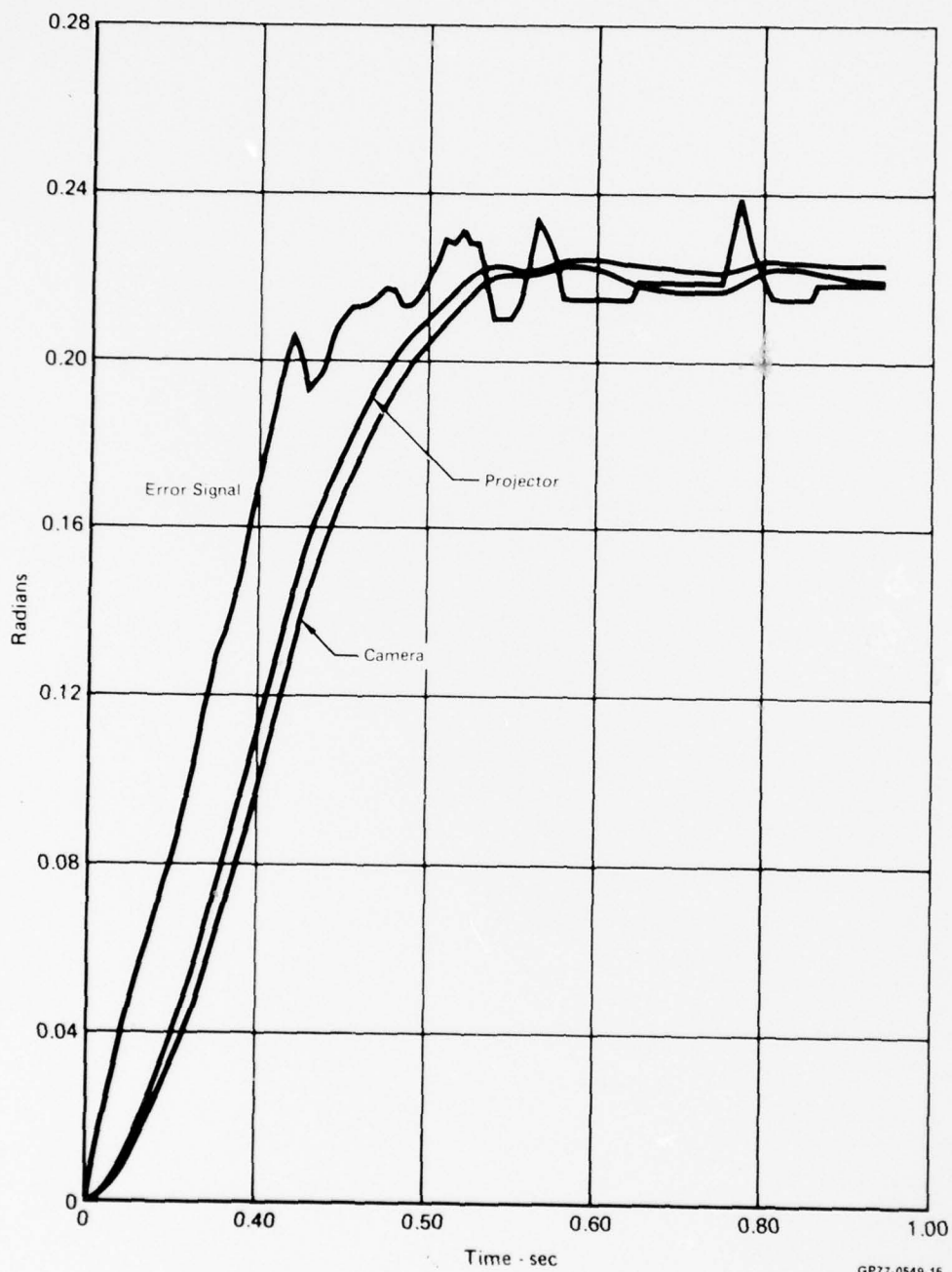


Figure 57 System Response for Ramp Input

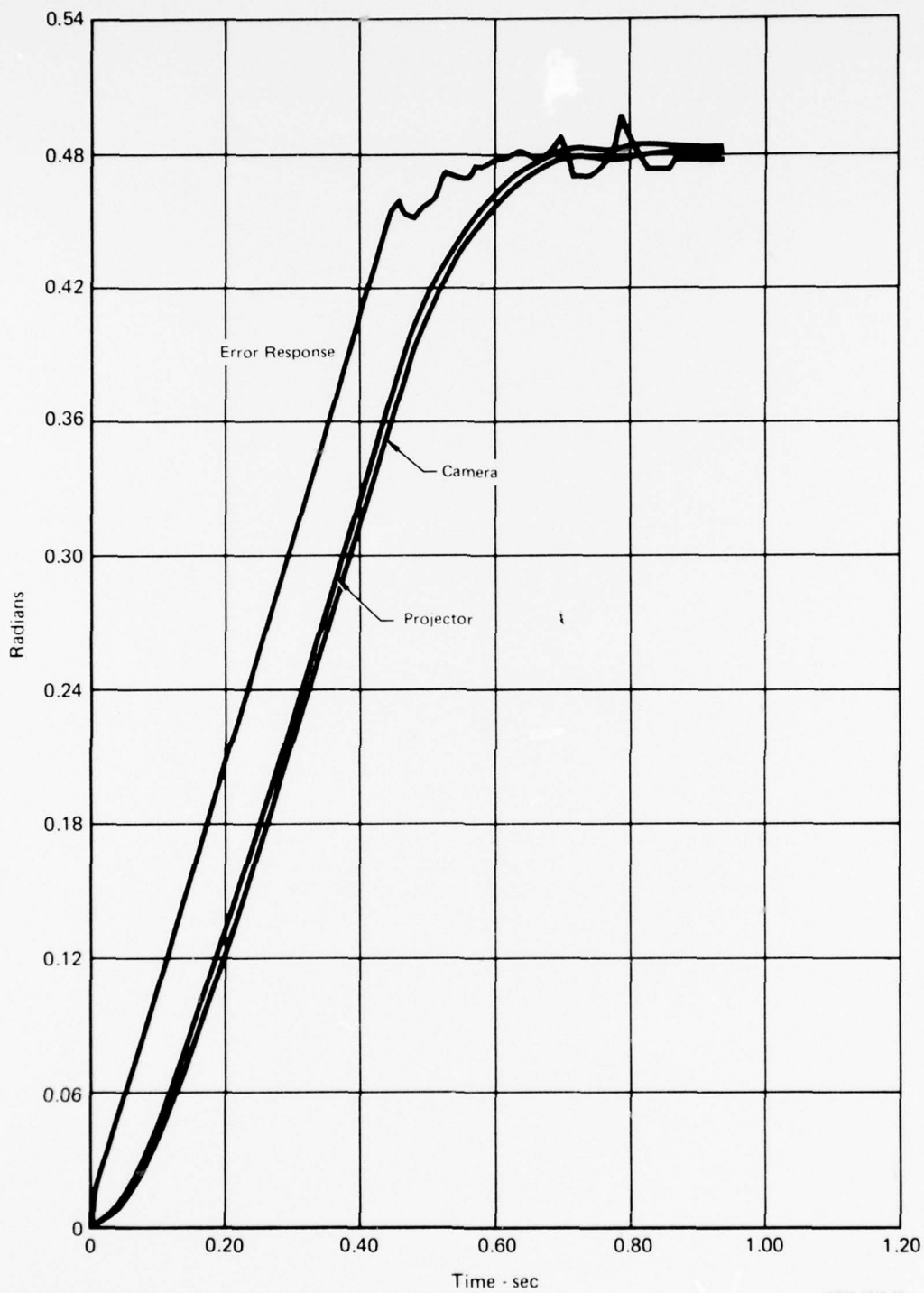


Figure 58 System Response for Step Input

GP77-0549-15

```

      C  PROJ CAMERA POSITION SERVOS STEP INPUT TORQ MTRS LIMITED
0001      INTEGER A,B,CAMR,DX,X,CER
0002      DIMENSION K(100),J(100),PROJ(100),V(100),M(100),JR(100),IDET(100)
0003      DIMENSION IV(100),IP(100),FST(100),DFST(100)
0004      DO 5 I=1,100
0005          IV(I)=0.0
0006          K(I)=0.0
0007          J(I)=0.0
0008          PROJ(I)=0.0
0009          DFST(I)=0.0
0010          FST(I)=0.0
0011          V(I)=0.0
0012          M(I)=0.0
0013          IP(I)=0.0
0014          JR(I)=0.0
0015      5  CONTINUE
0016          A=4
0017          B=-5
0018          E1N=0.25
0019          N=0
0020          CAMR=0
0021          DP=0.0
0022          PDOT=0.0
0023          DPDOT=0.0
0024          DT=0.010
0025          Z=0.00
0026          CR=0.0
0027          CRTE=0.0
0028          T=0.0
0029          RS=0.0
0030          DVDOT=0.0
0031          DV=0.0
0032          DO 100 I=3,100
0033              IDET(I)=((E1N-PROJ(I-1))*0.2)/0.000767
0034              KDRT=((PROJ(I-1)-PROJ(I-2))*2.0)/0.000767
0035              ID=IDET(I)*IDET(I)
0036              IF(ID.LE.16) IDET(I)=0
0037              CAMR=B*KDRT+A*IDET(I)
0038              IF(CAMR.GE.13) CAMR=13
0039              IF(CAMR.LE.-13) CAMR=-13
0040              DX=13
0041              N=N+1
0042              IF(N.GE.25) DX=0
0043              X=X+DX
0044              C=X*0.000767
0045              CER=X-IV(I-1)
0046              M(I)=CER
0047              DIP=M(I)*10.7*0.00244*1.333
0048              JR(I)=(V(I-2)-V(I-1))/0.000767
0049              CR=JR(I)/DT
0050              CRTE=CR*1.07*0.00244*1.333
0051              T=CRTE+DIP

```

Figure 59 System Math Model


```

0052      RS=T*T
0053      IF(T.GE.0.1)TQ=T-0.1
0054      IF(T.LE.0.1)TQ=T+0.1
0055      IF(RS.LE.0.01)TQ=0.0
0056      IF(RS.LE.0.01.AND.VDOT.GT.0.0)TQ=T-0.1
0057      IF(RS.LE.0.01.AND.VDOT.LT.0.0)TQ=T+0.1
0058      IF(T.GE.4.0)TQ=4.0
0059      IF(T.LE.-4.0)TQ=-4.0
0060      XLC=TQ-(VDOT*.1824)
0061      DVDOT=(XLC*DT)/0.113
0062      VDOT=VDOT+DVDOT
0063      DV=VDOT*DT
0064      V(I)=V(I-1)+DV
0065      IV(I)=V(I)/0.000767
0066      ERR=V(I)-PROJ(I-1)
0067      AERR=(ERR*180.0)/3.14159
0068      K(I)=ERR/0.000767
0069      DISP=K(I)*13.8*0.00244*0.5
0070      J(I)=(PROJ(I-2)-PROJ(I-1))/0.000767
0071      DFST(I)=(DX-FST(I-1))*0.10
0072      FST(I)=FST(I-1)+DFST(I)
0073      PRT=(J(I)+FST(I))/DT
0074      RATE=PRT*1.38*0.00244*0.5
0075      DZ=K(I)*0.000152
0076      Z=Z+DZ
0077      CHK=K(I)*0.0*K(I)
0078      IF(CHK.GE.4000)Z=0.0
0079      TRQE=RATE+DISP
0080      TRS=TRQE*TRQE
0081      IF(TRQE.GE.0.1)TRE=TRQE-0.1
0082      IF(TRQE.LE.-0.1)TRE=TRQE+0.1
0083      IF(TRS.LE.0.01)TRE=0.0
0084      IF(TRS.LE.0.01.AND.PDOT.GT.0.0)TRH=TRQE-0.1
0085      IF(TRS.LE.0.01.AND.PDOT.LT.0.0)TRH=TRQE+0.1
0086      IF(TRQE.GE.1.2)TRE=1.2
0087      IF(TRQE.LE.-1.2)TRE=-1.2
0088      XL=TRE-(PDOT*.02466666)
0089      DDPDOT=(XL*DT)/0.052
0090      PDOT=PDOT+DDPDOT
0091      DP=PDOT*DT
0092      PROJ(I)=PROJ(I-1)+DP
0093      IP(I)=PROJ(I)/0.000767
0094      WRITE(1,300) AERR,C,V(I),PROJ(I),TQ
0095      100 CONTINUE
0096      300 FORMAT (5(E11.4,1X))
0097      CALL EXIT
0098      END

```

ROUTINES CALLED:
EXIT

OPTIONS =/OP:2./GO

BLOCK LENGTH
MAIN. 3478 (015454)*

Figure 59 System Math Model (Concluded)

The system may be stopped at any time by turning the projector gain pots to zero. The processor may be stopped by pushing the HALT or the RESET button. The system may be restarted by repeating the sequence described above.

The mode of control may be switched between stick to head by actuating the toggle switch located on the rear panel of the microprocessor. When all gain pots are on, the system is in the stabilized mode. The projector pots can be left off for operation of system in non-stabilized display mode.

Basic Monitor Functions

The microprocessor has a self contained monitor program. An operator with an understanding of the servo control program, (See software section of this report) can use the monitor to troubleshoot not only software problems but also pin down the point of many electronic failures.

Using the monitor, the user can for instance examine the position data coming from the shaft encoders. To examine data, the following sequence should be used:

- o Depress halt (HLT) button
- o Depress examine memory (EM) button
- o Punch in memory address

When the address has been entered, the processor will display the 8 bit word stored at that address in a hexadecimal code. The location in memory following this address may be addressed by pushing the "CO" button. The low order bits are stored in the first location and the higher bits in the second. Camera pitch data is located at computer memory address 3D40 and 3D41. Camera yaw data is located at 3D42 and 3D43. The lower 13 bits contain the position information, highest order bits are not used and can be ignored. The lowest order bit is approximately equal to 2.6 minutes of arc.

A listing of the control program is available in the software section of this report. This listing, along with the monitor description in the same section will allow a person familiar with the 8080 programming language to alter the system parameters and fine tune the system. The control systems gains can be adjusted directly from the monitor, but a word of caution is in order. Due to the scaling complexities and interaction of the system gains it is suggested that change not be made without a complete and thorough understanding of the software.

The quad detector mounted on the helmet has approximately a 40° full field-of-view. If the IR spot that it senses is outside its field-of-view, the microprocessor will receive no control signals and the servo will remain at rest. The observer needs to turn his head, pointing the detector toward the high acuity portion of the display. As the user does this, the system will begin to slew toward him. The sensitivity of the head controller can be adjusted by adjusting the intensity of the source. The recommended settings of the light source are 5 Vac and 5 amps.

The joy stick control has zeroing pots so that the joy stick analog output signal can be adjusted within the system's software deadband eliminating servo drift.

The microprocessor LED readouts allow the operator to determine the operational mode of the microprocessor. Upon powerup, the readout will show 43210. The same readout will occur after the RST GO sequence. The halt (HLT) button will cause a "D" to be read into the first digit and the next four show the current program counter. The restart (RS) button changes the halt display to show a 6 in the first digit and leaves the other digits unchanged. If after depressing the halt button, a "D" is not located in the first digit, the microprocessor program is not running correctly is indicated. The user should then repeat to reset sequence (RST, GO).

The torque motor on the yaw axis of the projector can exert 100 ft. lb. of torque if the power amplifier or its input should fail in a hardover mode. Hard stops and motor shorting switches have been installed on this axis to protect the light valve in the unlikely event that such a failure should occur. If the motor shorting switches are tripped, the operator must stop the system and reset the switches.

In normal operation the software limits the camera and projector axes to $\pm 90^\circ$ in yaw and $\pm 45^\circ$ in pitch. These software limits prevent the operator from slewing the equipment into the mechanical stops and eliminate undue rapid deceleration of the hardware.

5.6 HEAD TRACKER INTERFACE ELECTRONICS

The control signals required for the head tracking mode are generated by a dual axis position sensor. This sensor provides pitch and yaw position information from a light spot imaged on the detector surface. The source of the light imaged on the detector is a 24 watt bulb in a lens assembly focused to image the filament of the bulb on the dome surface. The detector is helmet mounted, and the light source is mounted on the projector pitch axis. Although some axes crosstalk could have been eliminated by mounting the detector on the pitch axis and the light source on the helmet, the opposite arrangement was chosen in order to keep the helmet assembly as light as possible. Both the light source and the detector are filtered with Wratten 88A filters. The detector (PIN-SC-25) manufactured by United Detector, has a position sensitivity of .32 amp/watt/cm, and a series resistance of $5K\Omega$. The light source is a 1763, 6 volt, 4 ampere prefocus socket bulb. The detector output signal is amplified using the circuit shown in Figure 60. This amplifier is characterized by its low input impedance and high common mode rejection. The zener diodes located on the output stage clip the signal at approximately 4.7 volts to prevent overdriving the analog to digital input of the microprocessor.

The spot imaged on the detector (the filament of the bulb) nominally has a width of 0.06 inches. The detector has a usable width of 0.74 inch. A rough calculation shows that using a 0.9 inch focal length lens the detector will have an approximate field of view of 40° . If the source imaged on the dome is outside of the field of view of the detector the microprocessor receives no signals from the detector and the system will remain at rest. As the detector is pointed toward the image on the dome surface, the projector will begin to slew toward the detector. As the projector slews toward the detector* and locks onto the detector's signal, the system's feedback loop is completed and the system will be fully head controlled.

A typical signal output vs. command angle is shown in Figure 26. The amplitude of the signal output is not only a function of the CMR amplifier, but also of the light source intensity and positioning of the detector within the return cone of the source light.

The head control system may be finetuned by adjusting the light source to provide the appropriate response in the closed loop system.

* In actuality, the detector directs the camera to move and the projector follows the camera.

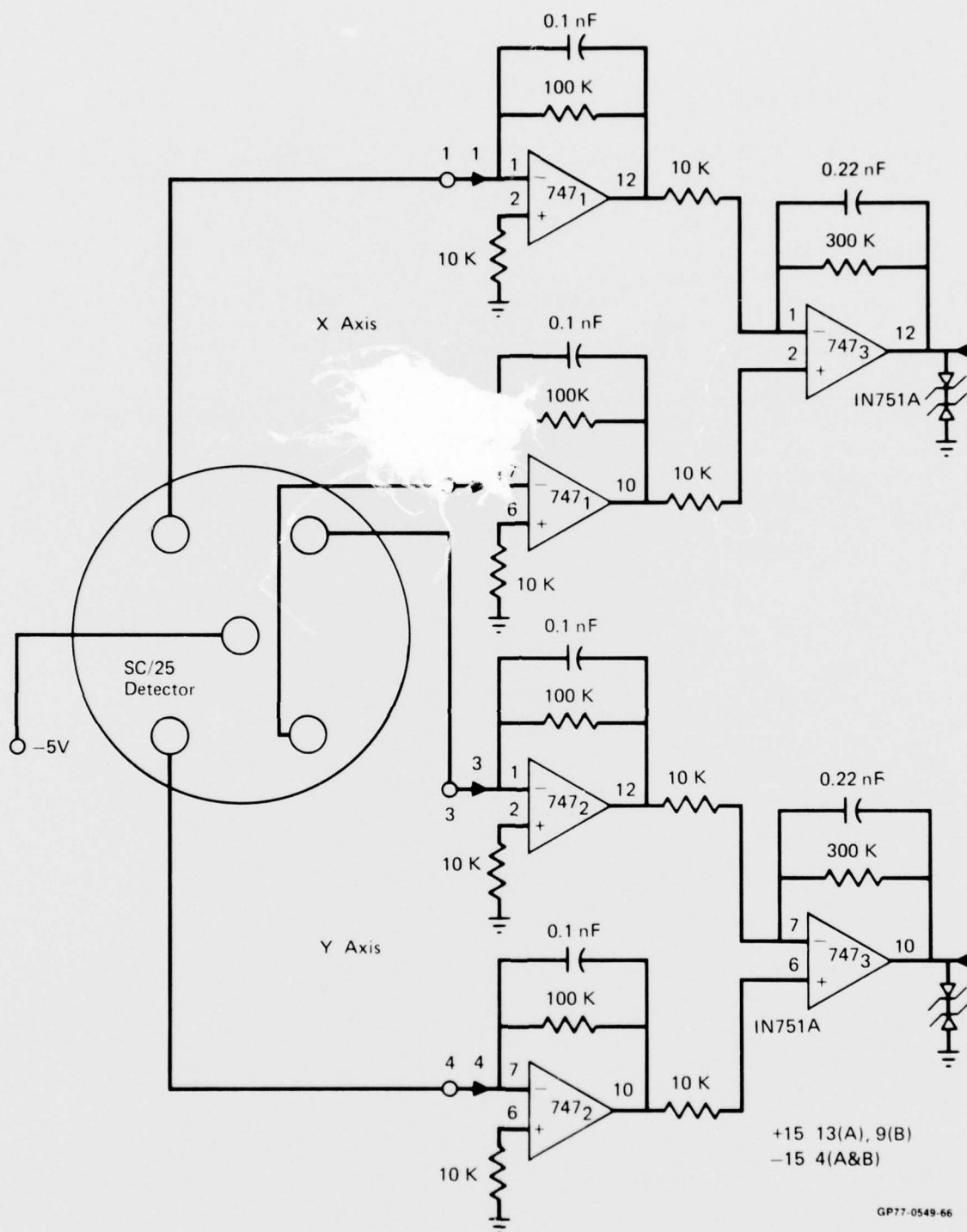


Figure 60 Head Control Detector Amplifier

Section 6

RESULTS AND CONCLUSIONS

This section details the tests that were made to document system performance as measured by system resolution and distortion and compares these data to theoretical predictions.

Resolution measurements of the total system were made using tribar targets. These measurements were made on the system as it was adjusted for the ONR demonstration. The system was set up for best overall focus, a situation which reduces on-axis resolution. The system focus problem is discussed in more detail in the focus corrector section of this report.

The lens distortion function causes no noticeable effect to radial lines while lines perpendicular to these (tangential lines) are compressed. For example, in the vertical direction, a vertical bar target which is readily resolvable has a horizontal counterpart which is not resolvable. These two target orientations were used to measure system resolution along and across the scanning line direction, (i.e. Horizontal bars used for vertical measurements).

The resolution measurements were made as a function of the angle from the optical axis (θ). These angles were computed from shaft position encoder data read from the microprocessor memory, the system geometry and lens nodal point shift data. Figure 61 shows the geometry involved to render a true θ from the encoder readings in order to determine vertical and horizontal resolution.

The target viewing distance was selected to be always greater than the lens hyperfocal distance as determined with an F11 system, and the focal length for the corresponding θ . The camera automatic iris control was disabled and set at the typical outdoor setting which was about F11. The resolution targets were illuminated using photoflood lamps, to provide proper target contrast. Now the vertical and horizontal resolution as a function of incoder reading will be determined.

The lens is located vertical distance (a) and horizontal distance (b) from the pivot point. The lens nodal point is located a horizontal distance (b-n) from the pivot point. The lens optical axes labeled 0a is pointed on azimuth angle (β_a) and elevation angle (β_e) with respect to the reference co-ordinate system xyz. The tibar target is located at angle θ with respect to the lens optical axis in a vertical plane.

For the vertical resolution, from the triangle with apex's labeled as 1-5-8 in Figure 61(a).

$$S_1 = \frac{L}{\cos \beta_a} \quad (68)$$

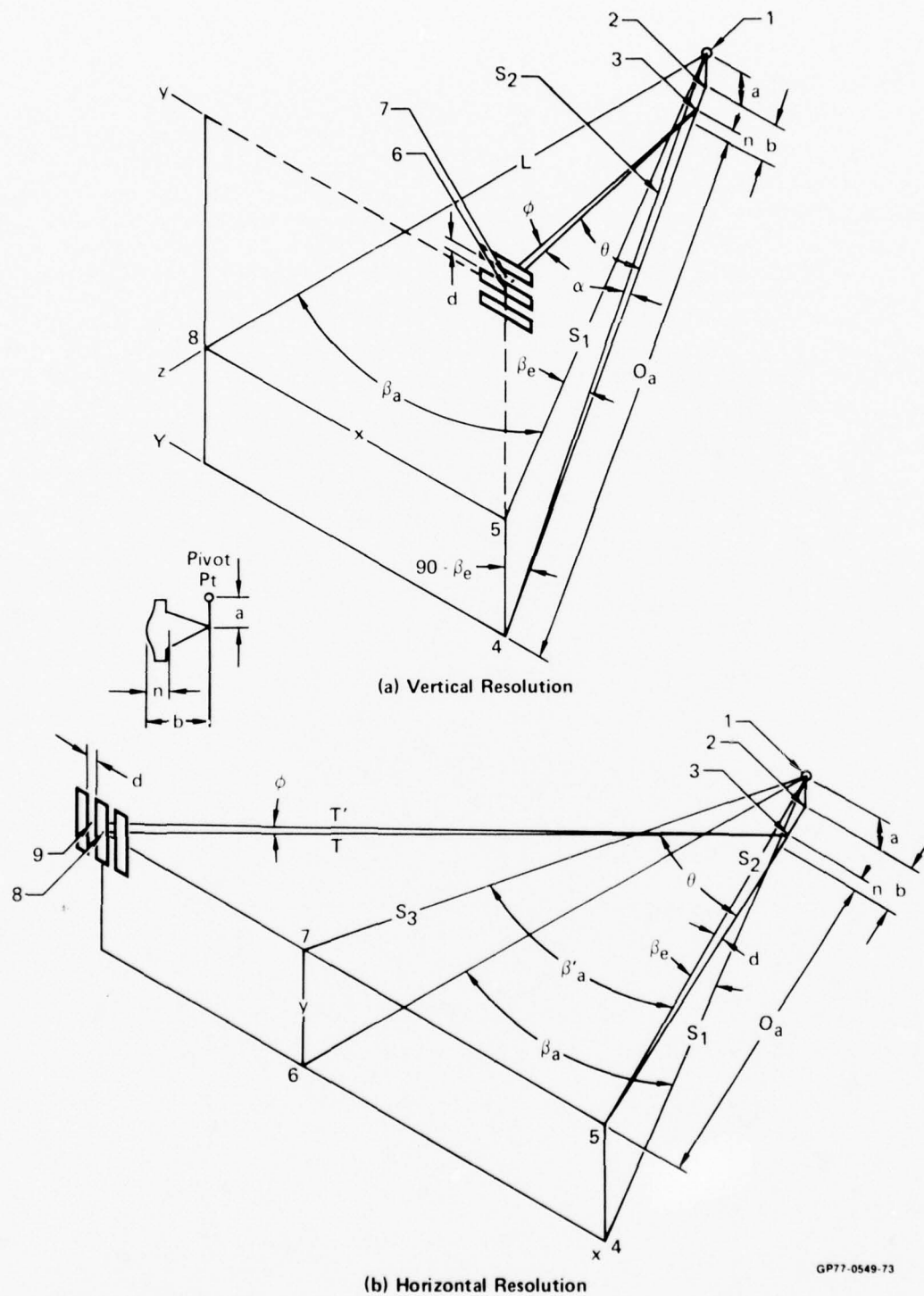


Figure 61 Geometry to Convert Shaft Encoders Readings to True Angles

From triangle 1-4-5

$$Y = S_1 \tan \beta_e \quad (69)$$

Also from triangle 1-4-5

$$S_2 = \frac{S_1}{\cos \beta_e} \quad (70)$$

From triangle 1-2-4

$$\alpha = \arcsin \frac{a}{S_2} \quad (71)$$

From triangle 1-2-4, the distance O_a is

$$O_a = S_2 \cos \alpha - b \quad (72)$$

From the oblique triangle 3-4-6, the distance T is

$$T = \sqrt{(Y + y)^2 + (O_a + n)^2 - 2(Y + y)(O_a + n) \cdot \cos(90 - \beta_e + \alpha)} \quad (73)$$

From the oblique triangle 3-4-6 the angle θ is defined as:

$$\theta = \arccos \left(\frac{-(Y + y)^2 + (O_a + n)^2 + T^2}{2 T (O_a + n)} \right) \quad (74)$$

From oblique triangle 3-4-7

$$T' = \sqrt{(Y + y + d)^2 + (O_a + n)^2 - 2(Y + y + d) \cdot (O_a + n) \cos(90 + \alpha - \beta_e)} \quad (75)$$

Also from oblique triangle 3-4-7 the angle θ' is defined as:

$$\theta' = \arccos \frac{-(Y + y + d)^2 + (O_a + n)^2 + (T')^2}{2 T' (O_a + n)} \quad (76)$$

The resolution \emptyset is then

$$\emptyset = \theta' - \theta \quad (77)$$

Now the horizontal resolution case shown on Figure 61(b) where the optical axis and line to target are in the horizontal plane. From the triangle with apex labeled 1-4-6,

$$S_1 = \frac{L}{\cos \beta_a} \quad (78)$$

From triangle 1-4-5

$$S_2 = \frac{S_1}{\cos \beta_e} \quad (79)$$

From triangle 1-2-5

$$\alpha = \arcsin \frac{a}{S_2} \quad (80)$$

From triangle 1-4-6

$$X = L \tan \beta_a \quad (81)$$

From triangle 1-2-5

$$O_a = S_2 \cos \alpha - b \quad (82)$$

From triangle 1-6-7

$$S_3 = \sqrt{L^2 + y^2} \quad (83)$$

From triangle 1-5-7

$$\beta'_a = \arctan \frac{X}{S_3} \quad (84)$$

From oblique triangle 3-5-8

$$T = \sqrt{(X + x)^2 + (O_a + n)^2 - 2(X + x)(O_a + n) \cos (90 - \beta'_a)} \quad (85)$$

Also from oblique triangle 3-5-8

$$\theta = \arccos \left(\frac{-(X + x)^2 + (O_a + n)^2 + T^2}{2 T (O_a + n)} \right) \quad (86)$$

From oblique triangle 3-5-9

$$T' = \sqrt{(X + x + d)^2 + (0_a + n)^2 - 2(X + x + d)(0_a + n) \cdot \cos(90 - \beta'_a)} \quad (87)$$

Also from triangle 3-5-9

$$\theta' = \arccos \left(\frac{-(X + x + d)^2 + (0_a + n)^2 + (T')^2}{2 T' (0_a + n)} \right) \quad (88)$$

The horizontal resolution is:

$$\emptyset = \theta' - \theta \quad (89)$$

6.1 CAMERA PERFORMANCE

Results of the camera performance tests are shown in Figures 62 and 63. Figure 63 shows resolution in the horizontal plane while Figure 63 is the same data for the vertical plane. The expected resolution as discussed in Section 3.0 is also shown on the figures. Note that in either case the on-axis angular resolution is about 1.7 times worse than was anticipated. In order to make some meaningful comparisons the computer model of Appendix E was degraded until the measured on-axis performance was achieved. This degradation was accomplished by increasing the Gaussian blur of the non-linear lens function. This required an increase from the ray trace data value of 5.5 microns (one sigma) to 50 microns. These data are shown by the solid line on the figures. Note that this data which was matched on-axis is near the actual performance for most other field angles. This indicates a uniform optical blur at the vidicon faceplate. A notable exception is the considerably worse performance in the 0.4 to 1.0 degree region caused by an incorrect aspheric element profile in the rear optical assembly of the non-linear lens. We attempted to correct for this during the contract by fabricating new elements using a new state-of-the-art pantagraph grinding technique and an air bearing spindle. Unfortunately, this was a failure. The new elements were even worse than the original hand fabricated elements. The fabricator is presently remaking these elements which will hopefully correct this problem in the near future. In this abnormal acuity region, performance drops by a factor of three. This is very distracting because performance should be best in this region to support foveal vision.

6.2 TOTAL SYSTEM PERFORMANCE

The measured performance of the overall system is shown in Figure 64 and 65 for the horizontal and vertical planes. Employing the same analytical method as in the camera case it was necessary to degrade display performance from the anticipated 15 microns (equivalent light valve spotsize) to 90 microns in order to predict horizontal on-axis performance. Then when

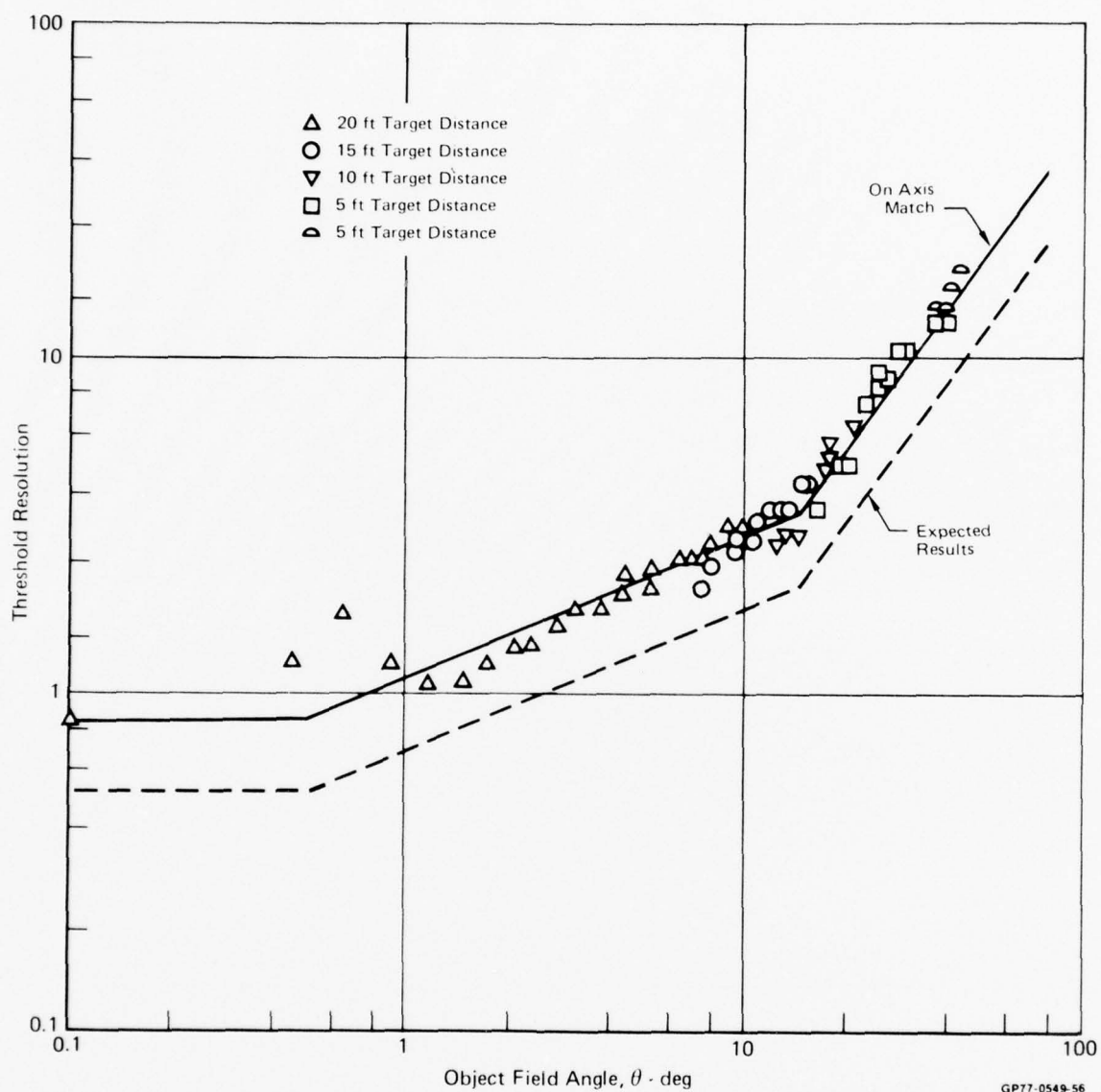


Figure 62 Threshold Resolution vs Angle from Optical Axis
Camera Only (Horizontal)

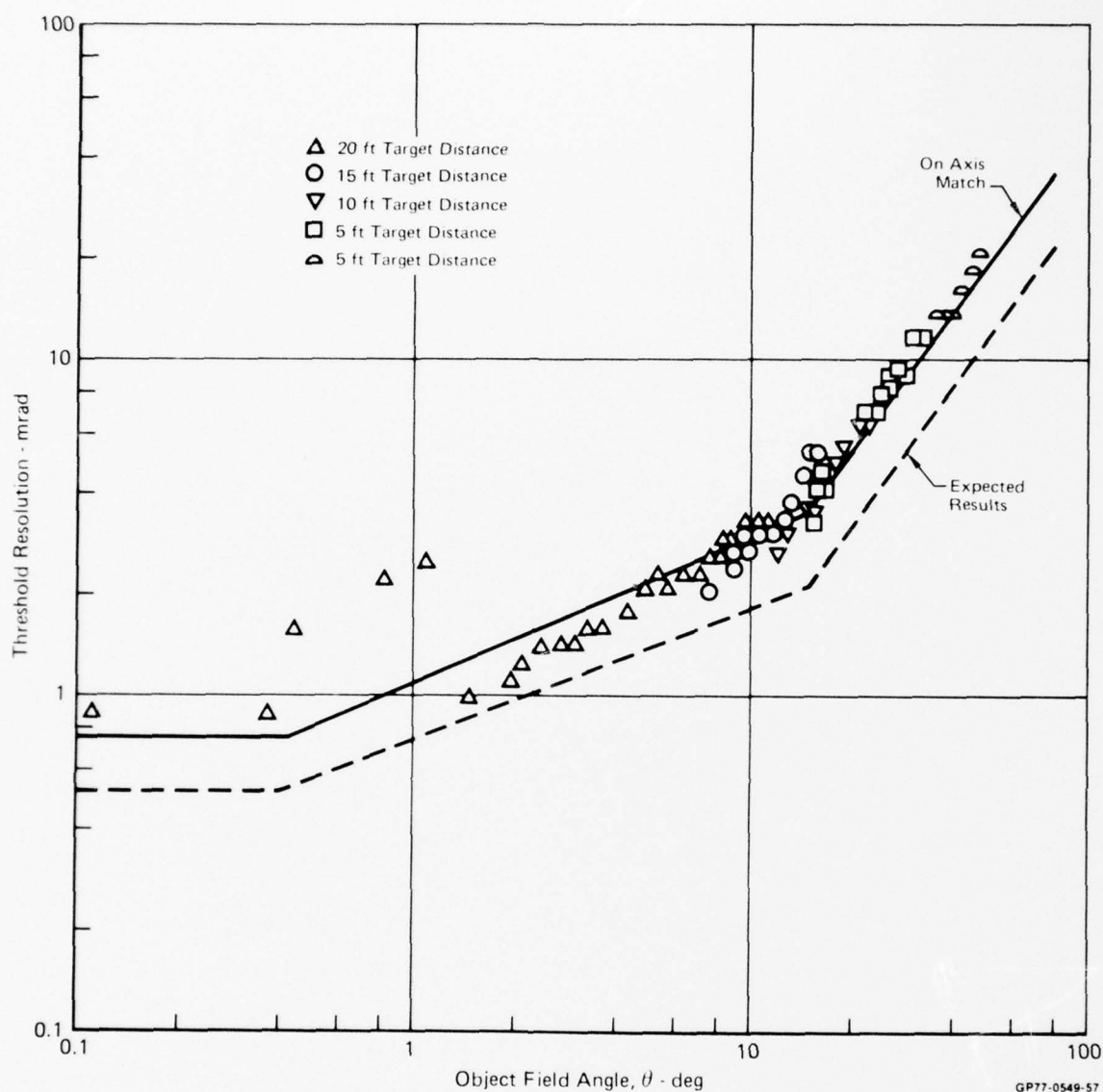


Figure 63 Threshold Resolution vs Angle from Optical Axis
Camera Only (Vertical)

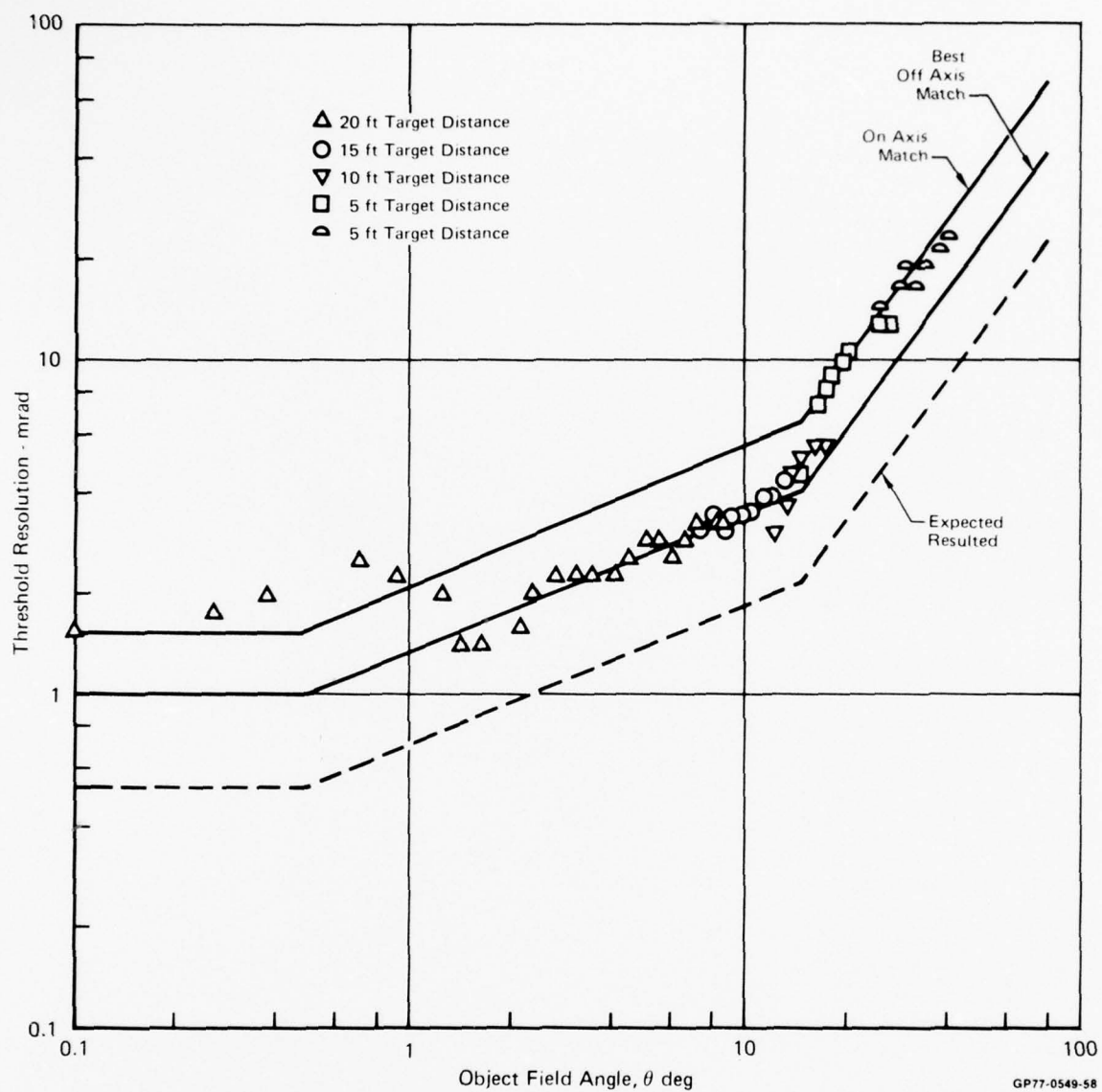
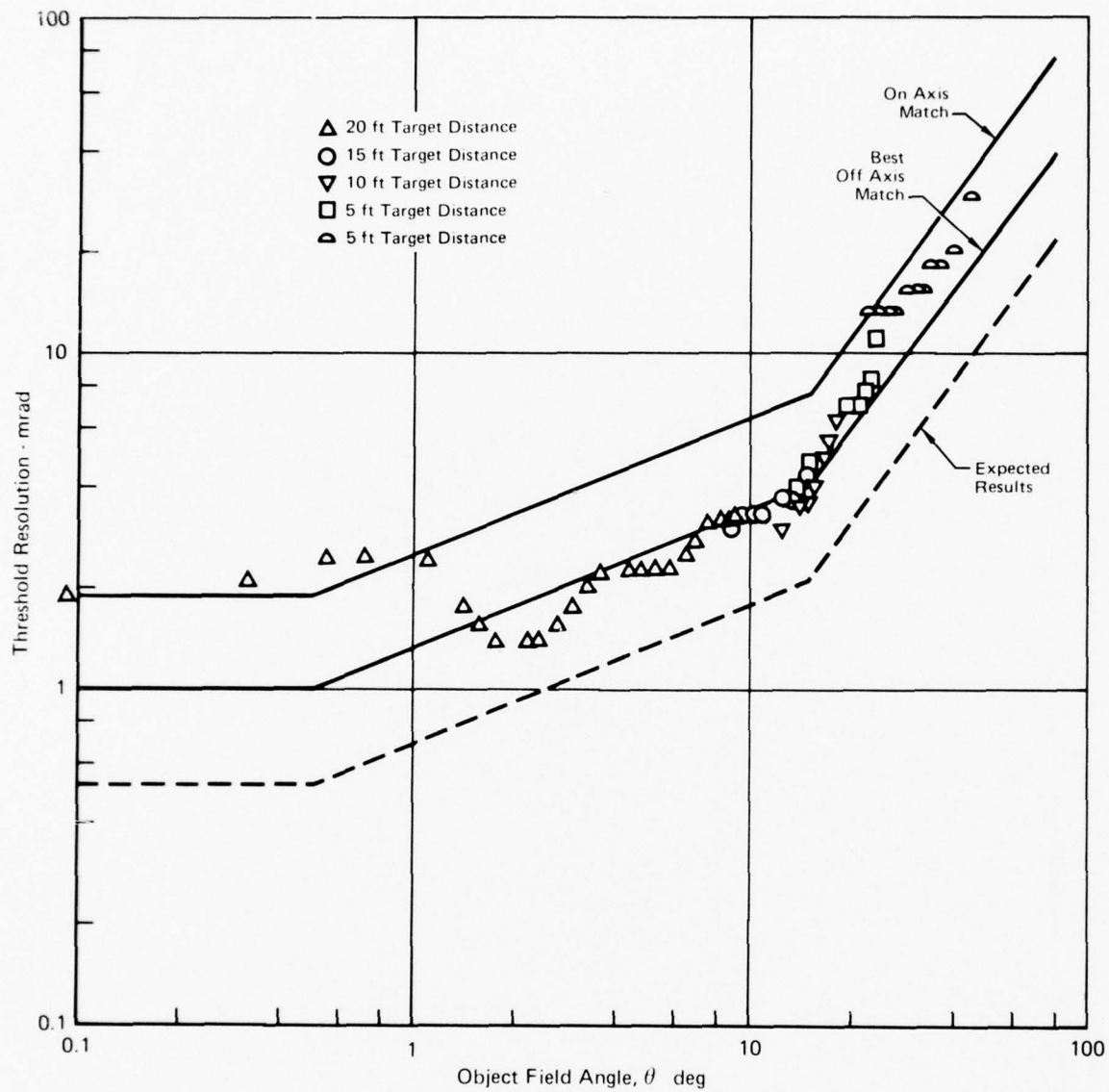


Figure 64 Threshold Resolution vs Angle from Optical Axis
Total System (Horizontal)



GP77-0549-59

Figure 65 Threshold Resolution vs Angle from Optical Axis
Total System (Vertical)

these data were plotted on Figures 64 and 65 very poor prediction of off-axis data is obtained. This implies a nonuniform degradation at the object plane of the projection non-linear lens with much higher blur on-axis. The reason for this is the diffraction problem created by the schlierin optics which was discussed in Section 3. However it appears to be considerably worse than anticipated. To assess the remainder of the field, the display blur was reduced until a good match was obtained off-axis. (The greatest emphasis was placed on the less than 15° region because of expected magnification problems which will be discussed later). A display blur of 30 microns matched the data very well for both horizontal and vertical planes as can be seen on the figures. This is a reasonable display quality value which would produce very little additional degradation to the camera if it applied on-axis as well. The on-axis performance would only degrade from 0.85 to 1.0 milliradian if the 30 micron display quality was maintained on-axis.

The disparity in on-axis system performance between horizontal and vertical planes (1.5 to 1.9 milliradians) is undoubtedly due to schlierin alignment (horizontal at the non-linear lens focal plane) which will yield a higher diffraction cutoff spatial frequency in the horizontal direction.

The system resolution, Figures 64 and 65, show the same local region of poor performance (around 1°) that was seen on the camera only curves. The projector appears to aggravate this region very little. The reason for this lies in the fact that the projector lens produces much better quality in this region apparently because it has a better rear lens cell.

The apparent lower system resolution at field angles larger than 20° is caused by incorrect magnification. This can be seen on Figures 66 and 67 which show measured vs. computed angular error in the projected display. Here the measured data is compared to 2%, 5% and 10% magnified images. The desired value is 2% while the horizontal magnification appears to be about 7% and the vertical about 4%.

6.2.1 Low Contrast Performance

Because of time constraints, direct measurement of low contrast performance was not possible. Therefore it is necessary to use the analytic model adjusted to yield the measured high contrast performance, to estimate performance at lower contrasts. These data are shown on Figure 68. Here the input modulation (contrast) required to resolve targets at various spatial frequencies are shown. Two curves are required for the system because of the projector problem noted above. It should be noted that the linear spatial frequency scale applies everywhere on the non-linear lens focal plane while the angular spatial frequency scale applies only on-axis. These two spatial frequency parameters are related as described in Appendix D.

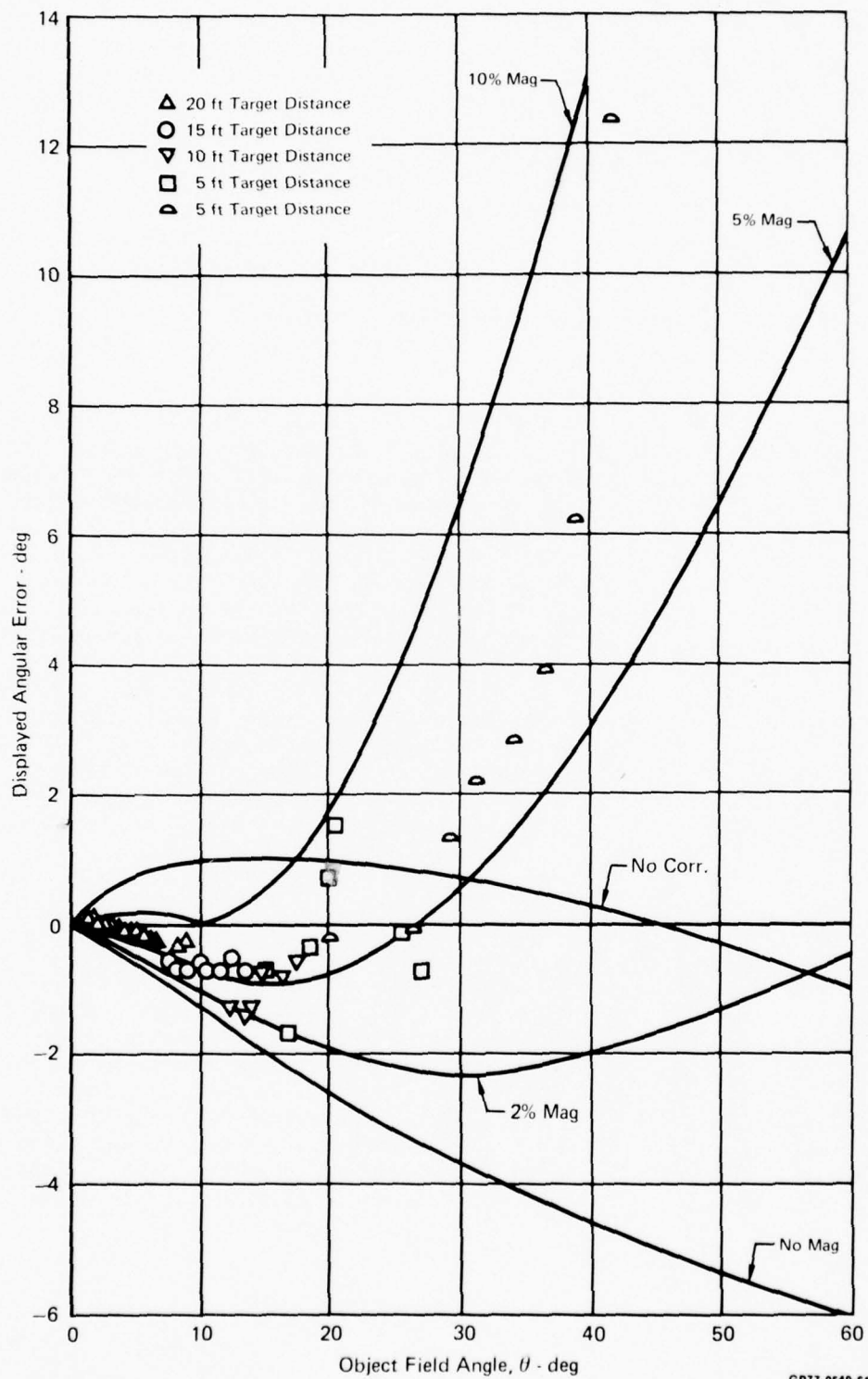


Figure 66 Horizontal Display Error vs Angle

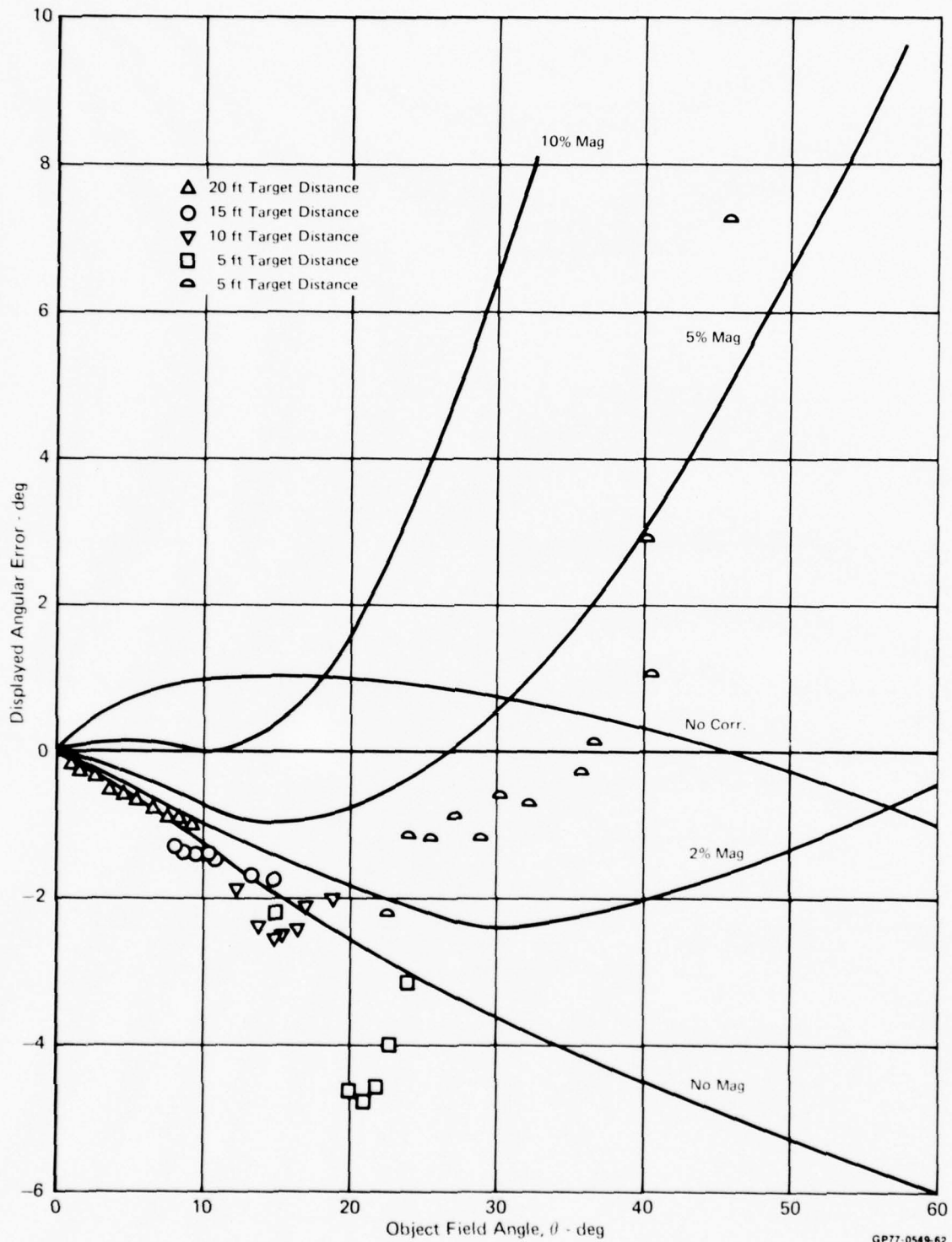
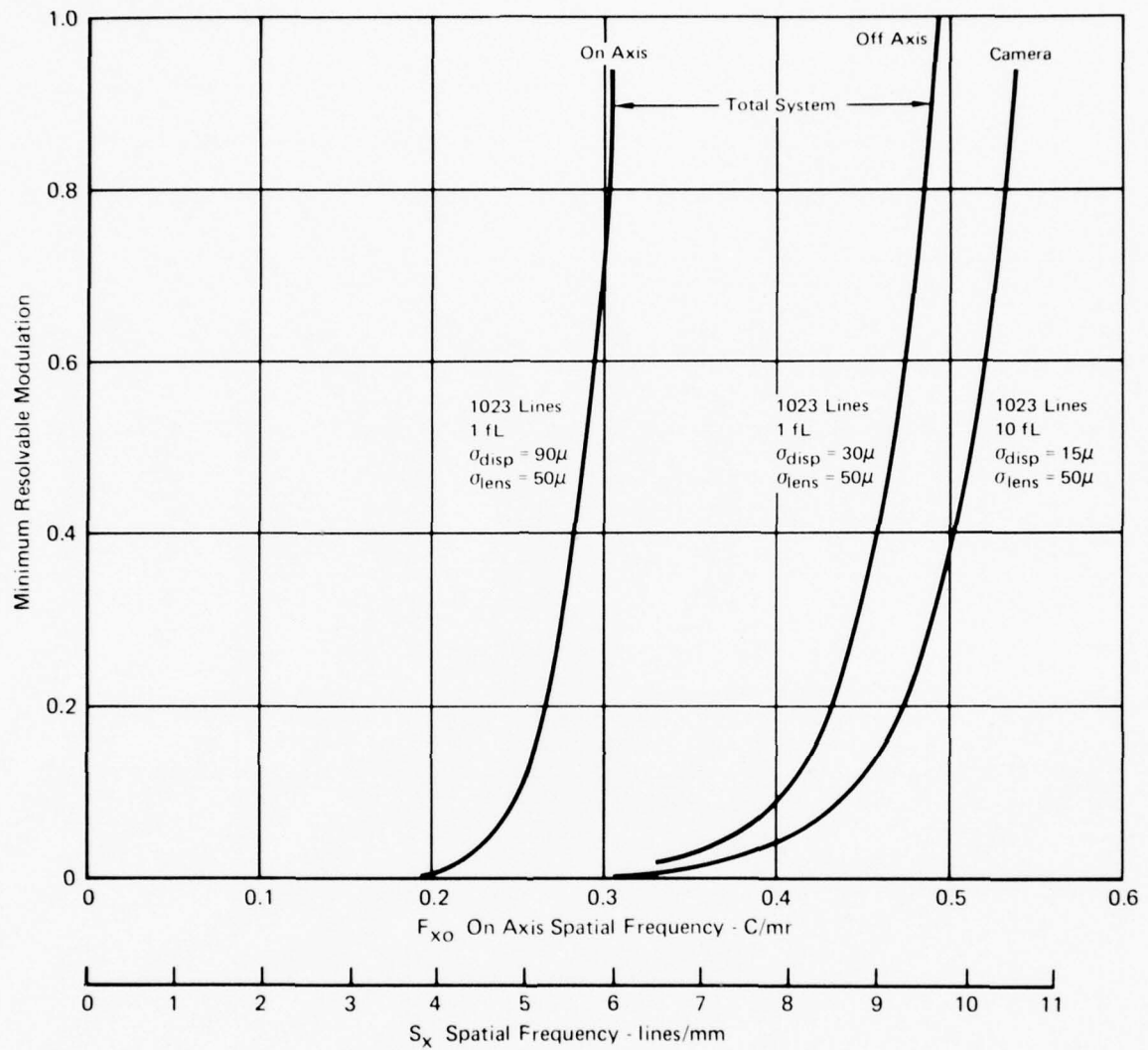


Figure 67 Vertical Display Error vs Actual Angle



GP77-0549-60

Figure 68 Minimum Resolvable Modulation Predictions

6.2.2 Demonstration Results

The system was demonstrated in the laboratory by placing the camera on the northwest corner of the roof of MCAIR Bldg. 102. A hard wire link was established to the display station which was located in the laboratory about 300 ft. away. The camera overlooked Lambert Field and Brown Road which borders the airport. A field of regard of 180° in azimuth and $\pm 60^\circ$ in elevation was established. For comparison a 525 line conventional TV camera with a remote control zoom lens was also placed on the roof. This camera was pointed towards a sign board about 1000 ft. distant. This sensor was displayed adjacent to the RVS camera video CRT display.

To compare resolution, the RVS camera was pointed toward the same sign board and the conventional camera was zoomed until the same detail could be seen on its display as the on-axis RVS was producing. This field-of-view was about $10^\circ \times 14^\circ$. The RVS projection field-of-view was then reduced by masking to this field-of-view. The operator was then given the task of searching the field of regard of the RVS sensor using joy stick control. The usual problems with narrow fields-of-view were noted in maintaining orientation in the total field of regard and in smooth tracking of moving vehicles.

Next the mask was removed so the operator could see the entire RVS field of view and the full up head control operation established. In general all viewers liked the wide field display, especially the ease in tracking moving targets. It should be noted here that the servo control performance was excellent. No perceptible display motion occurred under any dynamic condition. This requires that the camera and projector servos track within about 0.5 milliradian under the most extreme dynamic conditions.

Most observers noted the low on-axis performance even when made aware that it was comparable to a 14° FOV conventional system. Some observers were impressed by motion and glint cueing in the peripheral very low resolution area of the display while others felt lack of sharp spatial detail in these regions would degrade these visual cues.

6.3 CONCLUSIONS AND RECOMMENDATIONS

Considering this is the first device of this type, we feel the results were very encouraging. As should be expected the only serious problems were with the new technology or state-of-the-art advancement in non-linear optics. All conventional functions within the state-of-the-art worked perfectly including the servo control, TV camera, TV projector, head tracker, etc. The value of the digital control system was demonstrated through its outstanding performance and reliability which could have been achieved only with great effort if an analog system was employed.

It appears the greatest improvement in performance could be obtained by (a) replacing the rear splines elements of the non-linear lenses and (b) solving the diffraction problem in the projector relay. The first is underway and if successful should be corrected within one to two months. The latter has no easy solution at this time. As discussed in Section 3, increased relay magnification may help but complete correction may require a different type of light valve that does not require Schlieren optics. At least two are presently under development. A KDP light valve is being developed in France while a liquid crystal light valve is under development at Hughes Aircraft in the USA. Both of these operate on a controlled polarization principle and can use conventional optics. Another possibility is to construct a new non-linear lens with a small F/number so that it can utilize more of the light valve optical ray cone.

Finally we believe the laboratory demonstration, where a scene is viewed in which most spatial detail is stationary, does not show the true potential of the system in flight control and navigation. We have seen this when projecting tape recorded video taken through the windshield of an aircraft. It appears that the somewhat low on-axis resolution is not so objectionable under these dynamic conditions. Based on these observations it may be desirable to fly the sensor in order to obtain a true performance assessment in a dynamic environment.

Section 7
REFERENCE LIST

1. RVS Display Feasibility Study, Report No. MDC A3392, 28 Feb. 1975
McDonnell Aircraft Co., St. Louis, Mo. 63166
2. Remote Viewing System Technical Proposal Report No. MDC A2486, 21 Sept.
1973, McDonnell Aircraft Co., St. Louis, Mo. 63166
3. Head Controlled Remote Viewing System Technical Proposal Report No.
MDC A3020, 3 Sept. 1974, McDonnell Aircraft Co., St. Louis, Mo. 63166
4. Klaiber, R.J., Physical and Optical Properties of Projection Screens;
Technical Report NAVTRADEVCEV IH-63, December 1966

Appendix A

BRIEF DESCRIPTION OF THE REMOTE VIEWING SYSTEM (RVS)

The RVS concept is based on the fact that the human visual capability can be represented by a resolution capability of about 130,000 elements, provided that these elements are sized non-linearly according to the acuity function as shown in Figure A-1. An image with this characteristic requires only about 2 MHz video bandwidth at 30 Hz frame rates. In comparison, standard techniques would require over 1,000 MHz bandwidth for this field-of-view (180°) and resolution. Even at smaller fields-of-view, the bandwidth saving is significant. A comparison of bandwidth requirements for varying fields-of-view for the conventional linear acuity function and for the RVS foveal concept is shown in Figure A-2. Approximately two orders of magnitude decrease in BW is achieved with the foveal system at FOV's greater than 20 degrees. In order to mechanize the concept described above, a method must be devised to generate an image which satisfies the optical requirements of the eye. The RVS concept contains a lens system that creates optical "distortion" by varying the spacing of the angular resolution elements to duplicate the acuity function shown in Figure A-1. This process is illustrated in Figure A-3. The lens transfer characteristic required and the technique for reconstructing the image at a remote location is also shown on this figure. System operation is as follows:

The image transmission system scans the photocathode of the vidicon or photo-detectors of an imaging array, transmits this signal to the remote location, and recreates the image on a CRT or light valve tube. In the original RVS concept, the distorted image is expanded using a lens system with a transfer characteristic identical to the sensor lens and imaged on a spherical screen concentric with the nodal point of the lens.

Obviously, for the above image transmission system to perform adequately, the optical axes of both the sensor and projector must have the same alignment as the viewer's eye. The initial RVS system concept used the approach outlined in Figure A-4. The position of the projector is slaved to the camera by a high accuracy position servo, with the camera's angular position commanding the projector's position relative to fixed ground station reference coordinates. The viewer at the ground station thus has the same angular perspective as he would if he were located in the remote vehicle. The sensor and projector must also be aligned with the viewer's foveal axis. In the original concept a Honeywell oculometer was employed for this function. The oculometer measures the angle between the eye's foveal axis and the projector's optical axis. This error signal is transmitted to the remote vehicle and commands the camera to move until the angular error is reduced to zero. As the camera moves, the projector follows through the slaving loop. The control mode, presently under study, is somewhat different, however. The observer's head position instead of his eye position is utilized to point the remote camera. The operational difference resulting from this simplification is that when the viewer uses his peripheral vision, he must learn to rotate his head towards the area of interest rather than his eyes. A reticle may be required to show the observer the location of the highest acuity area of the display.

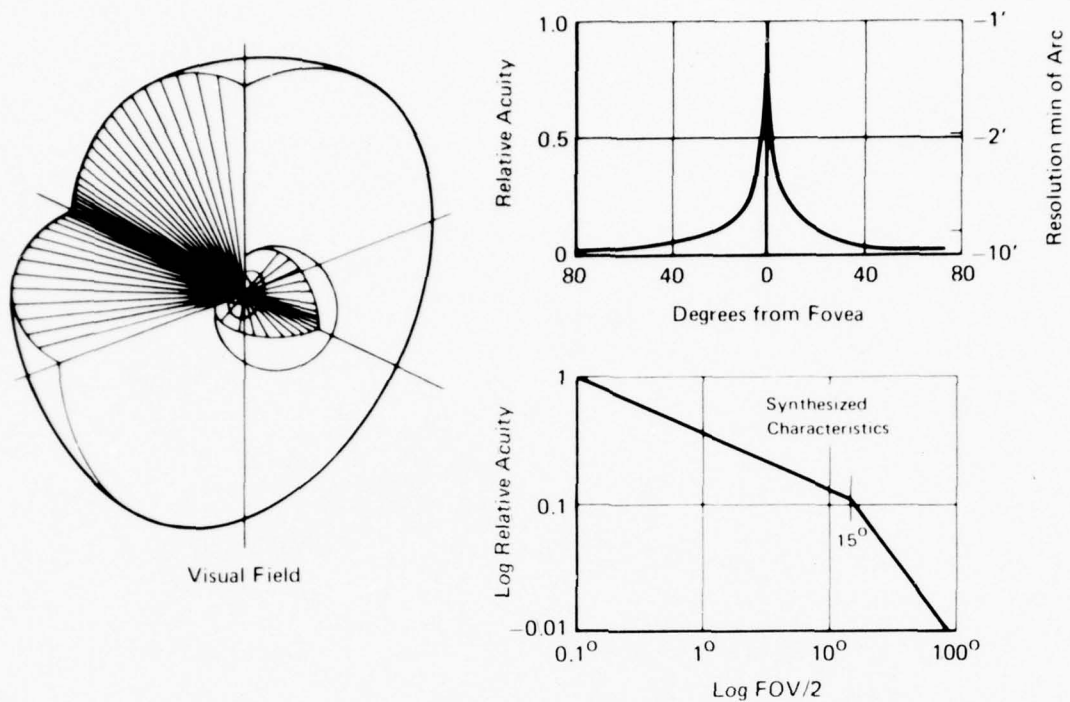


Figure A-1. Human Eye Characteristics

GP76-1037-112

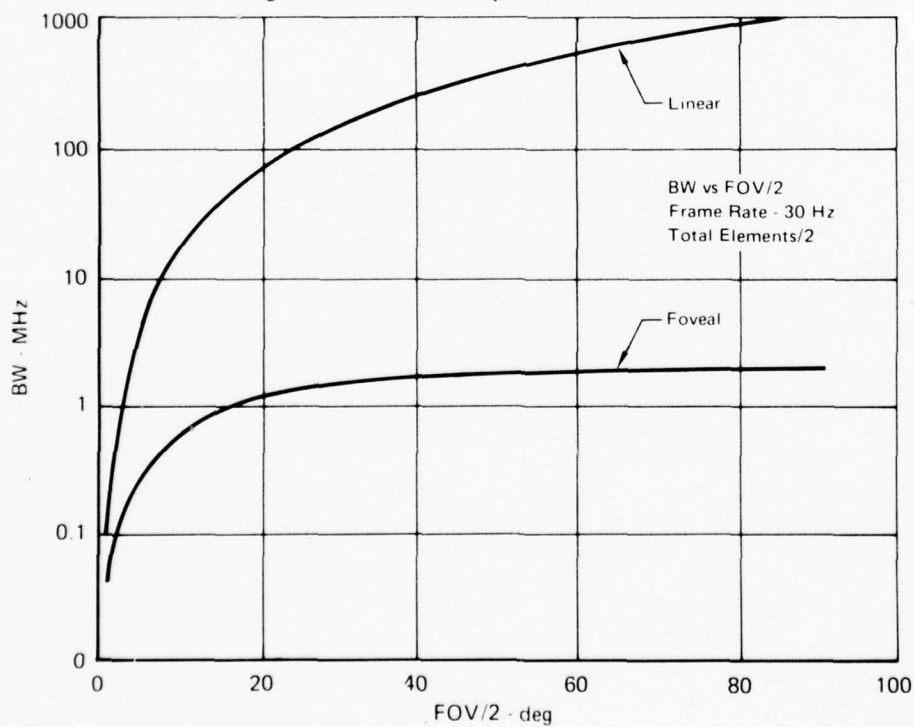
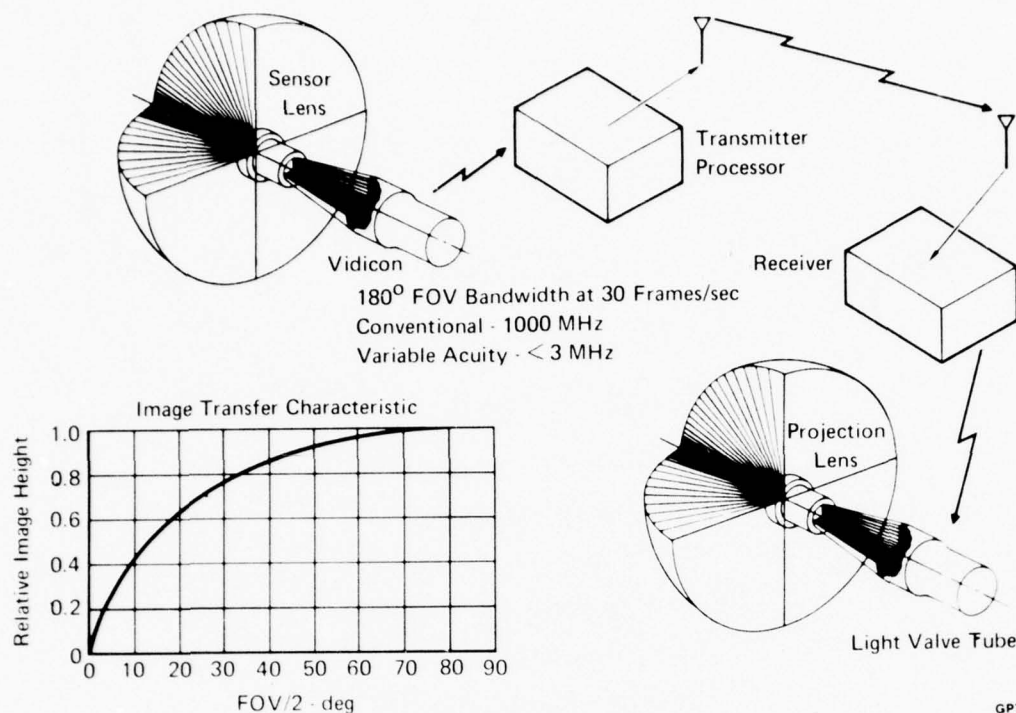


Figure A-2. Bandwidth Requirements

GP76-1037-113



GP76-1037-110

Figure A-3. Electro-Optical Schematic

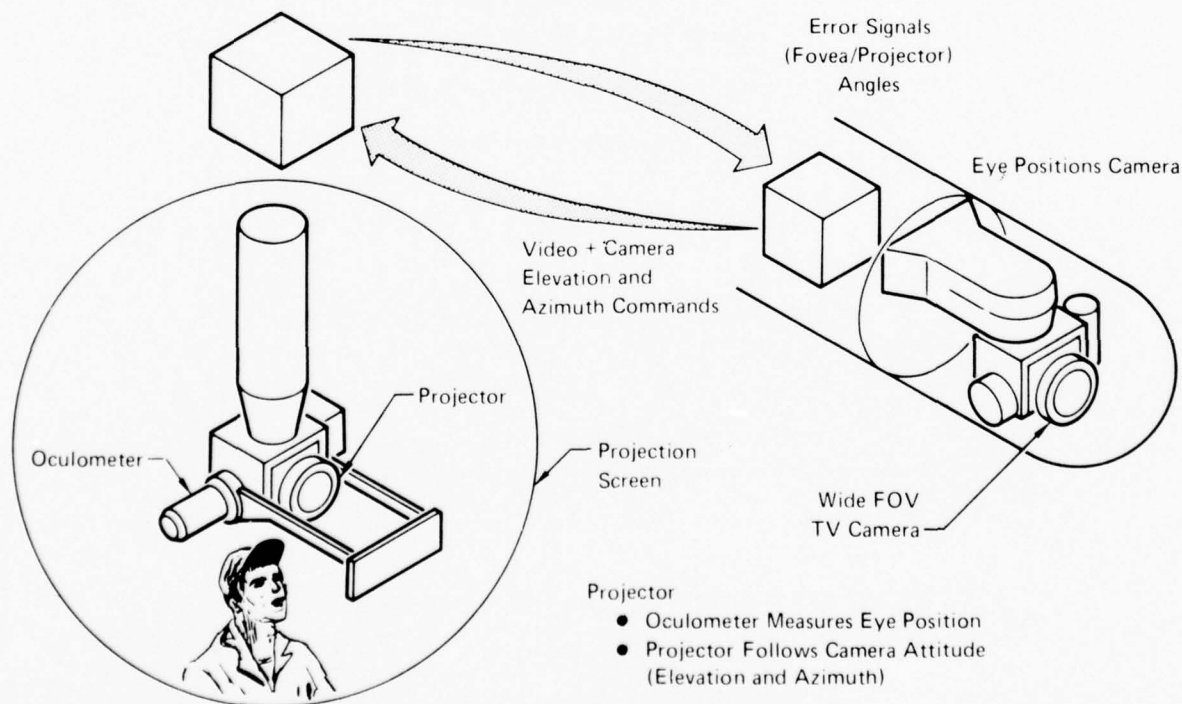


Figure A-4. Camera/Projector Interface

GP76-1037-111

Appendix B

CAMERA CONSIDERATIONS

LIGHT LEVEL CONTROL

Light level control must be accomplished by an iris in the camera optical relay. The relay is required for this purpose because no iris control is available in the non-linear lens. An iris control was not initially considered necessary because an $S_{b_2} S_3$ vidicon was contemplated which had sufficient dynamic range for good daylight performance with electronic light control. Solar damage considerations later dictated the use of a silicon vidicon which cannot be adapted to electronic light level control. The range required of the iris control is discussed below.

Assuming a GE Z7978 Epicon vidicon is utilized an average faceplate illumination of .25 ft-candles is recommended. Using conventional formulas, this relates to a scene brightness as follows:

$$E = \frac{\pi B}{4(F_{NO})^2} \quad (B-1)$$

If $E = .25$ ft-candles

$$B = \frac{.25 \times 4}{\pi} (F_{NO})^2 = .318 (F_{NO})^2 \frac{\text{Lumens}}{\text{Steradian-ft}^2}$$

Assuming a 1:1 relay between lens and vidicon the effective F number at the vidicon is identical to that of the non-linear lens - F/5.6. The brightness is:

$$B = 9.97 \frac{\text{Lumens}}{\text{Steradian-ft}^2} = 31.32 \text{ ft-lambert}$$

This is the minimum brightness level capability of the camera. It is sufficient to operate anywhere in the U.S., even under heavy cloud cover.

The maximum terrain brightness anticipated is about 5000 ft-lamberts. This approximates clear weather at 70° solar elevation and .16 terrain

reflectance. The F number required to attenuate this brightness to .25 ft-candles at the vidicon faceplate is (per Equation (B-1))

$$\begin{aligned}\frac{5000}{\pi} &= \frac{.25 \times 4}{\pi} (F_{NO})^2 \\ (F_{NO})^2 &= 5000 \\ F_{NO} &= 70.7\end{aligned}\tag{B-2}$$

This small aperture would cause serious diffraction in the image quality. For this reason, a filter is considered. Because of sensitivity of the silicon vidicon to IR radiation a Schott KG3 filter is recommended. This filter provides about 20% transmission in the visual spectrum. This reduces the maximum F number requirements to about F/16, which is easily obtainable in the optical relay between camera and lens.

In summary, the camera optical relay must have sufficient aperture to couple all the energy in the F/5.6 non-linear lens image ray bundle to the vidicon. The iris control in the relay must have the capability of reducing this F/5.6 ray bundle at the vidicon to F/16. This variable iris should be servo controlled to maintain the required vidicon faceplate illumination under varying terrain illumination and reflectance characteristics.

The average video level from the vidicon can be used as the drive signal. This is possible because the foveal region occupies most of the vidicon photocathode area. Therefore an average video level will optimize brightness in this area as desired.

SOLAR DAMAGE CONSIDERATIONS

Utilizing the sun brightness value of:

$$B_S = 2.09 \times 10^8 \frac{\text{Lumen}}{\text{Steradian ft}^2} \quad [\text{From Reference (B-1)}]$$

At F/5.6 the vidicon faceplate illumination would be [from Equation (B-1)]

$$E = \frac{\pi}{4} \frac{2.09 \times 10^8}{(5.6)^2} = .523 \times 10^7 \text{ foot candles}$$

This gives a 2x safety factor over the 10^7 foot candle maximum rating of the vidicon proposed for the RVS camera. Operationally the safety margin is considerably better than this because any time the sun is visible to the RVS the automatic light level control will certainly have the camera stopped down to F/8 or greater. The margin is at least 4x when this is considered. The IR filter discussed in the previous paragraph also increases the safety margin.

Appendix C

PROJECTOR STUDIES

INTRODUCTION

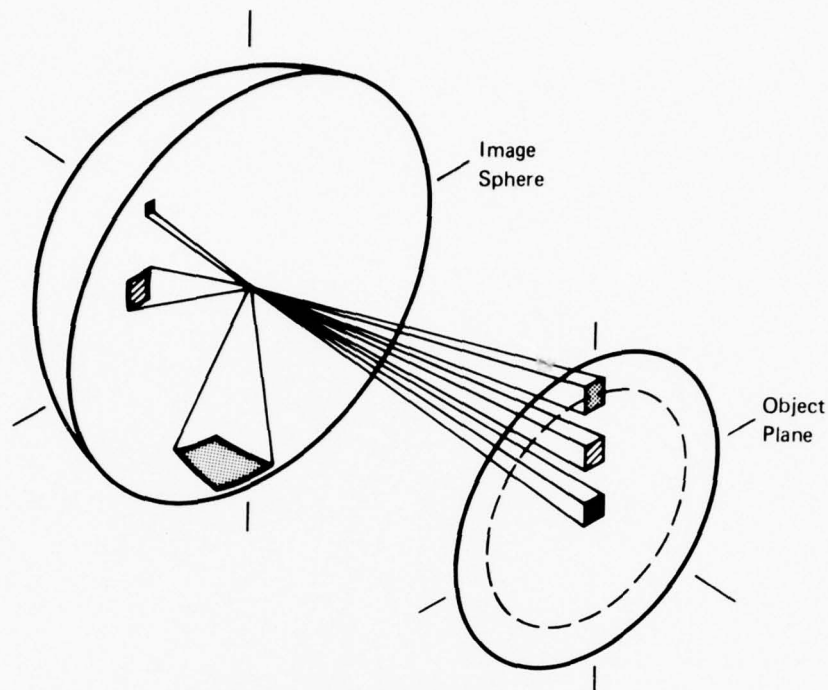
The projection brightness problem is illustrated in Figure C-1. Here uniform size area elements are shown in the projector object plane at three different distances from the optical axis. If the object plane is of uniform brightness (which is the case for the RVS intermediate image or projector object) the screen illumination decreases as object area elements displace from the optical axis. Each area in the object plane contains the same light flux, which is spread over a greater area on the projection screen. In the actual case, area elements are projected 1000 times larger in the extreme peripheral region (90°) than in the foveal region (0°) of the display. This, of course, is completely unacceptable to the viewer.

Two alternatives are possible for solving the above problem.

- (a) A variable density filter to properly attenuate the foveal area of projection so that it matches the peripheral field in screen brightness. This is, of course, feasible only if image brightness is sufficient to generate acceptable brightness in the peripheral field of the displayed image.
- (b) Employ a direct or virtual image viewing system. This is much more efficient and inherently results in uniform display brightness if the exit pupil is large enough to support the entire eye aperture (or the interocular spacing if binocular viewing is to be achieved).

Selection of the best display approach requires a thorough analysis of the two above approaches.

In the past year, MCAIR IRAD on the RVS has been 95% devoted to trade-offs of display concepts. The results of these studies, analyses, and tests are outlined below.



GP73-0782-25

FIGURE C-1
GENERAL PROJECTION GEOMETRY

PROJECTION SCREEN APPROACH

The geometry of the projection screen approach is shown in Figure C-2. An element of area dA with brightness B is projected through a lens of aperture D and focal length f to a viewing screen located at distance L . The image of dA on the viewing screen appears as dA_s . This area re-radiates over solid angle ω_s . The apparent screen brightness $B_s(\theta)$, as seen by the observer also at distance L , but offset by distance l , is calculated as follows.

The light flux through aperture D from image area dA is:

$$F = B \times \omega \times dA \quad (C-1)$$

where

ω is the solid angle of light collection by the projector lens.

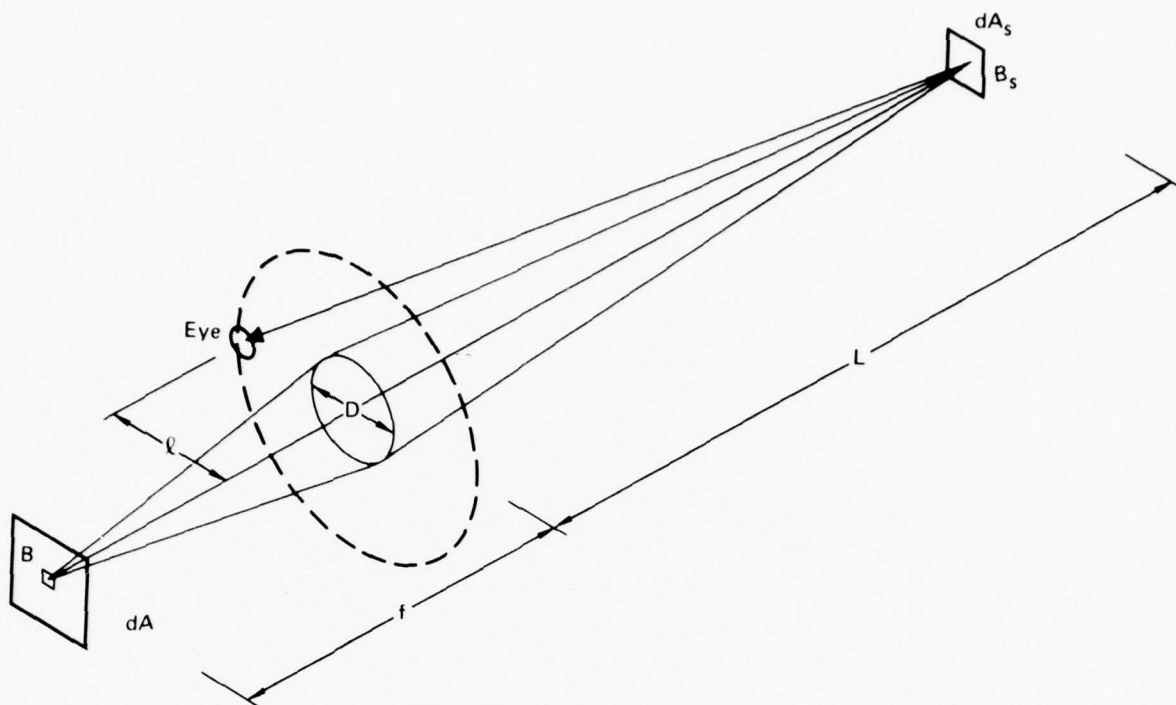


FIGURE C-2
DISPLAY BRIGHTNESS GEOMETRY

GP73-0782-24

Accordingly:

$$\omega = \frac{\pi [D(\theta)]^2}{4 [f(\theta)]^2} = \frac{\pi}{4 (F_{NO})^2} \quad (C-2)$$

Development of ω in terms of F_{NO} instead of lens aperture and focal length is preferred because both theory and experiment show that the latter vary with field angle (θ) on the non-linear lens while F_{NO} does not.

Combining these two equations yields:

$$F = \frac{B \pi dA}{4 (F_{NO})^2} \quad (C-3)$$

This is the total flux that illuminates dA_s at the screen.

Screen illumination (E) is:

$$E = \frac{F}{dA_s} = \frac{B\pi}{4 \left(F_{NO} \right)^2} \frac{dA}{dA_s(\theta)} \quad (C-4)$$

The screen brightness is therefore

$$B_s(\theta) = \frac{E}{\omega} = \frac{B\pi}{4 \left(F_{NO} \right)^2 \omega} \frac{dA}{dA_s(\theta)} \quad (C-5)$$

Note that B_s will have the same units as B if A and A_s have identical units.

For the on-axis case, zero subscript is used:

$$\frac{dA}{dA_s(0)} = \frac{[f(0)]^2}{L^2} = \frac{\left(F_{NO} \right)^2 [D(0)]^2}{L^2} \quad (C-6)$$

Therefore:

$$B_{s_0} = \frac{B\pi D(0)^2}{4\omega L^2} \quad (C-7)$$

For the developed lens, $D(0) = .356''$. Accordingly:

$$\frac{B_s(0)}{B} = \frac{.0995}{\omega L^2} \quad (C-8)$$

If $L = 60''$:

$$\frac{B_s(0)}{B} = \frac{2.76 \times 10^{-5}}{\omega} \quad (C-9)$$

WORST CASE

If the screen is perfectly diffuse

$$\omega = \pi \text{ steradians}$$

BEST CASE

If the screen has optimum characteristics

$$\omega \cong \frac{\pi \ell^2}{L^2}$$

WORST CASE

$$\frac{B_s(0)}{B} = 8.78 \times 10^{-6}$$

For $B_s(0) = 1$ ft-lambert

$$B = 114,000 \text{ ft-lambert}$$

If the screen is perfectly diffuse

BEST CASE

If $\ell = 10''$ (About the minimum projector/eye separation)

$$\omega = \pi \frac{10^2}{60} = .0873 \text{ steradians}$$

If the screen has optimum characteristics

$$\frac{B_s(0)}{B} = 3.161 \times 10^{-4}$$

For $B_s(0) = 1$ ft-lambert

$$B = 3160 \text{ ft-lambert}$$

The above calculations show an object brightness in the 3000 to 100,000 ft-lambert range is required for acceptable display brightness in the foveal region of the projected display. For reasons shown on Figure C-1, it is not the foveal region, but the peripheral region that puts the greatest requirement on B.

In calculating peripheral display brightness it is most convenient to normalize Equation (C-5) by the on-axis brightness. The result is a fall-off ratio of brightness anticipated in the projected display.

$$\frac{B_s(\theta)}{B_s(0)} = \frac{dA_s(0)}{dA_s(\theta)} \quad (C-10)$$

Equation (C-10) assumes a constant F_{NO} for the lens and ω for the screen. The former has been verified experimentally while the latter will be assured by spherical screen geometry and uniform coating.

The display brightness at any angle, θ , can be computed by determining the axial brightness using Equation (C-7) or (C-9) and multiplying by the ratio of Equation (C-10). The area ratios of Equation (C-10) are available from lens design data and have been

verified experimentally. These data are plotted on Figure C-3. Note that at 90° , brightness is down by 10^{-3} . It is obvious from this that the 3000 to 100,000 ft-lambert range required for on-axis brightness must be increased to 3,000,000 to

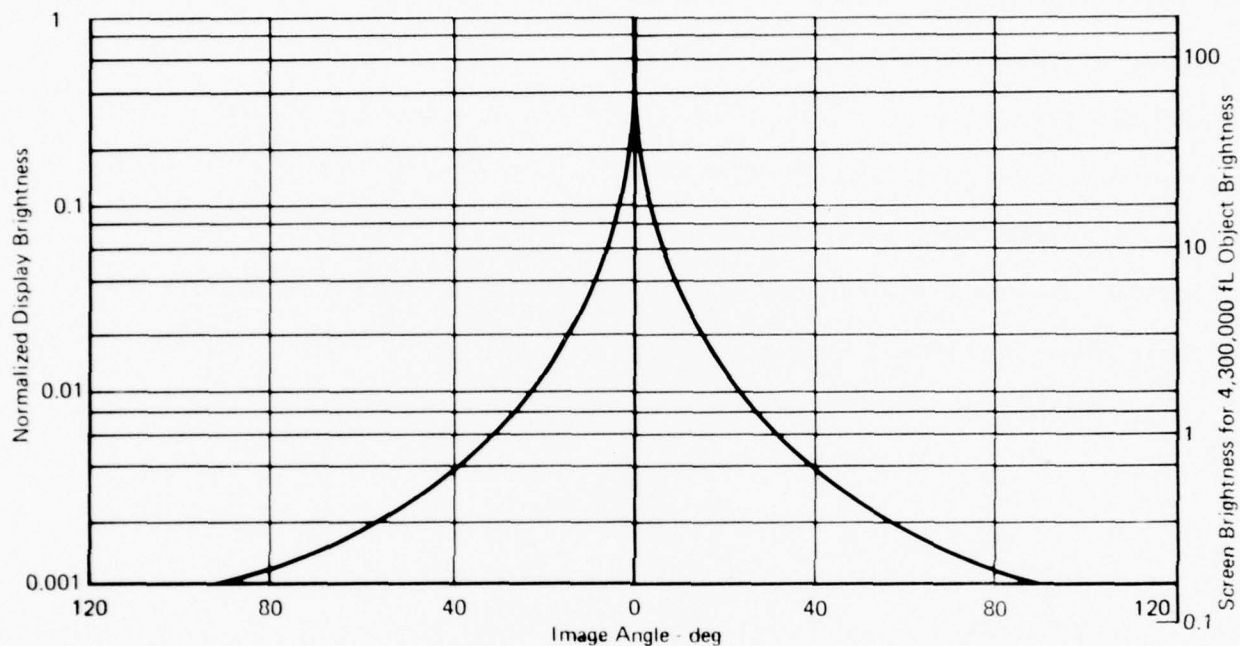


FIGURE C-3
NORMALIZED DISPLAY BRIGHTNESS

GP73-0782-47

100,000,000 ft-lambert to support peripheral vision. This exceedingly high requirement for object brightness initially led us to discard this approach and proceed to direct view display approaches. Difficulty in achieving sufficient exit pupil size and field of view (to be discussed later) with those approaches directed effort back to screen viewing techniques.

Since Equation (C-10) is constant (a function of the original concept) the clue to increasing display brightness must be found in the equation for axial brightness (Equation (C-7)).

Possible parameters are:

1. Screen Characteristics (ω)

2. Projection Lens Aperture (D)
3. Screen/Projector Distance (L)
4. Object Brightness (B)

Screen Solid Angle - In the previous example a minimum value of ω was computed to determine a lower limit of object brightness for the display projector. Since this minimum may not be practical it was studied in more detail. The first observation was that projector/viewer geometry could be improved for a specular coating. This is illustrated in Figure C-4. The eye and lens are equally displaced on each side of the sphere center. This aligns the centroid of the reflected light towards the eye position - making a large ω unnecessary.

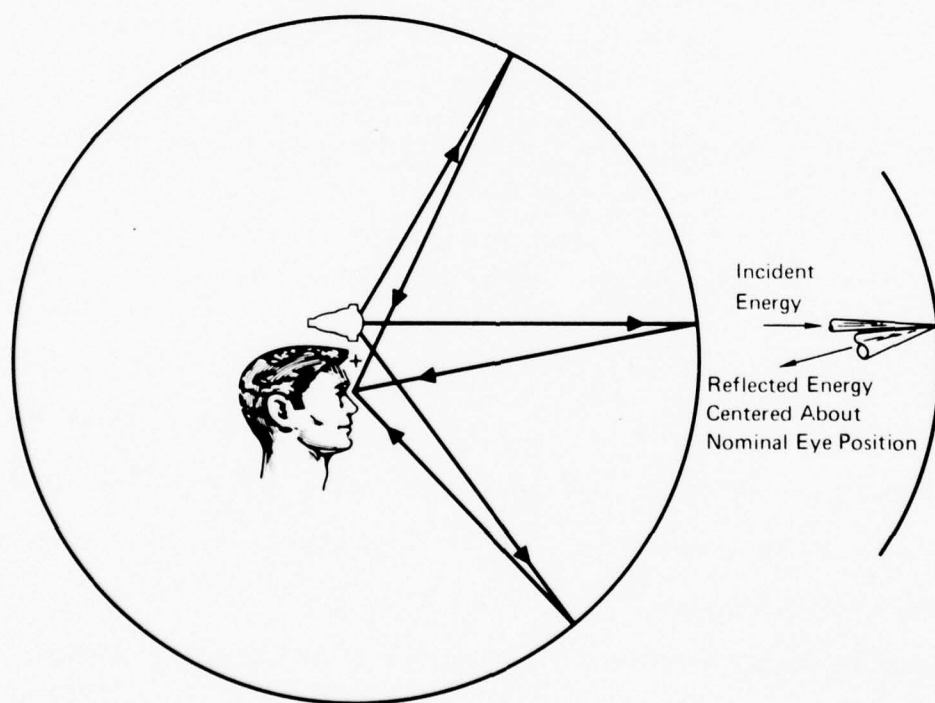


FIGURE C-4
OPTIMUM GEOMETRY FOR SPECULAR SCREEN COATINGS

GP73 0782 54

In reviewing available screen materials from Reference (C-1) Stewart Filmscreen Silvergrain appears good for our application. This screen has a gain of four. While higher gain screens exist, they tend to be retroreflective rather than specular.

Calculating object brightness requirements using this ω yields:

$$B = 25 \times 10^6 \text{ ft-lambert for a 1 ft-lambert screen brightness and full hemispheric projection}$$

The Stewart screen coating discussed above develops a considerably larger dispersion than is required by our concept - i.e., about $\frac{\pi}{4}$ steradians, which is equivalent to 30" dispersion at the head location if $L = 60$ inches. Using the geometry of Figure C-4 the dispersion required could be as small as half the interocular distance plus anticipated head motion. Allowing a 2 inch head motion, about 3 inches would be sufficient. Allowing an additional 2 inches for surface irregularities (about 2°) the solid angle would be

$$\omega = \frac{\pi 5^2}{60^2} = .0218 \text{ steradians}$$

From Equation (B-9)

$$\frac{B_s(0)}{B} = \frac{2.76 \times 10^{-5}}{.0218} = .00126$$

at 90° this requires

$$\frac{B_{90}}{1000} = \frac{B_{s0}}{1000} = 1.26 \times 10^{-6} B$$

For $B_{90} = 1 \text{ ft-lambert}$

$$B = \frac{1}{1.26 \times 10^{-6}} = 794,000 \text{ ft-lambert}$$

This is a substantial reduction below the 25×10^6 required using the Stewart coating.

The natural question at this point is if this type of screen could be fabricated. Theoretically it could be - as shown in Figure C-5. This figure shows the

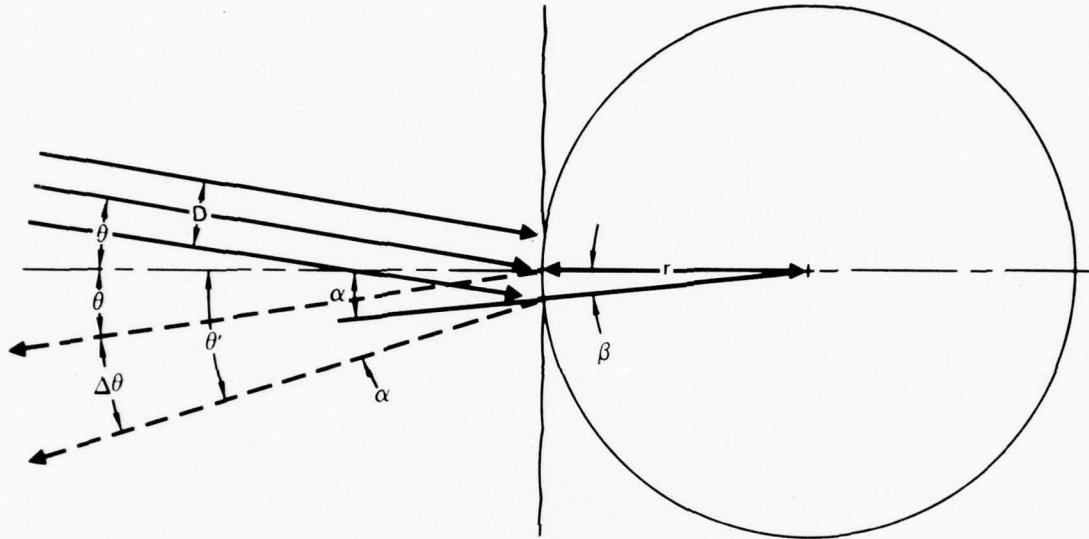


FIGURE C-5
OPTIMUM SCREEN COATING

GP73-0782-23

general construction that would receive the minimum beam dimension D and expand it into a diverging cone having a radius l at distances L ($D \ll l$).

From simple geometry it can be seen that

$$\cos \theta = \frac{D}{2h} \quad B = (\alpha - \theta)$$

$$h = \frac{D}{2 \cos \theta} \quad \alpha = \theta + B$$

$$\sin B = \frac{h}{r}$$

$$\theta' = \alpha + B = \theta + 2B$$

$$\Delta \theta = \theta' - \theta$$

$$\Delta \theta = 2 \arcsin \frac{h}{r}$$

$$\Delta\theta = 2 \arcsin \frac{D}{2r \cos \theta}$$

$$\sin \left(\frac{\theta}{2}\right) = \frac{D}{2r \cos \theta}$$

$$r = \frac{D}{2 \cos \theta \sin \left(\frac{\Delta\theta}{2}\right)}$$

The $\Delta\theta$ required to make 5" dispersion at 60" is

$$\theta = \arcsin \frac{5}{60} = 4.76^\circ$$

For our lens the minimum $D = .00356''$

θ is obtained from the projector lens/eye geometry which also is (by coincidence)

$$\theta = 4.76^\circ$$

Therefore,

$$r = \frac{.00356}{2 \cos 4.76 \sin \frac{4.76}{2}} = .043 \text{ inch}$$

Spacing of sphere centers would be $2h \approx D$

The optimum screen would therefore use specular reflective sections of .043 inch radius spheres - spaces at .0035" centers.

The above calculations show how the projector object brightness requirements could be reduced over 30 times through an optimized screen coating. Construction of such a coating might be expensive however.

Exit Aperture - Brightness requirements reduce by the square of the lens aperture D . Therefore, a new lens design would appear to be of significant value. For instance, if $F_{NO} = 1$ could be achieved, object brightness could be reduced by $(5.6)^2$ or about 30 times. Unfortunately the size of the projection lens would grow at least by 5.6 times. This means the present 9" diameter would increase to about 50". Besides being very expensive, a lens this size would force expansion

of screen geometry. If everything was scaled by 5.6, the advantage of the large aperture would be exactly negated by the increase in projection distance L . Barring a completely different lens design, it appears that questionable advantage can be gained by scaling lens geometry.

If through a new projector lens design, aperture could be made to increase with image angle θ , some compensation in B_s could be achieved while reducing B requirements. The limit of this would probably be $F_{NO} = 1$ in the peripheral field. Applying Equation (C-7), the object brightness requirements would now be:

$$B = 800,000 \text{ ft-lambert (Stewart Screen Coating)}$$

This level of improvement may be achievable through the expense and effort of a completely new non-linear lens design for projection only.

Considering the degree of technical advancement that was required to design a lens with correct distortion, such a redesign for projection appears to be a high risk.

Projection Distance L - Reducing the projection distance, L , is as effective as increasing D is reducing object brightness requirements. However, shown in Figure C-4, parallax angles of both projector/screen and viewer/screen are increased. Also, binocular viewing becomes impaired as L is reduced.

Quite arbitrarily at this time, a parallax of 5° is considered the maximum acceptable. Laboratory tests in projecting transparencies show that this value is acceptable in maintaining focus of the projected image. Since at the time of this writing a full hemispherical projection has not been achieved, it is impossible to determine if 5° is acceptable to the viewer.

It will be shown later that parallax can be eliminated and L reduced through hybrid projection techniques. They require considerable development, however, involving some technical risks.

Maintaining the 5° parallax angle with the existing non-linear lens requires about 60" projection distance. This is considered the minimum acceptable (L) at this time.

Object Brightness - At this point in the analysis it appears that between $.8 \times 10^6$ to 25×10^6 ft-lambert object brightness is required. Standard CRT's are in the 1000-3000 ft-lambert categories and are obviously unusable. Projection CRT's are better but still fall considerably short of the brightness requirements (10,000 - 20,000 ft-lambert) and add a x-ray radiation hazard that would probably make them unacceptable in the RVS application.

Eidophor light valve approaches eliminate the x-ray problem, but are quite large and have a mechanical pointing limit. Their high output, however, makes them a promising candidate. For this reason an available G.E. light valve was studied. The PJ 700 light valve has a monochrome output of 750 lumens and requires approximately F/3 relay optics. This indicates the geometry shown on Figure C-6. Since the non-linear lens requires only F/5.6 solid angle input and an image reduction is required to relay the light valve to the lens, the image brightness is equal to the light valve object brightness. This brightness can be computed as follows:

$$B = \frac{\text{Flux}}{\text{Area} \times \text{Solid Angle}} = \frac{750 \text{ lumens}}{6.3 \times 10^{-3} \times .0872}$$

$$B = 1,365,000 \frac{\text{lumens}}{\text{Ft}^2 \text{ steradian}} = 4,290,000 \text{ ft-lambert}$$

This value lies between requirements of the two screen coatings discussed above. For the Stewart coating, this value is about six times below that desired, or would deliver only .17 ft-lambert at 90° projection.

The scale to the right of Figure C-3 shows actual screen brightness that would be achieved versus field angle for the Stewart screen coating. This figure shows the desired 1 ft-lambert could be achieved out to 32° view angle. At 80°, the

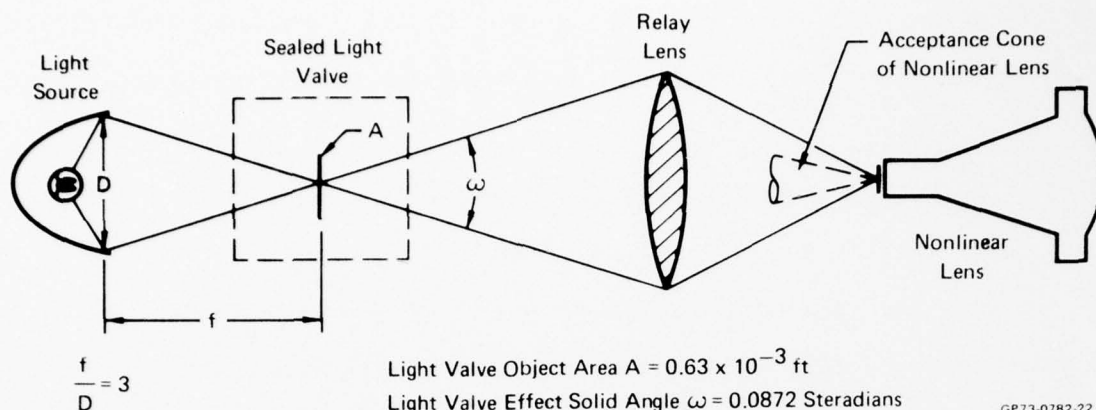


FIGURE C-6
LIGHT VALVE GEOMETRY

assured max field from the existing non-linear lens, the brightness is about .2 ft-lambert.

While Eidophor light valves exist with outputs as high as 4000 lumens, which is sufficient to achieve the desired display brightness, problems such as price, bulkiness, and reliability lead to the off-the-shelf G.E. system being a better choice for a near-term demonstration model. The .2 ft-lambert minimum screen brightness, we believe, is sufficient for these purposes. In the more distant future, single-crystal ferroelectric light valves can be expected to replace the Eidophor type [Reference (C-2)]. In addition to furnishing more light, these devices have a storage capability which will eliminate flicker in the peripheral field of the projected display - (an inherent problem in wide field displays). Therefore, we believe the light valve projection technique, using the existing non-linear lens and existing screen coatings, is a very feasible approach. If performance proves to be marginal, a specialized screen coating can correct the deficiency and assure a display brightness of over 5 ft-lambert.

Appendix D

PROM 1, PROM 2, PROM 3, AND
PROM 4 COMPUTER PROGRAM LISTINGS

Figure D-1 is a listing of the PROM No. 1 Computer Program. Figure D-2 is PROM No. 2, Figure D-3 is PROM No. 3, and Figure D-4 is PROM No. 4.

```

1          ; *****
2          ;
3          ;
4          ;
5          ;          SYSTEM EQUATES
6          ;
7          ;
8          ; *****
9          ;
10         ;
11         ;
12 0000     SETML    EQU      *HA14
13 0000     FIRST   EQU      *H3FE0
14 0000     OUTPT   EQU      *H981
15 0000     OSTAT   EQU      *H3D8A
16 0000     YAW     EQU      *H0400
17 0000     PITCH   EQU      *H0C00
18 0000     CAMAX   EQU      *H3D00
19 0000     CAMBX   EQU      *H3D01
20 0000     CAMAY   EQU      *H3D02
21 0000     CAMBY   EQU      *H3D03
22 0000     CCMAX   EQU      *H3D04
23 0000     CCMBX   EQU      *H3D05
24 0000     CCMAY   EQU      *H3D06
25 0000     CCMBY   EQU      *H3D07
26 0000     CPOAX   EQU      *H3D08
27 0000     CPOBX   EQU      *H3D09
28 0000     CPOAY   EQU      *H3D0A
29 0000     CPOBY   EQU      *H3D0B
30 0000     CPLAX   EQU      *H3D0C
31 0000     CPLBX   EQU      *H3D0D
32 0000     CPLAY   EQU      *H3D0E
33 0000     CPLBY   EQU      *H3D0F
34 0000     DETX    EQU      *H3D10
35 0000     DETY    EQU      *H3D11
36 0000     IPRJX   EQU      *H3D1A
37 0000     IPRJY   EQU      *H3D1C
38 0000     IPOSX   EQU      *H3D1E
39 0000     IPOSY   EQU      *H3D20
40 0000     MULCX   EQU      *H3D90
41 0000     MULDX   EQU      MULCX+20
42 0000     MXLVB   EQU      MULDX+20
43 0000     MXLVK   EQU      MXLVB+20
44 0000     MULAX   EQU      MXLVK+20
45 0000     MULBX   EQU      MULAX+20
46 0000     MULCY   EQU      MULBX+20
47 0000     MULDY   EQU      MULCY+20
48 0000     MYLVB   EQU      MULDY+20
49 0000     MYLVK   EQU      MYLVB+20
50 0000     MULAY   EQU      MYLVK+20

```

Figure D-1 Prom No. 1 Service Interrupt Handler Software

51	0000	MULBY	EQU	MULAY+20
52	0000	NCPOX	EQU	*H3D22
53	0000	NCPOY	EQU	*H3D24
54	0000	PRJAX	EQU	*H3D26
55	0000	PRJBX	EQU	*H3D27
56	0000	PRJAY	EQU	*H3D28
57	0000	PRJBY	EQU	*H3D29
58	0000	PRLAX	EQU	*H3D2A
59	0000	PRLBX	EQU	*H3D2B
60	0000	PRLAY	EQU	*H3D2C
61	0000	PRLBY	EQU	*H3D2D
62	0000	PVLAX	EQU	*H3D2E
63	0000	PVLBX	EQU	*H3D2F
64	0000	PVLAY	EQU	*H3D30
65	0000	PVLBY	EQU	*H3D31
66	0000	RSTRT	EQU	*H3D40
67	0000	RINT	EQU	*H3D34
68	0000	TSTRT	EQU	*H3D47
69	0000	TINT	EQU	*H3D38
70	0000	X	EQU	*H3D3A
71	0000	XY	EQU	*H3D3C
72	0000	XFLAG	EQU	*H3D3E
73	0000	YFLAG	EQU	*H3D3F
74	0000	USCMD	EQU	*H00ED
75	0000	USDAO	EQU	*H00EC
76	0000	USDAI	EQU	*H00EE
77	0000	PRTA1	EQU	*H0000
78	0000	PRTB1	EQU	*H0001
79	0000	PRTC1	EQU	*H0002
80	0000	PRTA2	EQU	*H0003
81	0000	PRTB2	EQU	*H00E5
82	0000	PRTC2	EQU	*H0000
83	0000	PRTD1	EQU	*H0001
84	0000	PRTD2	EQU	*H0002
85	0000	PRTD3	EQU	*H00E6
86	0000	PIOI1	EQU	*H00E7
87	0000	PIOI2	EQU	*H00EB
88	0000	MDW1	EQU	*H009B
89	0000	MDW2	EQU	*H0082
90	0000	N1	EQU	*H0001
91	0000	N2	EQU	*H0003
92	0000	PRSET	EQU	*HEA
93	0000	KYBD1	EQU	*H800
94	0000	KYBD2	EQU	*H9AB
95	0000	COMPAR	EQU	*H816
96	0000		ORG	0
97	0000 F3		DI	
98	0001 31FF3C		LXI	SP, #H3CFF
99	0004 CD8101		CALL	INIT
100	0007 3EC0		MVI	A, #HC0

Figure D-1 Prom No. 1 Service Interrupt Handler Software (Continued)

```

101 0009 328A3D      STA      OSTAT
102 000C 2F          CMA
103 000D D3EA      OUT      PRSET
104 000F 3EC7      MVI      A, #HC7
105 0011 2F          CMA
106 0012 D3EA      OUT      PRSET
107 0014 CDC301     CALL     SETUP
108 0017 FB          EI
109 0018 0604      MVI      B, #H04
110 001A 78          MOV      A, B
111 001B CD8109     CALL     OUTPT
112 001E 3E11      MVI      A, #H11
113 0020 80          ADD      B
114 0021 47          MOV      B, A
115 0022 FES9      CPI      #H59
116 0024 C21A00     JNZ      LEDS
117 0027 CD4401     CALL     ZERO
118 002A 76          HLT
119 002B 3EFF      MVI      A, #HFF
120 002D 2F          CMA
121 002E D3EA      OUT      PRSET
122 0030 C33300     BKWRD:  JMP     FRWRD
123 0033 C33000     FRWRD:  JMP     BKWRD
124 0036            DS      #H38-$
125 0038 C5          SRV:   PUSH     B      ;S
126 0039 D5          PUSH     D      ; A
127 003A E5          PUSH     H      ; V REG
128 003B F5          PUSH     PSW    ; E ITERS
129 003C DB01        IN       N1    ; INPUT LAST 3 BITS OF PROJ X
130 003E F61F        ORI      #H1F
131 0040 FE1F        CPI      #H1F
132 0042 CAD000      JZ       PTY
133 0045 47          MOV      B, A
134 0046 3EC0      MVI      A, #HC0
135 0048 2F          CMA
136 0049 D3EA      OUT      PRSET
137 004B 3EC7      MVI      A, #HC7
138 004D 2F          CMA
139 004E D3EA      OUT      PRSET
140 0050 78          MOV      A, B
141 0051 217B00     LXI      H, JTAB
142 0054 07          LOOP:   RLC
143 0055 DA7300     JC       ST
144 0058 23          INX      H
145 0059 23          INX      H
146 005A C35400     JMP      LOOP
147 005D DB03        PTY:   IN       N2
148 005F F61F        ORI      #H1F
149 0061 47          MOV      B, A
150 0062 3EC0      MVI      A, #HC0

```

Figure D-1 Prom No. 1 Service Interrupt Handler Software (Continued)

```

151 0064 2F          CMA
152 0065 D3EA        OUT    PRSET
153 0067 3EFF        MVI    A, #HFF
154 0069 2F          CMA
155 006A D3EA        OUT    PRSET
156 006C 7B          MOV    A, B
157 006D 218300       LXI    H, JTAB+8
158 0070 C35400       JMP    LOOP
159 0073 FB          ST:    EI
160 0074 EB          XCHG
161 0075 1A          LDAX   D
162 0076 67          MOV    L, A
163 0077 13          INX    D
164 0078 1A          LDAX   D
165 0079 67          MOV    H, A
166 007A E9          PCHL
167 007B 8B00        JTAB:  DI    KB1    ,J    T
168 007D 9100        DI    KB2    ,U    A
169 007F 9700        DI    COMPR  ,M    B
170 0081 AC00        DI    DBRF
171 0083 9D00        DI    RXRDY  ,P    L
172 0085 A300        DI    TXRDY  ,    E
173 0087 A900        DI    SYSCLK ,    S
174 0089 AC00        DI    DBRF
175 008B CD0008 KB1:  CALL  KYBD1  ,SERVICE
176 008E C3AC00       JMP    DBRF
177 0091 CDAB09 KB2:  CALL  KYBD2  ,ROUTINES
178 0094 C3AC00       JMP    DBRF
179 0097 CD1608 COMPR: CALL  COMPAR ,FOR
180 009A C3AC00       JMP    DBRF
181 009D CD5001 RXRDY: CALL  RX      ,INTER
182 00A0 C3AC00       JMP    DBRF
183 00A3 CD2D01 TXRDY: CALL  TX      ,RUPTS
184 00A6 C3AC00       JMP    DBRF
185 00A9 CDB100 SYSCLK: CALL  SYS    ,
186 00AC F1          DBRF:  POP    PSW  ,REST
187 00AD E1          POP    H      ,ORE
188 00AE D1          POP    D      ,REGIS
189 00AF C1          POP    B      ,TERS
190 00B0 C9          RET
191 00B1 21473D SYS:  LXI    H, TSTRT
192 00B4 7E          MOV    A, M
193 00B5 D3EC        OUT    USDAO
194 00B7 2B          DCX    H
195 00B8 22383D       SHLD   TINT
196 00BB 21403D       LXI    H, RSTRT
197 00BE 22343D       SHLD   RINT
198 00C1 213F3D       LXI    H, YFLAG
199 00C4 3E00        MVI    A, #H00
200 00C6 77          MOV    M, A

```

Figure D-1 Prom No. 1 Service Interrupt Handler Software (Continued)

201	00C7 213E3D	LXI	H,XFLAG
202	00CA 77	MOV	M,A
203	00CB DB00	IN	PRTA1
204	00CD 2F	CMA	
205	00CE 32263D	STA	PRJAX
206	00D1 DB01	IN	PRTB1
207	00D3 2F	CMA	
208	00D4 E61F	ANI	*H1F
209	00D6 32273D	STA	PRJBX
210	00D9 DB02	IN	PRTC1
211	00DB 2F	CMA	
212	00DC 32283D	STA	PRJAY
213	00DF DB03	IN	PRTA2
214	00E1 2F	CMA	
215	00E2 E61F	ANI	*H1F
216	00E4 32293D	STA	PRJBY
217	00E7 3A2E3D	LDA	PVLAX
218	00EA 2F	CMA	
219	00EB D300	OUT	PRTC2
220	00ED 3A2F3D	LDA	PVLBX
221	00F0 E60F	ANI	*H0F
222	00F2 322F3D	STA	PVLBX
223	00F5 3A313D	LDA	PVLBY
224	00F8 E6F0	ANI	*HF0
225	00FA 57	MOV	D,A
226	00FB 3A2F3D	LDA	PVLBX
227	00FE B2	ORA	D
228	00FF 2F	CMA	
229	0100 D301	OUT	PRTD1
230	0102 3A303D	LDA	PVLAY
231	0105 2F	CMA	
232	0106 D302	OUT	PRTD2
233	0108 DBE4	IN	*HE4
234	010A 07	RLC	
235	010B DA1101	JC	SCND
236	010E D20801	JNC	PORT
237	0111 DBE4	IN	*HE4
238	0113 07	RLC	
239	0114 07	RLC	
240	0115 D21101	JNC	SCND
241	0118 DBE6	IN	PRTD3
242	011A C680	ADI	*H80
243	011C 32103D	STA	DETX
244	011F DBE5	IN	PRTB2
245	0121 C680	ADI	*H80
246	0123 32113D	STA	DETY
247	0126 CD0004	CALL	YAW
248	0129 CD000C	CALL	PITCH
249	012C C9	RET	
250	012D 2A383D	LHLD	TINT

Figure D-1 Prom No. 1 Service Interrupt Handler Software (Continued)

251	0130 7D	MOV	A,L
252	0131 FE45	CPI	*H45
253	0133 CA4101	JZ	YF
254	0136 DA4001	JC	ET
255	0139 7E	CONT: MOV	A,M
256	013A 2B	DCX	H
257	013B 22303D	SHLD	TINT
258	013E D3EC	OUT	USDAO
259	0140 C9	ET: RET	
260	0141 213F3D	YF: LXI	H,YFLAG
261	0144 7E	MOV	A,M
262	0145 C600	ADI	*H00
263	0147 77	MOV	M,A
264	0148 1F	RAR	
265	0149 2A303D	LHLD	TINT
266	014C DA3901	JC	CONT
267	014F C9	RET	
268	0150 2A343D	RX: LHLD	RINT
269	0153 7D	MOV	A,L
270	0154 FE44	CPI	*H44
271	0156 CA7A01	JZ	CM
272	0159 DBEC	IN	USDAO
273	015B 77	MOV	M,A
274	015C 23	INX	H
275	015D 22343D	SHLD	RINT
276	0160 7D	MOV	A,L
277	0161 FE42	CPI	*H42
278	0163 CA7301	JZ	BM
279	0166 F743	CPI	*H43
280	0168 CA6C01	JZ	AM
281	016B C9	RET	
282	016C 2A303D	AM: LHLD	TINT
283	016F 7E	MOV	A,M
284	0170 D3EC	OUT	USDAO
285	0172 C9	RET	
286	0173 213E3D	BM: LXI	H,XFLAG
287	0176 3E01	MVI	A,*H01
288	0178 77	MOV	M,A
289	0179 C9	RET	
290	017A 2A0E3D	CM: LHLD	CPLAY
291	017D 220A3D	SHLD	CPOAY
292	0180 C9	RET	
293	0181 3E9B	INIT: MVI	A,MDW1
294	0183 D3E7	OUT	PIO11
295	0185 3E02	INIT1: MVI	A,MDW2
296	0187 D3EB	OUT	PIO12
297	0189 AF	UCLEAR: XRA	A
298	018A D3ED	OUT	USCMD
299	018C D3ED	OUT	USCMD
300	018E D3ED	OUT	USCMD

Figure D-1 Prom No. 1 Service Interrupt Handler Software (Continued)

```

301 0190 3E40      MVI      A, *H40
302 0192 D3ED      OUT      USCMD
303 0194 3E6E      MVI      A, *H6E
304 0196 D3ED      OUT      USCMD
305 0198 3E37      MVI      A, *H37
306 019A D3ED      OUT      USCMD
307 019C DBEE      IN       USDAI
308 019E DBEE      IN       USDAI
309 01A0 AF        XRA      A
310 01A1 D3EC      OUT      USDAO
311 01A3 C9        RET
312 01A4 210000     LXI      H, *H0000
313 01A7 223A3D     SHLD     *H3D3A
314 01AA 223C3D     SHLD     *H3D3C
315 01AD 22603D     SHLD     *H3D60
316 01B0 22703D     SHLD     *H3D70
317 01B3 22743D     SHLD     *H3D74
318 01B6 22783D     SHLD     *H3D78
319 01B9 22EE3F     SHLD     *H3FEE
320 01BC 22EA3F     SHLD     *H3FEA
321 01BF 22EC3F     SHLD     *H3FEC
322 01C2 C9        RET
323 01C3 AF        SETUP:  XRA      A
324 01C4 32E03F     STA      FIRST, FIRST=0, THEN FIRST=FF
325 01C7 CD140A     CALL     SETML
326 01CA 3EFF      MVI      A, *HFF
327 01CC 32E03F     STA      FIRST
328 01CF C9        RET
329 01D0            END

```

Figure D-1 Prom No. 1 Service Interrupt Handler Software (Continued)

INTEL 8086 .ROSS ASSEMBLER SYMBOL TABLE

PVLBX= 3D2F	PVLAY= 3D30	PVLBY= 3D31	RSTRT= 3D40
RINT = 3D34	TSTRT= 3D47	TINT = 3D38	X = 3D3A
XY = 3D3C	XFLAG= 3D3E	YFLAG= 3D3F	USCMD= 00ED
USDAO= 00EC	USDAI= 00EE	PRTA1= 0000	PRTB1= 0001
PRTC1= 0002	PRTA2= 0003	PRTB2= 00E5	PRTC2= 0000
PRTD1= 0001	PRTD2= 0002	PRTD3= 00E6	PRSET= 00EA
COMP= 0816	LEDS = 001A	BKWRD 0030	FRWRD 0033
SRV = 0038	LOOP 0054	PTY = 005D	ST = 0073
JTAB 007B	COMPR 0097	RXRDY 009D	TXRDY 00A3
SYSCL 00A9	SYS = 00B1	PORT = 0108	SCND = 0111
TX = 012D	CONT = 0139	ET = 0140	YF = 0141
RX = 0150	N1 = 0001	KB1 = 008B	KB2 = 0091
N2 = 0003	BM = 0173	CM = 017A	A = 0007
INIT = 0181	INIT1 = 0185	B = 0000	UCLEA = 0189
ZERO = 01A4	C = 0001	SETUP = 01C3	D = 0002
E = 0003	KYBD1= 0800	KYBD2= 09AB	PIO11= 00E7
MDW1 = 009B	MDW2 = 0082	PIO12= 00EB	DBRF = 00AC
AM = 016C	H = 0004	CAMAX= 3D00	CAMBX= 3D01
CAMAY= 3D02	CAMBY= 3D03	CCMAX= 3D04	CCMBX= 3D05
CCMAY= 3D06	CCMBY= 3D07	PITCH= 0C00	CPOAX= 3D08
CPLAX= 3D0C	L = 0005	CPOBX= 3D09	CPOAY= 3D0A
M = 0006	SETML= 0A14	CPOBY= 3D0B	FIRST= 3FE0
CPLBX= 3D0D	CPLAY= 3D0E	OSTAT= 3D8A	CPLBY= 3D0F
DETX = 3D10	YAW = 0400	DETY = 3D11	IPRJX= 3D1A
SP = 0006	IPRJY= 3D1C	IPOSX= 3D1E	OUTPT= 0981
IPOSY= 3D20	MULCX= 3D90	PSW = 0006	MULDY= 3D2A
MXLVB= 3DB8	MXLVK= 3DCC	MULAX= 3DE0	MULBX= 3DF4
MULCY= 3E08	MULDY= 3E1C	MYLVB= 3E30	MYLVK= 3E44
MULAY= 3E58	MULBY= 3E6C	NCPOX= 3D22	NCPOY= 3D24
PRJAX= 3D26	PRJBX= 3D27	PRJAY= 3D28	PRJBY= 3D29
PRLAX= 3D2A	PRLBX= 3D2B	PRLAY= 3D2C	PRLBY= 3D2D
PVLAX= 3D2E			

ERRORS DETECTED: 0

Figure D-1 Prom No. 1 Service Interrupt Handler Software (Concluded)

```

1          ; *****
2          ;
3          ;
4          ;
5          ;      SYSTEM EQUATES
6          ;
7          ;
8          ; *****
9          ;
10         ;
11         ;
12 0000     CAMAX   EQU    *H3D00
13 0000     CAMBX   EQU    *H3D01
14 0000     CAMAY   EQU    *H3D02
15 0000     CAMBY   EQU    *H3D03
16 0000     CCMAX   EQU    *H3D46
17 0000     CCMAY   EQU    *H3D44
18 0000     CPOAX   EQU    *H3D40
19 0000     CPOBX   EQU    *H3D41
20 0000     CPOAY   EQU    *H3D42
21 0000     CPOBY   EQU    *H3D43
22 0000     CPLAX   EQU    *H3D0C
23 0000     CPLBX   EQU    *H3D0D
24 0000     CPLAY   EQU    *H3D0E
25 0000     CPLBY   EQU    *H3D0F
26 0000     DETX    EQU    *H3D10
27 0000     DETY    EQU    *H3D11
28 0000     DDOTX   EQU    *H3D12
29 0000     DDOTY   EQU    *H3D14
30 0000     DOTIX   EQU    *H3D16
31 0000     DOTIY   EQU    *H3D18
32 0000     IPRJX   EQU    *H3D1A
33 0000     IPRJY   EQU    *H3D1C
34 0000     IPOSX   EQU    *H3D1E
35 0000     IPOSY   EQU    *H3D20
36 0000     MULCX   EQU    *H3D90
37 0000     MULDX   EQU    MULCX+20
38 0000     MXLVB   EQU    MULDX+20
39 0000     MXLVK   EQU    MXLVB+20
40 0000     MULAX   EQU    MXLVK+20
41 0000     MULBX   EQU    MULAX+20
42 0000     MULCY   EQU    MULBX+20
43 0000     MULDY   EQU    MULCY+20
44 0000     MYLVB   EQU    MULDY+20
45 0000     MYLVK   EQU    MYLVB+20
46 0000     MULAY   EQU    MYLVK+20
47 0000     MULBY   EQU    MULAY+20
48 0000     MICH    EQU    MULBY+20
49 0000     MICHY   EQU    MICH+20
50 0000     CMIY    EQU    MICHY+20

```

Figure D-2 Prom No. 2 Yaw Control Software


```

51 0000      CMIX      EQU      CMIX+20
52 0000      TORQY     EQU      CMIX+20
53 0000      TORQX     EQU      TORQY+20
54 0000      PTQX      EQU      TORQX+20
55 0000      NCPOX     EQU      *H3D22
56 0000      NCPOY     EQU      *H3D24
57 0000      PRJAX     EQU      *H3D26
58 0000      PRJBX     EQU      *H3D27
59 0000      PRJAY     EQU      *H3D28
60 0000      PRJBY     EQU      *H3D29
61 0000      PRLAX     EQU      *H3D2A
62 0000      PRLBX     EQU      *H3D2B
63 0000      PRLAY     EQU      *H3D2C
64 0000      PRLBY     EQU      *H3D2D
65 0000      PVLAX     EQU      *H3D2E
66 0000      PVLBX     EQU      *H3D2F
67 0000      PVLAY     EQU      *H3D30
68 0000      PVLBY     EQU      *H3D31
69 0000      RINT      EQU      *H3D34
70 0000      TINT      EQU      *H3D3B
71 0000      X          EQU      *H3D3A
72 0000      XY         EQU      *H3D3C
73 0000      XFLAG     EQU      *H3D3E
74 0000      YFLAG     EQU      *H3D3F
75 0000      DELY      EQU      *H3D68
76 0000      ICHY      EQU      *H3D70
77 0000      CDEL      EQU      *H3D72
78 0000      CIY       EQU      *H3D74
79 0000      USDAO     EQU      *H00EC
80 0000      PRTA1     EQU      *H0000
81 0000      PRTB1     EQU      *H0001
82 0000      PRTC1     EQU      *H0002
83 0000      PRTA2     EQU      *H0003
84 0000      PRTB2     EQU      *H00E5
85 0000      PRTC2     EQU      *H0000
86 0000      PRTD1     EQU      *H0001
87 0000      PRTD2     EQU      *H0002
88 0000      PRTD3     EQU      *H00E6
89
90      ;      SYSTEM COMPENSATION NETWORK
91      ;
92      ;
93 0400      ORG        *H400
94 0400 2A2C3D YAW:    LHLD     PRLAY
95 0403 EB          XCHG
96 0404 3A293D      LDA      PRJBY
97 0407 E610        ANI      *H10
98 0409 FE10        CPI      *H10
99 040B C21604      JNZ      RA
100 040E 3A293D      LDA      PRJBY

```

Figure D-2 Prom No. 2 Yaw Control Software (Continued)

101	0411 C6E0	ADI	*HE0
102	0413 32293D	STA	PRJBY
103	0416 2A283D RA:	LHLD	PRJAY
104	0419 CD4305	CALL	MINUS
105	041C 19	DAD	D
106	041D CD4305	CALL	MINUS
107	0420 EB	XCHG	
108	0421 CD083E	CALL	MULCY
109	0424 22143D	SHLD	DDOTY
110	0427 DBEC	IN	USDAO
111	0429 3A113D	LDA	DETY
112	042C FE04	CPI	*H04
113	042E F24004	JP	PAA
114	0431 FEFC	CPI	*HFC
115	0433 FA3B04	JM	MAN
116	0436 3E00	MVI	A.*H00
117	0438 C34204	JMP	ING
118	043B C604 MAN:	ADI	*H04
119	043D C34204	JMP	ING
120	0440 C6FC PAA:	ADI	*HFC
121	0442 5F ING:	MOV	E.A
122	0443 FE00	CPI	*H00
123	0445 3E00	MVI	A.*H00
124	0447 F24B04	JP	ZP
125	044A 2F	CMA	
126	044B 5F ZP:	MOV	D.A
127	044C CD1C3E	CALL	MULDY
128	044F EB	XCHG	
129	0450 2A143D	LHLD	DDOTY
130	0453 19	DAD	D
131	0454 EB	XCHG	
132	0455 7A	MOV	A.D
133	0456 07	RLC	
134	0457 DA6404	JC	FIVE
135	045A 21CCFF	LXI	H.*HFFCC
136	045D 19	DAD	D
137	045E DA7204	JC	PL
138	0461 C36B04	JMP	TWO
139	0464 213400 FIVE:	LXI	H.*H0034
140	0467 19	DAD	D
141	0468 D27B04	JNC	ML
142	046B EB TWO:	XCHG	
143	046C 22023D	SHLD	CAMAY
144	046F C38404	JMP	EXT
145	0472 213400 PL:	LXI	H.*H34
146	0475 22023D	SHLD	CAMAY
147	0478 C38404	JMP	EXT
148	047B 21CCFF ML:	LXI	H.*HFFCC
149	047E 22023D	SHLD	CAMAY
150	0481 C38404	JMP	EXT

Figure D-2 Prom No. 2 Yaw Control Software (Continued)

```

151      ;
152      ; CAMERA SERVO
153      ;
154 0484 3A433D EXT: LDA CPOBY
155 0487 E61F ANI *H1F
156 0489 32433D STA CPOBY
157 048C E610 ANI *H10
158 048E FE10 CPI *H10
159 0490 C29B04 JNZ WP
160 0493 3A433D LDA CPOBY
161 0496 C6E0 ADI *HE0
162 0498 32433D STA CPOBY
163 049B 2A423D WP: LHLD CPOAY
164 049E CD4305 CALL MINUS
165 04A1 22243D SHLD NCPOY
166 04A4 EB XCHG
167 04A5 2A0E3D LHLD CPLAY
168 04A8 19 DAD D
169 04A9 22F03F SHLD *H3FF0
170 04AC 29 DAD H
171 04AD 29 DAD H
172 04AE EB XCHG
173 04AF 2A423D LHLD CPOAY
174 04B2 220E3D SHLD CPLAY
175 04B5 7A MOV A,D
176 04B6 07 KLC
177 04B7 D2C404 JNC OGDR
178 04BA 211101 LXI H,*H111
179 04BD 19 DAD D
180 04BE D2D404 JNC DECR
181 04C1 C3DA04 JMP MUL
182 04C4 21EFFE OGDR: LXI H,*HFEEF
183 04C7 19 DAD D
184 04C8 DACE04 JC LMAR
185 04CB C3DA04 JMP MUL
186 04CE 210040 LMAR: LXI H,*H4000
187 04D1 C3DD04 JMP FLTR
188 04D4 2100C0 DECR: LXI H,*HC000
189 04D7 C3DD04 JMP FLTR
190 04DA CD303E MUL: CALL MYLVB
191 04DD CD4B05 FLTR: CALL SHIFT
192 04E0 CD4B05 CALL SHIFT
193 04E3 EB XCHG
194 04E4 2A803D LHLD *H3D80
195 04E7 19 DAD D
196 04E8 EB XCHG
197 04E9 22803D SHLD *H3D80
198 04EC 2A823D LHLD *H3D82
199 04EF CD4B05 CALL SHIFT
200 04F2 13 DAD D

```

Figure D-2 Prom No. 2 Yaw Control Software (Continued)

201	04F3	22823D	SHLD	*H3D82
202	04F6	22183D	SHLD	DOTIY
203	04F9	2A023D	LHLD	CAMAY
204	04FC	EB	XCHG	
205	04FD	2A3C3D	LHLD	XY
206	0500	19	DAD	D
207	0501	EB	XCHG	
208	0502	7A	MOV	A,D
209	0503	07	RLC	
210	0504	DA1205	JC	PAP
211	0507	21D0E2	LXI	H,*HE2D0
212	050A	19	DAD	D
213	050B	DA1D05	JC	ONE
214	050E	EB	XCHG	
215	050F	C33205	JMP	THRE
216	0512	21041E PAP:	LXI	H,*H1E04
217	0515	19	DAD	D
218	0516	D22905	JNC	FOUR
219	0519	EB	XCHG	
220	051A	C33205	JMP	THRE
221	051D	210000 ONE:	LXI	H,0
222	0520	22023D	SHLD	CAMAY
223	0523	21301D	LXI	H,*H1D30
224	0526	C33205	JMP	THRE
225	0529	210000 FOUR:	LXI	H,0
226	052C	22023D	SHLD	CAMAY
227	052F	21FCE1	LXI	H,*HE1FC
228	0532	223C3D THRE:	SHLD	XY
229	0535	EB	XCHG	
230	0536	2A243D	LHLD	NCPOY
231	0539	29	DAD	H
232	053A	29	DAD	H
233	053B	19	DAD	D
234	053C	22723D	SHLD	CDEL
235	053F	EB	XCHG	
236	0540	C30006	JMP	*H600
237	0543	7C MINUS:	MOV	A,H
238	0544	2F	CMA	
239	0545	67	MOV	H,A
240	0546	7D	MOV	A,L
241	0547	2F	CMA	
242	0548	6F	MOV	L,A
243	0549	23	INX	H
244	054A	C9	RET	
245	054E	7C SHIFT:	MOV	A,H
246	054C	07	RLC	
247	054D	7C	MOV	A,H
248	054E	1F	RAR	
249	054F	67	MOV	H,A
250	0550	7D	MOV	A,L

Figure D-2 Prom No. 2 Yaw Control Software (Continued)

251	0551	1F	RAR	
252	0552	6F	MOV	L,A
253	0553	C9	RET	
254	0554		END	

Figure D-2 Prom No. 2 Yaw Control Software (Continued)


```

1          ;*****
2          ;
3          ;
4          ;
5          ;      SYSTEM EQUATES
6          ;
7          ;
8          ;*****
9          ;
10         ;
11         ;
12 0000     LAGX     EQU     *H3F0C
13 0000     LAGY     EQU     *H3F20
14 0000     CDEL     EQU     *H3D72
15 0000     EOY      EQU     *H3FEC
16 0000     CAMAX    EQU     *H3D00
17 0000     CAMBX    EQU     *H3D01
18 0000     CAMAY    EQU     *H3D02
19 0000     CAMBY    EQU     *H3D03
20 0000     CCMAX    EQU     *H3D46
21 0000     CCMAY    EQU     *H3D44
22 0000     CPOAX    EQU     *H3D40
23 0000     CPOBX    EQU     *H3D41
24 0000     CPOAY    EQU     *H3D42
25 0000     CPOBY    EQU     *H3D43
26 0000     CPLAX    EQU     *H3D0C
27 0000     CPLBX    EQU     *H3D0D
28 0000     CPLAY    EQU     *H3D0E
29 0000     CPLBY    EQU     *H3D0F
30 0000     DETX     EQU     *H3D10
31 0000     DETY     EQU     *H3D11
32 0000     DDOTX    EQU     *H3D12
33 0000     DDOTY    EQU     *H3D14
34 0000     DOTIX    EQU     *H3D16
35 0000     DOTIY    EQU     *H3D18
36 0000     IPRJX    EQU     *H3D1A
37 0000     IPRJY    EQU     *H3D1C
38 0000     IPOSX    EQU     *H3D1E
39 0000     IPOSY    EQU     *H3D20
40 0000     MULCX    EQU     *H3D90
41 0000     MULDX    EQU     MULCX+20
42 0000     MXLVB    EQU     MULDX+20
43 0000     MXLVK    EQU     MXLVB+20
44 0000     MULAX    EQU     MXLVK+20
45 0000     MULBX    EQU     MULAX+20
46 0000     MULCY    EQU     MULBX+20
47 0000     MULDY    EQU     MULCY+20
48 0000     MYLVB    EQU     MULDY+20
49 0000     MYLVK    EQU     MYLVB+20
50 0000     MULAY    EQU     MYLVK+20

```

Figure D-2 Prom No. 2 Yaw Control Software (Continued)

51	0000	MULBY	EQU	MULAY+20
52	0000	MICH	EQU	MULBY+20
53	0000	MICHY	EQU	MICH+20
54	0000	CMY	EQU	MICHY+20
55	0000	CMIX	EQU	CMY+20
56	0000	TORQY	EQU	CMIX+20
57	0000	TORQX	EQU	TORQY+20
58	0000	PTQX	EQU	TORQX+20
59	0000	NCPOX	EQU	*H3D22
60	0000	NCPOY	EQU	*H3D24
61	0000	PRJAX	EQU	*H3D26
62	0000	PRJBX	EQU	*H3D27
63	0000	PRJAY	EQU	*H3D28
64	0000	PRJBY	EQU	*H3D29
65	0000	PRLAX	EQU	*H3D2A
66	0000	PRLBX	EQU	*H3D2B
67	0000	PRLAY	EQU	*H3D2C
68	0000	PRLBY	EQU	*H3D2D
69	0000	PVLAX	EQU	*H3D2E
70	0000	PVLBX	EQU	*H3D2F
71	0000	PVLAY	EQU	*H3D30
72	0000	PVLBY	EQU	*H3D31
73	0000	RINT	EQU	*H3D34
74	0000	TINT	EQU	*H3D38
75	0000	X	EQU	*H3D3A
76	0000	XY	EQU	*H3D3C
77	0000	XFLAG	EQU	*H3D3E
78	0000	YFLAG	EQU	*H3D3F
79	0000	DELY	EQU	*H3D68
80	0000	ICHY	EQU	*H3D70
81	0000	USDAO	EQU	*H00EC
82	0000	PRTA1	EQU	*H0000
83	0000	PRTB1	EQU	*H0001
84	0000	PRTC1	EQU	*H0002
85	0000	PRTA2	EQU	*H0003
86	0000	PRTB2	EQU	*H00E5
87	0000	PRTC2	EQU	*H0000
88	0000	PRTD1	EQU	*H0001
89	0000	PRTD2	EQU	*H0002
90	0000	PRTD3	EQU	*H00E6
91	0600		ORG	*H600
92	0600 7A		MOV	A, D
93	0601 07		RLC	
94	0602 DA1506		JC	YMI
95	0605 2100F0		LXI	H, *HF000
96	0608 19		DAD	D
97	0609 DA0F06		JC	YLM
98	060C C32506		JMP	KV
99	060F 210040	YLM:	LXI	H, *H4000
100	0612 C32806		JMP	YE

Figure D-2 Prom No. 2 Yaw Control Software (Continued)

```

101 0615 210010 YMI: LXI H,*H1000
102 0618 19 DAD D
103 0619 D21F06 JNC YDE
104 061C C32506 JMP KV
105 061F 2100C0 YDE: LXI H,*HC000
106 0622 C32806 JMP YE
107 0625 CD443E KV: CALL MYLVK
108 0628 EB YE: XCHG
109 0629 2A183D LHLD DOTIY
110 062C 19 DAD D
111 062D EB XCHG
112 062E 7A MOV A,D
113 062F 07 RLC
114 0630 DA4306 JC KAD
115 0633 21BCFB LXI H,*HFBBC
116 0636 19 DAD D
117 0637 DA3D06 JC OH
118 063A C35306 JMP GOSH
119 063D 210040 OH: LXI H,*H4000
120 0640 C35606 JMP OSH
121 0643 214404 KAD: LXI H,*H444
122 0646 19 DAD D
123 0647 D24D06 JNC WOW
124 064A C35306 JMP GOSH
125 064D 2100C0 WOW: LXI H,*HC000
126 0650 C35606 JMP OSH
127 0653 CDD03E GOSH: CALL TORQY
128 0656 22443D OSH: SHLD CCMAY
129 ;
130 ;PROJECTOR SERVO
131 ;
132 ;
133 0659 CDAC07 CALL LAG
134 065C 2A723D LHLD CDEL
135 065F EB XCHG
136 0660 7A MOV A,D
137 0661 07 RLC
138 0662 D26F06 JNC YYY
139 0665 210004 LXI H,*H400
140 0668 19 DAD D
141 0669 D27906 JNC LARGE
142 066C C38806 JMP GO
143 066F 2100FC YYY: LXI H,*HFC00
144 0672 19 DAD D
145 0673 DA7906 JC LARGE
146 0676 C38806 JMP GO
147 0679 2A3C3D LARGE: LHLD XY
148 067C CDA407 CALL MINUS
149 067F CD9B07 CALL SHIFT
150 0682 CD9B07 CALL SHIFT

```

Figure D-2 Prom No. 2 Yaw Control Software (Continued)

151	0685	22243D	SHLD	NCPOY
152	0688	2A283D GO:	LHLD	PRJAY
153	068B	CDA407	CALL	MINUS
154	068E	221C3D	SHLD	IPRJY
155	0691	EB	XCHG	
156	0692	2A243D	LHLD	NCPOY
157	0695	19	DAD	D
158	0696	22683D	SHLD	DELY
159	0699	EB	XCHG	
160	069A	7A	MOV	A,D
161	069B	07	RLC	
162	069C	D2B506	JNC	OGD
163	069F	216600	LXI	H.*H0066
164	06A2	19	DAD	D
165	06A3	D2AF06	JNC	DEC
166	06A6	C3BC06	JMP	BY
167	06A9	210040 LMA:	LXI	H.*H4000
168	06AC	C3BF06	JMP	IP
169	06AF	2100C0 DEC:	LXI	H.*HC000
170	06B2	C3BF06	JMP	IP
171	06B5	219AFF OGD:	LXI	H.*HFF9A
172	06B8	19	DAD	D
173	06B9	DAA906	JC	LMA
174	06BC	CD6C3E BY:	CALL	MULBY
175	06BF	22203D IP:	SHLD	IPOSY
176	06C2	2A683D	LHLD	DELY
177	06C5	EB	XCHG	
178	06C6	7A	MOV	A,D
179	06C7	07	RLC	
180	06C8	D2D506	JNC	CLA
181	06CB	213000	LXI	H.*H30
182	06CE	19	DAD	D
183	06CF	D21307	JNC	OUT
184	06D2	C3DC06	JMP	GAIN
185	06D5	21D0FF CLA:	LXI	H.*HFFD0
186	06D8	19	DAD	D
187	06D9	DA1307	JC	OUT
188	06DC	CD943E GAIN:	CALL	MICHY
189	06DF	EB	XCHG	
190	06E0	2A703D	LHLD	ICHY
191	06E3	19	DAD	D
192	06E4	22703D	SHLD	ICHY
193	06E7	EB	XCHG	
194	06E8	7A	MOV	A,D
195	06E9	07	RLC	
196	06EA	DAF706	JC	PA
197	06ED	2100C0	LXI	H.*HC000
198	06F0	19	DAD	D
199	06F1	DA0107	JC	PB
200	06F4	C30C07	JMP	PC

Figure D-2 Prom No. 2 Yaw Control Software (Continued)

201	06F7	210040 PA:	LXI	H, *H4000
202	06FA	19	DAD	D
203	06FB	D20B07	JNC	PD
204	06FE	C30C07	JMP	PC
205	0701	210040 PB:	LXI	H, *H4000
206	0704	EB	XCHG	
207	0705	C30C07	JMP	PC
208	0708	2100C0 PD:	LXI	H, *HC000
209	070B	EB	XCHG	
210	070C	2A203D PC:	LHLD	IPOSY
211	070F	19	DAD	D
212	0710	22203D	SHLD	IPOSY
213	0713	2A2C3D OUT:	LHLD	PRLAY
214	0716	EB	XCHG	
215	0717	2A2B3D	LHLD	PRJAY
216	071A	222C3D	SHLD	PRLAY
217	071D	2A1C3D	LHLD	IPRJJ
218	0720	19	DAD	D
219	0721	22F23F	SHLD	*H3FF2
220	0724	29	DAD	H
221	0725	29	DAD	H
222	0726	29	DAD	H
223	0727	29	DAD	H
224	0728	29	DAD	H
225	0729	EB	XCHG	
226	072A	2AEC3F	LHLD	EOY
227	072D	CDA407	CALL	MINUS
228	0730	19	DAD	D
229	0731	29	DAD	H
230	0732	EB	XCHG	
231	0733	7A	MOV	A, D
232	0734	07	RLC	
233	0735	D24207	JNC	OGDR
234	0738	210004	LXI	H, *H400
235	073B	19	DAD	D
236	073C	D25207	JNC	DECR
237	073F	C35B07	JMP	BXR
238	0742	2100FC OGDR:	LXI	H, *HFC00
239	0745	19	DAD	D
240	0746	DA4C07	JC	LMAR
241	0749	C35B07	JMP	BXR
242	074C	210040 LMAR:	LXI	H, *H4000
243	074F	C35B07	JMP	IPR
244	0752	2100C0 DECR:	LXI	H, *HC000
245	0755	C35B07	JMP	IPR
246	0758	CD5B3E BXR:	CALL	MULAY
247	075B	CD9B07 IPR:	CALL	SHIFT
248	075E	CD9B07	CALL	SHIFT
249	0761	EB	XCHG	
250	0762	2A623D	LHLD	*H3D62

Figure D-2 Prom No. 2 Yaw Control Software (Continued)

251	0765 19	DAD	D
252	0766 EB	XCHG	
253	0767 22623D	SHLD	*H3D62
254	076A 2A643D	LHLD	*H3D64
255	076D CD9B07	CALL	SHIFT
256	0770 19	DAD	D
257	0771 22643D	SHLD	*H3D64
258	0774 EB	XCHG	
259	0775 2A203D	LHLD	IPOSY
260	0778 19	DAD	D
261	0779 22303D	SHLD	PVLAY
262	077C 29	DAD	H
263	077D 29	DAD	H
264	077E 29	DAD	H
265	077F 29	DAD	H
266	0780 7C	MOV	A.H
267	0781 32303D	STA	PVLAY
268	0784 213F3D	LXI	H.YFLAG
269	0787 7E	MOV	A.M
270	0788 C601	ADI	*H01
271	078A 77	MOV	M.A
272	078B 07	RLC	
273	078C DA9007	JC	ALT
274	078F C9	RET	
275	0790 2A3B3D ALT:	LHLD	TINT
276	0793 7E	MOV	A.M
277	0794 2B	DCX	H
278	0795 223B3D	SHLD	TINT
279	0796 D3EC	OUT	USDAO
280	079A C9	RET	
281	079B 7C SHIFT:	MOV	A.H
282	079C 07	RLC	
283	079D 7C	MOV	A.H
284	079E 1F	RAR	
285	079F 67	MOV	H.A
286	07A0 7D	MOV	A.L
287	07A1 1F	RAR	
288	07A2 6F	MOV	L.A
289	07A3 C9	RET	
290	07A4 7C MINUS:	MOV	A.H
291	07A5 2F	CMA	
292	07A6 67	MOV	H.A
293	07A7 7D	MOV	A.L
294	07A8 2F	CMA	
295	07A9 6F	MOV	L.A
296	07AA 23	INX	H
297	07AB C9	RET	
298	07AC 2A023D LAG:	LHLD	CAMAY
299	07AF 29	DAD	H
300	07B0 29	DAD	H

Figure D-2 Prom No. 2 Yaw Control Software (Continued)

301	07B1 29	DAD	H
302	07B2 EB	XCHG	
303	07B3 2AEC3F	LHLD	EOY
304	07B6 CDA407	CALL	MINUS
305	07B9 19	DAD	D
306	07BA EB	XCHG	
307	07BB CDA83E	CALL	CMIY
308	07BE CD9B07	CALL	SHIFT
309	07C1 CD9B07	CALL	SHIFT
310	07C4 CD9B07	CALL	SHIFT
311	07C7 CD9B07	CALL	SHIFT
312	07CA CD9B07	CALL	SHIFT
313	07CD CD9B07	CALL	SHIFT
314	07D0 CD9B07	CALL	SHIFT
315	07D3 EB	XCHG	
316	07D4 2AEC3F	LHLD	EOY
317	07D7 19	DAD	D
318	07D8 22EC3F	SHLD	EOY
319	07DB C9	RET	
320	07DC	END	

Figure D-2 Prom No. 2 Yaw Control Software (Concluded)

```

1 0000          ORG    *H800
2 0000      KBIN2    EQU    *HE9      ;KEYBOARD INPUT PORT
3 0000      PRSET    EQU    *HEA      ;INTERRUPT FLIP-FLOP PRESET OUTPUT PO
4 0000      LEDCM    EQU    *HEB      ;LED AND COMPARATOR OUTPUT PORT
5 0000      SETML    EQU    *HA14
6 0000      OK       EQU    *HA64
7 0000      CHANG    EQU    *HA52
8 0000      READA    EQU    *H3D80    ;3D80 THRU 3D83 IS ADDRESS INFORMATIO
9 0000      READD    EQU    READA+4    ;3D84 THRU 3D85 IS DATA INFORMATION
10 0000      READF    EQU    READD+2    ;3D86 IS FUNCTION INFORMATION
11 0000      FSTAT    EQU    READF+1    ;3D87 IS FUNCTION STATUS
12 0000      PSAVE    EQU    FSTAT+1    ;PSAVE IS THE RETURN LOCATION IN INTE
13 0000      OSTAT    EQU    PSAVE+2    ;CODE FOR EXPECTED KEYBOARD INPUT
14          ;KBRD1 IS THE FUNCTION KEYBOARD SERVICE ROUTINE
15 0000 DBE9      KBRD1: IN      KBIN2    ;INPUT FUNCTION INFORMATION
16 0002 E6F0          ANI    *HF0      ;WE'RE ONLY INTERESTED IN HIGH ORDER
17 0004 47          MOV    B,A        ;SAVE FOR LATER
18 0005 32863D      STA    READF      ;STORE INFORMATION READ
19 0008 FE80          CPI    *H80      ;IS THIS A MAJOR OR MINOR FUNCTION
20 000A DA1F08      JC      FUNCT     ;MINOR FUNCTION-JUMP TO FUNCT
21          :      OSTAT=C0 MEANS MAJOR FUNCTION IS EXPECTED
22          :      OSTAT=20 MEANS MINOR MONITOR FUNCTION IS EXPECTED
23          :      OSTAT=10 MEANS MINOR SETML FUNCTION (CHANG OR OK) IS EXPE
24          :      OSTAT=8 MEANS NUMBER IS EXPECTED
25          :      LDA    OSTAT
26          :      CPI    *HC0
27          :      JNZ    ERROR
28 000D 78          MOV    A,B
29 000E FED0          CPI    *HD0      ;FIND PARTICULAR MAJOR FUNCTION
30 0010 DA140A      JC      SETML     ;JUMP TO SETML IF ACC=C0
31 0013 CAB309      JZ      START     ;JUMP TO START IF ACC=D0
32          :      ;COMPR IS THE ENTRY POINT WHEN A COMPARE INTERRUPT OCCURS
33 0016 3E20      COMPR: MVI    A,*H20 ;MONITOR OR COMPARE INTERRUPT HAS OCC
34 0018 328A3D      STA    OSTAT     ;GET READY FOR MONITOR MINOR FUNCTION
35 001B 78          MOV    A,B
36 001C C32E08      JMP    MONITR
37 001F FE80      FUNCT: CPI    *H80  ;CHECK FOR MONITOR MINOR OR SETML MIN
38 0021 DA2D08      JC      DIAG     ;IF LESS THAN 80 IT'S A MONITOR MINOR
39          :      LDA    OSTAT     ;CHECK FOR SETML MINOR FUNCTION
40          :      ANI    *H10
41          :      JZ      ERROR
42 0024 78          MOV    A,B      ;IS IT AN OK OR A CHANG
43 0025 FE90          CPI    *H90
44 0027 DA640A      JC      OK        ;IF ACC=80,OK
45 002A C3520A      JMP    CHANG
46          :      ;DIAG IS THE ROUTINE FOR MONITOR MINOR FUNCTIONS
47          :      ;DIAG: LDA    OSTAT ;CHECK TO SEE THAT THE
48          :      ANI    *H20      ; FUNCTION SELECTED
49          :      JZ      ERROR    ; WAS EXPECTED
50 002D C9      DIAG: RET

```

Figure D-3 Prom No. 3 Monitor Program

```

51 002E 3E70 MONITR: MVI A.#H70 ;GET READY
52 0030 32873D STA FSTAT ; FOR SINGLE STEP
53 0033 3FD8 MVI A.#HDB ;DISPLAY "D" ON HIGHEST
54 0035 CD8109 CALL OUTPT ; ORDER LED
55 0038 E1 POP H ;STORE THE OLD PROGRAM COUNTER AT LOC
56 0039 22883D SHLD PSAVE ; PSAVE(LOCATION IN INTERRUPT HANDLE
57 003C 210500 LXI H.8 ;POINT TO THE LOCATION CPU WAS EXECUT
58 003F 39 DAD SP ; WHEN INTERRUPT OCCURRED
59 0040 EB MCHG ;DISPLAY ADDRESS
60 0041 1A LDAX D ; OF INSTRUCTION
61 0042 CDD108 CALL SPLIT ; TO BE EXECUTED
62 0045 13 INX D ; AFTER RETURN
63 0046 1A LDAX D ; TO ORIGINAL
64 0047 CDD308 CALL SECND ; PROGRAM
65 004A 3E20 NEXT: MVI A.#H20 ;PREPARE FOR MONITOR MINOR FUNCTION
66 004C 328A3D STA OSTAT
67 004F 76 HLT ;WAIT FOR KEYBOARD INTERRUPT
68 0050 3A863D LDA READF ;LOAD FUNCTION
69 0053 CD1B09 ARND: CALL JUMP ;JUMP TO APPROPRIATE
70 0056 E9 PCHL ; ROUTINE
71 0057 6708 EM: DW EXAMM ; J
72 0059 7708 ER: DW EXAMR ; U
73 005B 8608 DM: DW DEPM ; M
74 005D 9508 DR: DW DEPR ; T P
75 005F A408 SS: DW SSTEP ; A
76 0061 AC08 CO: DW CONT ; B
77 0063 ED08 RS: DW RESET ; L
78 0065 CB08 CA: DW COMPA ; E
79 ;EXAMM IS THE MEMORY EXAMINATION ROUTINE
80 0067 CD0509 EXAMM: CALL E1 ;READ FOUR HEX DIGITS FROM KEYBOARD
81 006A CD5809 CALL CONCAT ;CONCATENATE INTO 16-BIT ADDRESS
82 006D CD7509 CALL ZERO ;ZERO OUT LOW ORDER FOUR DISPLAYS
83 0070 1A LDAX D ;DISPLAY CONTENTS
84 0071 CDD108 CALL SPLIT ; OF THAT ADDRESS
85 0074 C34A08 JMP NEXT
86 ;EXAMR EXAMINES THE CONTENTS OF A PARTICULAR REGISTER
87 0077 1601 EXAMR: MVI D.1 ;
88 0079 CD0509 CALL E2 ;READ ONE HEXADECIMAL DIGIT
89 007C CD3709 CALL MEMORY ;FIND LOCATION IN STACK
90 007F 7E MOV A.M ;DISPLAY CONTENTS OF
91 0080 CDD108 CALL SPLIT ; THAT REGISTER
92 0083 C34A08 JMP NEXT
93 ;DEPM DEPOSITS DATA INTO A SPECIFIED RAM LOCATION
94 0086 CD0309 DEPM: CALL E1 ;READ FOUR HEX DIGITS FROM KEYBOARD
95 0089 CD5809 CALL CONCAT ;CONCATENATE INTO 16-BIT ADDRESS
96 008C CD7509 CALL ZERO ;ZERO OUT LOW ORDER FOUR DISPLAYS
97 008F CD4309 CALL TWO ;READ IN TWO MORE DIGITS. CONCATENATE
98 0092 C34A08 JMP NEXT
99 ;DEPR DEPOSITS DATA INTO A SPECIFIED REGISTER
100 0095 1601 DEPR: MVI D.1

```

Figure D-3 Prom No. 3 Monitor Program (Continued)

```

101 0097 CD0509      CALL E2      ;READ IN ONE DIGIT
102 009A CD3709      CALL MEMORY  ;FIND LOCATION OF REGISTER IN STACK
103 009D EE          KCHG
104 009E CD4309      CALL TWO     ;READ IN TWO MORE DIGITS, CONCATENATE
105 00A1 C34A08      JMP NEXT
106                  ;SSTEP CAUSES ONE INSTRUCTION OF THE SOURCE PROGRAM TO BE
107                  ; EXECUTED FOLLOWED BY A RETURN TO THE DIAGNOSTIC
108                  ; ROUTINE
109 00A4 3E09 SSTEP: MVI A,9      ;SET THE CMPR FLIP-FLOP
110 00A6 CD8109      CALL OUTPT
111 00A9 C3BD08      JMP RESET
112                  ;CONT AUTOMATICALLY INCREMENTS THE TABLE POINTER FOR THE
113                  ; DEPM AND EXAMM FUNCTIONS
114 00AC 3A873D CONT: LDA FSTAT   ;EXAMM OR DEPM?
115 00AF CD1B09      CALL JUMP    ;GET READY TO JUMP TO 3RD
116 00B2 3E06      MVI A,6      ; INSTRUCTION OF DEPM OR
117 00B4 85        ADD L        ; EXAMM, ADDRESS IN RAM IS
118 00B5 6F        MOV L,A      ; INCREMENTED BY ONE
119 00B6 3E00      MVI A,0      ;ADD
120 00B8 17        RAL          ; CARRY
121 00B9 84        ADD H        ; OUT OF
122 00BA 67        MOV H,A      ; L TO H
123 00BB 13        INX D        ; INFORMATION AT READA THRU
124 00BC E9        PCHL        ; READA+3 IS UNCHANGED.
125                  ;RESET RESTORES THE REGISTERS AND INTERRUPT STATUS AND
126                  ; OLD PROGRAM COUNTER
127 00BD 3EC0 RESET: MVI A,#HC0   ;GET READY TO
128 00BF 328A3D      STA OSTAT    ; SAY GOODBYE
129 00C2 3EFF      MVI A,#HFF    ;ENABLE
130 00C4 2F        CMA          ; ALL INTERRUPT
131 00C5 D3EA      OUT PRSET     ; FLIP-FLOPS
132 00C7 2A883D      LHLD PSAVE   ;GET THE INTERRUPT HANDLER ADDRESS
133 00CA E9        PCHL        ;RETURN
134                  ;COMPA LOADS THE COMPARE ADDRESS BUFFERS AND THEN RETURNS
135                  ; TO THE SOURCE PROGRAM
136 00CB CD0009 COMPA: CALL E1     ;READ IN FOUR HEX DIGITS
137 00CE C3A403      JMP SSTEP    ; AND LOAD COMPARE ADDRESS
138                  ;SPLIT DECODES A 16-BIT NUMBER SO THAT IT CAN BE DISPLAYED
139                  ; ON THE FRONT PANEL
140 00D1 0E04 SPLIT: MVI C,4      ;REGISTER C POINTS TO LED DISPLAY
141 00D3 6F        SECND: MOV L,A ;SPLIT ACCUMULATOR INTO TWO HEX
142 00D4 29        DAD H        ; DIGITS,CONTAINED IN LOW ORDER
143 00D5 29        DAD H        ; FOUR BITS OF H AND L REGISTERS.
144 00D6 29        DAD H
145 00D7 29        DAD H
146 00D8 7D        MOV A,L
147 00D9 CDEF08      CALL LOW
148 00DC 0C        INR C
149 00DD 44        MOV B,H
150 00DE CDE808      CALL DATA

```

Figure D-3 Prom No. 3 Monitor Program (Continued)


```

151 00E1 0C          INR  C
152 00E2 C9          RET
153                ;STORE STORES THE DATA READ IN
154 00E3 E60F STORE: ANI  #HF      ;LOOK AT LOW ORDER FOUR
155 00E5 77          MOV  M,A      ; BITS READ IN. MOVE INTO READA
156 00E6 23          INX  H        ; INCREMENT READA TABLE POINTER.
157 00E7 47          MOV  B,A
158 00E8 78 DATA:  MOV  A,B      ;MOV DATA TO
159 00E9 E60F        ANI  #HF      ; HIGH ORDER
160 00EB 07          RLC           ; FOUR BITS
161 00EC 07          RLC
162 00ED 07          RLC
163 00EE 07          RLC
164 00EF B1 LOW:    ORA  C        ;OUTPUT DATA
165 00F0 CD8109      CALL OUTPT   ; TO APPROPRIATE
166 00F3 47          MOV  B,A      ; DISPLAY
167 00F4 3A873D      LDA  FSTAT   ; IS THIS PERHAPS A COMPARE
168 00F7 FE70        CPI  #H70    ; ADDRESS OR SINGLE STEP?
169 00F9 C0          RNZ
170 00FA 78          MOV  A,B      ; IF AC OR SS LOAD
171 00FB D604        SUI  4        ; COMPARE ADDRESS BUFFERS
172 00FD EEF0        XRI  #HF0     ; COMPLEMENT THE HIGH ORDER FOUR BITS
173 00FF CD8109      CALL OUTPT
174 0902 C9          RET
175                ;E1,E2,SHARE AND REPEAT ARE ENTRY POINTS TO A ROUTINE THAT
176                ; CONTROLS THE READING AND STORING OF DATA.
177 0903 1604 E1:    MVI  D,4      ;D CONTAINS # OF DIGITS OT BE READ.
178 0905 0E07 E2:    MVI  C,7      ;C CONTAINS DISPLAY POINTER
179 0907 21803D SHARE: LXI  H,READA
180 090A 3E08 REPEAT: MVI  A,B
181 090C 328A3D      STA  OSTAT
182 090F CD7109      CALL READ
183 0912 CDE308      CALL STORE   ;STORE AND
184 0915 0D          DCR  C        ; DISPLAY DIGIT
185 0916 15          DCR  D        ; READ
186 0917 C8          RZ
187 0918 C30A09      JMP  REPEAT
188                ;JUMP DETERMINES THE ADDRESS OF THE DIAGNOSTIC ROUTINE
189                ; TO BE USED
190 091B FE50 JUMP:  CPI  #H50     ;STORE THE FUNCTION READ AT FSTAT
191 091D CA2A09      JZ   AROUND   ; AND DISPLAY ON HIGH ORDER
192 0920 32873D      STA  FSTAT   ; DISPLAY (IF OTHER THAN CONT).
193 0923 F5          PUSH PSW
194 0924 F608        ORI  8
195 0926 CD8109      CALL OUTPT
196 0929 F1          POP  PSW
197 092A 0F AROUND: RRC           ; COMPUTE
198 092B 0F          RRC           ; JUMP
199 092C 0F          RRC           ; TABLE
200 092D 215708      LXI  H,EM     ; POSITION

```

Figure D-3 Prom No. 3 Monitor Program (Continued)

```

201 0930 85      ADD    L
202 0931 6F      MOV    L,A
203 0932 7E      MOV    A,M
204 0933 23      INX    H
205 0934 66      MOV    H,M
206 0935 6F      MOV    L,A
207 0936 C9      RET
208              ;MEMORY DETERMINES WHERE IN THE STACK A PARTICULAR
209              ; REGISTER IS STORED
210 0937 3A803D MEMORY: LDA    READA      ;STEP BACK 11 LOCATIONS THRU
211 093A 210900      LXI    H,9          ; STACK. H AND L POINT
212 093D 2F      CMA          ; TO B REGISTER
213 093E 3C      INR    A          ;NOW STEP FORWARD NUMBER
214 093F 85      ADD    L          ; OF LOCATIONS CORRESPONDING
215 0940 6F      MOV    L,A          ; TO REGISTER NUMBER.
216 0941 39      DAD    SP
217 0942 C9      RET
218              ;TWO READS IN TWO DIGITS FROM THE KEYBOARD AND FORMS
219              ; THESE INTO AN 8-BIT BYTE
220 0943 D5      TWO:  PUSH    D          ;STORE ADDRESS OF LOCATION
221 0944 1602      MVI    D,2          ; TO BE MODIFIED
222 0946 0E05      MVI    C,5
223 0948 21843D      LXI    H,READD      ;READ IN
224 094B CD0A09      CALL   REPEAT      ; TWO DIGITS
225 094E E1      POP    H
226 094F 01843D      LXI    B,READD      ;CONCATENATE
227 0952 CD5B09      CALL   ENT          ; AND
228 0955 72      MOV    M,D          ; STORE
229 0956 EB      XCHG          ;D AND E ARE AGAIN THE
230 0957 C9      RET          ; ADDRESS POINTER
231              ;CONCAT TAKES FOUR 4-BIT NUMBERS (STORED IN THE LOW ORDER
232              ; FOUR BITS OF FOUR MEMORY LOCATIONS) AND CONCATENATES THEM
233              ; INTO A 16-BIT NUMBER
234 0958 01803D CONCAT: LXI    B,READA      ;LOAD ACCUMULATOR WITH
235 095B 0A      ENT:  LDAX    B          ; HIGH ORDER HEX DIGIT
236 095C 07      RLC          ; OF READA TABLE
237 095D 07      RLC
238 095E 07      RLC
239 095F 07      RLC
240 0960 57      MOV    D,A
241 0961 03      INX    B
242 0962 0A      LDAX    B          ;CONCATENATE TWO HIGHEST ORDER
243 0963 B2      ORA    D          ; DIGITS BY OR-ING A WITH D.
244 0964 57      MOV    D,A          ;STORE RESULT IN D.
245 0965 03      INX    B          ;SAME THING WITH NEXT
246 0966 0A      LDAX    B          ; TWO DIGITS AND
247 0967 07      RLC          ; STORE IN E REGISTER.
248 0968 07      RLC
249 0969 07      RLC
250 096A 07      RLC

```

Figure D-3 Prom No. 3 Monitor Program (Continued)

```

251 096B 5F          MOV  E,A
252 096C 03          INX  B
253 096D 0A          LDAX B
254 096E B3          ORA  E
255 096F 5F          MOV  E,A
256 0970 C9          RET
257                ;READ READS IN THE DATA LINES OF THE KEYBOARD AND STORES
258                ; THIS SEQUENCE IN REGISTER A.
259 0971 76          READ:  HLT                ;WAIT FOR KEYBOARD INTERRUPT
260 0972 DBE9        IN    KBIN2
261 0974 C9          RET
262                ;ZERO WRITES ZEROES ON THE DISPLAYS
263 0975 3E04        ZERO:  MVI  A,4          ;OUTPUT ZEROES TO
264 0977 CD8109      LOOP:  CALL OUTPT        ; FOUR LOWEST ORDER DISPLAYS
265 097A 3C          INR   A
266 097B FE0B        CPI   B
267 097D C27709      JNZ   LOOP
268 0980 C9          RET
269 0981 F5          OUTPT: PUSH PSW          ;SAVE THE ACCUMULATOR
270 0982 2F          CMA                ;OUTPT THE NUMBER TO THE
271 0983 D3EB        OUT  LEDCM          ; LED AND COMPARATOR OUTPUT PORT
272 0985 3E47        MVI  A,*H47        ;TOGGLE
273 0987 2F          CMA                ; THE
274 0988 D3EA        OUT  PRSET          ; 74154
275 098A 3EC7        MVI  A,*HC7        ; ENABLE
276 098C 2F          CMA                ; PIN
277 098D D3EA        OUT  PRSET
278 098F F1          POP  PSW          ;RESTORE THE ACCUMULATOR
279 0990 C9          RET
280 0991 3EB8        ERROR: MVI  A,*HB8    ;OUTPUT ERROR MESSAGE
281 0993 CD8109      CALL OUTPT
282 0996 3E07        MVI  A,7
283 0998 CD8109      CALL OUTPT
284 099B 3E06        MVI  A,6
285 099D CD8109      CALL OUTPT
286 09A0 3EB5        MVI  A,*HB5
287 09A2 CD8109      CALL OUTPT
288 09A5 3EB4        MVI  A,*HB4
289 09A7 CD8109      CALL OUTPT
290 09AA C9          RET
291 09AB 3A8A3D      KBRD2: LDA  OSTAT      ;NUMERIC KEYBOARD SERVICE RETURN
292 09AE FE0B        CPI   B
293 09B0 C29109      JNZ   ERROR
294 09B3 C9          START: RET
295 09B4          END

```

Figure D-3 Prom No. 3 Monitor Program (Continued)

```

1 0A00          ORG    *HA00
2 0A00          FIRST EQU    *H3FE0
3 0A00          FSTAT EQU    *H3D87
4 0A00          ZERO   EQU    *H975
5 0A00          SPLIT  EQU    *H8D1
6 0A00          TWO    EQU    *H943
7 0A00          OSTAT  EQU    *H3D8A
8 0A00          TEMP   EQU    OSTAT+1
9 0A00          COUNT  EQU    TEMP+1
10 0A00         CNSNT  EQU    COUNT+1 ;3D8D HAS MULTIPLY CONSTANT READ FROM
11 0A00         MPNTR  EQU    CNSNT+1 ;3D8E THRU 3D8F HAS MULTIPLY ROUTINE
12 0A00         MULCX  EQU    MPNTR+2 ;3D90 HAS STARTING LOCATION OF 1ST MU
13              ;CTAB IS THE MULTIPLY CONSTANT TABLE
14 0A00 08       CTAB: DB    8
15 0A01 01       DB    1
16 0A02 3C       DB    *H3C
17 0A03 01       DB    1
18 0A04 04       DB    4
19 0A05 01       DB    1
20 0A06 06       DB    6
21 0A07 01       DB    1
22 0A08 3C       DB    *H3C
23 0A09 04       DB    4
24 0A0A 1A       DB    *H1A
25 0A0B A0       DB    *HA0
26 0A0C 00       DB    0
27 0A0D 00       DB    *H0
28 0A0E 0D       DB    *HD
29 0A0F 00       DB    0
30 0A10 09       DB    9
31 0A11 0A       DB    *HA
32 0A12 D0       DB    *HD0
33 0A13 0D       DB    *HD
34              ;SETML CREATES FAST MEMORY ROUTINES IN RAM
35 0A14 3E10     SETML: MVI    A,*H10 ;GET READY FOR SETML MINOR FUNCTION
36 0A16 328A3D   STA    OSTAT
37 0A19 3E00     MVI    A,0 ;CERTAIN SUBROUTINES USED BY THIS
38 0A1B 32873D   STA    FSTAT ;SECTION REQUIRE A VALUE FOR FSTAT
39 0A1E CD7509   CALL   ZERO ;ZERO OUT DISPLAY
40 0A21 21903D   LXI    H,MULCX
41 0A24 228E3D   SHLD   MPNTR ;INITIALIZE MULTIPLY ROUTINE POINTER
42 0A27 11000A   LXI    D,CTAB ;INITIALIZE TABLE POINTER
43 0A2A 3E14     MVI    A,20 ;INITIALIZE LOOP COUNT
44 0A2C 328C3D   INSPT: STA    COUNT
45 0A2F 1A       LDAX   D ;LOAD THE ACCUMULATOR WITH TABLE ENTR
46 0A30 328D3D   STA    CNSNT ;STORE TABLE ENTRY
47 0A33 CD0108   CALL   SPLIT ;DISPLAY TABLE ENTRY
48 0A36 31E03F   LDA    FIRST ;CHECK FOR FIRST TIME THRU
49 0A39 17       RAL      ;MSB DECIDES
50 0A3B DA438A   JC     HALT ;IF C=1, FIRST TIME THRU

```

Figure D-3. Prom No. 3 Monitor Program (Continued)

```

51 0A3D CD640A      CALL    OK      ;OTHERWISE, SET UP MULTIPLIES
52 0A40 C3440A      JMP      NEXT    ; INTERACTION FROM KEYBOARD
53 0A43 76          HALT:    HLT      ;WAIT FOR A KEYBOARD INTERRUPT
54 0A44 13          NEXT:    INX      ;PREPARE FOR NEXT TABLE ENTRY
55 0A45 3A8C3D      LDA      COUNT
56 0A48 3D          DCR      A        ;DECREMENT LOOP COUNTER
57 0A49 C22C0A      JNZ      INSPT
58 0A4C 3EC0        MVI      A,*HC0   ;PREPARE FOR NEXT MAJOR FUNCTION
59 0A4E 328A3D      STA      OSTAT
60 0A51 C9          RET
61                  ;CHANG READS TWO HEX NUMBERS FROM THE NUMERIC KEYBOARD AND USE
62                  ;NUMBER RATHER THAN THE ONE IN CTAB TO GENERATE A MULTIPLY ROU
63 0A52 118B3D      CHANG:    LXI      D,TEMP
64 0A55 CD4309      CALL     TWO      ;READ KEYBOARD
65 0A58 3E10        MVI      A,*H10   ;PREPARE FOR NEXT SETML MINOR FUNCTIO
66 0A5A 328A3D      STA      OSTAT
67 0A5D 3A8B3D      LDA      TEMP     ;THIS THE NEW MULTIPLY CONSTANT
68 0A60 CD700A      CALL     MULT     ;SET UP THE MULTIPLY ROUTINE
69 0A63 C9          RET
70                  ;OK TAKES THE NUMBER FROM THE TABLE AND GENERATES THE
71                  ;CORRESPONDING MULTIPLY ROUTINE
72 0A64 3E10      OK:      MVI      A,*H10 ;PREPARE FOR NEXT SETML MINOR FUNCTIO
73 0A66 328A3D      STA      OSTAT
74 0A69 3A8D3D      LDA      CNSNT    ;LOAD THE TABLE ENTRY INTO THE ACCUMU
75 0A6C CD700A      CALL     MULT     ;SET UP MULTIPLY ROUTINE
76 0A6F C9          RET
77                  ;MULT WRITES A ROUTINE IN RAM TO MULTIPLY VARIABLE BY SOME CON
78                  ;THE CONSTANT IS IN THE ACCUMULATOR. THE ROUTINE CORRESPONDING
79                  ;TO THE CONSTANT S IS GIVEN BELOW:
80                  ;
81                  ;          LXI H,0
82                  ;          DAD D
83                  ;          DAD H
84                  ;          DAD H
85                  ;          DAD D
86                  ;          RET
87 0A70 2ABE3D      MULT:    LHLD     MPNTR ;GET THE STARTING LOCATION FOR THE MU
88 0A73 3621        MVI      M,*H21    ;WRITE AN 'LXI H,0' INTO MEMORY
89 0A75 23          INX      H
90 0A76 3600        MVI      M,0
91 0A78 23          INX      H
92 0A79 3600        MVI      M,0
93 0A7B 23          INX      H
94 0A7C 0508        MVI      B,8       ;B IS THE LOOP COUNTER
95 0A7E 07          LPCY:    RLC        ;IGNORE LEADING ZEROES
96 0A7F DA890A      JC       OWT       ;JUMP OUT WHEN FIRST ONE IS FOUND
97 0A82 05          DCR      B
98 0A83 C27E0A      JNZ      LPCY
99 0A86 C3990A      JMP      ZCNT     ;NO ONES, NUMBER IS ZERO
100 0A89 0F          OWT:    RRC

```

Figure D-3 Prom No. 3 Monitor Program (Continued)


```

101 0A8A 07      TOP:      RLC          ;CHECK FOR ZERO OR ONE
102 0A8B D2910A      JNC      GO2      ;IF ZERO. JUST WRITE A 'DAD H'
103 0A8E 3619      GO1:      MVI      M,*H19 ;OTHERWISE WRITE A 'DAD D'
104 0A90 23          INX      H          ; AND THEN A 'DAD H'
105 0A91 3629      GO2:      MVI      M,*H29
106 0A93 23          INX      H
107 0A94 05          DCR      B          ;CONTINUE FOR ALL REMAINING BITS
108 0A95 C28A0A      JNZ      TOP
109 0A98 2E          JCX      H          ;WRITE OVER LAST 'DAD H'
110 0A99 36C9      ZCNT:      MVI      M,*HC9 ; WITH A 'RET'
111 0A9B 2A8E3D      LHLD     MPNTR      ;ADD 20 TO THE OLD STARTING
112 0A9E 011400      LXI      B,*H14    ; LOCATION TO GET THE NEW
113 0AA1 09          DAD      B          ;STARTING LOCATION
114 0AA2 228E3D      SHLD     MPNTR
115 0AA5 C9          RET
116 0000

```

INTEL 8080 CROSS ASSEMBLER SYMBOL TABLE

A = 0007	B = 0000	GO1 0A8E	GO2 0A91
C = 0001	D = 0002	E = 0003	CTAB 0A00
CHANG 0A52	H = 0004	HALT 0A43	L = 0005
M = 0006	FSTAT= 3D87	TEMP = 3D8B	FIRST= 3FE0
COUNT= 3D8C	CNSNT= 3D8D	SPLIT= 08D1	OSTAT= 3D8A
MULCX= 3D90	ZERO = 0975	MPNTR= 3D8E	SETML 0A14
SP = 0006	INSPT 0A2C	NEXT 0A44	OK = 0A64
MULT 0A70	LPCY 0A7E	PSW = 0006	TWO = 0943
OWT 0A89	TOP 0A8A	ZCNT 0A99	

ERRORS DETECTED: 0

Figure D-3 Prom No. 3 Monitor Program (Concluded)

```

1          ; *****
2          ;
3          ;
4          ;
5          ;      SYSTEM EQUATES
6          ;
7          ;
8          ; *****
9          ;
10         ;
11         ;
12 0000     CAMAX    EQU    #H3D00
13 0000     CAMBX    EQU    #H3D01
14 0000     CAMAY    EQU    #H3D02
15 0000     CAMBY    EQU    #H3D03
16 0000     CCMAX    EQU    #H3D46
17 0000     CCMAY    EQU    #H3D44
18 0000     CPOAX    EQU    #H3D40
19 0000     CPOBX    EQU    #H3D41
20 0000     CPOAY    EQU    #H3D42
21 0000     CPOBY    EQU    #H3D43
22 0000     CPLAX    EQU    #H3D0C
23 0000     CPLEX    EQU    #H3D0D
24 0000     CPLAY    EQU    #H3D0E
25 0000     CPLBY    EQU    #H3D0F
26 0000     DETX     EQU    #H3D10
27 0000     DETY     EQU    #H3D11
28 0000     DDOTX    EQU    #H3D12
29 0000     DDOTY    EQU    #H3D14
30 0000     DOTIX    EQU    #H3D16
31 0000     DOTIY    EQU    #H3D18
32 0000     IPRJX    EQU    #H3D1A
33 0000     IPRJY    EQU    #H3D1C
34 0000     IPOSX    EQU    #H3D1E
35 0000     IPOSY    EQU    #H3D20
36 0000     MULCX    EQU    #H3D90
37 0000     MULDX    EQU    MULCX+20
38 0000     MXLVB    EQU    MULDX+20
39 0000     MXLVK    EQU    MXLVB+20
40 0000     MULAX    EQU    MXLVK+20
41 0000     MULBX    EQU    MULAX+20
42 0000     MULCY    EQU    MULBX+20
43 0000     MULDY    EQU    MULCY+20
44 0000     MYLVB    EQU    MULDY+20
45 0000     MYLVK    EQU    MYLVB+20
46 0000     MULAY    EQU    MYLVK+20
47 0000     MULBY    EQU    MULAY+20
48 0000     MICH     EQU    MULBY+20
49 0000     MICHY    EQU    MICH+20
50 0000     CMIY     EQU    MICHY+20

```

Figure D-4 Prom No. 4 Pitch Control Software

```

51 0000      CMIX      EQU      CMIY+20
52 0000      NCPOX     EQU      *H3D22
53 0000      NCPOY     EQU      *H3D24
54 0000      PRJAX     EQU      *H3D26
55 0000      PRJBX     EQU      *H3D27
56 0000      PRJAY     EQU      *H3D28
57 0000      PRJBY     EQU      *H3D29
58 0000      PRLAX     EQU      *H3D2A
59 0000      PRLBX     EQU      *H3D2B
60 0000      PRLAY     EQU      *H3D2C
61 0000      PRLBY     EQU      *H3D2D
62 0000      PVLAX     EQU      *H3D2E
63 0000      PVLBX     EQU      *H3D2F
64 0000      PVLAY     EQU      *H3D30
65 0000      PVLBY     EQU      *H3D31
66 0000      RINT      EQU      *H3D34
67 0000      TINT      EQU      *H3D38
68 0000      X          EQU      *H3D3A
69 0000      XY         EQU      *H3D3C
70 0000      XFLAG     EQU      *H3D3E
71 0000      YFLAG     EQU      *H3D3F
72 0000      CDELX     EQU      *H3D76
73 0000      CIX       EQU      *H3D76
74 0000      USDAO     EQU      *H00EC
75 0000      PRTA1     EQU      *H0000
76 0000      PRTB1     EQU      *H0001
77 0000      PRTC1     EQU      *H0002
78 0000      PRTA2     EQU      *H0003
79 0000      PRTB2     EQU      *H00E5
80 0000      PRTC2     EQU      *H0000
81 0000      PRTD1     EQU      *H0001
82 0000      PRTD2     EQU      *H0002
83 0000      PRTD3     EQU      *H00E6
84 0000      ORG        EQU      *HC00
85          ;
86          ;   SYSTEM COMPENSATION NETWORK
87          ;
88          ;
89 0C00 213E3D PITCH: LXI      H,XFLAG
90 0C03 7E      MOV      A,M
91 0C04 1F      RAR
92 0C05 D2000C  JNC      PITCH
93 0C08 2A2A3D  LHLD     PRLAX
94 0C0B EB      XCHG
95 0C0C 3A273D  LDA      PRJBX
96 0C0F E610    ANI      *H10
97 0C11 FE10    CPI      *H10
98 0C13 C21E0C  JNZ      RA
99 0C16 3A273D  LDA      PRJBX
100 0C19 CF00   ADI      *HE0

```

Figure D-4 Prom No. 4 Pitch Control Software (Continued)

```

101 0C1B 32273D      STA      PRJBX
102 0C1E 2A263D RA:  LHLD     PRJAX
103 0C21 CDD20D      CALL    MINUS
104 0C24 19          DAD      D
105 0C25 EB          XCHG
106                ; *****SPECIAL LEAD NETWORK
107                ;
108                ; *****
109 0C26 2A573D      LHLD     #H3D52
110 0C29 EB          XCHG
111 0C2A 2AEA3F      LHLD     #H3FEA
112 0C2D CDDA0D      CALL    SHIFT
113 0C30 CDD20D      CALL    MINUS
114 0C33 19          DAD      D
115 0C34 CDDA0D      CALL    SHIFT
116 0C37 CDDA0D      CALL    SHIFT
117                ;
118 0C3A 22123D      SHLD     DDOTX
119 0C3D EB          XCHG
120 0C3E 7A          MOV      A,D
121 0C3F 07          RLC
122 0C40 DA530C      JC       FEE
123 0C43 21FEFF      LXI     H,#HFFFE
124 0C46 19          DAD      D
125 0C47 DA600C      JC       DET
126 0C4A 210000      LXI     H,0
127 0C4D 22123D      SHL     DDOTX
128 0C50 C3600C      JMP     DET
129 0C53 210200 FEE: LXI     H,2
130 0C56 19          DAD      D
131 0C57 D2600C      JNC     DET
132 0C5A 210000      LXI     H,0
133 0C5D 22123D      SHLD    DDOTX
134 0C60 3A103D DET: LDA     DETX
135 0C63 FE04        CPI     #H04
136 0C65 F2770C      JP      PDL
137 0C68 FEFC        CPI     #HFC
138 0C6A FA720C      JM      MDL
139 0C6D 3E00        MVI     A,#H00
140 0C6F C3790C      JMP     ING
141 0C72 C604 MDL:   ADI     #H04
142 0C74 C3790C      JMP     ING
143 0C77 C6FC PDL:   ADI     #HFC
144 0C79 5F ING:     MOV     E,A
145 0C7A FE00        CPI     #H00
146 0C7C 3E00        MVI     A,#H00
147 0C7E F2B20C      JP      ZAP
148 0C81 2F          CMA
149 0C82 57 ZAP:     MOV     D,A
150 0C83 CDA43D      CALL    MULDX

```

Figure D-4 Prom No. 4 Pitch Control Software (Continued)

```

151 0C86 EB          XCHG
152 0C87 2A123D      LHLD   DDOTX
153 0C8A 19          DAD    D
154 0C8B EB          XCHG
155 0C8C 7A          MOV    A,D
156 0C8D 07          RLC
157 0C8E DA9B0C      JC     FIVE
158 0C91 21CCFF      LXI    H,*HFFCC
159 0C94 19          DAD    D
160 0C95 DAA90C      JC     PLMT
161 0C98 C3A20C      JMP    TWO
162 0C9B 213400 FIVE: LXI    H,*H0034
163 0C9E 19          DAD    D
164 0C9F 02B20C      JNC    MLMT
165 0CA2 EB          TWO:  XCHG
166 0CA3 22003D      SHLD   CAMAX
167 0CA5 C3BB0C      JMP    EXIT
168 0CA9 213400 PLMT: LXI    H,*H34
169 0CAC 22003D      SHLD   CAMAX
170 0CAF C3BB0C      JMP    EXIT
171 0CB2 21CCFF MLMT: LXI    H,*HFFCC
172 0CB5 22003D      SHLD   CAMAX
173 0CB8 C3BB0C      JMP    EXIT
174                :
175                :     CAMERA SERVO
176                :
177 0CBB 3A413D EXIT: LDA    CPOBX
178 0CBE E61F        ANI    *H1F
179 0CC0 32413D      STA    CPOBX
180 0CC3 E610        ANI    *H10
181 0CC5 FE10        CPI    *H10
182 0CC7 C2D20C      JNZ    WP
183 0CCA 3A413D      LDA    CPOBX
184 0CCD C6E0        ADI    *HE0
185 0CCF 32413D      STA    CPOBX
186 0CD2 3A403D WP:  LDA    CPOAX
187 0CD5 2F          CMA
188 0CD6 6F          MOV    L,A
189 0CD7 3A413D      LDA    CPOBX
190 0CDA 2F          CMA
191 0CDB 67          MOV    H,A
192 0CDC 23          INX    H
193 0CDD 22223D      SHLD   NCPOX
194 0CE0 EB          XCHG
195 0CE1 2A0C3D      LHLD   CPLAX
196 0CE4 19          DAD    D
197 0CE5 22F45F      SHLD   *H3FF4
198 0CE8 29          DAD    H
199 0CE9 29          DAD    H
200 0CEA 3F          XCHG

```

Figure D-4 Prom No. 4 Pitch Control Software (Continued)

201	0CEB 2A403D	LHLD	CPOAX
202	0CEE 220C3D	SHLD	CPLAX
203	0CF1 7A	MOV	A,D
204	0CF2 07	RLC	
205	0CF3 D2000D	JNC	OGDR
206	0CF6 211101	LXI	H,*H111
207	0CF9 19	DAD	D
208	0CFA D2100D	JNC	DECR
209	0CFD C3160D	JMP	MUL
210	0D00 21EFFE OGDR:	LXI	H,*HFEEF
211	0D03 19	DAD	D
212	0D04 DA0A0D	JC	LMAR
213	0D07 C3160D	JMP	MUL
214	0D0A 210040 LMAR:	LXI	H,*H4000
215	0D0D C3190D	JMP	FLTR
216	0D10 2100C0 DECR:	LXI	H,*HC000
217	0D13 C3190D	JMP	FLTR
218	0D16 CDB83D MUL:	CALL	MXLVB
219	0D19 CDDA0D FLTR:	CALL	SHIFT
220	0D1C CDDA0D	CALL	SHIFT
221	0D1F EB	XCHG	
222	0D20 2A843D	LHLD	*H3D84
223	0D23 19	DAD	D
224	0D24 EB	XCHG	
225	0D25 22843D	SHLD	*H3D84
226	0D28 2A863D	LHLD	*H3D86
227	0D2B CDDA0D	CALL	SHIFT
228	0D2E 19	DAD	D
229	0D2F 22863D	SHLD	*H3D86
230	0D32 22163D	SHLD	DOTIX
231	0D35 2A903D	LHLD	CAMAX
232	0D3C EB	XCHG	
233	0D39 2A3A3D	LHLD	X
234	0D3C 19	DAD	D
235	0D3D EB	XCHG	
236	0D3E 7A	MOV	A,D
237	0D3F 07	RLC	
238	0D40 DA4E0D	JC	PAP
239	0D43 2100F2	LXI	H,*HF200
240	0D46 19	DAD	D
241	0D47 DA590D	JC	ONE
242	0D4A EB	XCHG	
243	0D4B C36E0D	JMP	THRE
244	0D4E 21100B PAP:	LXI	H,*H0B10
245	0D51 19	DAD	D
246	0D52 22650D	JNC	FOUR
247	0D55 EB	XCHG	
248	0D56 C36E0D	JMP	THRE
249	0D59 210000 ONE:	LXI	H,*H0
250	0D5C 22003D	SHLD	CAMAX

165 165

Figure D-4 Prom No. 4 Pitch Control Software (Continued)

251	0D5F 21000E	LXI	H, #H0E00
252	0D62 C36E0D	JMP	THRE
253	0D65 210000 FOUR:	LXI	H, 0
254	0D68 22003D	SHLD	CAMAX
255	0D6B 21F0F4	LXI	H, #HF4F0
256	0D6E 223A3D THRE:	SHLD	X
257	0D71 EB	XCHG	
258	0D72 2A223D	LHLD	NCPOX
259	0D75 29	DAD	H
260	0D76 29	DAD	H
261	0D77 19	DAD	D
262	0D78 29	DAD	H
263	0D79 29	DAD	H
264	0D7A 22763D	SHLD	CDELX
265	0D7D EB	XCHG	
266	0D7E 7A	MOV	A, D
267	0D7F 07	RLC	
268	0D80 D28D0D	JNC	CLA
269	0D83 213000	LXI	H, #H30
270	0D86 19	DAD	D
271	0D87 D2CB0D	JNC	OUT
272	0D8A C3940D	JMP	GAIN
273	0D8D 21D0FF CLA:	LXI	H, #HFFD0
274	0D90 19	DAD	D
275	0D91 DACB0D	JC	OUT
276	0D94 CDBCB3E GAIN:	CALL	CMIX
277	0D97 EB	XCHG	
278	0D98 2A783D	LHLD	CIX
279	0D9B 19	DAD	D
280	0D9C 22783D	SHLD	CIX
281	0D9F EB	XCHG	
282	0DA0 7A	MOV	A, D
283	0DA1 07	RLC	
284	0DA2 DAAFF0D	JC	PA
285	0DA5 2100C0	LXI	H, #HC000
286	0DA8 19	DAD	D
287	0DA9 DAB90D	JC	PB
288	0DAC C3C40D	JMP	PC
289	0DAF 210040 PA:	LXI	H, #H4000
290	0DB2 19	DAD	D
291	0DB3 D2C00D	JNC	PD
292	0DB6 C3C40D	JMP	PC
293	0DB9 210040 PB:	LXI	H, #H4000
294	0DBC EB	XCHG	
295	0DBD C3C40D	JMP	PC
296	0DC0 2100C0 PD:	LXI	H, #HC000
297	0DC3 EB	XCHG	
298	0DC4 2A163D PC:	LHLD	DOTIX
299	0DC7 19	DAD	D
300	0DCB 22163D	SHLD	DOTIX

Figure D-4 Prom No. 4 Pitch Control Software (Continued)

```
301 0DCB 2A763D OUT:  LHL  CDELX
302 0DCE EB          XCHG
303 0DCF C3E60D      JMP  *HDE6
304 0DD2 7C          MOV  A,H
305 0DD3 2F          CMA
306 0DD4 57          MOV  H,A
307 0DD5 7D          MOV  A,L
308 0DD6 2F          CMA
309 0DD7 6F          MOV  L,A
310 0DD8 23          INX  H
311 0DD9 C9          RET
312 0DDA 7C          SHIFT: MOV  A,H
313 0ddb 07          RLC
314 0DDC 7C          MOV  A,H
315 0DDD 1F          RAR
316 0DDE 67          MOV  H,A
317 0DDF 7D          MOV  A,L
318 0DE0 1F          RAR
319 0DE1 6F          MOV  L,A
320 0DE2 C9          RET
321 0DE3              END
```

Figure D-4 Prom No. 4 Pitch Control Software (Continued)

```

1          ; *****
2          ;
3          ;
4          ;
5          ;      SYSTEM EQUATES
6          ;
7          ;
8          ; *****
9          ;
10         ;
11         ;
12 0000     CAMAX    EQU    #H3D00
13 0000     EOX      EQU    #H3FEA
14 0000     CAMBX    EQU    #H3D01
15 0000     CAMAY    EQU    #H3D02
16 0000     CAMBY    EQU    #H3D03
17 0000     CCMAX    EQU    #H3D46
18 0000     CCMAY    EQU    #H3D44
19 0000     CPOAX    EQU    #H3D40
20 0000     CPOBX    EQU    #H3D41
21 0000     CPOAY    EQU    #H3D42
22 0000     CPOBY    EQU    #H3D43
23 0000     CPLAX    EQU    #H3D0C
24 0000     CPLBX    EQU    #H3D0D
25 0000     CPLAY    EQU    #H3D0E
26 0000     CPLBY    EQU    #H3D0F
27 0000     DETX     EQU    #H3D10
28 0000     DETY     EQU    #H3D11
29 0000     DDOTX    EQU    #H3D12
30 0000     DDOTY    EQU    #H3D14
31 0000     DOTIX    EQU    #H3D16
32 0000     DOTIY    EQU    #H3D18
33 0000     IPRJX    EQU    #H3D1A
34 0000     IPRJY    EQU    #H3D1C
35 0000     IPOSX    EQU    #H3D1E
36 0000     IPOSY    EQU    #H3D20
37 0000     MULCX    EQU    #H3D90
38 0000     MULDX    EQU    MULCX+20
39 0000     MXLVB    EQU    MULDX+20
40 0000     MXLVK    EQU    MXLVB+20
41 0000     MULAX    EQU    MXLVK+20
42 0000     MULBX    EQU    MULAX+20
43 0000     MULCY    EQU    MULBX+20
44 0000     MULDY    EQU    MULCY+20
45 0000     MYLVB    EQU    MULDY+20
46 0000     MYLVK    EQU    MYLVB+20
47 0000     MULAY    EQU    MYLVK+20
48 0000     MULBY    EQU    MULAY+20
49 0000     MICH     EQU    MULBY+20
50 0000     MICHY    EQU    MICH+20

```

Figure D-4 Prom No. 4 Pitch Control Software (Continued)

51	0000	CMIY	EQU	MICHY+20
52	0000	CMIX	EQU	CMIX+20
53	0000	TORQY	EQU	CMIX+20
54	0000	TORQX	EQU	TORQY+20
55	0000	PTQX	EQU	TORQX+20
56	0000	NCPOX	EQU	*H3D22
57	0000	NCPOY	EQU	*H3D24
58	0000	PRJAX	EQU	*H3D26
59	0000	PRJBX	EQU	*H3D27
60	0000	PRJAY	EQU	*H3D28
61	0000	PRJBY	EQU	*H3D29
62	0000	PRLAX	EQU	*H3D2A
63	0000	PRLBX	EQU	*H3D2B
64	0000	PRLAY	EQU	*H3D2C
65	0000	PRLBY	EQU	*H3D2D
66	0000	PVLAX	EQU	*H3D2E
67	0000	PVLBX	EQU	*H3D2F
68	0000	PVLAY	EQU	*H3D30
69	0000	PVLBY	EQU	*H3D31
70	0000	RINT	EQU	*H3D34
71	0000	TINT	EQU	*H3D38
72	0000	X	EQU	*H3D3A
73	0000	XY	EQU	*H3D3C
74	0000	XFLAG	EQU	*H3D3E
75	0000	YFLAG	EQU	*H3D3F
76	0000	DELTA	EQU	*H3D58
77	0000	ICHAN	EQU	*H3D60
78	0000	USDAO	EQU	*H00EC
79	0000	PRTA1	EQU	*H0000
80	0000	PRTB1	EQU	*H0001
81	0000	PRTC1	EQU	*H0002
82	0000	PRTA2	EQU	*H0003
83	0000	PRTB2	EQU	*H00E5
84	0000	FRTC2	EQU	*H0000
85	0000	PRTD1	EQU	*H0001
86	0000	PRTD2	EQU	*H0002
87	0000	PRTD3	EQU	*H00E6
88	0DE6		ORG	*HDE6
89	0DE6 7A		MOV	A,D
90	0DE7 07		RLC	
91	0DE8 DAF50D		JC	MIB
92	0DEB 2100C0		LXI	H,*H0000
93	0DEE 19		DAD	D
94	0DEF DAFF0D		JC	ALM
95	0DF2 C30B0E		JMP	XVK
96	0DFS 210040 MIB:		LXI	H,*H4000
97	0DF8 19		DAD	D
98	0DF9 D2050E		JNC	CDE
99	0DFC C30D0E		JMP	XVK
100	0DFF 210040 ALM:		LXI	H,*H4000

Figure D-4 Prom No. 4 Pitch Control Software (Continued)


```

101 0E02 C30E0E      JMP      ETR
102 0E05 2100C0 CDE: LXI      H, #HC000
103 0E08 C30E0E      JMP      ETR
104 0E0B CDCC3D XVK:  CALL    MXLVK
105 0E0E EB          ETR:  XCHG
106 0E0F 2A163D      LHLD    DOTIX
107 0E12 19          DAD     D
108 0E13 EB          XCHG
109 0E14 7A          MOV     A, D
110 0E15 07          RLC
111 0E16 DA290E      JC      KAD
112 0E19 219AF9      LXI      H, #HF99A
113 0E1C 19          DAD     D
114 0E1D DA230E      JC      OH
115 0E20 C3390E      JMP      GOSH
116 0E23 210040 OH:  LXI      H, #H4000
117 0E26 C33C0E      JMP      OSH
118 0E29 216606 KAD: LXI      H, #H666
119 0E2C 19          DAD     D
120 0E2D D2330E      JNC     WOW
121 0E30 C3390E      JMP      GOSH
122 0E33 2100C0 WOW: LXI      H, #HC000
123 0E36 C33C0E      JMP      OSH
124 0E39 CDE43E GOSH: CALL    TOROX
125 0E3C 22463D OSH:  SHLD    CCMAX
126
127                :PROJECTOR SERVO
128
129
130 0E3F CDCE0F      CALL    LAG
131 0E42 2A2C3D      LHLD    PRJAX
132 0E45 CDB40F      CALL    MINUS
133 0E48 221A3D      SHLD    IPRJX
134 0E4B EB          XCHG
135 0E4C 2A403D      LHLD    CPOAX
136 0E4F 19          DAD     D
137 0E50 22583D      SHLD    DELTA
138 0E53 EB          XCHG
139 0E54 7A          MOV     A, D
140 0E55 07          RLC
141 0E56 D2630E      JNC     OGD
142 0E59 210040      LXI      H, #H4000
143 0E5C 19          DAD     D
144 0E5D D2730E      JNC     DEC
145 0E60 C3790E      JMP      BX
146 0E63 2100C0 OGD: LXI      H, #HC000
147 0E66 19          DAD     D
148 0E67 DA6D0E      JC      LMA
149 0E6A C3790E      JMP      BX
150 0E6D 210040 LMA:  LXI      H, #H4000

```

Figure D-4 Prom No. 4 Pitch Control Software (Continued)

151	0E70 C37C0E	JMP	IP
152	0E73 2100C0 DEC:	LXI	H, #HC000
153	0E76 C37C0E	JMP	IP
154	0E79 CDF43D BX:	CALL	MULBX
155	0E7C 221E3D IP:	SHLD	IPOSX
156	0E7F 2A583D	LHLD	DELTA
157	0E82 EB	XCHG	
158	0E83 7A	MOV	A, D
159	0E84 07	RLC	
160	0E85 D2920E	JNC	CLA
161	0E88 213000	LXI	H, #H30
162	0E8B 19	DAD	D
163	0E8C D2D00E	JNC	OUT
164	0E8F C3990E	JMP	GAIN
165	0E92 21D0FF CLA:	LXI	H, #HFFD0
166	0E95 19	DAD	D
167	0E96 DAD00E	JC	OUT
168	0E99 CD803E GAIN:	CALL	MICH
169	0E9C EB	XCHG	
170	0E9D 2A603D	LHLD	ICHAN
171	0EA0 19	DAD	D
172	0EA1 22603D	SHLD	ICHAN
173	0EA4 EB	XCHG	
174	0EA5 7A	MOV	A, D
175	0EA6 07	RLC	
176	0EA7 DAB40E	JC	PA
177	0EAA 2100C0	LXI	H, #HC000
178	0EAD 19	DAD	D
179	0EAE DABF0E	JC	PB
180	0EB1 C3C90E	JMP	PC
181	0EB4 210040 PA:	LXI	H, #H4000
182	0EB7 19	DAD	D
183	0EB8 D2C50E	JNC	PD
184	0EBB C3C90E	JMP	PC
185	0EBE 210040 PB:	LXI	H, #H4000
186	0EC1 EB	XCHG	
187	0EC2 C3C90F	JMP	PC
188	0EC5 2100C0 PD:	LXI	H, #HC000
189	0EC8 EB	XCHG	
190	0EC9 2A1E3D PC:	LHLD	IPOSX
191	0ECC 19	DAD	D
192	0ECD 221E3D	SHLD	IPOSX
193	0ED0 2A2A3D OUT:	LHLD	PRLAX
194	0ED3 EB	XCHG	
195	0ED4 2A263D	LHLD	PRJAX
196	0ED7 222A3D	SHLD	PRLAX
197	0EDA 2A1A3D	LHLD	IPRJX
198	0EDD 19	DAD	D
199	0EDE 22F63F	SHLD	#H3FF6
200	0EE1 20	DAD	H

Figure D-4 Prom No. 4 Pitch Control Software (Continued)

AD-A046 704

MCDONNELL AIRCRAFT CO ST LOUIS MO
REMOTE VIEWING SYSTEM.(U)
JUN 77 R W FISHER

F/G 17/2

UNCLASSIFIED

3 OF 3
ADA
046704

ONR-CR213-129-2F

N00014-75-C-0660
NL



201	0EE2 29	DAD	H
202	0EE3 29	DAD	H
203	0EE4 29	DAD	H
204	0EE5 29	DAD	H
205	0EF6 EB	XCHG	
206	0EE7 2AEA3F	LHLD	EOX
207	0EEA 19	DAD	D
208	0EEB CD7B0F	CALL	SHIFT
209	0EEE CD7B0F	CALL	SHIFT
210	0EF1 CD7B0F	CALL	SHIFT
211	0EF4 EB	XCHG	
212	0EFS 7A	MOV	A, D
213	0EF6 07	RLC	
214	0EF7 D2040F	JNC	OGDR
215	0EFA 215515	LXI	H, #H1555
216	0EFD 19	DAD	D
217	0EFE D2140F	JNC	DECR
218	0F01 C31A0F	JMP	BXR
219	0F04 21ABEA OGDR:	LXI	H, #HEAAB
220	0F07 19	DAD	D
221	0F08 DA0E0F	JC	LMAR
222	0F0B C31A0F	JMP	BXR
223	0F0E 210040 LMAR:	LXI	H, #H4000
224	0F11 C31D0F	JMP	IPR
225	0F14 2100C0 DECR:	LXI	H, #HC000
226	0F17 C31D0F	JMP	IPR
227	0F1A CDE03D BXR:	CALL	MULAX
228	0F1D CD7B0F IPR:	CALL	SHIFT
229	0F20 CD7B0F	CALL	SHIFT
230	0F23 EB	XCHG	
231	0F24 2A503D	LHLD	#H3D50
232	0F27 19	DAD	D
233	0F28 EB	XCHG	
234	0F29 22503D	SHLD	#H3D50
235	0F2C 2A523D	LHLD	#H3D52
236	0F2F CD7B0F	CALL	SHIFT
237	0F32 19	DAD	D
238	0F33 22523D	SHLD	#H3D52
239	0F36 EB	XCHG	
240	0F37 2A1E3D	LHLD	IPOSX
241	0F3A 19	DAD	D
242	0F3B EB	XCHG	
243	0F3C 7A	MOV	A, D
244	0F3D 07	RLC	
245	0F3E D24B0F	JNC	VOGD
246	0F41 214F00	LXI	H, #H4E
247	0F44 19	DAD	D
248	0F45 D25B0F	JNC	VDEC
249	0F48 C3610F	JMP	VBX
250	0F4B 21B2FF VOGD:	LXI	H, #HFFB2

Figure D-4 Prom No. 4 Pitch Control Software (Continued)

251	0F4E 19	DAD	D
252	0F4F DA550F	JC	VLMA
253	0F52 C3610F	JMP	VBX
254	0F55 210040 VLMA:	LXI	H.*H4000
255	0F58 C3640F	JMP	VIP
256	0F5B 2100C0 VDEC:	LXI	H.*HC000
257	0F5E C3640F	JMP	VIP
258	0F61 CDF83E VBX:	CALL	PTQX
259	0F64 7C VIP:	MOV	A.H
260	0F65 0F	RRC	
261	0F66 0F	RRC	
262	0F67 0F	RRC	
263	0F68 0F	RRC	
264	0F69 322F3D	STA	PVLBX
265	0F6C E6F0	ANI	*HF0
266	0F6E 67	MOV	H.A
267	0F6F 7D	MOV	A.L
268	0F70 01	RRC	
269	0F71 0F	RRC	
270	0F72 0F	RRC	
271	0F73 0F	RRC	
272	0F74 E60F	ANI	*H0F
273	0F76 B4	ORA	H
274	0F77 322E3D	STA	PVLAX
275	0F7A C9	RET	
276	0F7B 7C SHIFT:	MOV	A.H
277	0F7C 07	RLC	
278	0F7D 7C	MOV	A.H
279	0F7E 1F	RAR	
280	0F7F 67	MOV	H.A
281	0F80 7D	MOV	A.L
282	0F81 1F	RAR	
283	0F82 6F	MOV	L.A
284	0F83 C9	RET	
285	0F84 7C MINUS:	MOV	A.H
286	0F85 2F	CMA	
287	0F86 67	MOV	H.A
288	0F87 7D	MOV	A.L
289	0F88 2F	CMA	
290	0F89 6F	MOV	L.A
291	0F8A 23	INX	H
292	0F8B C9	RET	
293	0F8C 21523D	LXI	H.*H3D52
294	0F8F 34	INR	M
295	0F90 7E	MOV	A.M
296	0F91 FE64	CPI	*H64
297	0F93 FAB00F	JM	ALED
298	0F96 FEC8	CPI	*HC8
299	0F98 FA9E0F	JM	BLED
300	0F9B 3E00	MVI	A.*H00

Figure D-4 Prom No. 4 Pitch Control Software (Continued)


```

301 0F9D 77      MOV      M,A
302 0F9E 0654    BLED:    MVI      B,*H54
303 0FA0 78      SLED:    MOV      A,B
304 0FA1 CDC00F  CALL     OUTPT
305 0FA4 3E11      MVI      A,*H11
306 0FA6 80      ADD      B
307 0FA7 47      MOV      B,A
308 0FAB FEA9      CPI      *HA9
309 0FAA C2A00F  JNZ      SLED
310 0FAD C3BF0F  JMP      BOX
311 0FB0 06A4    ALED:    MVI      B,*HA4
312 0FB2 78      PLED:    MOV      A,B
313 0FB3 CDC00F  CALL     OUTPT
314 0FB6 3E11      MVI      A,*H11
315 0FB8 80      ADD      B
316 0FB9 47      MOV      B,A
317 0FBA FEF9      CPI      *HF9
318 0FBC C2B20F  JNZ      PLED
319 0FBF C9      BOX:     RET
320 0FC0 2F      OUTPT:   CMA
321 0FC1 D3E8      OUT      *HE8
322 0FC3 3E3F      MVI      A,*H3F
323 0FC5 2F      CMA
324 0FC6 D3EA      OUT      *HEA
325 0FC8 3EFF      MVI      A,*HFF
326 0FCA 2F      CMA
327 0FCB D3EA      OUT      *HEA
328 0FCD C9      RET
329 0FCE 2A003D  LAG:     LHLD     CAMAX
330 0FD1 29      DAD      H
331 0FD2 29      DAD      H
332 0FD3 29      DAD      H
333 0FD4 EB      XCHG
334 0FD5 2AEA3F  LHLD     EOX
335 0FD8 CD840F  CALL     MINUS
336 0FDB 19      DAD      D
337 0FDC EB      XCHG
338 0FDD CD0C3F  CALL     *H3F0C
339 0FE0 CD7B0F  CALL     SHIFT
340 0FE3 CD7B0F  CALL     SHIFT
341 0FE6 CD7B0F  CALL     SHIFT
342 0FE9 CD7B0F  CALL     SHIFT
343 0FEC CD7B0F  CALL     SHIFT
344 0FEF CD7B0F  CALL     SHIFT
345 0FF2 CD7B0F  CALL     SHIFT
346 0FF5 EB      XCHG
347 0FF6 2AEA3F  LHLD     EOX
348 0FF9 19      DAD      D
349 0FFA 22EA3F  SHLD     EOX
350 0FFD C9      RET

```

Figure D-4 Prom No. 4 Pitch Control Software (Continued)

351 0FFE

END

Figure D-4 Prom No. 4 Pitch Control Software (Continued)

INTEL 8086 CROSS ASSEMBLER SYMBOL TABLE

PRLAX= 3D2A	PRLBX= 3D2B	PRLAY= 3D2C	PRLBY= 3D2D
PVLAX= 3D2E	PVLBX= 3D2F	PVLAY= 3D30	PVLBY= 3D31
RINT = 3D34	TINT = 3D38	X = 3D3A	XY = 3D3C
YFLAG= 3D3F	DELTA= 3D58	USDAO= 00EC	PRTA1= 0000
PRTB1= 0001	PRTC1= 0002	PRTA2= 0003	PRTB2= 00E5
PATC2= 0000	PRTD1= 0001	PRTD2= 0002	PRTD3= 00E6
MIB 0DF5	ALM 0DFF	XVK 0E0B	ETR 0E0E
OH 0E23	WOW 0E33	GOSH 0E39	OSH 0E3C
OGD 0E63	LMA 0E6D	BX 0E79	IP 0E7C
PA 0EB4	PB 0EEE	PD 0EC5	PC 0EC9
OUT 0ED0	OGDR 0F04	LMAR 0F0E	BXR 0F1A
IPR 0F1D	VOGD 0F4B	VLMA 0F55	VDEC 0F5B
VBX 0F61	VIP 0F64	SHIFT 0F7B	A = 0007
MINUS 0F84	SLED 0FA0	B = 0000	PLED 0FB2
BOX 0FBF	C = 0001	OUTPT 0FC0	D = 0002
CDE 0E05	DEC 0E73	E = 0003	KAD 0E29
CLA 0E92	BLED 0F9E	ALED 0FB0	LAG 0FCE
ICHAN= 3D60	GAIN 0E99	DECR 0F14	H = 0004
CAMAX= 3D00	CAMBX= 3D01	CAMAY= 3D02	CAMBY= 3D03
CCMAX= 3D46	CCMAY= 3D44	MICH = 3E80	XFLAG= 3D3E
CPOAX= 3D40	CPLAX= 3D0C	CPLBX= 3D0D	L = 0005
CPOBX= 3D41	CPOAY= 3D42	M = 0006	CPOBY= 3D43
CPLAY= 3D0E	EOX = 3FEA	CPLBY= 3D0F	DETX = 3D10
PETY = 3D11	DDOTX= 3D12	DDOTY= 3D14	DOTIX= 3D16
DOTIY= 3D18	IPRJX= 3D1A	SP = 0006	IPRJY= 3D1C
IPOSX= 3D1E	IPOSY= 3D20	MULCX= 3D90	MULDX= 3DA4
PSW = 0006	MXLVB= 3DB8	MXLVK= 3DCC	MULAX= 3DE0
MULBX= 3DF4	MULCY= 3E08	MULDY= 3E1C	MYLVB= 3E30
MYLVK= 3E44	MULAY= 3E58	MULBY= 3E6C	MICHY= 3E94
CMIY = 3EAB	CMIX = 3EBC	TORQY= 3ED0	TORQX= 3EE4
PTQX = 3EF8	NCPOX= 3D22	NCPOY= 3D24	PRJAX= 3D26
PRJBX= 3D27	PRJAY= 3D28	PRJBY= 3D29	

ERRORS DETECTED: 0

Figure D-4 Prom No. 4 Pitch Control Software (Concluded)

Appendix E

APPLICATION OF THE NIGHT VISION LABORATORY (NVL) THERMAL VIEWING SYSTEM STATIC PERFORMANCE MODEL TO THE RVS

It was suggested that the NVL Thermal Viewing System Static Performance Model, Reference (E-1) be used to evaluate the performance of the Remote Viewing System (RVS). However, repeated attempts to convert the RCS parameters directly to the NVL model have led to the following problem. The radial distortion function of the foveal lens does not lend itself to an MTF analysis as a function of object field angular spatial frequency as called for in the NVL model. All parameters can be converted successfully except for the scan velocity term because a linear raster scan on the lens image plane will create a variable angular velocity and variable direction scan in the object field. This is depicted in Figure E-1. Extreme complexity results when attempts are made to convert spatial into temporal frequency. This is illustrated by the rotation of the f_x bar pattern in the lens image plane shown in Figure E-1. Given enough time, an analysis could be made in a manner compatible with the NVL model. However, the analysis is much simpler if performed, not in object field angular frequency (cycles/milliradian) but in spatial frequency terms (cycles/millimeter). For our purpose of optimizing the RVS lens, it is simpler to work in terms of spatial frequency on the foveal lens focal plane.

This simplicity arises because seven of the nine MTF's are independent of object field angle at this foveal lens focal plane location, and the scan velocity is unidirectional and uniform at this location, thereby making easy conversion from spatial to temporal parameters. The only non-linear conversions necessary are simple geometrical ones which translate from focal plane to object field and display space. The advantages of working in the spatial frequency terms will become clear as the analysis is developed. In the following development, the NVL model approach will be used precisely but will be applied in the foveal lens focal plane as a function of linear spatial frequency (cy/mm). Parameters will be covered in the same order as they are in the NVL Report Reference E-1, which describes the model in detail.

E.1 MTF's

Optical MTF The optical MTF's consist of a diffraction MTF and a Gaussian MTF.

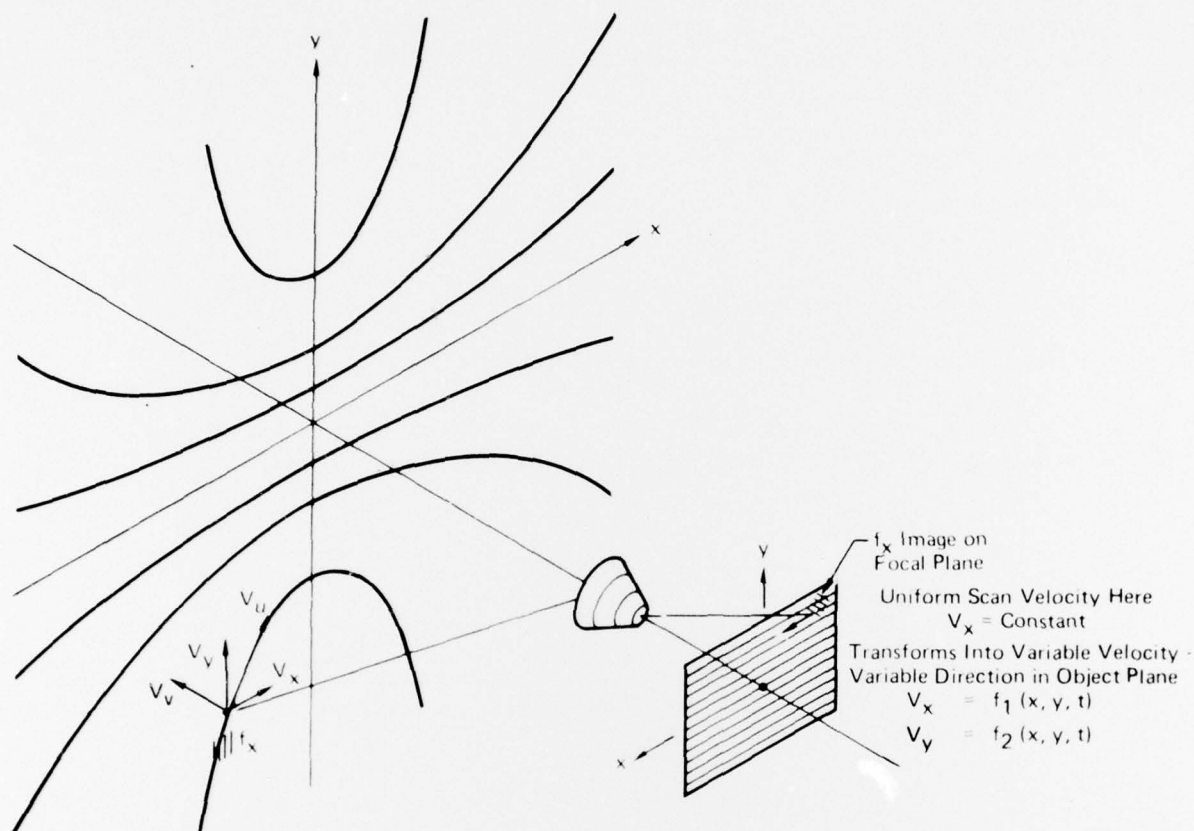
(a) Diffraction In angular terms, the diffraction MTF is referenced as Equations (9) and (10) of the NVL report:

$$H_{\text{opt}}(f_x, \theta) = \frac{2}{\pi} [\cos^{-1} A - A(1 - A^2)^{1/2}] \quad (\text{E-1})$$

$$\text{where, } A = \lambda F_{\#} f_x / L(\theta) \quad (\text{E-2})$$

where $L(\theta)$ is the equivalent focal length which changes over a 50/1 range as object field angle θ changes. The angle θ is the absolute angle between the point of interest and the lens optical axis. At the foveal lens image plane

$$S_x = \frac{f_{\mu}}{L(\theta)} \quad (\text{E-3})$$



GP77-0475-40

FIGURE E-1
SCAN DISTORTION INTRODUCED BY FOVEAL LENS

where S_x is the image plane spatial frequency and f is its object field angular^x equivalent measured along the scan line projection in the object field (μ direction on Figure E-1). Solving for f_μ in Equation (E-3) and substituting this for f_x in Equation (E-2),

$$A = \lambda F_{\#} S_x \quad (E-4)$$

Since the F/number of our lens is constant, the diffraction MTF is no longer a function of object field angle. Thus we may write $H_{\text{diff}}(S_x)$ which indicates that the MTF is a function of the independent variable S_x only. Note, however, that conversion to object field angular spatial frequency is very simple because focal length is constant over small angular increments and may be determined from

$$f_{\mu} = S_x L(\theta) \quad (\text{E-5})$$

where μ is along the scan line projection in the object field

likewise

$$f_w = S_y L(\theta) \quad (\text{E-6})$$

where w is normal to the scan direction in the object field

(b) Blur - A similar simplicity exists here. The MTF equation with the angular term b of Equation (11) of Reference(E-1) replaced with its equivalent is:

$$H_{\text{blur}}(f_x, \theta) = \exp \left[- \frac{2\pi^2 \sigma^2}{L(\theta)^2} f_x^2 \right] \quad (\text{E-7})$$

The foveal lens inherently has a constant spatial blur over its entire focal plane, so that the sigma (σ) of Equation(E-7) is a constant. Substituting Equation(E-5) into (E-7) we see the blur MTF simplifies to

$$H_{\text{blur}}(S_x) = \exp \left[- 2\pi^2 \sigma^2 S_x^2 \right] \quad (\text{E-8})$$

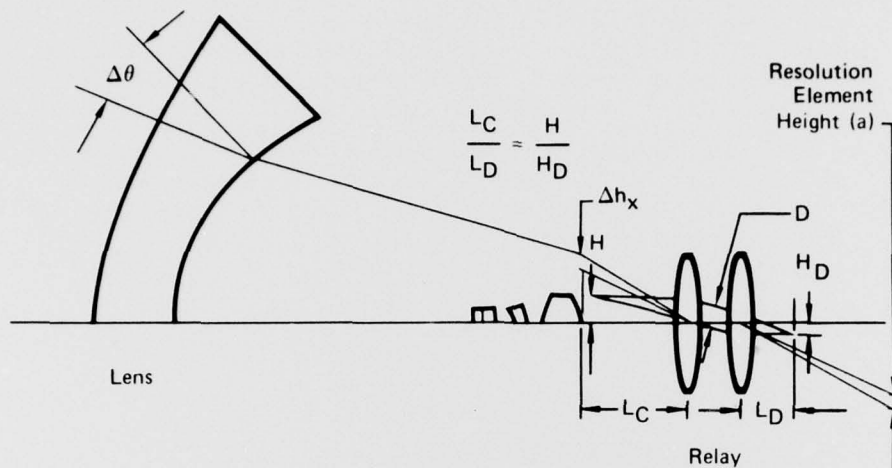
Thus this MTF like the diffraction MTF, is no longer a function of object field angle because the focal length variable has been removed.

Detection MTF - The spatial filter MTF of the detector is defined as:

$$H_{\text{Det}}(f_x, \theta) = \frac{\sin(\pi f_x \Delta x)}{\pi f_x \Delta x} \triangleq \text{Sinc}(f_x \Delta x) \quad (\text{E-9})$$

It is also complex in our system because the angular projection of the detector into the object field ($\Delta\theta$) in this equation varies with absolute object field angle (θ). Since the detector height is still uniform at the lens focal plane, shown in Figure(E-2) as Δh , Equation(D-9) can be restated as:

$$H_{\text{Det}}(S_x) = \frac{\sin(\pi S_x \Delta h_x)}{\pi S_x \Delta h_x} \quad (\text{E-10})$$



GP77-0475-32

FIGURE E-2
OPTICAL RELAY PARAMETERS

Again the MTF becomes independent of object field angle. Note from Figure(E-2) that the detector height (Δh_x) is a function of detector size(a), detector system focal length (L_D), and relay focal length (L_C), viz:

$$\Delta h_x \approx a_x \frac{L_C}{L_D} \quad (E-11)$$

If the detector characteristics are known, the focal lengths are a function of detector size (Δh) projected unto the image plane as shown in Figure(E-2). Detector size Δh can be computed directly from either the on-axis resolution required, the number of scan lines required across the vertical FOV, or bandwidth/response restrictions and frame rate requirements. The focal lengths, L_C and L_D , are then selected to make the detector dimension appear as the required Δh at the foveal lens focal plane. The detector MTF becomes:

$$H_{Det}(S_x) = \text{Sinc} \frac{S_x a_x L_C}{L_D} \quad (E-15)$$

Again this MTF is independent of object field angle.

Detector Electronics MTF - It is in the MTF, the detector electrical response, that we get into real trouble trying to work in object field angular space. For a conventional linear optical system, a linear detector scan velocity converts into a scaled but linear angular scan in the object field. This is not true in our system as was shown in Figure E-1. A linear scan in the x direction on the image plane results in angular velocities in both θ_x and θ_y directions in the angular object field. Both of these angular components are nonlinear functions of both x and y position on the image plane. Thus, converting from spatial frequency to temporal frequency becomes very complex. All of this can be avoided by working in linear spatial plane terms. If the scanner has an angular scan velocity β , then the linear motion of the instantaneous FOV on the foveal lens image is

$$V_x = \beta L_C \quad (E-16)$$

The conversion to temporal frequency (f) is therefore

$$f = V_x S_x \quad (E-17)$$

This is a constant conversion and not a function of time. Therefore, all electronic MTF's of the NVL model are valid. These are

$$\begin{aligned} H'_{\text{Det}}(f) \\ H_{\text{Elect}}(f) \\ H_B(f) \end{aligned}$$

Display - The RVS display is the inverse of the foveal lens, which results in a conventional linear raster generated on the CRT. The CRT has a constant spot size and the expansion optics has a constant blur at the object focal plane. Again this MTF, if derived in the linear spatial plane, will not be a function of object angle. If the optical blur and CRT spot size are combined and assumed to have a Gaussian MTF, a composite sigma (σ_d) results and the MTF is:

$$H_{\text{Disp}}(S_x) = \exp \left[-2\pi^2 (r\sigma_d)^2 S_x^2 \right] \quad (E-18)$$

where r is the physical ratio of format sizes; viz

$$r = \frac{H_{\text{LENS IMAGE}}}{H_{\text{DISPLAY CRT}}} \quad (E-19)$$

By contrast, if this were accomplished in the object angular plane, the MTF would be much more complex, viz

$$H_{\text{Disp}}(f_x, \theta, M) = \exp \left[- \frac{2\pi^2 (r\sigma_d)^2 f_x^2}{L(\theta)^2 M^2} \right] \quad (\text{E-20})$$

where M is any system angular magnification from object field to the viewer. Again the simplicity is obvious.

Stabilization and Eyeball - The remaining two MTF's are the only two that are not simplified by working in linear spatial rather than angular terms. First, stabilization tends to be angular input to the system. Using the MTF from the NVL report:

$$H_{\text{Los}}(f_x) = \exp(-P f_x^2) \quad (\text{E-21})$$

Converting to the foveal lens image plane results in

$$H_{\text{Los}}(S_x, \theta) = \exp[-P S_x^2 L(\theta)^2] \quad (\text{E-22})$$

Similarly, the eye views the display in angular terms. The NVL MTF is

$$H_{\text{Eye}}(f_x) = \exp \left[- \frac{P f_x^2}{M} \right] \quad (\text{E-23})$$

Equation(E-23) must be converted to the foveal lens image plane

$$H_{\text{Eye}}(S_x, \theta) = \exp \left[- \frac{P S_x L(\theta)}{M} \right] \quad (\text{E-24})$$

In conclusion, seven MTF's have been simplified at the expense of two that have been made slightly more complex by the conversion to linear spatial frequency.

E.2 NOISE EQUIVALENT MODULATION (NEM)

For visual spectrum applications noise equivalent modulation must replace NEAT in the NVL model. In the visual model, the primary noise source is the detector which is a silicon vidicon. Its NEM was extracted from data of Reference (E-2). These data show vidicon S/N as a function of faceplate illumination for a specific bandwidth. The basic function is approximately

$$\frac{\text{peak-to-peak signal}}{\text{noise (rms)}} = 100 E \quad (\text{E-21})$$

where E is faceplate illumination in LUX. The noise equivalent signal is (signal input that just equal noise)

$$NEM = \frac{\text{noise}}{\text{signal}} = \frac{1}{100E} \quad (E-22)$$

assuming that the noise is proportional to the square root of the bandwidth (Δf) of $4(10^8)$ Hz. For data given:

$$NEM = \frac{\Delta f}{100E \sqrt{4 \times 10^6}} = 5 \times 10^{-6} \frac{\sqrt{\Delta f}}{E} \quad (E \text{ in LUX}) \quad (E-23)$$

For E in footcandles:

$$NEM = \frac{4.64 \times 10^{-7} \sqrt{\Delta f}}{E} \quad (E \text{ in Foot-Candles}) \quad (E-24)$$

The faceplate illumination can be calculated from system geometry as follows:

$$E_f = \frac{B T_a T_o}{4 F_{no}^2} \quad (E-25)$$

Where

B=Scene brightness in footlamberts

T_a = Atmospheric transmission

T_o = Optical transmission within sensor

F_{no} = The equivalent F/number or F/number actually supplying the vidicon. This is the lens F/number modified by the relay and from basic geometrical optical theory is:

$$F_{noe} = F_{no} \frac{L_D}{L_c} \quad (E-26)$$

If the sensor employs an automatic light level control which operates on vidicon target current, E will be accurately maintained. Therefore, Equation (E-24) applies as written for the level of E which is preset. For the silicon vidicon under study, best performance is obtained when the level is about 0.1 lumens/ft². Equation (E-23) then becomes:

$$NEM = 4.64 \times 10^{-6} \sqrt{\Delta f} \quad (E-27)$$

E.3 MRM CALCULATIONS

The following MRM equation modifications are required so that the computation may be performed in linear spatial frequency terms. First, in the NVL MRT equation, Δy must be replaced by the apparent detector size at the foveal lens image plane, i.e., it must be the Δh defined on Figure E-2. As previously demonstrated in Equation (E-11).

$$\Delta h_y = a_y \frac{L_C}{L_D} \quad (E-28)$$

Also, in the MRM equation, it is best to compute the Q integral in terms of temporal frequency. This eliminates the velocity term in the MRT equation and makes the Q integral easier to compute. The Q integral is therefore

$$Q(f, \theta) = \int_0^\infty \frac{S(f)}{S(f_0)} H_N^2(f) H_w\left(\frac{f}{V_x}\right)^2 H_{Eye}\left(\frac{f}{V_x}\right) df \quad (E-29)$$

Of these terms, only H_w , the transfer function for a rectangular bar of width w , has not been defined. This transfer function is in linear rather than angular dimensions, i.e.,

$$H_w\left(\frac{f_x}{V_x}\right) = \text{Sinc } w\left(\frac{f_x}{V_x}\right) = \text{Sinc } \left(WS_x\right) \quad (E-30)$$

where

$$w \triangleq \frac{1}{2S_x} \quad (E-31)$$

The MRM equation written to show the dependency of two variables is

$$\text{MRM}(S_x, \theta) = \frac{\text{SNR} \pi^2 \text{NEM}}{4\sqrt{14} \text{MTF}_{\text{TOTAL}}(S_x, \theta)} \left[\frac{\Delta h_y S_x Q(f, \theta)}{\Delta f_N F_R t_e \eta_{\text{OVSC}}} \right]^{1/2} \quad (E-32)$$

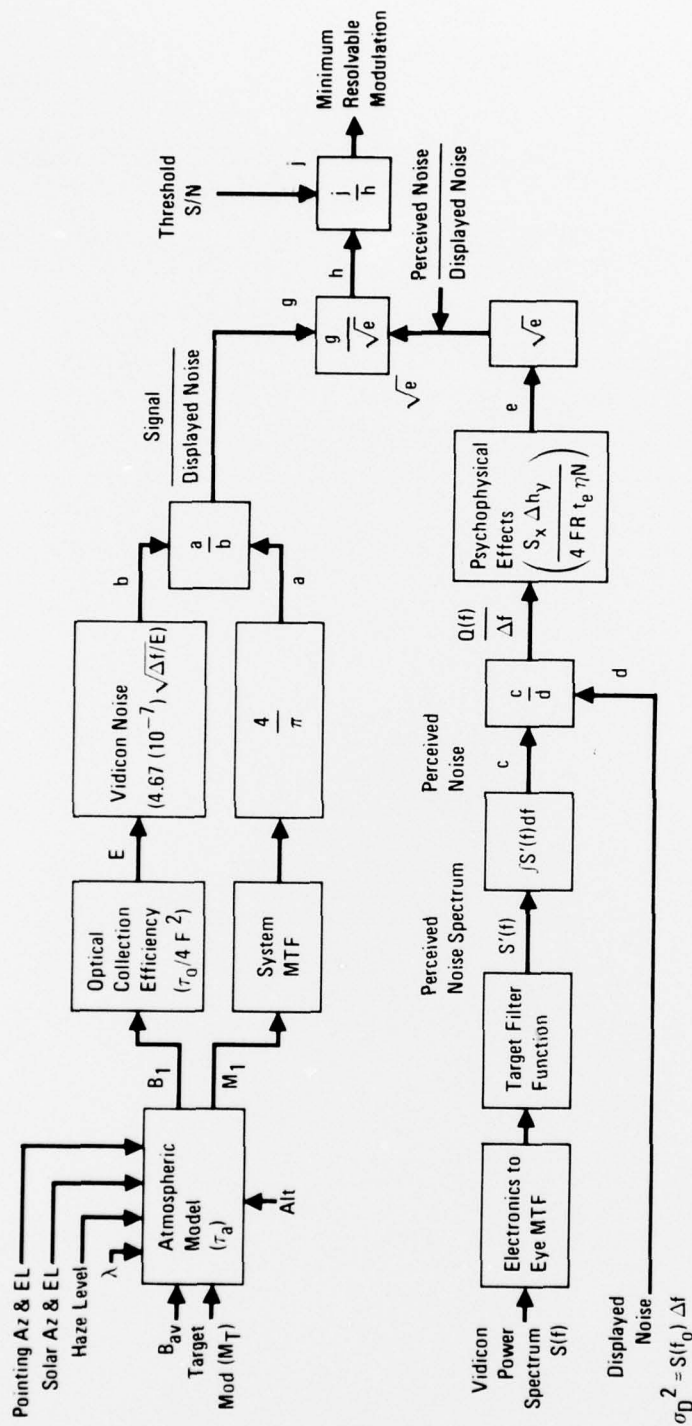
This equation results in an MRT very weakly dependent on θ . To obtain the MRM for any field angle θ , we convert the spatial frequency term S_x into an angular frequency term by using Equation(E-9) containing the focal length function:

$$f_\mu = S_x L(\theta)$$

Note this will be the angular spatial frequency in the scan direction (target bars normal to the scan direction). It could be related to f_x and f_y but this does not appear to be required at this point.

E.4 CONCLUSIONS

To conclude this effort, a block diagram of the NVL model converted to the VARVS Concept in the visual spectrum is shown in Figure E-3. This model was used in the study to compute Minimum Resolvable Modulation to predict performance.



GP77 0475 7

FIGURE E-3
NVL MODEL ADAPTED TO VARVS
FOR VISUAL SPECTRUM

APPENDIX
LIST OF REFERENCES

- C-1 Klaiber, R.J., Physical and Optical Properties of Projection Screens;
Technical Report NAVTRADEVCEH IH-63, December 1966
- C-2 Single Crystal Ferroelectronics and Their Application in Light Valve
Display Devices; Proceedings of the IEEE Vol. 61, No. 7, July 1973
- E-1 Ratches, James, et al, Night Vision Laboratory Static Performance
Model For Thermal Viewing Systems, Army Electronics Cmd., Fort Monmouth,
N.J., Report No. 7043, April 1975.
- E-2 RCA, Inc., 4532A Camera Tube Specification Sheet RCA Corp., Harrison,
N.J., Jan. 1973

DISTRIBUTION LIST

Chief of Naval Research		Naval Material Command	
800 North Quincy Street		Washington, DC 20360	
Arlington, VA 22217		ATTN: MAT 08T231	1
ATTN: Code 221	10		
455	1	Headquarters, U.S. Marine Corps	
421	1	Washington, DC 20380	
		ATTN: RD-1	1
Defense Documentation Center			
Cameron Station		Naval Air Systems Command	
Alexandria, VA 23314	12	Washington, DC 20360	
		ATTN: AIR 5103F	1
Naval Research Laboratory		5105	1
Washington, DC 20375		340D	1
ATTN: Tech Info Division	1	340F	1
Library, Code 2039		360E	1
		PMA 247	1
Office of Naval Research Branch			
Office		Naval Sea Systems Command	
New York Area Office		Washington, DC 20360	
715 Broadway (5th Floor)		ATTN: NSEA 0341	1
New York, NY 10003	1	NSEA 653C	1
Office of Naval Research Branch			
Office		Naval Electronic Systems Command	
1030 East Green Street		Washington, DC 20360	
Pasadena, CA 91106	1	ATTN: ELEX 320	1
		330	1
Office of Naval Research Branch			
Office		U.S. Naval Air Development Center	
495 Summer Street		Warminster, PA 18974	
Boston, MA 02210	1	ATTN: Code 402	1
		304	1
Office of Naval Research Branch		54P3	1
Office		30P8	3
536 Clark Street		6011	1
Chicago, IL 60605	1		
Director of Defense Research		Naval Ocean Systems Center	
and Engineering		271 Catalina Boulevard	
Washington, DC 20350		San Diego, CA 92152	
ATTN: ODDR&E/E&PS	1	ATTN: Code 8235	1
ODDR&E/E&LS	1		
Chief of Naval Operations		Naval Weapons Center	
Washington, DC 20350		China Lake, CA 93555	
ATTN: OP 987	1	ATTN: Code 3925	1
OP 986	1	Code 3175	1
OP 982	1		
OP 596	1	Naval Weapons Center	
OP 506	1	Dahlgren, VA 22448	
		ATTN: Mr. K. Ferris	3

Naval Training Equipment Orlando, FL 32813 ATTN: Code N-2224	1	U.S. Army Night Vision Lab Fort Belvoir, VA 22060 ATTN: DRSEL-NV-SD	1
Naval Air Test Center Service Test Division Aero Medical Branch Patuxent River, MD 20670 ATTN: Mr. Fred Hoerner	1	U.S. Army Research and Development Command P.O. Box 209 St. Louis, MO 63166 ATTN: DRSAB-EV	1
Naval Avionics Facility 6000 E. 21st Street Indianapolis, IN 46218 ATTN: Technical Library	1	U.S. Army Aviation Center Ft. Rucker, AL 36362 ATTN: ATQZ-D-SGA	1
Dean of Research Administration Naval Postgraduate School Monterey, CA 93940 ATTN: Dr. J. Powers	1	Human Engineering Labs Aberdeen Proving Grounds, MD 21105 ATTN: DRXRD-HEL	1
U.S. Coast Guard Headquarters 400 7th Street, NW Washington, DC 20591 ATTN: GDST/62 TRPT	1	Headquarters Aeronautical Systems Division Air Force Systems Command Wright-Patterson AFB, OH 45433 ATTN: AFAL/AA AFAL/CC AFAL/RWI	1 1 1
HQS Army Research Institute 1300 Wilson Boulevard Arlington, VA 22209	1	Air Force Flight Dynamics Laboratory Air Force Systems Command Wright-Patterson AFB, OH 45433 ATTN: AFFDL/FG	1
Headquarters U.S. Army Washington, DC 20350 ATTN: DAMA-WSA DAMA-ZE DAMA-WSM DAMA-ARZ	1 1 1 1	Aero Medical Research Laboratory Wright-Patterson AFB, OH 45433 ATTN: AMRL/HE	1
U.S. Army Avionics Laboratory U.S. Army R&D Command Fort Monmouth, NJ 07703 ATTN: DAVAA-F (Mr. Respass) DAVAA-E (Mr. Gurman)	2 1	Air Force Office of Scientific Research 4100 Wilson Boulevard Arlington, VA 22209	1
U.S. Army Material Command Washington, DC 20315 ATTN: DRCDR-HA DRCPM-AAH DRCPM-GCM-WF	1 1 1	Federal Aviation Agency NAFEC Bldg. 10 Atlantic City, NJ 03405 ATTN: Mr. D. Elliott	1
		Headquarters Aeronautical Systems Division Air Force Systems Command Wright-Patterson AFB, OH 45433 ATTN: ASD/YRD ASD/SD	1 1

Defense Advanced Research
Project Agency
1400 Wilson Blvd.
Arlington, VA 22209
ATTN: Dr. Strom

1

National Aeronautical and
Space Administration
Langley Research Center
Mail Stop 1574
Hampton, VA 23665
ATTN: Mr. R. Morris

1

National Aeronautical and
Space Administration
Ames Research Center
Mail Stop 200-10
Moffett Field, CA 94035
ATTN: Mr. J. Dusterberry

1

Institute for Defense Analysis
400 Army-Navy Drive
Arlington, VA 22204
ATTN: Mr. L. Biberman
Dr. A. Schnitzler

1

1